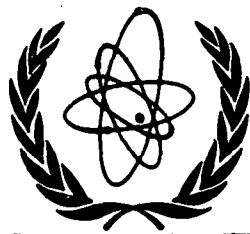


International Atomic Energy Agency



**INDC**

**INTERNATIONAL NUCLEAR DATA COMMITTEE**

CONSOLIDATED PROGRESS REPORT FOR 1975

ON NUCLEAR DATA ACTIVITIES

IN THE NDS SERVICE AREA

Argentina  
Bangladesh  
Brazil  
Bulgaria  
Hungary  
India  
Iran  
Iraq  
Israel  
Pakistan  
Poland  
Romania  
South Africa  
Yugoslavia

January 1976

**IAEA NUCLEAR DATA SECTION, KÄRNTNER RING 11, A-1010 VIENNA**

Reproduced by the IAEA in Austria  
January 1976  
75-10110

CONSOLIDATED PROGRESS REPORT FOR 1975

ON NUCLEAR DATA ACTIVITIES

IN THE NDS SERVICE AREA

Argentina

Bangladesh

Brazil

Bulgaria

Hungary

India

Iran

Iraq

Israel

Pakistan

Poland

Romania

South Africa

Yugoslavia

January 1976

## FOREWORD

This consolidated progress report for 1975 has been prepared for the countries in the NDS service area. It is intended to encourage a closer relationship between Member States and provide for a wider circulation of unpublished progress reports from countries within the Nuclear Data Section service area. A second report INDC(SEC)-51/L covers countries outside the NDS service area.

The report is arranged alphabetically by country, and reproduces the content of each individual report as it was received by the INDC Secretariat. Also included in the Table of Contents is a list of each laboratory, institute and university referred to in the report, preceded by its internationally used EXFOR code.

As in all progress reports the information included here is partly preliminary and is to be considered as private communication. Consequently, the individual reports are not to be quoted without the permission of the authors.



TABLE OF CONTENTS

	pages
<u>Argentina</u> .....	1-4
(3ARGCNE) CNEA - Comision Nacional de Energia Atomica at Constituyentes	
(3ARGCAB) Universidad San Carlos y Centro Atomico, Bariloche	
<u>Bangladesh</u> .....	5-16
(3BANRAM) Atomic Energy Center, Ramna, Dacca	
(3BANITD) Institute of Nuclear Technology, Dacca	
<u>Brazil</u> .....	17-47
(3BZLUSP) Instituto de Fisica, Universidade de Sao Paulo, Sao Paulo	
(3BZLIEA) Instituto de Energia Atomica, Sao Paulo	
(3BZLRIO) Centro Brasileiro de Pesquisas Fisicas, Rio de Janeiro	
(3BZLIEN) Instituto de Engenharia Nuclear, Rio de Janeiro	
(3BZLIDF) Instituto de Fisica, Universidade Federal do Rio Grande do Sul, Porto Alegre	
<u>Bulgaria</u> .....	49-56
(3BULBLA) Institute of Nuclear Research and Nuclear Energy, Sofia	
<u>Hungary</u> .....	57-126
(3HUNKFI) Hungarian Academy of Sciences, Central Research Institute for Physics, Budapest	
(3HUNKOS) Institute of Experimental Physics, Kossuth Univer- sity, Debrecen	
(3HUNDEB) Hungarian Academy of Sciences, Institute of Nuclear Research, Debrecen	
(3HUNELU) Roland Eoetus University, Budapest	

	pages
<u>India</u> .....	127-207
(3INDTRM) Bhabha Atomic Research Centre, Bombay	
(3INDTAT) Tata Institute of Fundamental Research, Bombay	
(3INDSAH) Saha Institute of Nuclear Physics, Calcutta	
(3INDAUW) Andhra University, Visakhapatnam	
(3INDBHU) Banaras Hindu University, Varanasi	
(3INDBIT) Birla Institute of Technology, Pilani and Ranchi	
(3INDBUU) Burdwan University, Burdwan	
(3INDDIU) Dibrugarh University, Assam	
(3INDITK) Indian Institute of Technology, Kanpur	
(3INDKUK) Kurukshetra University, Kurukshetra	
(3INDMAU) Marathwada University, Aurangabad (M.S.)	
(3INDPRA) Physical Research Laboratory, Ahmedabad	
(3INDPUC) Punjab University, Chandigarh	
(3INDPAT) Punjab University, Patiala	
(3INDDLH) University of Delhi, Delhi	
(3INDUMA) University of Madras, Madras	
(3INDKAL) Reactor Research Centre, Kalpakkam	
<u>Iran</u> .....	209-241
(3IRNTEH) Tehran University Nuclear Centre Tehran	
<u>Iraq</u> .....	243-300
(3IRQNRI) Nuclear Research Institute, Tuwaitha, Baghdad	
<u>Israel</u> .....	301-347
(3ISLTEL) Tel Aviv University	
(3ISLIRC) Israel AEC Research Centres	
(3ISLBGU) Ben Gurion University, Beer Sheba	
(3ISLWZI) Weizmann Institute of Science, Rehovot	

	pages
<u>Pakistan</u> .....	349-355
(3PAKNIL) Pakistan Institute of Nuclear Science and Technology Rawalpindi	
<u>Poland</u> .....	357-401
(3POLIBJ) Institute of Nuclear Research, Warsaw	
(3POLWWA) University of Warsaw	
<u>Romania</u> .....	403-426
(3RUMBUC) Institute of Atomic Physics, Bucharest	
<u>Republic of South Africa</u> .....	427-436
(3SAFPEL) Physics Division, Atomic Energy Board, Pelindaba	
(3SAFSUN) Southern Universities Nuclear Institute, Faure	
<u>Yugoslavia</u> .....	437-457
(3YUGNJS) Institute "Jozef Stefan" Ljubljana	
(3YUGRBZ) Institute "Ruder Boskovic", Zagreb	

P R O G R E S S R E P O R T

NUCLEAR DATA IN ARGENTINA 1975

Compiled and selected by

G.H. RICABARRA

Progress Report Argentina

1. Research on the decay scheme data of  $^{141}\text{La}$

D. Otero, A.N. Proto, G. Kalberman, F.C. Iglesias

The decay scheme data of  $^{141}\text{La}$  feed by the beta decay of  $^{141}\text{Ba}$  was studied, a detector of Ge(Li) (2.2 keV resolution) was used together with a coincidence system slow and slow-fast. Using a detector of Si(Li) for electrons and a Ge(Li) detector the internal conversion coefficient  $\alpha_k$  was determined for the transitions of:

113.04, 276.93, 304.18, 343.66, 457.5, 462.24 and 467.18 keV.

2. "Study of the  $^{141}\text{Xe} \rightarrow ^{141}\text{Cs}$  beta decay"

D. Otero, A.N. Proto, F.C. Iglesias

a)  $^{141}\text{Xe}$

211 gamma transitions were identified. Internal coefficients ( $\alpha_k$ ) were calculated for the following transitions: 118.71 (0.2  $\pm$  0.08), 187.6 (0.16  $\pm$  0.06), 362.02 (0.024  $\pm$  0.015), 369.5 ( $\pm$  0.023), 388.98 (0.02  $\pm$  0.01), 459.12 (0.013  $\pm$  0.006), 467.8 (0.015  $\pm$  0.006), 539.9 (0.011  $\pm$  0.003) and 556.61 (0.008  $\pm$  0.003) keV.

Gamma gamma coincidences were measured, and by this technique were measured the following levels: 68.98  $\pm$  0.03, 105.96  $\pm$  0.03, 187.72  $\pm$  0.04, 206.69  $\pm$  0.03, 467.93  $\pm$  0.07, 557.10  $\pm$  0.18, 664.25  $\pm$  0.17, 946.01  $\pm$  0.12, 961.98  $\pm$  0.04, 977.53  $\pm$  0.34, 979.86  $\pm$  0.08, 1097.26  $\pm$  0.12, 1234.82  $\pm$  0.04, 1245.11  $\pm$  0.06, 1518.28  $\pm$  0.31 and 1556.71  $\pm$  0.11 keV.

The decay scheme data of  $^{141}\text{Cs}$  with 39 levels is presented that includes 95% of the total gamma intensity.

b)  $^{141}\text{Cs}$

189 gamma transitions were identified. The internal conversion electron coefficients was calculated for the transitions of 48.48 (6.6  $\pm$  0.9) keV. Level schemes were established by gamma-gamma coincidence for the following transitions: 48.48  $\pm$  0.05, 588.55  $\pm$  0.04, 1194.16, 1748.90  $\pm$  0.1 and 2397.66  $\pm$  0.4 keV. The decay scheme with 27 levels of  $^{141}\text{Ba}$  is presented.

3. Study of  $^{72}\text{As}$  and  $^{74}\text{As}$  by means of the nuclear reactions  $(\alpha, np)$  and  $(\alpha, 3np)$  with  $^{70}\text{Ge}$  and  $^{72}\text{Ge}$ .

A.M. Hernandez, A. Filevich, M. Behar and G. García Bermúdez and M.A.J. Mariscotti.

Using the external beam of the Buenos Aires Sincrocyclotron, nuclear reactions  $(\alpha, xnp)$  on enriched targets of  $^{70}\text{Ge}$  and  $^{72}\text{Ge}$  were studied with energies in between 30 and 55 MeV. The decay scheme level were also studied by a coincidence system with two Ge(Li) detectors.

4. Spin and parity of the level of 1958 keV in the  $^{124}\text{Te}$ .

M.C. Cambiaggio, M. Behar, G. García Bermúdez y A. Filevich.

The results of the present experiment shows that the level of 1958 keV is  $4^+$ , with the mixing parameter of the transition 709 keV being  $\delta = 0.035 \pm 0.040$ .

5. "System for the measure of the half-life in the range of msec-sec in the Sincrocyclotron of Buenos Aires".

E.A. Santi, N. Fazzini, J. Sinderman and M.A.J. Mariscotti

A simple electronic and mechanical system has been built designed to measure short half-lives.

The following half-lives has been measured:

$^{197}\text{Au}(\alpha, 4n)^{197}\text{Tl}$	$T_{1/2} = 497 \pm 8 \text{ msc.}$
$^{197}\text{Au}(\alpha, 2n)^{199}\text{Tl}$	$T_{1/2} = 25 \pm 2 \text{ msec.}$
$\text{Hg}(\alpha, xn)^{180}\text{W}$	$T_{1/2} = 5.47 \pm 0.1 \text{ msec.}$
$^{141}\text{Pr}(\alpha, 3n)^{142}\text{Pm}$	$T_{1/2} = 2.18 \pm 0.03 \text{ msec.}$

6. Study of the decay of  $^{49}\text{Sc} \rightarrow ^{49}\text{Ti}$

M.T. Bodio, A.M. Hernández, M.A.J. Mariscotti

In the present work the decay of  $\text{Sc}$  was measured by means of the nuclear reaction  $^{48}\text{Ca}(n, \text{gamma})^{49}\text{Ca} \rightarrow ^{49}\text{Sc} \rightarrow ^{49}\text{Ti}$ .

A sample of  $\text{CO}_3\text{Ca}$  was irradiated in the R.A.3 and by this means a sample of  $^{49}\text{Sc}$  was obtained.

For the first time the transitions of 380.5 keV and 1381.5 keV of  $^{49}\text{Ti}$  were observed, however the lines observed were weak.

7. Half-life systematic of neutron deficient radio-isotopes

L.P. Chimento and M.A.J. Mariscotti

An analysis has been made that includes known isotopes which are placed at the left of the stability line with  $Z \geq 82$  and  $W > 250$  keV. The variation of  $T_{1/2}$  is in between  $10^{-2}$  sec. and  $10^8$  sec.

For odd  $\Delta = N - Z$  (220 isotopes) the lineal approximation:

$$\log T_{1/2}(\text{sec}) = 5 a_{\Delta} (-\log W (\text{MeV}) + b_{\Delta} )$$

describe within an order of magnitude 84% of the cases.

If the analysis is limited to  $W \geq 2$  MeV the deviation are reduced to 7.5%.

8. Total cross section of Cr for neutrons in the thermal and sub-thermal range.

F. Kropff, J.R. Granada, L.A. Remez, A. Vasile

The total cross section was measured between  $1.3 \cdot 10^{-4}$  and 30 eV, using the time of flight technique with the linear accelerator of Bari-loche. A theoretical calculation together with a fitting of the experimental results was used to obtain the value  $\sigma_{\text{th}}(2200 \text{ m/s}) = 3.25 \pm 0.15$  barn for the thermal absorption cross section of Cr.

**Progress Report**

**on**

**Nuclear Data Activities in**

**Bangladesh**

1974

**Compiled by**

**M. Mizanul Islam  
Atomic Energy Centre,  
Dacca.**

Bangladesh Nuclear Data Committee

- |                                        |                                                |
|----------------------------------------|------------------------------------------------|
| 1. Prof. M. Innaas Ali<br>(convener)   | Bangladesh Atomic Energy<br>Commission, Dacca. |
| 2. Dr. M. Mizanul Islam<br>(Secretary) | Atomic Energy Centre,<br>Dacca.                |
| 3. Dr. Mizanur Rahman <sup>*</sup>     | Atomic Energy Centre, Dacca.                   |
| 4. Dr. A.H. Khan                       | Atomic Energy Centre, Dacca.                   |
| 5. Dr. M.A. Wadud Mondal               | Institute of Nuclear<br>Technology, Dacca.     |
| 6. Prof. A.K.M. Siddiq                 | Department of physics<br>Dacca University      |
| 7. Prof. Ahmed Husain                  | Department of physics<br>Rajshahi University   |
| 8. Dr. Ekhlauddin Ahmed                | Department of physics<br>Chittagong University |

---

\*

Present address: Department of Mathematics,  
Rajshahi University.

Atomic Energy Centre  
P.O. Box No. 164  
Ramna, Dacca,  
Bangladesh.

1. Fast neutron induced fission

(N.M. Islam, A.H. Khan, M. Khaliquzzaman, M.A. Rahman,  
M. Enayetullah and D.A.M. Abdullah)

A scattering chamber has been specially designed and fabricated to study the fast neutron induced fission using the 3 MeV Van de Graaff accelerator of the Atomic Energy Centre, Dacca. The fragments are detected with ORTEC heavy ion detectors. Measurements are in progress for the study of anisotropy of fission fragments produced by neutron interaction on  $^{235}\text{U}$  at a number neutron energies and on the mass-energy correlation of fission fragments as a function of neutron energy.

2. Fast Neutron Scattering

(M. Mizanul Islam)

The Neutron pit area has been covered with metallic sheets to facilitate the movement of detectors for angular distribution measurements. A neutron detector has been fabricated consisting of a NE 213 liquid scintillator 2" in dia. & 2" in length viewed directly by a RCA 8585 photomultiplier mounted on a constant fraction timing base, model ORTEC 270. One large detector shielding made up of brass and filled with paraffin has been also fabricated.

Work will start on the measurement of ~~angular distribution of~~ angular distribution of elastically scattered neutrons on carbon in the incident neutron energy range of 200 keV to 2 MeV using  $^7\text{Li}(p,n)$

and  $T(p,n)$  reactions. Measurements will then be continued on heavy elements and reactor structural materials depending on the availability of the samples.

3. Measurement of Total Neutron cross-section of Ce and Ho  
(M. Hussain\*, M. Husain, M. Enayetullah, N. Islam and M. Shajhan\*).

Total neutron cross sections of Ce and Ho were measured in the energy ranges 4.04 to 5.62 MeV, 16.40 to 18.98 MeV and 3.74 to 5.69 MeV. The results had statistical errors of 3% for Ce and 2% for Ho. The present data along with the earlier ones were used for Optical model analysis following the procedures of Emmerich and Buck.

4. Measurement of total Neutron cross section for V and Te  
(M. Hussain\*, M. Husain, M. Enayetullah, N. Islam and M. Das\*).

Neutron total cross sections for V and Te between energy range 1.0 to 2.0 MeV at 10 keV energy steps were measured using oxide samples. The cross-sections have been compared with other available data and were found to be in good agreement.

5. Studies of interaction and fission of uranium by fast neutrons employing nuclear emulsion.

( M.M. Kasim )

In order to study the fission process employing nuclear emulsion technique, four K1 emulsion plates of size 5" x 2" x 100  $\mu$ m were exposed to 17.35 MeV neutrons. The neutrons were obtained from  $T(d,n) He^4$  reaction using 1.6 mg/cm<sup>2</sup> titanium backed tritium target and deuteron beam of 1.5 MeV from Van de Graaff. The plates

---

\* Dacca University

were exposed for three hours. The distance between front edge of emulsion and target was 7 cm. The plates were then processed by the usual procedure. ID19 developer (diluted 1+9) and 30% plain hypo were used during developing and fixing respectively. Large number of recoil proton tracks were found when these plates were examined under microscopes. Scanning work is in progress for finding out  $(n,\alpha)$  reaction with Ag and Br nuclei of emulsion.

6. The elastic scattering of protons from  $^{27}\text{Al}(p,p_0)$  reaction.

(N.A. Rahman, M.A. Awal, M. Rahman and H.M. Sen Gupta\*)

The  $^{27}\text{Al}(p,p_0)$  resonance reaction was investigated in the energy region  $E_p = 0.85$  to  $3.00$  MeV and eleven isolated resonances have been observed.

The resonances have been analysed to obtain their properties.

Experimental measurements:

The experiment has been performed with the proton beam provided by the 3 MeV Van de Graaff accelerator at the AEC, Dacca. Beam energy spread was about 850 eV. Natural aluminium targets of thickness  $5-20 \mu\text{gm}/\text{cm}^2$  (2.2 keV at  $E_p = 2$  MeV) were prepared by Vacuum evaporation on carbon backings of  $5-20 \mu\text{gm}/\text{cm}^2$  thick and used in the experiment. Two ORTEC surface barrier detectors of  $100 \text{ mm}^2$  sensitive area and depletion depths of  $500 \mu\text{m}$  and  $1000 \mu\text{m}$  respectively were used for the detection of elastically scattered protons. The target was kept at an angle of  $45^\circ$  with respect to

---

\* Dacca University

the proton beam inside a scattering chamber. The protons after passing through the target were collected in a Faraday cup. Each point on the measurement corresponds to 100  $\mu\text{C}$  of charge. The desired peak area of the elastically scattered protons from the target is gated by the discriminator levels of the single channel analyzer ORTEC 420. The discriminator levels are adjusted for every 5 - 10 keV increase in proton energy.

Measurements were carried out at c.m. angles  $90^\circ$ ,  $125^\circ$  and  $141^\circ$  in the energy region  $E_p = 0.85-3.0$  MeV. A number of resonances were observed and only the eleven isolated resonances at  $E_p = 1.117$ , 1.199, 1.363, 1.452, 1.496, 1.574, 1.793, 2.028, 2.472, 2.548 and 2.866 MeV have been studied in the present work.

#### Analyses of data

The differential elastic scattering cross-section for protons from a target nucleus near an isolated resonance relative to the non-resonant potential scattering cross-section is expressed by the relation<sup>1)</sup>

$$\frac{\sigma}{\sigma_R}(\theta, E) = 1 + \frac{(E-E_0)A(\theta)}{(E-E_0)^2 + (\Gamma/2)^2} + \frac{B(\theta)}{(E-E_0)^2 + (\Gamma/2)^2} \dots \quad (1.1)$$

where  $E$  is the energy of incident projectile,  $E_0$  is the resonance energy and  $A(\theta)$  and  $B(\theta)$  are angle factors which depend on  $l, J$ , total resonance width  $\Gamma$  and ratio between proton and total resonance width  $\Gamma_p/\Gamma$ .

The parameters  $E_0$ ,  $l, J, \Gamma_p$  and  $\Gamma$  were given as input for analysis and were allowed to vary till an acceptable fit is obtained.

The resonance at  $E_p = 2.548$  MeV was fitted with  $l = 2$ . The shape of the resonance at  $90^\circ$  is different from all other resonances at this angle. All other resonances needed  $l = 1$ .

Two of the resonances at  $E_p = 1.117$  and  $1.793$  MeV were identified as analogues of the  $3.461$  and  $4.030$  MeV levels in  $^{28}\text{Al}$  respectively. For these two states a comparison is made with spectroscopic factors given by  $(d,p)$  stripping reactions<sup>2,3)</sup> leading to the corresponding parent states.

#### References

- 1) R. Bloch, R.E. Pixley and H. Winkler, *Helv. Phys. Acta* **40**, 832 (1967).
- 2) S. Chen, J. Rapaport, H. Enge and W.W. Buechaer, *Nucl. Phys.* **A197**, 97 (1972).
- 3) T.P.G. Carola and G. Van der Bann, *Nucl. Phys.* **A173**, 414 (1971).
7. Angular distribution of  $\gamma$ -rays from the  $^{27}\text{Al}(p,\gamma)^{28}\text{Si}$  resonance reaction.  
(M.A. Rahman, M.A. Awal, M. Rahman and H.M. Sen Gupta\*)

The present work is concerned with the angular distribution measurement of gamma rays from the  $^{27}\text{Al}(p,\gamma)^{28}\text{Si}$  resonance reaction at  $E_p = 2.482, 2.511$  and  $2.735$  MeV. The properties of the resonance levels are obtained.

---

\* Dacca University

### Experimental Procedure

The experiments were performed by using the proton beam provided by the 5.5 MeV Van de Graaff of Bhaba Atomic Research Centre, Bombay, India. The targets nominally  $20 \mu\text{g}/\text{cm}^2$  thick were prepared by depositing natural aluminium on tantalum backings by vacuum evaporation. The target was placed at an angle of  $45^\circ$  with respect to beam direction. A 20 c.c. co-axial Ge(Li) detector was used for the detection of gamma rays. The angular distribution of gamma rays were measured at angles of  $0^\circ$ ,  $30^\circ$ ,  $55^\circ$  and  $90^\circ$  with the Ge(Li) detector. A  $5'' \times 6''$  NaI(Tl) detector placed at a distance of 5 cm from the target and at an angle of  $90^\circ$  to the beam direction served as a monitor.

The spins of nuclear states are determined by angular distribution measurements. The theoretical angular distribution is expressed by the relation

$$W(\theta) = A_0 + A_2 Q_2 P_2(\cos \theta) + A_4 Q_4 P_4(\cos \theta)$$

where  $W(\theta)$  is the intensity observed at an angle  $\theta$  and  $Q_2$  and  $Q_4$  are the attenuation factors due to finite size of the detector.

The ratios  $A_2/A_0 = a_2$  and  $A_4/A_0 = a_4$  depend on the spins of the initial and final states  $J_i$  and  $J_f$  and on the multipole mixing ratio  $\delta$ . The data analysis was done by varying  $\arctan \delta$  in the range of  $-90^\circ$  to  $+90^\circ$  for an assumed value of  $J_i$  ( $J_f$  being known).

Quality of each fit is given by

$$\chi^2 = \frac{1}{n-1} \sum_{i=1}^n (Y_i - W_i)^2 / E_i^2$$

where  $n$  is the number of data points,  $Y_1$  and  $W_1$  are experimental and theoretical yields respectively and  $E_1$  is the error in experimental yield.

Results of the angular distribution measurements of  $\gamma$ -rays emitted by resonance levels at 13.980, 14.007 and 14.223 MeV of  $^{28}\text{Si}$  at  $E_p = 2.482, 2.511$  and  $2.735$  MeV show that they are analogues to the levels at 4.685, 4.741 and 4.928 MeV of  $^{28}\text{Al}$ .

8. Analogue states in  $^{57}\text{Co}$  and  $^{46}\text{Ti}$  from proton capture reactions in  $^{56}\text{Fe}$  and  $^{45}\text{Sc}$ .

(M.A. Rahman, M.A. Awal, M. Rahman and H.M. Sen Gupta\*)

The  $^{56}\text{Fe}(p,\gamma)^{57}\text{Co}$  resonance reaction have been studied in the energy region  $E_p = 1.20 - 3.03$  MeV to identify the isobaric analogue states in the compound nucleus  $^{57}\text{Co}$  corresponding to the ground and low-lying levels of the parent nucleus  $^{57}\text{Fe}$ .

The  $(p,\gamma)$  yield curve displays a number of strong resonances. In the present investigation nine analogue states at  $E_p = 1.246, 1.262, 1.416, 1.652, 2.065, 2.310, 2.525, 2.588, 2.680$  and  $3.002$  MeV corresponding to ground,  $0.014, 0.136, 0.367, 0.707, 1.004, 1.196, 1.265, 1.356$  and  $1.627$  MeV states of  $^{57}\text{Fe}$  have been tentatively identified. The coulomb displacement energy for the isobaric pair  $^{57}\text{Fe} - ^{57}\text{Co}$  has been found to be  $8.890 \pm 0.052$  MeV. .

The  $(p,\gamma)$  yield curve from  $^{45}\text{Sc}$  target has been investigated in the energy range  $E_p = 0.86 - 3.03$  MeV. Coulomb displacement energy as obtained in the present measurements is  $\Delta E_c = (7.611 \pm 0.063)$ .

---

\* Dacca University

9. Proton induced X-ray fluorescence spectroscopy

(A.H. Khan, M.M. Islam, M.A. Rahman, M.B. Zaman and M.A. Awal)

An experimental setup for charged particle induced X-ray measurements has been established. The purpose of the setup is to measure the inner shell ionization cross sections due to ion-atom collisions. At present a gas filled proportional X-ray spectrometer is in use. This is being replaced by a Si(Li) X-ray spectrometer.

With the present setup the spectrometer has been calibrated using a variable energy X-ray source prepared by Radio chemical Centre, Amersham. It has been used to identify the characteristic X-rays of Cu, Ti, Pb and U produced by 1.2 MeV proton bombardment. In addition, X-rays from fission fragments from 252-Cf will be measured with the Si(Li) detector in order to study the nuclear charge dispersion phenomenon in fission.

10. Application of the Resonating group formalism.

(S.A. Afsal and S. Ali)

Application of the resonating group formalism is done to the case of  $\alpha$ - $\alpha$  phase shifts for  $l = 0$ ,  $2A^4$  with different types of N-N interactions. Consistent rms. radius and lower bound of energy had been taken into account. Out of five N-N interactions studied, two give good agreement with experimental results.

11. Three body problem.

(M. Rahman and S.M.M.R. Chowdhury)

After successful applications of the separable potential in reproducing the two body phase-shifts it has been thought worthwhile to apply the same technique to study the three body problem. There has been a few attempts on the three body problem in the past; most of them are in the momentum representation where coulomb interaction has either been neglected or only approximately accounted for.

In this project we want to formulate the three body problem in coordinate representation which has not been done yet and take into account of the coulomb interaction exactly. For simplicity we take the case of  $^{12}\text{C}$  and study the same as  $3 - \alpha$

The analytical work on the problem is in progress.

12.  $\alpha$ -d Model of  $\text{Li}^6$

(S.A. Afzal)

Following resonating group formalism  $\alpha$ -d model of  $\text{Li}^6$  has been critically examined from the point of view of Pauli Exclusion Principle. A review of literature is in progress.

13. An Analysis of  $^{12}\text{C}(^{16}\text{O}, \alpha)^{24}\text{Mg}$  Reaction.

(S.A. Afzal and A.A.Z. Ahmed)

An analysis of the nucleon reaction  $^{12}\text{C}(^{16}\text{O}, \alpha)^{24}\text{Mg}$  has been started. It is of interest to see the validity of clustering in  $^{12}\text{C}$ ,  $^{16}\text{O}$ ,  $^{24}\text{Mg}$  as  $\alpha$ -particles. With the availability of beams of heavy ions lot of experimental data for this reaction are available but satisfactory theoretical analysis of this reaction from the clustering point of view has not yet been made. With this point in view the present project has been taken up.

Institute of Nuclear Technology,  
Dacca.

1. "Time behaviour of a neutron pulse in a homogeneous multiplying medium"

( M.A.W. Mondal )

From a review of the literature, it appears that not much works have been done to study the behaviour of neutron slowing down times in multiplying medium. For this reason in this project we wish to study the slowing down times of a neutron pulse in homogeneous multiplying media. The problem has been formulated with the help of the time moments of the neutron distribution using a multi-energy group technique. Using the group constants compiled by Abagyan et al<sup>1)</sup> some results for a homogeneous U<sup>235</sup> water system have been obtained. The results indicate that near criticality the average slowing down times become very large. This is not surprising, since in a nearly critical system it becomes difficult to separate source neutrons from fission neutrons.

Further works are in progress.

1) Abagyan, L.P., Bazasyants, N.O., Bondarenko, I.E., and Nikolaev, M.N., 1964, Group constants for Nuclear Reactor calculations (New York: Consultants Bureau).

2. "Calculation of core parameters for the design of the proposed 1 MW(th) research reactor for Bangladesh Atomic Energy Commission".

(M.A.W. Mondal, S.A.M.M. Siddiqui, Q. Sharfuddin and M.A.Mannan)

Using a two-group diffusion theory model, a preliminary estimate for the neutron flux and critical mass has been obtained. Some calculations for the shielding design have also been done. Further detailed calculations are in progress.

Instituto de Física da Universidade de São Paulo  
Cidade Universitária - Caixa Postal 20516 São Paulo  
Brasil

PROGRESS REPORT ON NUCLEAR DATA IN BRAZIL\*

(June 1974 - May 1975)

Compiled by

S.B.Herdade

Liasion Officer for Brazil, International Nuclear Data  
Committee.

\*Work supported by Comissão Nacional de Energia Nuclear  
and Instituto de Física, Universidade de São Paulo.

## 1. INTRODUCTION

This Progress Report has been written on the basis of:

a) published papers; b) institutes and universities annual reports; c) abstracts of papers presented at the Annual Meeting of the Brazilian Society for the Advancement of Science, Belo Horizonte, July 1975, and d) private communications.

The material has been selected having in mind the eventual interest to nuclear data compilers and evaluators. Although it was tried not to miss any appropriate institution or individual there might have been some oversight.

The information herein contained should not be quoted without author's permission.

## 2. MAIN EXPERIMENTAL FACILITIES FOR NUCLEAR PHYSICS RESEARCH.

For data on type, location, characteristics, and utilization of accelerators and research reactors in Brazil, readers should be referred to the last "Progress Report on Nuclear Data in Brazil (June 1973-May 1974)", IFUSP/P-esp. or INDC(SEC)-422, December 1974.

### Progress report on new facilities :

Variable Energy Cyclotron (Instituto de Engenharia Nuclear - Rio de Janeiro).

Characteristics: Cyclotron Corporation Model CV-28; can deliver over 50 $\mu$ A of external beams of 2 to 24 MeV protons, 3 to 14 MeV deuterons, 5 to 38 MeV  $^3\text{He}^{++}$ , and 6 to 28 MeV  $^4\text{He}^{++}$ . Heavier ions can also be accelerated.

Status: operation has started in October 1974; preliminary experiments on beam alignment and energy calibration have been

carried out with 14 MeV deuteron and 28 MeV alpha particles; some excitation functions of targets of interest for radioisotope production have been measured.

The machine is going to be used for the production of neutron deficient radionuclides for medical uses, activation analysis, nuclear chemistry, radiation damage studies, nuclear reaction studies, and neutron cross-section measurements.

"Pelletron Accelerator" (Instituto de Física-Universidade de São Paulo).

A split-pole high resolution magnetic spectrometer, and a time of-flight fast-neutron spectrometer have been installed in the experimental area in addition to other equipment for nuclear reaction and spectroscopy studies. A Honeywell DDP-516 computer coupled to a IBM/360-44 is being used for automatic data collection and analysis of several experiments .

Beams of  $^{16}\text{O}$  (36-40 MeV)  $^3\text{He}$  (20 MeV), deuterons, and protons have been utilized in nuclear physics, (see itens 6 and 7 of this report).

### 3. NUCLEAR SPECTROSCOPY

#### 3.1 - Shell model calculations of the $^{40}\text{K}$ energy levels.

S.A.S.Vitiello and I.D.Goldman (Instituto de Física - Universidade de São Paulo).

Energies and spins of the odd parity excited states of  $^{40}\text{K}$  have been calculated considering particle-hole configurations and a residual interaction of the type  $V_{12} = V_0 (1 + \chi \sigma_1 \cdot \sigma_2) \cdot \delta(\vec{r}_1 - \vec{r}_2)$  as the one adopted by Szpikowski (Acta Physica Polonica, 25: 169, 1964). The particle-hole interaction has been treated as a perturbation of the central field where the

nucleons move. This perturbation has been assumed to have a very short range and being represented by forces of the type  $\delta(\vec{r}_1 - \vec{r}_2)$ . For proton holes we used successively:

I)  $d_{3/2}$  and  $s_{1/2}$ ; II)  $d_{5/2}$ ,  $s_{1/2}$ , and  $d_{3/2}$ ; and for neutrons:  
I)  $f_{7/2}$  and  $p_{3/2}$ ; II)  $f_{7/2}$ ,  $p_{3/2}$ ,  $f_{5/2}$ , and  $p_{1/2}$ . Harmonic oscillator wave functions have been adopted in the calculations.

### 3.2 - Decay study of $^{178}\text{Ta}$

O.A.M.Helene and I.D.Goldman (Instituto de Física - Universidade de São Paulo).

A line of 216.7 KeV has been observed in the gamma transitions of  $^{178}\text{Hf}$ , formed by the EC decay of  $^{178m}\text{Ta}$  (2.1 h), and has been interpreted as a transition between rotational levels in the  $K = 8^-$  band. This transition would imply the formation of the  $9^-$  state of  $^{178}\text{Hf}$  with an intensity of approximately 0.25%. From the present result and other previous data for other transitions we can determine log ft values for the states  $8^-$  (1148 KeV),  $8^-$  (1480 KeV),  $9^-$ , and  $10^-$ , which are 4.9, 4.9, 7.0, and 7.3, respectively. Of the possible values for the spin and parity of this  $^{178}\text{Ta}$  isomer,  $7^-$ ,  $8^-$  and  $9^-$ , the value  $7^-$  is eliminated because it is incompatible with log ft = 7.0 found for the  $9^-$  state of  $^{178}\text{Hf}$ .  $^{178}\text{Ta}$  has been obtained from the reaction  $^{181}\text{Ta}(\gamma, 3n)$  at the IF-USP LINAC.

### 3.3 - Measurements of mean lives of nuclear excited states and stopping power for heavy ions.

E.P.Madeira, R.V.Ribas, W.M.Roney, W.A.Seale, and T.Polga (Instituto de Física-Universidade de São Paulo).

Measurements of mean lives of nuclear excited states by the plunger method (Phys.Rev. 173:(4), 177,1969), and of stopping power of some materials for heavy ions are being carried out. The

technique employed is the observation of the Doppler shift of the gamma-rays emitted by the recoil nucleus following Coulomb excitation caused by the bombardment with  $^{16}\text{O}$  ions.

3.4 - Decay of an isobaric analog resonance in  $^{123}\text{Sb}$ .

H.Miyake and A.F.R.Toledo Piza (Instituto de Física - Universidade de São Paulo).

The resonance observed at 8.60 MeV in proton inelastic scattering experiments, for  $2^+$  collective excited states in  $^{122}\text{Sn}$ , is usually attributed to the state  $1\ g_{7/2}$ . Comparison of the calculated values for the spectroscopic amplitudes and partial widths for decay with the corresponding experimental values indicates that such resonance is due to the  $2\ f_{7/2}$  state. The Toledo Piza and Kerman formalism is employed and delta, quadrupole-quadrupole and octopole-octopole interaction are included.

3.5 -  $^{90}\text{Zr}$  states detected in the reaction  $^{91}\text{Zn}(d,t)^{90}\text{Zr}$ .

L.C.Gomes, F.C.Sampaio, O.Dietzsch, E.W.Hamburger and G. Rao (Instituto de Física - Universidade de São Paulo).

A  $^{11}\text{Zr}$  (95% enriched) target has been bombarded by a deuteron beam at the University of Pittsburgh tandem accelerator, and the resulting tritons have been detected in nuclear emulsions after energy separation in a magnetic spectrograph. Exposures have been carried out at seven angles with an incident deuteron energy of 16 MeV. Data analysis carried out at the University of São Paulo has lead us to the identification of triton groups corresponding to 16 excited states of  $^{90}\text{Zr}$ : 0.0, 1.761, 2.190, 2.322, 2.750, 3.077, 3.307, 3.846, 4.234, 4.460, 4.699, 4.832, 5.070, 5.080, 5.348, 5.383 MeV.

Due to the long exposure times it was possible to detect weak-

ly excited levels with a reasonable statistics. The DWBA calculations fitted to the angular distribution curves allowed the determination of the spectroscopic factors and of the relative contributions of different orbital angular momenta. In this way it is possible to describe the  $^{91}\text{Zr}$  ground state wave function in terms of the  $^{90}\text{Zr}$  states coupled to the single particle states of the transferred neutron.

### 3.6 - Study of neutron hole states in $^{123}\text{Te}$ .

N.A.G.Fernandes, M.N.Rao and N.Ueta (Instituto de Física - Universidade de São Paulo).

Energy levels of  $^{123}\text{Te}$  have been studied by the  $^{124}\text{Te}(^3\text{He},\alpha)^{123}\text{Te}$  reaction induced by 20 MeV  $^3\text{He}$  particles. The obtained experimental angular distributions have been compared with the ones calculated by DWBA using the DWUCK program. The transferred angular momenta and the spectroscopic factors corresponding to several transitions are determined.

### 3.7 - Multipole admixture $\delta(E2/M1)$ of gamma transition in $^{71}\text{Ga}$ .

R.N.Saxena, A.Bairrio Nuevo Jr (Instituto de Energia Atômica - São Paulo) and F.C.Zawislak (Instituto de Física - Universidade Federal do Rio Grande do Sul).

The directional correlation of  $\gamma$ -transitions in  $^{71}\text{Ga}$  have been measured from the  $\beta$ -decay of  $^{71m}\text{Zn}$  using automated Ge(Li)-NaI(Tl) gamma spectrometer. The spin assignments to the levels at 390 ( $1/2^-$ ), 487 ( $5/2^-$ ), 512 ( $3/2^-$ ) 964 ( $5/2^-$ ), 1107 ( $7/2^-$ ), 1494 ( $9/2^+$ ), and 2247KeV ( $7/2^+$ ) confirm the results of several previous studies on this nucleus. The directional correlation data have been analysed in terms of the multipole mixing ratios  $\delta(E2/M1)$  for several  $\gamma$ -transitions. The results are:  $\delta(121) = -0.2^{+0.3}_{-2.4}$ ,  $\delta(142) = 0.04^{+0.04}$ ,  $\delta(386) = 0.06^{+0.04}$ ,  $\delta(487) = 0.04^{+0.03}$ ,  $\delta(512) = -0.14^{+0.10}$ ,  $\delta(620) = 1.3^{+0.8}_{-0.3}$ ,  $\delta(753) = 0.0^{+0.01}$  and  $\delta(964) =$

$\pm \begin{matrix} 0.9 \\ 0.3 \end{matrix}$ . The experimental results are discussed in terms of various nuclear models which are applicable for the odd-A nuclei in this mass region.

### 3.8 - Multipole admixture $\delta(E2/M1)$ of gamma transition in $^{69}\text{Ga}$ .

R.N.Saxena, A.Bairrio, Nuevo Jr (Instituto de Energia Atômica-São Paulo), F.C.Zawislak (Instituto de Física-Universidade Federal do Rio Grande do Sul) and I.D.Goldman (Instituto de Física-Universidade de São Paulo).

The directional correlation of  $\gamma$ -transitions in  $^{69}\text{Ga}$  have been measured from the decay of  $^{69}\text{Ge}$  using an automated Ge(Li)-NaI(Tl) gamma spectrometer. The measurements have been carried out for the following gamma cascades at 553-318, 787-318, 1206-318, 234-872, 1051-872, 1349-574 and 587-1336 KeV energies. Preliminary analysis of the results confirm  $1/2^-$  spin assignment for the 318 KeV level in  $^{69}\text{Ga}$ . The results are further being analysed in terms of the multipolarities of 234, 1050 and 1349 KeV  $\gamma$ -transitions. In addition the spin assignments to several levels in  $^{69}\text{Ga}$  will be established.

## 4. PHOTONUCLEAR REACTIONS

### 4.1 - The $(\gamma, n)$ reaction in $^{12}\text{C}$ and $^{14}\text{N}$ and $(\gamma, 2n)$ reaction in $^9\text{Be}$ at energies between 0.3 GeV and 1 GeV.

V.di Napoli, M.L.Terranova (Istituto di Chimica Generale ed Inorganica dell'Università, Roma) and H.G. de Carvalho, and J.B.Martins (Centro Brasileiro de Pesquisas Físicas - Rio de Janeiro, Brasil).

Cross sections per equivalent quantum of the reactions  $^{12}\text{C}(\gamma, n)^{11}\text{C}$ ,  $^{14}\text{N}(\gamma, n)^{13}\text{N}$ , and  $^9\text{Be}(\gamma, n)^8\text{Be}$  have been measured in the energy range 0.3 - 1.0 GeV. Average absolute cross-sections

have been calculated of  $(0.90 \pm 0.10)$  mb and  $(0.021 \pm 0.002)$  mb for the  $^{12}\text{C}(\gamma, n)^{11}\text{C}$  and  $^9\text{Be}(\gamma, n)^8\text{Be}$  reactions, respectively, over the whole energy range considered, by means of the photon difference method. As far as the  $^{14}\text{N}(\gamma, n)^{13}\text{N}$  reaction is concerned, the relatively smaller values of the cross sections per equivalent quantum and the larger experimental errors did not allow to calculate any absolute cross section value.

#### 4.2 - $(\gamma, n)$ reactions in complex nuclei at intermediate energies.

V.di Napoli, F.Salvetti, M.L.Terranova (Istituto de Chimica Generale ed Inorganica dell'Universit , Roma) and H.G.de Carvalho, J.B.Martins, O.A.P.Tavares (Centro Brasileiro de Pesquisas F sicas - Rio de Janeiro, Brazil).

The work reports measurements of the cross sections per equivalent quantum of the  $(\gamma, n)$  reaction in  $^{31}\text{P}$ ,  $^{52}\text{Cr}$ ,  $^{55}\text{Mn}$ ,  $^{59}\text{Co}$ ,  $^{75}\text{As}$ ,  $^{127}\text{I}$ , and  $^{197}\text{Au}$  at bremsstrahlung energies ranging between 0.3 GeV and 1.0 GeV. Mean absolute cross sections have been calculated of  $(1.6 \pm 0.1)$  mb,  $(2.5 \pm 0.5)$  mb,  $(3.5 \pm 0.5)$  mb,  $(3.0 \pm 0.5)$  mb,  $(4 \pm 1)$  mb,  $(5 \pm 2)$  mb, and  $(8 \pm 3)$  mb, for the above listed nuclei respectively.

#### 4.3 - On the isomeric-yield ratio of $^{52}\text{Mn}^g$ and $^{52}\text{Mn}^m$ photoproduction from $^{55}\text{Mn}$ at intermediate energies.

V.di Napoli, G.Persichelli, M.L.Terranova (Istituto di Chimica Generale ed Inorganica dell'Universit , Roma) and J.B.Martins (Centro Brasileiro de Pesquisas F sicas Rio de Janeiro).

Photonuclear reactions yielding, as final products, pairs of nuclear isomeric states are very useful in estimating the relative probabilities of producing each isomer. The knowledge of the

isomeric-yield ratios can provide information about the spin dependence of the nuclear-level density in the nucleus under investigation and the mechanism of the reaction. We have carried out yield measurements of the photoproduction of  $^{52}_{\text{Mn}}^{\text{g}}$  and  $^{52}_{\text{Mn}}^{\text{m}}$  from  $^{55}_{\text{Mn}}$  at bremsstrahlung energies from 0,3 GeV to 1,0 GeV. Previous results for rhodium isotopes are also discussed.

#### 4.4 - On the yield ratio of $^{164}\text{Ho}$ isomeric states.

V.R.Vanin and I.D.Goldman (Instituto de Física - Universidade de São Paulo).

Holmium oxide targets have been irradiated by the bremsstrahlung beam of the IF/USP LINAC with energies between 14 and 28 MeV. The isomeric yield ratio has been measured by the residual activity in the samples with a Ge-Li detector. The yield ratio of the  $6^-$  state is approximately constant and equal to 0.25 in the above mentioned energy range. This result is compatible with the predictions based on the statistical model.

#### 4.5 - Isomeric yield ratios of $^{87}\text{Y}$ and $^{86}\text{Y}$ by $(\gamma, xn)$ reactions as a function of energy.

C.M.Faria (Faculdade de Filosofia, Ciências e Letras de Rio Claro, S.Paulo) and I.D.Goldman (Instituto de Física Universidade de São Paulo).

Yttrium oxide targets have been irradiated by a bremsstrahlung beam (tantalum radiator) of the IF/USP LINAC, in the energy range 32-45 MeV. The residual activities of  $^{87}\text{Y}$  corresponding to the metaestable state  $9/2^+$  (14h) and ground state  $1/2^-$  (80h) have been determined by means of the 381 KeV and 483 KeV transitions, respectively. For  $^{86}\text{Y}$  the 208 KeV and 1078 KeV lines have been observed for the metaestable state  $8^+$  (48 min) and ground state  $4^-$  (14.6 h), respectively. An increase of the yield ratio as a function of

energy have been observed in both cases: from 0.28 (32 MeV) to 0.42 (45 MeV) for  $^{87}\text{Y}$ , and from 0.012 (36 MeV) to 0.017 (45 MeV) for  $^{86}\text{Y}$ .

4.6 - Study of the  $^{55}\text{Mn}(\gamma, 3n)^{52g}\text{Mn}$  reaction up to 46 MeV.

M.Nielsen and I.D.Goldman (Instituto de Física - Universidade de São Paulo).

Mettalic manganese has been irradiated with the bremsstrahlung beam of the IF/USP LINAC, in the energy range 32-46 MeV. The yield of  $^{54}\text{Mn}$  and  $^{52g}\text{Mn}$  for, the reactions  $^{55}\text{Mn}(\gamma, n)$  and  $^{55}\text{Mn}(\gamma, 3n)$ , respectively, have been determined by the residual activities in the samples. The activities have been measured by a Ge-Li detector (3 KeV resolution for the  $^{60}\text{Co}$  1332 KeV line) following the 835 KeV transition ( $T = 314$  days) of  $^{54}\text{Mn}$ , and the 744, 935, and 1434 KeV transitions of  $^{52}\text{Mn}$  ( $T = 5,7$  days). The yield ratio, of  $^{52g}\text{Mn}$  relatives to  $^{54}\text{Mn}$  has been found to be  $1.4 \times 10^{-3}$  at 46 MeV.

4.7 - Study of the isomeric yield ratio of  $^{117}\text{In}$  by the photo-alpha reaction in antimony.

E.A.Finotti and I.D.Goldman (Instituto de Física - Universidade de São Paulo).

The reaction  $^{121}\text{Sb}(\gamma, \alpha)^{117g}\text{In}$ ,  $^{117m}\text{In}$  has been studied experimentally by observing the lines 552.9 KeV ( $T_{1/2} = 44$  min) from  $^{117g}\text{In}$ , and 315 KeV ( $T_{1/2} = 117$  min) from  $^{117m}\text{In}$ , with a Ge-Li detector. To avoid the interference of the 564 KeV transition from  $^{122}\text{Sb}$  produced by neutron capture in the target, indium has been chemically separated from the antimony sample. The isomeric yield ratio obtained was 0.8 at a bremsstrahlung energy of 35 MeV.

4.8 - Measurements of the differential gamma-ray scattering cross sections in platinum, tungsten, and silver.

P.Pitanga, S.de Barros (Instituto de Física - Universidade Federal do Rio de Janeiro) and R.Moreira (Instituto de Física - Universidade de São Paulo).

Measurements of the elastic scattering cross sections of 412 KeV gamma rays in platinum, tungsten, and silver has been carried out at angles of 40°, 60°, 90°, and 120°. The scattered radiation has been detected by a 22 cm<sup>3</sup> Ge-Li detector with 2.5 KeV resolution, which allowed a good separation between the elastic and inelastic scattering. The experimental results in this energy, where Rayleigh and Thomson amplitudes are dominant, are compared with theoretical calculation on the basis of the form factor method.

4.9 - Electric quadrupole resonances

E.Woly nec and C.A.Botelho (Instituto de Física - Universidade de São Paulo).

Quadrupole resonances have been studied by many researchers that have utilized (e,e'x) reactions at certain scattering angles in order to enhance electricquadrupole interaction relative to electric dipole. These studies have the disadvantage of using a phenomenological analysis for the form factor, which does not discriminate between E2 and E0, that have the same angular dependence, or the assumption of a nuclear model, in order to obtain the differential cross sections. We have performed computer simulation of yield measurements of the electrodisintegration of nuclei, suposing the existence of quadrupole components in the photoabsorption, and we have shown that the electrodisintegration yield is very sensitive to quadrupole transitions. It is possible

to obtain the quadrupole resonance cross-sections by analysing the electrodisintegration yield measurements on the basis of the virtual photon formalism, taking into account the Coulomb distortion in the calculation. This method has the advantage of being model independent, depending only on the validity of quantum electrodynamics.

#### 4.10 - Spin 0 and 1 effects in deep inelastic electron-proton scattering.

A.Knoth (Instituto de Física - Universidade Federal do Rio de Janeiro)

Recent experimental measurements of the R ratio for deep inelastic electron-proton scattering, where  $R = \frac{\sigma(\text{longitudinal})}{\sigma(\text{transverse})}$  and the  $\sigma$ 's represent the virtual photon cross section, have shown a quite rapid increase in R for small values of the variables  $x$  ( $x < 0.2$ ). Generally, parton models for this case have been constructed using only spin 1/2 parton. We will attempt to demonstrate how the spin 0 and 1 effects can be explained while still preserving a strictly spin 1/2 parton model. Also, why do these effects only seem to appear at small  $x$  and not large  $x$ .

#### 4.11 - Influence of Coulomb distortion in the virtual photon spectrum.

I.C.Nascimento and E.Wolyneć (Instituto de Física - Universidade de São Paulo), and D.S.Onley (Ohio University, Athens, Ohio - U.S.A).

Measurements of the ratio  $\sigma^-/\sigma^+$  between the nuclear excitation cross-sections for electrons and positrons, published in the literature, are compared with calculated ratios using photon spectra determined in DWBA. The behaviour of this ratio as a function of target atomic number  $Z$  and incident electron energy  $E_0$

is shown to be mainly due to Coulomb distortion. These curves do not present structures corresponding to resonances in the photo-absorption cross-section, but they are very sensitive to the presence of quadrupole absorption.

#### 4.12 - Influence of Coulomb distortion in the bremsstrahlung spectrum.

A.N.Fagundes, B.S.Bhandari and I.C.Nascimento (Instituto de Física - Universidade de São Paulo).

The bremsstrahlung spectrum, calculated in first order Born approximation is largely utilized in the study of photonuclear reactions. Nevertheless, in a recent paper Gargaro and Onley indicate that effects of Coulomb distortion may be very significant, specially in heavy nuclei. Measurements of the bremsstrahlung spectrum have not been performed in the giant resonance region, so that the precision of the formulas utilized are not known. In the present experiment the electron beam of the IF/USP LINAC has been used to bombard several different radiators with increasing atomic number  $Z$ , at the energy of 25 MeV, producing bremsstrahlung, that was detected by the activation of copper foils. Taking  $^{12}\text{C}$  as a standard radiator for normalization purposes, the relative yields due to different radiators are compared with calculations using conventional formulas in order to have an idea of the importance of the Coulomb distortion.

### 5. FISSION AND NUCLEAR MODELS

#### 5.1 - Present status of photofission of actinides near threshold.

B.S.Bhandari and I.C.Nascimento (Instituto de Física Universidade de São Paulo).

The phenomenon of photofission near threshold has received se

rious attention in the last few years due to its relative importance in studying the shape of the recently suggested "double humped fission barrier" and also mainly because of better gamma ray facilities becoming available at several laboratories. Measurements of photofission cross sections and of the angular distribution of fission fragments permit the determination of the relative contributions of the various fission channels at different excitation energies.

Presently available data on photofission cross sections, photo neutron cross section and on angular distribution of photofission fragments of actinides have been reviewed and some suggestions for additional studies have been made with the aim towards a better understanding of "threshold fission" phenomena in the framework of a double humped barrier in fission.

#### 5.2 - Photofission of $^{238}\text{U}$ below threshold

B.S.Bhandari (Instituto de Física - Universidade de São Paulo) and D.S.Onley (Ohio University, Athens, Ohio, USA)

Photofission cross-sections of  $^{238}\text{U}$  below threshold have been calculated using a double humped potential barrier parameterized by smoothly joining four parabolas and a Coulomb potential at and beyond the scission point. The primary potential well is made arbitrarily wide in order to reproduce a density of states comparable with that known to exist in the compound nucleus and which manifests itself as fine structure on the transmission resonances. A "spreading width" method is introduced by taking an average over this fine structure which results in a broadening of the transmission coefficient peaks. Relative strength in the fission channel has been calculated and an attempt has been made to reconcile the apparent resonance structures observed recently in photofission experiments and the isomeric and ground state spontaneous

fission halflives in terms of a single suitable set of parameters of a double humped barrier for  $^{238}\text{U}$ . In addition to reproducing satisfactorily the observed resonance structure near threshold the calculation also predicts several low energy resonances in the cross-sections.

5.3 - Quadrupole component in the  $^{238}\text{U}$  photofission at low energies.

J.D.T.Arruda Neto, S.B.Herdade, B.S.Bhandari and I.C. Nascimento (Instituto de Física - Universidade de São Paulo).

All nuclei exhibit a resonance in the photonuclear reaction cross section attributed to the E1 excitation mode. Recently, Bohr and Mottelson have made theoretical predictions of a E2 collective excitation occurring at  $58A^{-1/3}$  ( $A =$  mass number). Several angular distribution experiments have evidenced the occurrence of a E2 excitation, but with a very low intensity relative to the E1 excitation, making difficult its detection. In the present work we have developed a method to obtain the quadrupole photofission cross section from the total electrofission and photofission yields, and the virtual photon spectrum calculated in DWBA on the basis of the Gargaro and Onley formalism. The sensitivity of this method is due to the fact that the ratio of the yields for E2 and E1 is much greater in electrofission than in photofission. A preliminary analysis of our data have shown the existence of a quadrupole resonance at about 9 MeV, which is consistent to the value predicted by Bohr and Mottelson (9.4 MeV).

5.4 - Electron induced fission fragment angular distribution of  $^{238}\text{U}$ .

J.H.Vuolo, S.B.Herdade, B.S.Bhandari and I.C.Nascimento (Instituto de Física - Universidade de São Paulo).

The angular distributions of the fragments in the electro-fission of  $^{238}\text{U}$  have been measured in the energy range 5.78 - 14.38 MeV. The electron beam of the Universidade of São Paulo LINAC was used to irradiate a thin uranium target and the fragments were detected using makrofol. For the data analysis, theoretical angular distributions of fragments in the electron induced fission of an even-even nucleus have been calculated in terms of the usual rotation matrices and the virtual photon spectrum has been taken from the DWBA formalism given by Gargaro and Onley. Since the virtual photons are not transverse waves, they don't contain the different multipole components in equal amounts. In particular we hope to use the much stronger quadrupole intensity in virtual photon spectrum to analyse quadrupole components in the nuclear spectrum in more detail than is possible with real photons alone.

5.5 - Measurement of the delayed neutrons in the photofission of  $^{238}\text{U}$  and  $^{232}\text{Th}$ .

Y.Miyao, M.N.Martins, O.D.Gonçalves, L.M.Lunardi, S. de Barros, and G. Moscati (Instituto de Física - Universidade de São Paulo).

Pellets of  $\text{U}_3\text{O}_8$  and  $\text{ThO}_2$ , with thickness 1 to 3  $\text{g}/\text{cm}^2$ , have been irradiated with bremsstrahlung at the University of São Paulo LINAC in the energy range 12 to 30 MeV. The counting system was formed by a multichannel analyser operated in the multiscaler mode, which accumulated the neutron counts and the electron beam charge measured by a secondary emission monitor. The neutrons have been detected by BF3 counters immersed in a paraffin moderator. The data have been analysed by decomposing the decay curves in components of fixed half-lives, corresponding to the yields of

precursor groups. The analysis of the results shows that the yields of the different groups do not vary with energy, which limits the possible precursors to the peak regions in the fission fragment mass distribution curve.

5.6 Penetrability through a three humped barrier in quasi-classical approximation.

B.S.Bhandari (Instituto de Física -Universidade de São Paulo).

A three humped barrier has been parameterized by smoothly joining five parabolic potentials. Expression for the penetrability through such a barrier has been obtained in quasi-classical approximation and the behaviour of penetrability versus energy has been studied. In the light of recently suggested evidence for a third minimum in the potential energy surface of thorium isotopes, a plausible explanation of their sub-barrier fission characteristics is given in terms of a three humped barrier.

5.7 - Calculation of the penetrability through a two-dimensional fission barrier in the scattering formalism.

T.Kodama and R.A.M.S.Nazareth (Centro Brasileiro de Pesquisas Físicas - Rio de Janeiro).

The complete understanding of the fission process requires a dynamical description of the system. Due to the difficulty to describe the dynamics as a multidimensional process, several authors solved the problem for the unidimensional case. More recently, Hofmann introduced a two dimensional treatment. The objective of this work is to determine the penetrability for a certain fission barrier using the method proposed by Hofmann and to compare the result with the existing experimental values. In this method a bidimensional collective Hamiltonian is constructed in

which one of the coordinates (the fission coordinate) defines the fission path and the other is represented by harmonic oscillations transverse to the fission path. The frequencies of the transverse harmonic oscillations are responsible by the coupling between the two degrees of freedom of the problem and so contributing to the evaluation of the fission barrier. In our preliminary work it has been introduced a correct path for fission through the simple potential barrier given by Brack. The inertia coefficients related to the two degrees of freedom, given by Hasse, are also used.

5.8 - Exact calculation of the penetrability through a barrier for fission of heavy ions in a simple two-dimensional case.

T.Kodama (Centro Brasileiro de Pesquisas Físicas - Rio de Janeiro), R.A.M.S.Nazareth (Instituto de Física - Universidade Federal do Rio de Janeiro), and J.R.Nix (Los Alamos Scientific Laboratory - USA).

In the study of the effect of zero-point quantum oscillations of nuclei in their fusion cross-sections at low energies, we have calculated exactly the penetrability through a simple two-dimensional barrier  $V(x,y)$ . The coordinate  $x$  is related to the distance between the centers of mass of the two nuclei and  $y$  is related to the sum of their deformations along a common symmetry axis. The parabolic potential in  $x$  is one of the two harmonic oscillators in  $y$ , depending of the value of  $x$  relative to a critical value  $x_1$ . Both oscillations differ by the positions of their minima and by their curvatures. This simulates the dominant characteristics in the two dimensional surface energy potential with two aligned valleys (the fission and fusion valleys) sepa-

rated by a hump between them. When an incident wave which is located in the fusion valley reaches the potential barrier, it is partially transmitted and partially reflected in waves that correspond to different excited states in the transverse direction and to different energy increments in the direction of fusion. The amplitude of these waves are determined by imposing the condition of continuity to the wave functions (exactly expressed in terms of cylindrical-parabolic functions) and to their derivatives in  $x_1$ . The penetrability is then obtained from the amplitudes of the transmitted waves. The presence of the hump and of the fusion valley increases the penetrability for all incident energies, but the relative increment is bigger for low energies. The penetrability is found to vary less with energy than the one calculated for the same one-dimensional barrier. This effect explain part of the anomaly that appears among the experimental values of the curvature parameter  $n_x$  obtained by analysing the low energy fusion penetrability in terms of a one-dimensional barrier and the calculated values. The experimental values are substantially smaller than the calculated ones.

5.9 - Non-lanthanide fragment yields in  $^{238}\text{U}$  fission induced by 14 MeV neutrons.

A.V.Bellido and G.M.de Macedo Grassi (Instituto de Engenharia Nuclear, and COPPE- Universidade Federal do Rio de Janeiro).

$^{238}\text{U}$  has been irradiated by 14 MeV neutrons, and from a nitric solution of the target, the lanthanides have been separated by precipitation with HF and the non fissioned uranium by extraction with TBP. The resulting solution has been analysed with a high resolution Ge<sub>Li</sub> detector. Relative yields have been obtained of mass chains 91,92,93,101,104,105,107,128,129,131,132,133,134,135,

141 and 142, and converted to absolute yields by normalization with mass yields already published in the literature.

5.10 - The Wigner and higher order terms in the droplet mass formula.

T.Kodama (Centro Brasileiro de Pesquisas Físicas - Rio de Janeiro) and K.Takahashi (University of Köln, Germany).

The mass formula of the droplet model proposed by Myers and Swiatecki is a generalization of the one obtained from the liquid drop model, in which the concept of density distribution of the nucleons is taken into account explicitly. Several authors have obtained the droplet parameters and the resulting formulas are satisfactory at least for the masses in the ground state. Nevertheless, the experimental data are available only in a very narrow band of the N-Z plane and, besides this, perturbed by even-odd and shell effects. This makes the least square fit of the parameters very unstable. The so called Wigner terms and the high order ones are particularly very difficult to determine. These terms are carefully investigated in the present work. There are some indications that the coefficient for the higher order symmetry is much bigger than the values previously assumed.

5.11 - Monopole and dipole resonances and the droplet model mass formula.

T.Kodama (Centro Brasileiro de Pesquisas Físicas - Rio de Janeiro) and E.R.Hill (Th, Darmstadt, Germany)

By calculating the change in potential energy in the droplet formula due to the change in the density distribution parameters, we can investigate the giant resonance phenomenon more satisfactorily than by the utilization of the usual mass formula.

The kinetic energy for the droplet parameter can be also calculated. The resonance energy is obtained by diagonalising the total hamiltonian with respect to these parameters. Comparison with the experimental value gives information about the droplet parameters which cannot be obtained from the nuclear masses in the ground state. It is also discussed the pulsing mode of the nucleus in this model.

## 6. LIGHT AND HEAVY ION REACTIONS

### 6.1 - Distortion effects in (p,2p) quasi-free scattering

P.M.Mors (Instituto de Física - Universidade do Rio Grande do Sul).

Results of (p,2p) experiments have been presented, in general, in the form of energy spectrum and angular correlation curves. In this work, the presentation of part of these results in the form of momentum distribution contour diagrams in momenta space, as suggested by Jacob and Maris, has been investigated. The contour diagrams drawn from a theoretical calculation for the  $^{16}\text{O}$  (p,2p)  $^{15}\text{N}$  reaction, for the 1s and 1p states, at bombarding energies 200 MeV and 378 MeV, are very sensitive to the distortion caused by the optical potential on the incident and emergent protons, presenting deformations and dislocations, as compared to the circular forms centered in the origin that they should have without distortion. The dislocation and deformation of each diagram are attributed, respectively, to the real and imaginary parts of the optical potential that actuates on the protons involved in the reaction.

### 6.2 - On the inversion of the potential scattering problem on the basis of the harmonic oscillator.

A.F.R. de Toledo Piza and M.M.Watanabe (Instituto de

Física - Universidade de São Paulo).

The representation of a nucleon-nucleon potential on the basis of the harmonic oscillators from scattering (phase shifts) informations only, following the procedure utilized by the University of Sussex group (Elliott et al, Nucl.Phys. A121: 241,1968) is analysed for the case of phase shifts produced by known potentials. The adequacy of the method is proved for regular potentials. Nevertheless, the introduction of repulsive cores leads to serious problems in the interpretation of the results in the procedure suggest in Sussex. The effects of possible contributions outside the energy surface are studied through the potential short range unitarian transformations, that maintain the phase shifts invariant.

6.3 - Study of the reaction  ${}^7\text{Li}(p,n){}^7\text{Be}$  with a time-of-flight system.

W.R.Wylie, E.W.Cybulska, R.A.Douglas, and E.F.Pessoa  
(Instituto de Física - Universidade de São Paulo).

A three-stage beam pulsing system has been designed and build at the University of São Paulo Pelletron accelerator. The obtained pulse width was less than 2nsec, and the compression factor more than 10. Neutron angular distributions for the reaction  ${}^7\text{Li}(p,n){}^7\text{Be}$ , with 8.5 MeV incident protons, have been measured.

6.4 - Study of the  ${}^{91}\text{Zr}(d,p){}^{92}\text{Zr}$  reactions.

T.Borello-Lewin, L.B.Horodynski Matsushigue, C.M. Oliv  
van, and F.Sampaio (Instituto de Física - Universida-  
de de São Paulo)

The study of the  ${}^{91}\text{Zr}(d,p){}^{92}\text{Zr}$  reaction relates to a program for obtaining detailed experimental informations on nuclei with number of protons or neutrons near closed shells (Rev.Bras.

Fis., 2:157,1972). A self-sustained target, enriched to 89% in  $^{91}\text{Zr}$ , of  $540 \mu\text{g}/\text{cm}^2$  thickness, has been bombarded by 12 MeV deuterons at the University of Pittsburg tandem. The resulting protons have been analysed by a magnetic spectrograph and detected in nuclear emulsions, located at 9 scattering angles, between  $8^\circ$  and  $55^\circ$ , with a resolution of 12 KeV. The decomposition of the experimental angular distributions in contributions corresponding to the compatible angular momenta will be made using DWBA calculations and least square fits. It is expected that that the results will contribute to the description of collective aspects of the even nucleus  $^{92}\text{Zr}$ .

6.5 - Collective model analysis of deuteron inelastic scattering in  $^{91}\text{Zr}$ .

L.B.Horodynski-Matsushigue, T.Borello-Lewin, O.Dietzsch, E.Hamburger and H.Miyake (Instituto de Física-Universidade de São Paulo).

Nuclear emulsions plates have been exposed in the University of Pittsburg tandem magnetic spectrometer for the study of the  $^{91}\text{Zr}(d,d')$  reaction, as part of a program on detailed spectroscopic studies of nuclei near magic numbers. About 50 levels have been detected and 27 angular distributions obtained. These distributions may be classified by a visual analysis, in three main groups. The situation of  $^{91}\text{Zr}$ , with only one neutron besides the magic nucleus  $^{90}\text{Zr}$ , is adequate to the de-Shalit simple model, which consider the coupling of each collective state of the even nucleus with the extra particle. The description of the excitation process of these even nucleus levels is usually made within the DWBA formalism. Extensive calculation have been carried out with the DWUCK program, and macroscopic interaction (R.H.Bassel

et al, Phys.Rev. 128: 2693,1962). The inclusion of the imaginary part in the interaction has a pronounced effect on the angular distributions. For deuterons of 17 MeV incident energy, consideration of Coulomb excitation was important, specially for low multipolarity states. These calculations have shown that the three above mentioned groups correspond to transferred angular momenta  $L = 2, 3, \text{ and } 5$ , in accordance with the more strongly excited states in the neighbour nuclei  $^{90}\text{Zr}$  and  $^{92}\text{Zr}$ . The obtained average deformation parameter  $\beta_L$  are, for the case of  $L=2$ , closer to the values for  $^{92}\text{Zr}$ . We are engaged in a more fundamental description of the  $^{91}\text{Zr}$  levels, using the BCS + RPA approximations for describing the even nucleus states and constructing the odd nucleus states assuming contributions of more than one configuration.

#### 6.6 - Relative Q-values for (d,t) reactions in Zr stable isotopes.

L.C.Gomes and O.Dietzsch (Instituto de Física - Universidade de São Paulo).

Relative Q-values for (d,t) reactions induced in zirconium isotopes ( $A=90,91,92,94, \text{ and } 96$ ) have been determined by a simultaneous observation of triton groups corresponding to transitions to the ground states. The target contained all the mentioned isotopes, and the tritons have been detected by nuclear emulsion plates located in the focal plane of the University of Pittsburg magnetic spectrometer. The Q-values have been normalized, for the one of  $^{92}\text{Zr}$  obtained from the mass excess table of Wapstra and Gove (Nuclear Data, A9:303,1971). The Q(d,t) results obtained in this experiment for the mass 90 and 91 isotopes are in good agreement with the ones of the above mentioned table. Nevertheless,

our results indicate discrepancies in the  $Q(d,t)$  values of the mass 94 and 96 Zr isotopes (27,5 KeV and 22,1 KeV, respectively) and, therefore, a disagreement in the masses of the isotopes 93 and/or 94, and 95 and/or 96.

6.7 - Inelastic scattering of  $^3\text{He}$  and  $\alpha$  in  $^{124}\text{Sn}$  and  $^{124}\text{Te}$

C.A.Appoloni, S.Salém, M.N.Rao, and N.Ueta (Instituto de Física -Universidade de São Paulo).

Angular distributions have been determined for the elastic and inelastic scattering of alpha and  $^3\text{He}$  particles, of approximately 20 MeV, in  $^{124}\text{Sn}$  and  $^{124}\text{Te}$  targets. The inelastic scattering angular distributions corresponding to one phonon ( $2^+$  and  $3^-$ ) levels have been analysed by DWBA, using the optical parameters obtained in the analysis of the elastic scattering. Results of this analysis and the deformation parameters of  $^{124}\text{Sn}$  and  $^{124}\text{Te}$  are presented.

6.8 - Optical model parameters for  $^3\text{He}$  and alpha particle beams in  $Z \approx 50$  nuclei.

A.T.M.Mendes, N.Ueta and M.N.Rao (Instituto de Física Universidade de São Paulo)

Angular distributions have been measured for the elastic scattering of  $^3\text{He}$  and alpha particles in  $^{124}\text{Sn}$ ,  $^{124}\text{Te}$  and  $^{123}\text{Sb}$  targets, in energies of approximately 20 MeV. The experimental results have been analysed in order to determine optical model parameters. These parameters will be utilized in DWBA analysis of transfer reactions induced by alpha and  $^3\text{He}$  particles.

6.9 - Study of one proton transfer reactions in tellurium isotopes.

A.S.Toledo, M.N.Rao, N.Ueta and O.Sala (Instituto de Física - Universidade de São Paulo)

Levels of  $^{125}\text{I}$  have been studied by the reaction  $^{124}\text{Te} (^3\text{He}, d)^{125}\text{I}$  with an incident energy of 19,5 MeV. The deuteron angular distributions have been measured by utilizing surface barrier telescopes and particle analog identification. The transferred angular momenta ( $l_p$ ) and the spectroscopic factors for several transitions have been obtained by DWBA calculations. The studies will be extended to the reactions  $(^3\text{He}, d)$  and  $(\alpha, t)$  in  $^{122}\text{Te}$  and  $^{124}\text{Te}$ .

6.10 - Preliminary results for reactions induced by  $^{16}\text{O}$  in  $^{27}\text{Al}$ .

J.C.Acquadro, D.Pereira, O.Sala, and N.D.Vieira Jr  
(Instituto de Física - Universidade de São Paulo).

Reactions induced by  $^{16}\text{O}$  in  $^{27}\text{Al}$  are studied by identifying the resulting particles with a proportional counter coupled to a semiconductor detector. Preliminary results indicate the possibility of determining cross sections for the transfer of a few particles, as well as for the formation of a compound nucleus or partial fusion.

6.11 - Study of the reaction  $^{10}\text{B} (^{16}\text{O}, \alpha)^{22}\text{Na}$

J.Hirata, M.J.Bechara, T.Borello-Lewin, E.R.Cruz,  
L.C.Gomes, A.I.Hamburger, L.B.Horodyski-Matsushige,  
K.Koide, F.Sampaio, E.M.Takagui, N.Marquardt,  
and O.Dietzsch (Instituto de Física - Universidade de São Paulo).

Excitation functions of several  $\alpha$  particle groups, corresponding to low excitation levels of  $^{22}\text{Na}$ , populated in the interaction  $^{10}\text{B} + ^{16}\text{O}$ , have been determined at  $\theta_{\text{LAB}} = 0^\circ$ , in steps of 250 KeV, in the bombarding energy range 36.0 - 39.5 MeV. A surface barrier semiconductor detector, protected by Ni and Al

foils with thickness sufficient to stop the incident  $^{16}\text{O}$  beam and other heavy ions, has been used to detect the alpha particles. The  $^{16}\text{O}$  beam has been produced in the University of São Paulo Pelletron accelerator. Any structure has been observed corresponding to the states 0.58 and 1.9 MeV in  $^{22}\text{Na}$ , contrarily to the observations of other authors in the energy range 40-46 MeV (Campo et al, Phys.Rev.C, 9:1258,1974). However, our results suggests structures of 400 KeV width at  $E_{\text{LAB}} =$  MeV for the transition corresponding to the ground state and at  $E_{\text{LAB}} = 37$  MeV for the state of  $E_x = 1.53$  MeV.

6.12 - Threshold energies for  $D(^{16}\text{O},n)^{17}\text{F}$  reactions

V.H.Rotberg (Instituto de Física - Universidade de São Paulo).

Threshold energies for  $D(^{16}\text{O},n)^{17}\text{F}$  reactions, in the charge states  $4^+$  and  $3^+$  of the  $^{16}\text{O}$  ion, have been utilized for the energy calibration of the University of São Paulo Pelletron accelerator. The neutrons have been detected by a long counter and the threshold energies utilized to determine the calibration constant of the 90° analysing magnet coupled to the accelerator. These energies have been re-calculated in the present work and the results presented discrepancies when compared to the values adopted in other laboratories as calibration references. These discrepancies are due to approximations that are usually valid for kinematic calculations of endoergic reactions induced by light particles in heavier targets, but that are not applied to the present situation.

6.13 - Excitation of  $^{24}\text{Mg}$  by the interaction  $^{10}\text{B} + ^{14}\text{N}$

K.Koide, A.Ceballos, N.Marquardt, and O.Dietzsch  
(Instituto de Física - Universidade de São Paulo).

Excitations curves have been determined by the reaction  $^{10}\text{B}(^{14}\text{N},\alpha)^{20}\text{Ne}$  at  $\theta_{\text{LAB}} = 0^\circ$ , and for the reaction  $^{10}\text{B}(^{14}\text{N},p)^{23}\text{Na}$  at  $\theta_{\text{LAB}} = 165^\circ$ , in the bombarding energy range 9,5 to 13 MeV. The experimental data have been obtained in the Laboratory of Nuclear Physics of the University of Montreal by utilizing a high intensity ion beam at a tandem Van de Graaff. In both reactions no evidence has been found for the strong resonance (corresponding to a excitation energy of 33.2 MeV in  $^{24}\text{Mg}$ ) observed by other authors in the interaction  $^{12}\text{C} + ^{12}\text{C}$ . Our data gives a direct evidence that the formation of this resonant state in  $^{24}\text{Mg}$  depends strongly on the entrance channel.

## 7. NEUTRON PHYSICS

### 7.1 - Slow Neutron Cross Section of Deoxyribonucleic Acid, ex-Thymus.

R.Fulfaro, V.S.Walder, L.A.Vinhas and L.Q.Amaral\*  
(Instituto de Energia Atômica - São Paulo).

In order to study the dynamics of water in biological molecules and the freedom of motion of the hydrogen atoms, the neutron transmission through a DNA sample was measured in the neutron wave-length interval 4.0 to 6.5 Å using a crystal spectrometer. The knowledgement of the bounding state of the water present in DNA is very useful to study the structures and the function of biological macromolecules. NMR studies suggest some from of ice-like coordination for  $\text{H}_2\text{O}$  in biological molecules, where as results obtained from neutron inelastic scattering in polyglutamic acid suggest a behaviour similar to liquid water. In the present work, measurements were performed at room temperature for a dry sample and for a wet sample with 7.8% moisture. The total cross sections,  $\sigma$ , and the scattering cross sections per hydro-

\* Presently at the Instituto de Física-Universidade de São Paulo

gen atom,  $\sigma_{S/H}$ , were determined in each case, thus obtaining the cross section of  $H_2O$  present in DNA. This cross section shows that the water in DNA presents a behaviour similar to that of liquid water. By analysing the  $\sigma_{S/H}$  curve for dry DNA it is observed that the hydrogen atoms have not much freedom of motion in this biological molecule. Also, the cold neutron inelastic scattering for DNA samples were measured; the results are being analysed.

### 7.2 - Liquid-Solid Transition in Cyclohexanol by Neutron Transmission.

R.Fulfaro and L.A.Vinhas (Instituto de Energia Atômica -São Paulo).

The total cross section of the cyclohexanol was measured for  $6.13\text{\AA}$  wavelength neutrons, varying the sample temperature in a range that includes the melting point. From these experimental results and by comparison with theoretical calculations it was possible to obtain the Debye temperatures for both states. These temperatures were used to calculate the disorder entropy variation near the fusion point.

### 7.3 - Multiple Neutron Diffraction Experiment with Temperature Variation.

C.B.R.Parente and R.S.da Costa

Multiple neutron diffraction patterns have been obtained with an aluminum single crystal at different temperatures. For a temperature change of  $70^\circ\text{C}$  the patterns show a distinct variation in the angular position of the peaks ranging from about  $0.02^\circ$  to  $0.2^\circ$ . To perform the experiment so that it could be used for the determination of the cell parameter in each temperature, a careful crystal mounting and alignment were done. The mechanical precision of all movable parts of the  $2\theta$  and  $\theta$  axes of the neu-

tron diffractometer allows an angular positioning with an error within 0.01°. The goniometer used to set the scattering vector of the primary reflection along the proper direction as well as to turn the crystal around it has an angular precision of the same order. The counting time was 6 minutes which gave an statistical fluctuation of the order 0.5% and the angular steps were taken as 0.05° for narrow peaks and 0.10 for the broad peaks. The cell parameter values determined by the angular positions of the peaks presented calculated errors of the order of  $3 \times 10^{-3} \text{ \AA}$ .

#### 7.4 - Hydrogen Concentration Determined by the Neutron Transmission Method.

L.A.Vinhas, R.Fulfaro, V.S.Walder and C.B.R.Parente.

It has been developed the techniques for determining the hydrogen content of hydrogenous compounds by neutron transmission. The method is based in the large slow neutron scattering cross section of hydrogen compared to carbon and other elements. Using the crystal spectrometer of IEA, selecting neutrons of energy 0.145 eV, the experimental transmission of 14 standard compounds have been measured. The precision and accuracy of the method were studied.

#### 7.5 - Measurement of the relative cross-section for the reaction $^{103}\text{Rh}(n,n')^{103m}\text{Rh}$ by activation.

S.B.Herdade, E.W.Cybulska, R.A.Douglas, E.F.Pessoa, and W.R.Wylie (Instituto de Física - Universidade de São Paulo)

Following the recommendation contained in INDC(NDS) - 47/L (1972), the relative cross-section for the reaction  $^{103}\text{Rh}(n,n')$   $^{103}\text{Rh}$  has been measured in the energy range 4.0 - 8.0 MeV. The reaction  $^7\text{Li}(p,n)^7\text{Be}$  produced at the University of São Paulo Pel-

letron accelerator has been utilized as neutron source. The neutron spectra of this reaction, for 8,5 MeV incident protons, has been determined at several angles by the time-of-flight method. The activation of the rhodium foils has been detected by means of the X-rays following internal conversion of the 40 KeV transition, with a NaI(Tl) detector through a thin Be window. Preliminary results are in agreement with previous measurements by Santry and Buttler (Can.J.Phys. 52:1421,1974).

---

Addresses of Institutions mentioned in this Progress Report

Instituto de Física - Universidade de São Paulo  
Caixa Postal 20516 - São Paulo, S.P.-Brasil

Instituto de Energia Atômica  
Caixa Postal 11049 - Pinheiros  
São Paulo, S.P.-Brasil

Centro Brasileiro de Pesquisas Físicas  
Av. Wenceslau Bráz, 71  
Rio de Janeiro - RJ, Brasil

Instituto de Engenharia Nuclear  
Caixa Postal 2186 - ZC-00  
20000 Rio de Janeiro-RJ- Brasil

Instituto de Física  
Universidade Federal do Rio Grande do Sul  
Av. Luiz Englert s/n  
90000 Porto Alegre- R.S.- Brasil



Progress Report  
on Nuclear Data Activities in Bulgaria  
1974 - June 1975

Compiled by E.Nadjakov  
Liaison Officer to the INDC for Bulgaria  
Institute of Nuclear Research and Nuclear Energy  
Bulgarian Academy of Sciences, Sofia 13, Bulgaria

All the activities have taken place at the Institute mentioned above, some of them in collaboration with the Joint Institute for Nuclear Research (JINR), Dubna.

1. Neutron nuclear data

1. Nuclear material safeguards developed in Bulgaria (N.Bachvarov, V.Christov et al)

a) Special nuclear material concentration measurements.

Two techniques have been developed. 1) Beta reflectometry: beta scattering technique has been developed and portable instruments - fabricated. Used for determination of U, Pu or Th concentrations with a precision of 0.1 - 0.3 per cent. 2) Beta excitation analysis - by using Ge(Li) or scintillation spectrometers, precision 0.1 per cent - under development.

b) Measurement of fresh fuel assemblies.

Four techniques are being used or are under development. 1) Gamma spectrometric measurements of the fuel enrichment. 2) Gamma spectrometric measurements of  $^{238}\text{U}$  concentration. 3) Neutron counting measurements of  $^{238}\text{U}$ . 4) Weighing of the whole fuel assembly.

c) Measurement of irradiated fuel assemblies.

Included are: 1) Gamma spectrometric measurements; 2) Neutron and neutron coincidence measurements; 3) In core reactor measurements; 4) Reactor physics calculations.

2. Determination of thermalization parameter  $M_2$  and neutron temperature in a water lattice by pulsed source and "non  $1/V$ " absorber (A.Stanolov, V.Christov)

The method of poisoning with a "non  $1/V$ " absorber is used to determine the neutron thermalization parameter  $M_2$  in a water lattice, containing hollow tubes with a step of 2 cm, and  $p=0.2442$ . The pulsed experiments have been carried out in Sofia at the reactor IRT-2000 by a fast mechanical chopper.

The value of  $M_2$  obtained for water  $5.097 \text{ cm}^{-1}$  is compared with the theoretical values calculated by Honeck. The value of  $M_2$  measured for the investigated lattice  $2.92 \text{ cm}^{-1}$  is regularly smaller as compared with the experimental value for water. This is due to the relative decrease of scattering kernels concentration, and probably also to the neutron spectra modification in the lattice caused by the diffusion cooling effect. Neutron temperatures in homogeneous water solutions and in water lattices have been determined.

3. Determination of the albedo in a moderator with a big spherical hollow (A.Stanolov, K.Ilieva, V.Christov)

The nonstationary transport of neutrons in a spherical block of water moderator, containing a big spherical hollow, has been investigated. The quasi-asymptotic decay constants of the neutron flux have been measured, and the albedo - determined. A comparison between experimental and calculated data shows that the diffusion approximation is applicable to calculations of the albedo  $K_0$  in such systems.

The results are shown in Table 1. Notations: R - spherical hollow radius, H - water moderator thickness. Moreover:

$$K_0(\lambda) = \frac{1 - 2(R^{-1} + L^{-1} \coth((H+Z_0)/L))D/\langle V \rangle_T}{1 + 2(R^{-1} + L^{-1} \coth((H+Z_0)/L))D/\langle V \rangle_T} \quad (1)$$

$$D = D_0(1 - (\langle V \Sigma_c \rangle_T + \lambda)3D_0/\langle V \rangle_T^2), \quad L = (D/(\langle V \Sigma_c \rangle_T + \lambda))^{\frac{1}{2}}$$

$Z_0 = 0.34 \text{ cm}$ ;  $\langle V \rangle_T = 2(\pi)^{-\frac{1}{2}}V_T$ ;  $D_0$  - pulse experiment diffusion coefficient;

$$K_0(\lambda) = (\text{Re } f(x - |2R\lambda/V_T|))^{-1} \quad (2)$$

and for  $x \leq 1$  ( $C=0.5772\dots$ ):

$$f(x) = 1 - \frac{\sqrt{\pi}}{3}x + \frac{1}{4}x^2 - \frac{\sqrt{\pi}}{15}x^3 + \frac{1}{144}\left(\frac{9}{4} - 3C - \ln x\right)x^4$$

4. Two-level analysis of  $^{239}\text{Pu}$  neutron induced fission cross section in the neutron resonances energy region (S.A.Toshkov, N.B.Yaneva)

The formula for reaction cross section based on the R-matrix formalism considering the interference between two neighbouring resonances, referred to the same value of total momentum, has been used for analysis of cross sections of  $^{239}\text{Pu}$  resonance neutron induced fission. Experimental resolution and thermal motion of the target nuclei have been calculated by numerical integration.

The results of such an analysis of experimental data received from the IAEA have been presented at the 3rd Soviet Neutron Conference (Kiev, 9-13. 6. 75). The parameters of some resonances can be seen in Table 2.

## 2. Non-neutron nuclear data

1. New data on the decay of  $^{131}\text{La}$  and  $^{133}\text{La}$  (S.Avramov, Ts.Vylov, S.Batsev, M.Enikova, Zh.Zhelev, I.Penev, H.Protochristov, V. Fominych)

The activities have been produced by bombarding a Gd target with 660 MeV protons in the synchrocyclotron of JINR, Dubna. After a standard radiochemical procedure the La fraction has been further mass-separated. All gamma spectra have been measured with a Ge(Li) spectrometer (volume  $47\text{ cm}^3$ , resolution 2.5 keV at 1.33 MeV).  $35\text{ cm}^3$  coaxial Ge(Li) detectors have been used for measuring the gamma-gamma coincidences in  $^{133}\text{La}$ .

The gamma energies and intensities E, I, of  $^{131}\text{La}$  and  $^{133}\text{La}$  are given respectively in Tables 4 and 5. The results of the coincident experiment with  $^{133}\text{La}$  are presented in Table 3.

Table 1

R cm	H cm	$\rho$ ( $H_3BO_3$ ) mg/cm <sup>3</sup>	$\lambda_{meas}$	$K_o(\lambda_{meas})$ acc. to (1)	$K_o(\lambda_{meas})$ acc. to (2)
5.3	12.3		4090 $\pm$ 15	0.8338 $\pm$ 0.0011	0.8812
8.0	9.6		3280 $\pm$ 15	0.8367 $\pm$ 0.0012	0.8476
5.3	12.3	5.96	12650 $\pm$ 400	0.7902 $\pm$ 0.0240	0.6754
8.0	9.6	5.96	8470 $\pm$ 250	0.7340 $\pm$ 0.0160	0.6484
14.0	3.6	5.96	7470 $\pm$ 250	0.7230 $\pm$ 0.0200	0.5540
5.3	12.3	14.9	21000 $\pm$ 700	0.6901 $\pm$ 0.0350	0.4980
8.0	9.6	14.9	20640 $\pm$ 750	0.6770 $\pm$ 0.0400	0.3500
14.0	3.6	14.9	8280 $\pm$ 200	0.6202 $\pm$ 0.0150	0.4883

Table 2

E (eV)	$2g\Gamma_n^0$ (eV)	$\Gamma_f$ (eV)	J
10.96	0.00444	-0.220	1
11.93	0.00031	0.115	1
14.30	0.00026	-0.080	1
14.74	0.00148	0.102	1
22.34	0.00104	0.114	1
23.95	0.00003	-0.015	1
26.34	0.00284	-0.074	1

Table 3

279.5 keV with:	340.1, 385.6, (565.6 + 567.7), 571.2, 584.6, 595.8, 751.5, 820.9, 1061.4 keV
302.0 keV with:	(290.6 + 291.7), 556.3, 584.6, 621.5, 809.8 keV
(565.6 + 567.7) keV with:	279.5, (290.6 + 291.7), 534.8, 751.6, 428.9 keV
595.8 keV with:	279.5, (290.6 + 291.7) keV
850.3 keV with:	279.5 keV

Table 4

E (keV)	I	E (keV)	I	E (keV)	I	E (keV)	I
79.8	4.3	434.6	2.5	879.1	1.4	1793.5	0.4
107.8	109.3	437.1	0.8	932.8	0.3	1823.7	0.7
140.2	0.4	447.8	2.4	974.4	4.2	1874.4	0.5
147.9	1.2	453.7	35.2	1082.	0.2	1881.4	0.2
153.3	1.1	525.8	49.1	1107.3	0.3	1947.8	0.5
160.5	10.7	561.7	7.2	1129.1	0.2	1956.8	0.8
177.8	1.6	567.3	0.9	1136.0	0.7	2087.6	0.4
194.9	0.2	594.1	10.5	1154.9	0.6	2107.3	0.2
204.2	5.6	611.2	5.9	1178.1	2.2	2164.3	0.2
208.5	17.7	628.6	0.9	1291.9	0.7	2167.9	0.2
244.8	1.3	657.7	1.8	1368.4	0.3	2180.9	0.2
257.0	18.2	661.3	0.9	1386.7	0.3	2195.7	0.2
276.9	0.8	718.5	1.0	1390.9	0.5	2206.3	0.2
285.3	63.4	740.0	0.2	1443.9	0.4	2216.2	0.2
316.9	6.1	752.8	0.6	1455.6	0.3	2271.5	0.2
353.6	3.4	766.1	0.6	1476.2	0.3	2357.7	0.1
362.2	7.4	770.4	1.0	1495.2	0.7	2370.4	0.1
365.2	88.8	773.3	0.2	1500.7	1.3		
386.7	0.5	838.4	0.5	1696.6	0.4		
403.4	4.5	845.1	1.3	1700.8	0.4		
417.8	100	866.2	7.0	1718.3	0.3		

Table 5

E (keV)	I	E (keV)	I	E (keV)	I	E (keV)	I
228.2	4.8	571.2	9.4	911.4	64	1318.6	3.6
239.3	3.6	580.8	6.8	920.7	10	1376.0	2.0
257.0	9.4	584.6	91	949.9	1.3	1387.1	2.8
279.5	1000	591.9	16	965.7	1.1	1398.3	2.9
287.0	75	595.8	200	980.0	1.5	1403.6	1.8
290.6	500	618.2	440	984.0	1.4	1416.1	2.4
291.7	320	621.5	270	991.0	1.6	1494.8	1.5
302.9	66	632.5	530	994.5	1.7	1500.4	1.1
326.5	5.0	653.1	4.4	1009.2	40	1528.3	2.3
328.7	8.3	664.0	39	1021.4	2.3	1551.2	6.0
340.1	14.0	671.9	15	1043.0	4.8	1563.4	4.5
353.0	8.0	676.3	12	1095.5	3.7	1608.0	28
374.3	2.8	718.3	2.2	1099.8	115	1631.2	0.5
385.6	32	722.1	1.6	1113.1	3.3	1660.2	1.2
428.8	2.1	751.6	2.5	1175.9	2.2	1677.5	1.9
435.8	3.9	784.7	2.3	1182.4	1.1	1694.6	2.4
469.2	9.7	809.8	29	1199.5	12	1730.7	1.2
527.4	35	820.9	6.6	1211.7	25	1757.5	1.2
534.8	20	846.0	240	1220.0	1.7	1769.5	4.5
556.3	52	850.3	16	1239.0	3.0	1831.7	1.2
559.7	11	858.4	200	1260.8	15		
565.6	250	874.7	28	1284.0	35		
567.7	110	887.0	11	1316.8	11		

2. Lifetime and side feeding measurements of nuclear yrast levels (B.Bochev, R.Kalpakchieva, S.A.Karamian, T.Kutsarova, E.Nadjakov, Yu.Ts.Oganesian et al)

The recoil-distance Doppler-shift method has been applied in (HI, 4n) reactions at the U-300 heavy ion cyclotron of JINR, Dubna. A new high precision Doppler chamber has been used. It allowed measurements on high spin yrast levels in the back bending region. Not only lifetimes, but also side feeding intensities and times could be obtained.

The results of four Yb isotopes up the bands are presented in Table 6 and compared to the rigid rotor model. Similar data about the  $^{160}\text{Er}$  and  $^{166}\text{Hf}$ ,  $^{168}\text{Hf}$ ,  $^{170}\text{Hf}$  isotopes are under preparation. A systematics of deduced energy and lifetime parameters of the Yb isotopes down the bands, together with preliminary results on the Er and Hf isotopes, is shown in Table 7.

July 1975

Table 6

Transition energies  $E_{I \rightarrow I-2}$ , relative side feeding intensities  $P_I$ , mean side feeding times  $\varphi_I$  and mean lifetimes  $\tau_I$  (at spin I) in the yrast bands of four Yb isotopes

Nucleus	Level I	$E_{I \rightarrow I-2}$ (keV)	$P_I$	$\varphi_I$ (ps)	$\tau_I$ (ps)		Rigid rotor	
					Experiment			
$^{160}_{70}\text{Yb}_{90}$	2	243.1	0		182	+	6	182 <sup>*</sup> )
	4	395.4	0		11.60	+	0.60	12.38
	6	508.8	0		2.73	+	0.30	3.235
	8	588.7	0		1.29	+	0.30	1.498
	10	636	1		12.5	±	2	0.993
$^{162}_{70}\text{Yb}_{92}$	2	166.5	0		578	+	85	578 <sup>*</sup> )
	4	320.3	0		20.3	+	3.0	21.71
	6	436.2	0		4.6	+	0.9	4.352
	8	521.4	1		10	±	3	1.720
$^{164}_{70}\text{Yb}_{94}$	2	123.5	0		1272	+	50	1272 <sup>*</sup> )
	4	262.8	0		42.8	+	3.0	44.54
	6	375.0	0		7.24	+	0.50	7.298
	8	463.0	0.16	+ 0.01	6.3	±	5.3	2.472
	10	530.9	0.17	± 0.01	5.1	±	4.2	1.222
	12	576.9	0.14	± 0.01	4.8	±	3.2	0.794
	14	569.7	0.06	± 0.01	2.3	±	1.1	0.836
	16	490	0.12	± 0.015	1.3	±	0.5	1.748
18	543	0.35	± 0.035	5.3	±	1.5	1.042	
$^{166}_{70}\text{Yb}_{96}$	2	102.3	0		1789	+	90	1789 <sup>*</sup> )
	4	227.8	0		76.3	+	5.0	75.10
	6	337.7	0		11.24	+	0.80	10.64
	8	430.2	0.12	± 0.02	3.8	±	1.8	3.109
	10	507.3	0.14	± 0.04	3.7	±	3.1	1.339
	12	570.1	0.10	± 0.03	2.5	±	2.2	0.737
	14	603.9	0.11	± 0.03	3.0	±	2.2	0.547
	16	494.1	0.13	± 0.03	3.0	±	1.5	1.467
	18	509.3	0.14	± 0.04	2.0	±	2.3	1.253
20	588.5	0.26	± 0.05	2.8	±	2.1	0.608	

\* ) Normalized to experiment

Table 7

Moments of inertia  $J = 3/E_{2 \rightarrow 0}$ , energy ratios  $E_4/E_2 = (E_{4 \rightarrow 2} + E_{2 \rightarrow 0})/E_{2 \rightarrow 0}$ , intrinsic E2 moments  $Q$  and quadrupole deformation parameters  $\beta$  of four Yb isotopes, and preliminary results on one Er and three Hf isotopes

Nucleus	$J$ (MeV <sup>-1</sup> )	$E_4/E_2$	$Q$ (barn)	$\beta$
<sup>160</sup> <sub>70</sub> Yb <sub>90</sub>	12.34	2.626	4.81 ± 0.08	0.207 ± 0.003
<sup>162</sup> <sub>70</sub> Yb <sub>92</sub>	18.02	2.924	6.07 ± 0.45	0.257 ± 0.019
<sup>164</sup> <sub>70</sub> Yb <sub>94</sub>	24.29	3.128	6.79 ± 0.13	0.284 ± 0.006
<sup>166</sup> <sub>70</sub> Yb <sub>96</sub>	29.33	3.227	7.26 ± 0.18	0.301 ± 0.008
<sup>160</sup> <sub>68</sub> Er <sub>92</sub>	23.89	3.100	6.54 ± 0.71	0.286 ± 0.031
<sup>166</sup> <sub>72</sub> Hf <sub>94</sub>	18.90	2.965	5.94 ± 0.14	0.241 ± 0.006
<sup>168</sup> <sub>72</sub> Hf <sub>96</sub>	24.25	3.114	7.12 ± 0.13	0.285 ± 0.005
<sup>170</sup> <sub>72</sub> Hf <sub>98</sub>	29.91	3.202	7.21 ± 0.46	0.286 ± 0.018

**P R O G R E S S R E P O R T**

**Nuclear Data Programme**

**in**

**H u n g a r y**

**1975**

P R O G R E S S R E P O R T

CENTRAL RESEARCH INSTITUTE FOR PHYSICS OF THE HUNGARIAN ACADEMY OF SCIENCES, Budapest	59
INSTITUTE OF EXPERIMENTAL PHYSICS, KOSSUTH UNIVERSITY, Debrecen	92
INSTITUTE OF NUCLEAR RESEARCH OF THE HUNGARIAN ACADEMY OF SCIENCES, Debrecen	105
ROLAND EÖTVÖS UNIVERSITY, DEPARTMENT FOR ATOMIC PHYSICS, Budapest	124

H U N G A R Y

1975

Compiled by  
Gy. Kluge  
Central Research Institute for Physics  
of the Hungarian Academy of Sciences, Budapest

CENTRAL RESEARCH INSTITUTE FOR PHYSICS  
OF THE HUNGARIAN ACADEMY OF SCIENCES

BUDAPEST

CENTRAL RESEARCH INSTITUTE FOR PHYSICS  
NUCLEAR PHYSICS DEPARTMENT, BUDAPEST

1./ Van de Graaff-accelerator with the following parameters:

energy range: 0,8 - 5,0 MeV  
accelerated ions:  $H^+$ ,  $D^+$ ,  $^4He^+$   
long-time energy stability:  $\Delta E/E = 2 \times 10^{-4}$  FWHM  
short-time energy stability:  $\Delta E/E = 1,2 \times 10^{-4}$  FWHM  
target places: 3  
max. target current: 5  $\mu A$   
working time: 4000 hours/year  
type: EG-2R /home made/

2./ Neutron-generator:

max. voltage: 200 kV  
working voltage: 150-180 kV  
accelerated ions:  $H^+$ ,  $D^+$   
max.ion current: 500  $\mu A$   
neutronflux:  $3 \times 10^9$  n/cm<sup>2</sup>.s  
/1 cm distance from the target at 10  $\mu A$  deuteron current/  
target places: 2  
working time: 2500 hours/year  
type: NG-200 /home made/

3./ A fast-slow coincidence unit for positron annihilation lifetime measurements with time resolution 0,6 ns /PAN/

4./ A setup for positron annihilation angular correlation measurements /PANNI/

5./ A fast-slow coincidence unit for the investigation of nuclear fission /gas-scintillation chambers, vacuum-system, etc./

6./ An automatically controlled three-detector system with fast-slow coincidence circuits for the differential and integral perturbed angular correlation /PAC/ measurements

- 7./ Three-axis goniometer for channeling and back-scattering experiments.
- 8./ 2 small computers /developped by the electronic department of CRIP/ with memory capacity 4k and 8k respectively /type TPA-1001/ for on-line measurements and for preliminary data analysis.
- 9./ 4096-channel analyser with matrix analog-digital converter.
- 10./ 1024-channel analysers /NTA-512 B/.
- 11./ 512 - channel analysers /NTA-512 A/.
- 12./ 2 Mössbauer-spectrometers, cryostats and furnaces
- 13./ Ge/Li/ semiconductor detectors /4 cm<sup>3</sup> - 80 cm<sup>3</sup>/.
- 14./ Ge/Li/ X-ray detector /NE-5290/.
- 15./ Multiwire proportional chambers.

INVESTIGATION OF THE REACTION  ${}^2\text{H}(n,np)$  AT  $\vartheta_n=0^\circ$  +

J. KECSKEMÉTI and T. CZIBÓK

Central Research Institute for Physics, Budapest

B. ZEITNITZ

II. Institut für Experimentalphysik, Universität Hamburg

The differential cross section of the  ${}^2\text{H}(n,np)$  reaction was measured at  $\vartheta_n=0^\circ$ . Because of the applied special geometry the experimental data extend over a large fraction of the phase space, including several final state interaction regions as well as regions far from the dominance of quasi-two-body processes. The experiment was analysed with an exact three-body calculation using s-wave separable potentials. The analysis of the n-n and n-p final state interaction peaks gave  $a_{nn}=-16.3 \pm 2.0$  fm for the n-n  ${}^1S_0$  scattering length and  $r_{nn}=3.15 \pm 0.7$  fm for the effective range. Remarkable deviations from the calculated cross sections were found in regions where no strong final state interaction was present.

+This work was supported in part by the Bundesministerium für Forschung und Technologie, Germany.

Publications: Phys. Rev. Letters 32, /1063-1067/ 1974  
to be published in Nuclear Physics

Small - angle scattering of 1.6 MeV neutrons

G. Hrehuss and G. Pálka

Central Research Institute for Physics, Budapest,  
Hungary

The differential cross section of Pb for elastic scattering of 1.6 MeV neutrons from the  ${}^7\text{Li}(p,n){}^7\text{Be}$  reaction is measured at the angular range  $0-2.5^\circ$ . The interaction between the magnetic moment of neutrons and the nuclear Coulomb field is investigated at the extremely small angle elastic scattering. The data collection is in progress.

Investigation of low-energy charged particle reaction  
cross sections on light nuclei

I. Szentpétery

Central Research Institute for Physics, Budapest, Hungary

Recently, because of possible interest in energy-producing processes, growing world-wide attention is paid to low energy charged particle reaction data. The body of the experimental results collected up til now is far not complete and, on the other hand, some data sets measured repeatedly by different groups are not consistent. It should also be noted that the vast majority of the data in question was measured around the early fifties under very unadvanced technical conditions as it can be judged looking back from today. Consequently, there is a rather urgent need for really "good", reliable, consistent data for low energy cross sections.

In order to contribute to this important field low-energy cross section studies have been started in our Institute. The measurements of the  ${}^9\text{Be}(p,d)$  and  ${}^9\text{Be}(p,\alpha)$  absolute cross sections in the proton energy region  $E_p = 50-200$  keV are in progress. The emphasis is put on the exactness of the experimental data. The absolute errors of the measurements are expected to be 20 % maximally. This measurement should be finished in 1975. The next program is the study of the  ${}^{11}\text{B}(p,\alpha)$  reaction. For the near future the investigation of the  ${}^6\text{Li}+d$  system is planned.

$g_{9/2}$  analogue resonances in the  $^{64}\text{Zn}$  nucleus

I. Fodor, I. Szentpétery, A. Schmiedekamp<sup>‡</sup>

Central Research Institute for Physics, Budapest, Hungary

K. Beckert, H.U. Gersch

Zentralinstitut für Kernforschung, Rossendorf bei Dresden GDR

J. Delanuy, B. Delaunay, R. Ballini

Centre d'Etudes Nucléaire, Saclay, France

/to be published in Nuclear Physics/

Two  $g_{9/2}$  analogue resonances have been found in  $^{64}\text{Zn}$ , corresponding to the 1.546 and 1.589 MeV levels in the parent nucleus  $^{64}\text{Cu}$ . The resonances were located through the  $^{63}\text{Cu}(p,\gamma)$  reaction at proton bombarding energies  $E_p^{\text{lab}}=3.217$  and 3.251 MeV respectively. The gamma ray transitions from the isobaric analogue resonances to the lower lying levels in  $^{64}\text{Zn}$  were studied with a Ge(Li) detector. The asymmetry ratios,  $I(0^\circ)/I(90^\circ)$ , were measured for a few prominent gamma transitions. Based on these studies both the resonances were assigned as  $3^-$  spin and parity. From the analogue resonances a large M1 transition strength of about 0.1 W.U. was found to branch to a level at excitation energy 3.002 MeV which was identified as the main component of the antianalogue state. The structure of the analogue states is supposed to be  $[p_{3/2} g_{9/2}] 3^-$  and a possible mixing with  $3^-$  octupole vibrational states is discussed.

<sup>‡</sup>On leave of absence from University of Texas, Austin, Texas, USA

## FISSION NEUTRON SPECTRUM STUDIES <sup>x</sup>

L. Jéki, Gy. Kluge, A. Lajtai and I. Vinnay  
Central Research Institute for Physics,  
Budapest

Possible contribution of hypothetical retarded neutrons to the energy spectrum of prompt fission neutrons below 400 keV is measured. For neutron energies above 400 keV the relative yield of the retarded neutrons was found to be at most 0.3 % of all neutrons.

## MEASUREMENT OF ENERGY AND ANGULAR DISTRIBUTION OF PROMPT FISSION NEUTRONS FROM THE SPONTANEOUS FISSION OF <sup>252</sup>Cf. <sup>x</sup>

L. Jéki, Gy. Kluge, A. Lajtai and I. Vinnay  
Central Research Institute for Physics,  
Budapest

The angular and energy distributions of prompt neutrons from the spontaneous fission of <sup>252</sup>Cf as functions of fragment mass are measured in the energy range 2 keV - 1 MeV. This multi-parameter measurement is being carried out to get information on the emission mechanism of neutrons of low energy.

<sup>x</sup> In cooperation with Institute of Physics and Power Engineering, Obninsk, USSR.

ENERGY SPECTRUM MEASUREMENT OF NEUTRONS FROM  
 $^{235}\text{U}/n_{\text{th},f}/$  REACTION IN ENERGY RANGE OF 0.05 - 1 MeV. <sup>x</sup>

L.Jéki, Gy.Kluge, A.Lajtai and I.Vinnay  
Central Research Institute for Physics,  
Budapest

Prompt fission neutron spectrum from 0.05 MeV to 1 MeV is measured for  $^{235}\text{U}/n_{\text{th},f}/$  reaction. The existence of low energy surplus neutrons relative to the overall Maxwell distribution is investigated. Due to the large background of neutrons and gammas from the reactor an especially long data collection is necessary. The data accumulation is in progress at the Central Research Institute for Physics.

MEASUREMENT OF PERTURBED ANGULAR DISTRIBUTION OF GAMMA-RAYS EMITTED FROM SPONTANEOUS FISSION OF  $^{252}\text{Cf}$ . <sup>x</sup>

L.Jéki, Gy.Kluge, A.Lajtai and I.Vinnay  
Central Research Institute for Physics,  
Budapest

The influence of extranuclear effects to the angular distribution of fission gammas is studied. The angular distribution of gamma-rays emitted from the fission fragments is measured as a function of pressure of the gas containing the fragment paths. As a next step, the angular distributions of gamma-rays from fragments let through thin foils of different thicknesses are measured.

<sup>x</sup> In cooperation with Institute of Physics and Power Engineering, Obninsk, USSR.

EXCITATION OF THE COLLECTIVE STATES OF THE EVEN-EVEN  
Sm ISOTOPES BY INELASTIC SCATTERING OF 40 MeV HELIONS<sup>‡</sup>

G. Páll, Central Research Institute for Physics  
Budapest, Hungary

C. Pegel, I. Institut für Experimentalphysik,  
Universität Hamburg, Germany

In order to investigate the structure of the low lying collective states and its variation in the Sm isotopes, which represent such a nuclear range, where a transition from the spherical shape to the deformed one occurs, the coupled channel method is applied using phenomenological collective models, namely the harmonic-anharmonic vibrator, symmetric and asymmetric rotator in case of the  $^{144}$ ,  $^{148}$  Sm,  $^{150}$ Sm and  $^{152,154}$ Sm nuclei respectively. The values of the  $\beta_\lambda$  parameters characterising the vibrational states, the one-phonon component of the two-phonon states, furthermore the  $\gamma$  asymmetry and  $\beta_2$ ,  $\beta_4$  deformations are determined. The values of the deformation parameters characterising the nuclear distributions from /p,p'/ analysis are compared to the corresponding values characterising the interaction potential describing the helion scattering.

<sup>‡</sup>This work has been done at I. Institut für Experimentalphysik, Universität Hamburg.

Supported in part by the Alexander von Humboldt-Foundation

Publications: Z. Physik 268, /51-55/ 1974

Proc. on Frühjahrstagung den Haag 1975, C3.6

QUASIELASTIC SCATTERING OF 670 MeV PROTONS ON  
DEUTERON CLUSTERS IN  ${}^6\text{Li}$  and  ${}^7\text{Li}$  NUCLEI

D. Albrecht, G. Chemnitz, J. Erő, Z. Fodor,  
Hong Sung Mu, B.A. Khomenko, N.N. Khovansky, P. Koncz,  
S. Koncz, Z.V. Krumstein, Yu.P. Merekov, V.I. Petrukhin,  
Z. Seres, M. Tóth.

Joint Institute for Nuclear Research, Dubna and  
Central Research Institute for Physics, Budapest

Preprint JINR E1-8935 /1975/

Kinematically complete measurements of  
quasielastic scattering of 670 MeV protons on deuteron  
clusters in  ${}^6\text{Li}$  and  ${}^7\text{Li}$  nuclei have been made at an  
angle of  $165^\circ$  c.m.s. In the  ${}^6\text{Li} /p, pd/ {}^4\text{He}$  reaction  
alpha particle is produced mostly in the ground state.  
For the  ${}^7\text{Li} /p, pd/ {}^5\text{He}$  reaction those events are more  
probable when the residual nucleus is produced in the  
excited state. The half width of intranuclear momentum  
distribution of deuteron clusters has been determined  
and is  $\sim 50$  MeV/c for  ${}^6\text{Li}$  and  $\sim 65$  MeV/c for  ${}^7\text{Li}$ .

Investigation of Space-sensitive multiwire proportional chambers with high detector area

L. Vályi, Zs. Kajcsos

We have continued the investigation and design of the new types of the Space-sensitive detectors of high detecting area, the most progressive detecting methods.

We carried out a systematic examination of the physical and operational properties of the 1000 x 600 mm<sup>2</sup> sensitive detector area multiwire proportional chamber with X and Y coordinate signal planes, using electron- and  $\gamma$ -rays of <sup>90</sup>Sr and <sup>55</sup>Fe radioactive isotopes respectively with different filling gas compositions.

The measured energy spectrum of <sup>55</sup>Fe significant for the signal wires of the MWPC, it shows the energy resolution at this energies  $\sim 20$  %.

The efficiency of the MWPC is  $\sim 100$  % in at operation applied voltage range of /300-350 V/.

Operation and Development at the 5 MeV Electrostatic Ion Accelerator of the Central Research Institute for Physics, Budapest, Hungary.

G.Bürger, E.Klopfer, P.Kostka, Á.Kovács, J.Pazonyi and  
J.Roósz

The main results of development at the 5 MeV Van de Graaff pressurized ion accelerator which continued in the period of 1974-75 have been the increase of energy stability, of reliability of the machine and of running time for the experiment. A new rf-ion source with a relative long life-time was tested and installed. Its life-time is about 1200 - 1500 hours. Application a special charging system with brushes instead of needles and using a conventional manufactured belt, the long-time energy stability is less than  $2 \times 10^{-4}$ . Protons, deuterons and helium ions may be accelerated and changed within a short time without shut down. The target area was extended up to three beamlines. Usual target currents are about 1 - 5  $\mu\text{A}$ . In 1974, the accelerator was running more than 5000 hours, during the first half year of 1975 over 2200 hours for the experiments in basic and applied nuclear physics.

Work at the 200 keV Cascade Accelerator of the Central  
Research Institute for Physics, Budapest, Hungary.

G. Bürger and I. Szentpétery

The 200 keV open-air cascade type ion accelerator was  
formerly used as a fast neutron source. During the last  
year it was used as a proton accelerator only. For this  
purpose the vacuum system was reconstructed and a speci-  
al beam-line was mounted.

## Lattice location of arsenic implanted into silicon<sup>+</sup>

G. Mezey, E. Uggerhøj<sup>++</sup>

Channeling effect was used to study the lattice location of arsenic implanted into silicon. The substrate temperature was maintained at 400 °C or 500 °C during implantation. The doses of implantation were between  $10^{14}$  and  $10^{15}$  As/cm<sup>2</sup>.

Angular scans through the  $\langle 111 \rangle$  and  $\langle 110 \rangle$  axes show that the channeling dips obtained on 1.5 MeV  $^4\text{He}^+$  ion scattering measurements were narrower for arsenic than for the Si host lattice. This suggests that some or all arsenic atoms are displaced from the lattice sites.

The minimum yield data show that the arsenic has a highly substitutional character. The substitutional component was between 70-80 per cent in the dose range used in present experiment.

<sup>+</sup>This work was done in the University of Aarhus, Denmark

<sup>++</sup>Permanent address: University of Aarhus

Drive-in diffusion studies on antimony and gallium  
implanted into silicon<sup>+</sup>

J. Gyulai, L. Csepregi, T. Nagy, G. Mezey, E. Kótai,  
P. Révész, A. Manuaba, J.W. Mayer<sup>++</sup>

Diffusion of antimony and gallium from an implanted predeposition was investigated. To prevent antimony out-diffusion during drive in, a low-temperature /850 °C/ and 5 minutes oxidation was used after implantation. The diffusion processes were carried out at 1050 °C. Diffusion of antimony was accordance with diffusion theory. Channeling measurements showed that the Sb atoms sit predominantly on substitutional lattice sites.

In the case of Ga implants, the experiments, using low temperature oxidation as encapsulation, led to different results compared with antimony. Because of the high solubility of Ga in SiO<sub>2</sub> almost all of the gallium diffused instantly onto the outer surface of the oxide. Completely different picture was found when a reactively sputtered Si<sub>3</sub>N<sub>4</sub> layer was used for encapsulation. Under this condition extremely fast diffusion was observed and the resulting distribution was almost flat for extreme depths.

<sup>+</sup>This work was done on the basis of CRIP - CALTECH agreement

<sup>++</sup>Permanent adress:  
California Institute of Technology, Pasadena

Publication: Le Vide 174, 416, 1974

Lattice location of group III. and V. elements implanted  
into silicon

G. Mezey, T. Nagy, E. Kótai, J. Gyulai, P. Révész,  
L. Csepregi

Lattice location experiments were made on As, Sb or Ga implanted silicon during isochronal annealing up to 900 °C. The substrates were at room temperature during implantation. The Sb implant exhibited increasing substitutional component up to 700 °C during the annealing process. The maximum value of substitutional component was about 80 %. At higher annealing lattice sites.

The implanted As exhibited high 80 per cent substitutional component too. However, in the temperature range of 700-800 °C this component showed a reverse characteristic.

The Ga-doped silicon gave practically no substitutional component up to 800 °C anneals. This differs surprisingly from results of different authors.

Enhanced oxidation studies by means of  $^{16}\text{O}(\alpha, \alpha)^{16}\text{O}$   
elastic scattering

T. Nagy, E. Kótai, A. Manuaba, G. Mezey, J. Gyulai

The differential cross section for elastic scattering of alfa particles by  $^{16}\text{O}$  exhibit strong deviation at 3050 keV energy. This is due to a given energy level of  $^{20}\text{Ne}$  nuclei. Therefore the sensitivity for detecting oxigen using a beam of 3.05 MeV  $^4\text{He}^+$  is increased by a factor of 30. The effect on surface oxidation of group III. and V. elements implanted into silicon is being investigated.

Positron Lifetime Measurements in Aliphatic Hydrocarbons

Zs. Kajcsos, I. Dézsi, D. Horváth

Appl. Phys; 5, 53, /1974/

The positron lifetimes and relative intensities were measured in highly purified liquid and solid hydrocarbons. It was found that most of the lifetime parameters changed at the melting point of the samples and their values were lower in the solid than in the liquid phase. A study of hexane isomers was also performed and there was found only very small difference for different isomers.

Positron annihilation in ionic crystals

Á. Balogh, I. Dézsi, D. Horváth, Zs. Kajcsos

/Appl. Phys. 6, 21-23 /1975/

Izotóptechnika, 17, 473 /1974//

Positron lifetime measurements were made on  $\text{Ca}^{2+}$  doped NaCl,  $\text{Ba}^{2+}$  doped NaCl and X-ray-and additively-coloured KCl crystals. In the NaCl(Ca) system a correlation which could be approximated by a power equation was found between the dopant concentration and the positron annihilation parameters. In the NaCl(Ba) system the decay parameters do not change significantly as expected.

Positron annihilation in amino acids

I. Dézsi, D. Horváth, Zs. Kajcsos

/Chem. Phys. Lett., 24, 514 /1974//.

Positron lifetime measurements were performed on eight different amino acids  $\tau_1$ ,  $\tau_2$  and  $I_2$  values were observed at around 0,35 ns, 0,7-1,2 ns and 20-30 % respectively. The long-lived component seems to be produced by positronium states trapped in the crystalline lattice or by positronium bound to molecules.

Ground state conversion in  $\text{Fe}(\text{BF}_4)_2 \cdot 6 \text{H}_2\text{O}$

L. Asch<sup>†</sup>, I. Dézsi, T. Lohner and B. Molnár

The study of the phase transformation in  $\text{Fe}(\text{BF}_4)_2 \cdot 6 \text{H}_2\text{O}$ . The temperature dependence of the Mössbauer spectra showed that the later crystals undergo the same ground state conversion as the ferrous perchlorate hexahydrate did. The transition enthalpies were also determined by calorimetric measurements.

<sup>†</sup>Physik Department, Technische Universität München,  
Garching, F.R.G.

Interpretation of experimental Mössbauer  
quadrupole splittings of iron pentacyanide  
complexes using molecular orbital theory

A. Trautwein<sup>+</sup>, F.E. Harris<sup>++</sup>, I. Dézsi

Theoret. Chim. Acta /Berl./ 35, 231 /1974/

Semiempirical self-consistent-field molecular orbital calculations were carried out for six ironpentacyanide complexes and were used to interpret their experimental quadrupole splittings. Probable orientations were identified for the  $C_6H_5$  and  $NO_2^-$  groups in  $Fe(CN)_5 NOC_6H_5^{-3}$  and  $Fe(CN)_5 NO_2^{2-4}$ . Calculations on  $Fe(CN)_5 NO^{-2}$  and  $Fe(CN)_5 NO^{-3}$  could simultaneously be brought into agreement with experiment by reparametrization to make the NO group more positively charged. All the calculations indicated the importance of including all the Fe 3d and 4p orbitals in the calculations and of considering neighbouring-atom effects.

<sup>+</sup>Fachbereich Angewandte Physik, Universität des Saarlandes, Saarbrücken, F.R.G.

<sup>++</sup>Department of Physics, University of Utah, Salt Lake City, Utah, USA

Spin relaxation effects in  $\text{Fe}/\text{NO}_3/3$  and  $\text{Fe}/\text{ClO}_4/3$   
frozen solutions and in  $\text{Fe}/\text{ClO}_4/3$  crystal hydrates

F. Sontheimer<sup>†</sup>, D.L. Nagy, I. Dézsi, T. Lohner,  
G. Ritter<sup>†</sup>, D. Seyboth<sup>†</sup>, H. Wegener<sup>†</sup>

J. de Physique, 35, C6-443 /1974/

Spin relaxation was studied in  $\text{Fe}/\text{NO}_3/3$  and  $\text{Fe}/\text{ClO}_4/3$  frozen solutions and in  $\text{Fe}/\text{ClO}_4/3$  crystal hydrates. Mössbauer spectra have also been measured in various magnetic fields up to 80 kG. All these substances showed pronounced relaxation effects. The relaxation time in the frozen solutions was found to be field dependent and rather long in high fields /  $\sim 10^{-7}$  s/. In crystal hydrates the relaxation times turned out to be field independent and much shorter /  $\sim 10^{-9}$  s/. The zero field spectra of the crystal hydrates showed an intermediate character between isotropic and longitudinal relaxation.

<sup>†</sup>Physikalisches Institut II. der Universität  
Erlangen - Nürnberg, Erlangen, F.R.G.

Morin transition in  $\alpha$   $\text{Fe}_2\text{O}_3$  diluted with  
trivalent metallic ions

I. Dézsi, T. Lohner, B. Molnár, D.L. Nagy

In: Proc. Int. Conf. Mössbauer Spect., Cracow, 1975.

Phase transformation studies have been performed on the system  $(1-x) \alpha\text{-Fe}_2\text{O}_3 - x \text{Al}_2\text{O}_3$ .  $x = 1-8$  mol %. Increasing Al-concentration was found to decrease the Morin-temperature and to increase the angle between the spin direction and the [111] axis. No intermediate magnetic phase with  $\Delta E_Q = 0$  was found.

Mössbauer Effect Study of  $\text{Co}^{57}$  and  $\text{Fe}^{57}$  Impurities  
in Ferroelectric  $\text{LiNbO}_3$

W. Keune,<sup>++</sup> S.K. Date<sup>+</sup>, I. Dézsi, U. Gonser<sup>++</sup>

to be published in J. Appl. Phys.

The Mössbauer effect observed with  $\text{LiNbO}_3$ :  
 $\text{Co}^{57}$  /source/ and  $\text{LiNbO}_3$ : $\text{Fe}^{57}$  /absorber/ crystals  
showed the existence of high spin  $\text{Fe}^{2+}$  and  $\text{Fe}^{3+}$   
valence states. The  $\text{Fe}^{2+}/\text{Fe}^{3+}$  ratio could be  
changed by reducing or oxidizing heat treatment.  
 $\text{Fe}^{3+}$  in sources and absorbers shows Mössbauer  
spectra which are typical for slow electronic  
relaxation between the crystal field states of the  
 ${}^6\text{S}_{5/2}$  state ion. For both,  $\text{Fe}^{3+}$  and  $\text{Fe}^{2+}$ , the  
principal axis of the electric field gradient is  
found to be parallel to the crystallographic c-axis.  
For ferric iron  $V_{zz}$  is positive, while  $V_{zz}$  is  
negative and strongly temperature dependent for  
ferrous iron. The impurity site substitution and  
charge compensation mechanism are discussed.

<sup>+</sup>permanent address: Tata Institute of Fundamental  
Research, Bombay, India

<sup>++</sup>Fachbereich Angewandte Physik, Universität des  
Saarlandes, Saarbrücken, F.R.G.

Mössbauer spectroscopy of Fe-HEDTA frozen solutions

I. Dézsi, T. Lohner, D.L. Nagy, G. Ritter<sup>‡</sup>,  
H. Spiering<sup>‡</sup>

In: Proc. Conf. Mössbauer Spect., Cracow, 1975.

Different ionic species have been identified in Fe<sup>III</sup>-HEDTA /HEDTA=hydroxyethylethylene diaminetriacetic acid/aqueous solutions. The minimum of the magnetic susceptibility found at pH=5 was explained by the existence of antiferromagnetically coupled dimeric species with a net spin S=0. This species were identified by recording spectra in an applied magnetic field of 50 kG.

<sup>‡</sup>Physikalisches Institut II der Universität  
Erlangen-Nürnberg, Erlangen, F.R.G.

Ferroelectric phase transformation in  $\text{CH}_3\text{NH}_3\text{Fe}/\text{SO}_4/2 \cdot 12 \text{H}_2\text{O}$

I. Dézsi, T. Lohner, D.L. Nagy

In: Proc. Int. Conf. Mössbauer Spect., Cracow, 1975.

Studies of  $\text{CH}_3\text{NH}_3\text{Fe}/\text{SO}_4/2 \cdot 12 \text{H}_2\text{O}$  have been devoted to the ferroelectric phase transition which occurs at 169 K. A minimum of the absorption area as a function of temperature at  $T_c$  was found which suggests that the phonon spectrum of the crystal anomalously changes around the phase transition temperature.

Paramagnetic relaxation phenomena in alums

I. Dézsi, T. Lohner, D.L. Nagy, A.M. Afanasiev\*

J. de Physique, 35, C6-449 /1974/

Paramagnetic spin relaxation has been studied in alums  $AFe/SO_4/2 \cdot 12 H_2O$  / $A=NH_4, K, Tl, Rb, Cs$  and  $CH_3NH_3/$ . It was found that in the first four cases / $\alpha$ -alums/ where the local symmetry of the  $Fe^{3+}$  ions is almost cubic the tensor of the transition probabilities is isotropic. In the last two cases / $\beta$ -alums/ the local environment of  $Fe^{3+}$  is slightly distorted which results in an isotropic transverse characteristics of the relaxation tensor.

\*I.V. Kurchatov Institute of Atomic Energy  
Moscow, U.S.S.R.

Can we prepare texture-free Mössbauer samples?

D.L. Nagy, I. Dézsi, K. Kulcsár

In: Proc. Int. Conf. Mössbauer Spect., Cracow, 1975.

A reason for the appearance of texture in Mössbauer absorbers is a small pressure on the surface of the sample. The effect of such pressures on the asymmetry of a quadrupole doublet was discussed and it was found that a relatively small /e.g. 20 %/ deformation of the sample may result in an asymmetry as high as e.g. 8 %. Using this fact the method of preparing texture-free samples has been worked out.

Ligand field theory and hyperfine interaction in  
siderite

H. Spiering<sup>‡</sup>, R. Zimmermann<sup>‡</sup>, D.L. Nagy

In: Proc. Int. Conf. Mössbauer Spect., Cracow, 1975.

The ligand field theory has successfully been applied to describe the hyperfine interactions in  $\text{FeCO}_3$ . Supposing a small mixing of the  $E_g^2$  doublet to the  $E_g$  ground state doublet the temperature dependence of the hyperfine field was understood using a single exchange constant.

<sup>‡</sup>Physikalisches Institut II. der Universität Erlangen-Nürnberg, Erlangen, F.R.G.

Magnetic field induced texture in Mössbauer absorbers

D.L. Nagy, K. Kulcsár, G. Ritter<sup>✱</sup>, H. Spiering<sup>✱</sup>,  
H. Vogel<sup>✱</sup>, R. Zimmermann<sup>✱</sup>, I. Dézsi, M. Pardavi-Horváth

Phys. Chem. Solids, 36, 759 /1975/

The reason for the appearance of texture in Mössbauer absorbers was studied. As a model, polycrystalline  $\text{FeCO}_3$  mixed with active carbon powder was used. It was found that magnetic fields of some kG are able to induce a considerable texture. The effect was due to the anisotropy of the magnetic susceptibility and could be described by a simple phenomenological model. Similar effects have been observed in  $\text{FeSO}_4 \cdot \text{H}_2\text{O}$  and  $\text{FeCl}_2 \cdot 4 \text{H}_2\text{O}$  powders mixed with active carbon.

<sup>✱</sup>Physikalisches Institut II der Universität Erlangen-Nürnberg, Erlangen, F.R.G.

Production of group constants from the evaluated  
nuclear data distributed by IAEA

P. Vértes

Central Research Institute for Physics, Budapest

In order to supply group constants for the calculations to be performed in the framework of the ZR-6 project, a new program system has been elaborated which is able to convert cross-sections given point-wise or by resonance parameters into infinite diluted or screened group averaged cross-sections and into inelastic and elastic group transfer matrix. The group-system and averaging spectrum are arbitrary. Up to now the program system can use files in KEDAK or UK format, but it will be extended to SOKRATOR and ENDF/B format.

**INSTITUTE OF EXPERIMENTAL PHYSICS,**

**KOSSUTH UNIVERSITY**

**DEBRECEN**

## EXPERIMENTAL FACILITIES

1. A 0.45 mg Cf-252 /fission/ neutron source;
2. 200 kV /2 mA/ neutron generator /home made/;
3. 180 kV /1.2 mA/ Activatron-111 neutron generator, it can be pulsed, pulse period: down to 10 microsec;
4. Pu-Be neutron sources from 0.5 to 5 Ci ;
5. 40 cm<sup>3</sup> Ge/Li/ detector with 3 keV FWHM at 1332 keV, and Si/Li/ X-ray spectrometer with 350 eV FWHM at 6.4 keV;
6. 4000 channel DIDAC /Intertechnique/ analyser and MULTI-20 Plurimat N data processing system with peripherals; three 100 channel analysers;
7. Li-6J/Eu/crystal spectrometer; He-3 proportional counter; time-of-flight system with associated particle and klystron bunching method for fast neutrons is under construction;
8. Low-background proportional counter for measuring weak beta and/or gamma rays, e.g. tritium, with a sensitivity of a few pCi;  $4\pi$  -  $\beta$  flow gas counter.

ANGULAR DISTRIBUTION OF FRAGMENTS IN THE  
FISSION OF URANIUM AND THORIUM

M.Várnagy, S.Juhász, J.Csikai

The angular distribution of fragments from the neutron induced fission of  $^{238}\text{U}$  and  $^{232}\text{Th}$  had been measured with a polycarbonate /Makrofol E/ detector at  $E_n=14.1$  MeV neutron energy [1,2] .

Now a method has been developed for the automatic evaluation of angular distribution of fission fragments from  $^{238}\text{U}$  and  $^{232}\text{Th}$  induced by  $^{252}\text{Cf}$ -neutrons. This method is based on the jumping spark counting. A simultaneous measurement was also applied using the optical method described in ref. [1]. The results obtained by the two independent methods are in good agreement.

- [1] E. Baratçugil, S. Juhász, M.Várnagy, S.Nagy, J.Csikai, Nucl. Phys. A 173 /1971/ 571
- [2] E.Baratçugil, S.Juhász, M.Várnagy, S.Nagy, J.Csikai, Neutronnaja Fizika /Izd. Naukoza Dumka, Kiev 1972/ I-240.

CALCULATION OF AVERAGE /n,2n/ CROSS-SECTIONS  
FOR Cf-252 FISSION NEUTRONS

Z.T.Bódy

Fission spectrum average /n,2n/ cross-sections were calculated for Cf-252 fission neutrons from experimental excitation functions [1] and from most probable /absolute/ cross-section values at 14.7 MeV [2]. Different temperatures for fission were supposed between the 1.4 - 1.6 MeV range. A 10 % variation in the temperature alters the average cross-sections roughly by a factor of two. The comparison with experimental data makes it possible - in principle - to choose such a temperature by which the commonly used square root times exponential type model spectrum gives the best fit to the experimental values. However, in practice, this choice can not be still done owing to the lack of the sufficient number of experimental data.

[1] Z.T.Bódy, ATOMKI Közlemények 16/4. 351, /1974/.

[2] Z.T.Bódy, J.Csikai, Atomic Energy Rev., 11 153, /1973/.

$^{252}\text{Cf}$  NEUTRON IRRADIATION FACILITIES

M.Buczko, M.H.Al-Mundheri<sup>+</sup>, J.Csikai, Z.Dezso

An activation facility has been designed for the accomodation and safe-handling up to 50 mg of Cf-252 neutron source. The absolute values of thermal, epithermal and fast neutron fluxes were determined by foil activation method using In, Dy, Au, Al and Fe detectors, and compared with other experimental results and theoretical estimations.

+ On leave from Iraqi Atomic Energy Commision, Baghdad

APPLICATION OF SSNTDs FOR NEUTRON RADIOGRAPHY

S.Juhász, M.Várnagy

Radiographs of a microswitch and other electric parts were made with Lexan polycarbonate using  $U_3O_8$  /20%  $^{235}U$ / /n,f/ converter as well as CA-8015 cellulosenitrate /manufactured by Kodak Pathe, France/ using  $^6LiF$  /n, $\alpha$ / converter. The thermal neutron exposure time was 50 h.  $^{252}Cf$  was used as a neutron source.

DETERMINATION OF THE BITUMEN CONTENT IN ASPHALT  
CONCRETE USING A NEUTRON REFLECTION METHOD

M.Buczko, Z.Dezso, J.Csikai

A neutron physical method for the fast, nondestructive determination of the bitumen content in asphalt concrete has been developed [1,2,3]. The determination is performed on cylindrical asphalt concrete samples containing desiccated rubble matrix. Using samples of ~1000 g and measuring times of 20 min, the reproducibility of the bitumen determination is  $\pm 0.15$  w%, the sensitivity is  $3 \cdot 10^{-3}$  g/g.

[1] M.Buczko, Z.Dezso, J.Csikai, J.Radiol.Chem.  
25, 179 /1975/

[2] S.Nagy, P.Raics, S.Daroczy, G.Peto, Z.Dezso,  
M.Buczko, J.Csikai, Research Report 1971. KÉV  
Debrecen, Contract No. 14223/1970.

[3] E.Pittlik, M.Husi, E.Szucs, J.Csikai, M.Buczko,  
S.Daroczy, S.Nagy, G.Peto, P.Raics, Z.Dezso,  
Patent Appl., UE-24, 8 Aug. 1972.

TITANIUM CONTENT DETERMINATION IN BAUXITE:  
A COMPARISON OF NEUTRON ACTIVATION ANALYSIS WITH  
X-RAY FLUORESCENCE METHOD

M.Buczko, S.Mukherjee, Z.Dezso, M.Hegedus, M.Varady

ABSTRACT

Titanium content determination has been investigated using bauxite samples of various origin, by thermal neutron activation and x-ray analysis using  $^{252}\text{Cf}$ -fission neutron source and Ge/Li/ detector as well as  $^3\text{H}$ -exciting source and Si/Li/ detector. For the same measuring time the sensitivity of the activation method is 0.35 w% Ti, with an absolute statistical error less than 10% in the case of 8<sup>g</sup> sample weight, while for the x-ray method is 0.06 w% Ti with an absolute statistical error less than 5 %.

APPLICATION OF T-CELLIT DETECTOR FOR THE  
STUDY OF NUCLEAR REACTIONS

M.Várnagy, J.Csikai, J.Szabó and S.Szegedi

The T-cellit detector was successfully used for measuring the angular distribution of alpha-groups from  $^{19}\text{F} /d,\alpha/ ^{17}\text{O}$  [1,2] and  $^9\text{Be} /d,\alpha/ ^7\text{Li}$  [3,4] reactions as well as for the determination of the cross section of the reactions  $^9\text{Be} /d,\alpha/ ^7\text{Li}$  [3,4] and  $^{10}\text{B} /p,\alpha/ ^7\text{Be}$  [5,6].

Now a method has been developed for the simultaneous determination of the angular distributions of the  $^3\text{He}$  and  $^4\text{He}$  particles from the  $^{6,7}\text{Li} /p,\alpha/ ^{3,4}\text{He}$  reactions [7] as well as of the  $^1\text{H}$ ,  $^7\text{Li}$  and  $^4\text{He}$  particles from the  $^6\text{Li} /d,p/ ^7\text{Li}$  and  $^6\text{Li} /d,\alpha/ ^4\text{He}$  reactions in the energy region relevant for nuclear astrophysics. Cross sections for the reaction  $^6\text{Li} /p,\alpha/ ^3\text{He}$  have also been determined [7].

- [1] Somogyi Gy., Schlenk B., Várnagy M., Meskó L., Valek A., ATOMKI KÖZLEMÉNYEK 10 /1968/ 33
- [2] G.Somogyi, B.Schlenk, M.Várnagy, L.Meskó, A.Valek, Nuclear Instruments and Methods 63 /1968/ 189
- [3] Szegedi S., Thesis /Kossuth University, Debrecen 1970/
- [4] S.Szegedi, Acta Phys. Acad, Sci. Hungary 34 /1973/ 215
- [5] Szabó J., Thesis /Kossuth University, Debrecen, 1971/
- [6] J.Szabó, J.Csikai, M.Várnagy Nucl.Phys. A195 /1972/ 527
- [7] M.Várnagy, J.Csikai, J.Szabó, S.Szegedi, J.Bánhalmi, Nucl. Instr. and Meth. 119 /1974/ 451

SPARK COUNTING TECHNIQUES OF ETCHED NUCLEAR  
TRACKS FOR NEUTRON DOSIMETRY AND SAFEGUARDS

M.Várnagy, E.Gyarmati, J.Csikai and T.Sztaricskai

A new method based on the Fraunhofer diffraction had been worked out for the determination of the average diameter of the particle tracks in solid-state nuclear track detectors [1].

Now, a jumping spark counter /JSC/ has been constructed for the fission fragment counting and its characteristic features were studied. The JSC is suitable either for step by step or continuous counting of thin /5-18  $\mu\text{m}$ / polymer foils with etched nuclear tracks. A method has been developed for the rapid determination of the optimum values for the factors which may influence the characteristics of the JSC. The JSC is applicable in the interval of 0.1 - 5000 spark/cm<sup>2</sup>. The efficiency is ~100% up to 100 track/cm<sup>2</sup> if the fission fragments enter at right angles to the detector surface. The reproducibility of the counting is ~2% even at ~5000 spark/cm<sup>2</sup>. The number of counts determined by JSC is in good agreement with that observed with optical microscope. The investigations showed that there is no effect of gamma exposures on the counting of fission tracks in the 2,5 - 34,5 Mrad interval.

The decay of the sparking rate and the amplitude distributions of the sparks were studied with a 4000 multi-channel pulse-height analyser.

The JSC method can be used in the personal and emergency neutron dosimetry, safeguards of nuclear materials and evaluation of angular distribution of fission fragments.

- [1] M.Várnagy, J.Szabó, S.Juhász, J.Csikai,  
Nucl.Instr. and Meth. 106 1973 30
- [2] E.Gyarmati, Prize essay /Kossuth University, 1975/
- [3] M.Várnagy, Scientific Session at Kossuth University  
/May 12-13, 1975/ Debrecen
- [4] J.Csikai, IAEA Seminar on the Uses of Cf 252 in  
Teaching and Research /14-18 April, 1975. Karlsruhe/

ESR STUDY OF IRRADIATED POLYMERS

M. Várnagy

The types and kinetics of long-lived free radicals formed upon  $\gamma$ , UV- and neutron irradiation of Lexan, Makrofol E and Makrofol KG polycarbonates, Melinex O polyester, Triafol TN, Triafol TX and T-cellit cellulose-acetates, cellulose-aceto-butirates and cellulose nitrates were studied at 77°K and room temperatures in air and nitrogen atmospheres and in vacuum [1].

These investigations are important to study the characteristics of the solid state nuclear track detectors [2 - 7].

- [1] M.Várnagy, Scientific Session at the Kossuth University /May 12-13, 1975/
- [2] G.Somogyi, M.Várnagy, G.Pető, Nucl. Instr. and Meth. 59 /1968/ 299
- [3] G.Somogyi, M.Várnagy, L.Medveczky  
JOURENTRA /Clermont-Ferrand, 1969/ III-86
- [4] G.Somogyi, M.Várnagy, L.Medveczky  
Radiat. Eff. 5 /1970/ 111
- [5] M.Várnagy, Thesis /Kossuth University, 1970/
- [6] M.Várnagy, J.Csikai, S.Szegedi, S.Nagy,  
Nucl. Instr. and Meth. 89 /1970/ 27
- [7] M.Várnagy, 2nd Meeting of Hungarian Nuclear Physicists /Debrecen, 4-8 June, 1973/

MEASUREMENT OF ELECTRON, X-RAY AND GAMMA  
RAY DOSES WITH SSCTDS

M.Várnagy, M.Osvay, J.Csikai and S.Szegedi

The T-cellit cellulose acetate foil had been found to be suitable for the measurement of doses higher than 1 Mrad [1 - 2].

Now, investigations are in progress to apply polycarbonate, polyester, cellulose-acetate, cellulose-nitrate and cellulose-acetate-butirate foils for the measurement of gamma doses in the 1 - 100 Mrad interval.

[1] M.Várnagy, J.Csikai, S.Szegedi,  
Nucl. Instr. and Meth. 119 /1974/ 261

[2] M.Várnagy, J.Csikai, S.Szegedi,  
Izotóptechnika 17 /1974/ 480

NONDESTRUCTIVE MEASUREMENTS OF SURFACE DENSITY  
ON ROADS

A.Pázsit and S.Sudár

A portable probe has been developed using radioactive isotope for the nondestructive measurement of road surface density. With the equipment one can determine the density of both hot and ready roads within 10 minutes with error of  $\pm 0,01 \text{ g/cm}^3$ . The contribution to the total scattering events from the upper 4 cm thick layer is 97,5 %.

**INSTITUTE OF NUCLEAR RESEARCH**

**OF THE HUNGARIAN ACADEMY OF SCIENCES**

**DEBRECEN**

INSTITUTE OF NUCLEAR RESEARCH OF THE  
HUNGARIAN ACADEMY OF SCIENCES, DEBRECEN

Large experimental equipments of INR.

1./ 5 MV Van de Graaff generator of proton, deuteron and alpha beams

Measuring arrangements for the energy and angular distributions of charged particles have been built, the building of assemblies for gamma and neutron distribution measurements is in progress. The measuring centre of the generator consists of a Nuclear Data 50/50 data collecting and processing system.

2./ 1 MV Van de Graaff generator

This accelerator extends the lower energy limit covered by the generator a/ from 0,8 MeV down to 0,3 MeV. In the accelerator types a/ and b/ basic research of nuclear reactions /reaction mechanism, nuclear data collection/ has been started.

3./ An equipment and program for the "in-beam" measurement of conversion electrons is being now prepared utilizing of semiconductor detectors and superconductive transport magnet, destined for operation in connection with the 5 MeV Van de Graaff generator.

4./ Cockroft-Walton generator with maximum operational voltage of 700 kV

The generator is suitable for the acceleration of protons deuterons and electrons. The available measuring arrangement covers the cross sections for and the angular distributions of /d,p/, /d,alpha/ reactions. Research facilities for use with electron acceleration are now under investigation.

5./ Program for the application of nuclear spectroscopic methods in other disciplines and practice /Nuclear physics, chemical information from internal conversion measurements, ESCA, radioisotopic x-ray fluorescence/.

6./ Neutron Generator

for the production of D+T neutrons with  $D^+$  ions analysed at 150 kV opera-

tional voltage, max. ion current of 500  $\mu$ A. In the recent past  $^{70}\text{Zn}/n,p/$ ,  $^{198}\text{Pt}/n,2n/$ ,  $/n,\text{gamma}/$ ,  $/n,p/$ ,  $/n,d/$  and  $/n,\text{alpha}/$  reactions were studied /cross section measurement, half-life determination and gamma spectroscopy/.

## FAST NEUTRON CROSS-SECTIONS OF Os ISOTOPES

P. Kovács, I. Uray

Cross-section measurements were carried out at 14,7 MeV neutron-energy for several reactions using Os target with the following results.

Reaction:	cross-section [mb]	Reaction:	cross-section [mb]
$^{184}\text{Os}(n,2n)^{183\text{m}}\text{Os}$	$383 \pm 75 \sqrt{\epsilon}$	$^{184}\text{Os}(n,p)^{184\text{g}}\text{Re}$	$100 < \sigma_g < 400$
$^{184}\text{Os}(n,2n)^{183\text{g}}\text{Os}$	$760 \pm 155$	$^{188}\text{Os}(n,p)^{188}\text{Re}$	$6,0 \pm 1,2$
$^{186}\text{Os}(n,2n)^{185}\text{Os}$	$1403 \pm 282$	$^{189}\text{Os}(n,p)^{189}\text{Re}$	$6,5 \pm 1,3$
$^{192}\text{Os}(n,2n)^{191\text{m}}\text{Os}$	$892 \pm 186$	$^{190}\text{Os}(n,p)^{190\text{m}}\text{Re}$	$0,1 \pm 0,02$
$^{192}\text{Os}(n,2n)^{191\text{g}}\text{Os}$	$1176 \pm 196$	$^{190}\text{Os}(n,p)^{190\text{g}}\text{Re}$	$2,4 \pm 0,3$
$^{192}\text{Os}(n, \alpha)^{189}\text{Os}$	$0,15 \pm 0,03$	$^{190}\text{Os}(n, \gamma)^{193}\text{Re}$	$4,0 \pm 0,7$

## DOPPLER BROADENING OF THE LINE AND ANGULAR DISTRIBUTION OF ALPHA PARTICLES IN THE ${}^9\text{Be}(p, \alpha_2){}^6\text{Li}$ NUCLEAR REACTION

Á. Kiss, E. Koltay, Gy. Szabó

Measurements have been performed in order to check the possibilities using line shape analysis of the Doppler broadened gamma lines  $\gamma_i$  instead of measuring the angular distribution of the light particles  $b_i$  emitted in nuclear reactions. The results obtained for the case  ${}^9\text{Be}(p, \alpha_2){}^6\text{Li}$  at bombarding energy  $E_p=2.567$  keV indicate the usefulness of the present method.

## A STUDY OF THE MECHANISM OF $^{14}\text{N}(d,p)^{15}\text{N}$ REACTION AT LOW BOMBARDING ENERGIES

I. Hunyadi, B. Schlenk, A. Valek and T. Vertse

Angular distributions of the proton groups  $p_0$ ,  $p_1+p_2$ ,  $p_3$ ,  $p_4$ ,  $p_5$  from the  $^{14}\text{N}(d,p)^{15}\text{N}$  reaction have been measured between 0.32 and 0.63 MeV deuteron bombarding energy. The experimental data were compared to the incoherent sum of the DWBA and Hauser-Feshbach cross-sections. In most cases the measured and calculated cross-sections agree quite well.

## INVESTIGATION OF THE $^{27}\text{Al}(p,\alpha)^{24}\text{Mg}$ REACTION

I. Hunyadi, E. Koltay, L. Zolnai

Measuring the excitation function and angular distribution curves of the  $^{27}\text{Al}(p,\alpha)^{24}\text{Mg}$  reaction level characteristics have been determined for the resonances at 1568, 1580, 1647, 1662, 1725, 1842, 1899, 1909, 1985, 2040, 2135, 2165, 2179, 2206 keV bombarding proton energies. In the case of the first eight resonances where solid state track detector technique was used both  $\alpha_0$  and  $\alpha_1$  groups have been observed.

# LEVELS OF $^{41}\text{Sc}$ FROM THE $^{40}\text{Ca}(p,p)^{40}\text{Ca}$ REACTION

E. Koltay, L. Végh

To be published in Nuclear Physics

The R-matrix formalism for multilevel cross-sections has been used to analyse the data obtained in the elastic scattering measurements performed on the 5 MV Van de Graaff generator of the Institute. Excitation energies, width and spin-parity values have been given for 30 excited levels of  $^{41}\text{Sc}$  as follows:

3.412 MeV,	1	keV,	$1/2^+$ ;	3.478 MeV,	80	keV,	$1/2^-$ ;
3.728 MeV,	12	keV,	$1/2^-$ ;	3.771 MeV,	0.4	keV,	$3/2^-$ ;
4.500 MeV,	1	keV,	$3/2^+$ ;	4.533 MeV,	12	keV,	$3/2^-$ ;
4.642 MeV,	36	keV,	$1/2^-$ ;	4.775 MeV,	3	keV,	$3/2^+$ ;
4.865 MeV,	2	keV,	$5/2^+$ ;	4.945 MeV,	1	keV,	$5/2^+$ ;
4.947 MeV,	2	keV,	$5/2^-$ ;	5.020 MeV,	6	keV,	$1/2^+$ ;
5.036 MeV,	0.4	keV,	$9/2^+$ ;	5.071 MeV,	3	keV,	$1/2^-$ ;
5.082 MeV,	0.7	keV,	$3/2^+$ ;	5.141 MeV,	3	keV,	$3/2^-$ ;
5.353 MeV,	3	keV,	$3/2^+$ ;	5.372 MeV,	7	keV,	$5/2^+$ ;
5.393 MeV,	4	keV,	$3/2^-$ ;	5.417 MeV,	18	keV,	$5/2^+$ ;
5.488 MeV,	12	keV,	$1/2^-$ ;	5.491 MeV,	1	keV,	$1/2^+$ ;
5.518 MeV,	0.5	keV,	$5/2^-$ ;	5.531 MeV,	20	keV,	$3/2^-$ ;
5.574 MeV,	6	keV,	$3/2^-$ ;	5.647 MeV,	3	keV,	$5/2^-$ ;
5.688 MeV,	1	keV,	$1/2^-$ ;	5.702 MeV,	12	keV,	$1/2^-$ ;
5.706 MeV,	12	keV,	$5/2^-$ ;	5.753 MeV,	7	keV,	$3/2^-$ ;

## INVESTIGATION OF THE STRUCTURE OF $^{45}\text{Sc}$ NUCLEUS

Dang H.U., Fényes T., Gulyás J., Kiss Á., Koltay E., Máté Z.

To be published in ATOMKI Közlemények

The scattered proton and  $\gamma$ -radiations of the  $^{45}\text{Sc}(p,p'\gamma)^{45}\text{Sc}$  reaction have been studied with surface-barrier Si, and Ge(Li) detectors at 2; 2.5; 3; 3.5 and 4 MeV bombarding proton energies. From the 48 gamma rays, associated with the decay of  $^{45}\text{Sc}$  excited levels, 11 are new. The intensity of gamma-rays was measured as a function of the bombarding proton energy. In the proton spectrum 18 inelastically scattered proton groups were observed, which are connected with  $^{45}\text{Sc}$  excited states. The  $\gamma$ -radiation of the  $^{45}\text{Ti} \rightarrow ^{45}\text{Sc}$  decay was also investigated. On the basis of experimental results we propose a new level scheme of the  $^{45}\text{Sc}$  nucleus. Gamma-ray branching ratios have been obtained for the excited levels. From the experimental results and different theoretical calculations conclusions are drawn on the structure of the  $^{45}\text{Sc}$  nucleus.

## DECAY MODES OF $^{190}\text{Re}$

P. Kovács, I. Uray

The decay modes of  $^{190}\text{Re}$  have been investigated by means of (n,p) reaction using 14,7 MeV neutrons. Our measurements indicate that the 3.2 min half-life belongs to the ground state, while the 3.0 h half-life belongs to the metastable state of the  $^{190}\text{Re}$ . The measured gamma transitions indicate that the population of the 1387,3; 1995,5 and 2352,5 keV levels follows the ground-state  $\beta^-$  decay, while energy levels at 1446,5; 1682,0; 1836,6; 2069,7 and 2121,2 keV energies manifest themselves after the  $\beta^-$  decay of the metastable state.

## K-SHELL IONIZATION BY PROTONS FOR Cr, Cu, In AND BY ALPHA-PARTICLES FOR Cr, Cu

E. Koltay, D. Berényi, I. Kiss and S. Ricz

K-shell ionization cross-section by proton and alpha impact was determined in the 0.9-4 MeV region of bombarding energies for Cr and Cu targets as well as for In by protons in the 0.9-2.5 region. The measurements were performed using a 5 MV Van de Graaff generator and Si(Li) X-ray detector. The results are given in tabulation and compared with BEA (binary-encounter approximation).

The publication is in preparation.

## L-SHELL IONIZATION BY ELECTRON IMPACT

B. Schlenk, A. Valek, S. Ricz and D. Berényi

Total L-shell ionization cross-section was determined by electron impact using a Cockroft-Walton generator for Yb and Au in the region from 250 keV to 650 keV by steps of 50 keV. The cross-section values are varied around 900 barn for Yb and around 300 barn for Au. The details are given in table.

The publication is in preparation.

## SEARCH FOR VIRTUAL ELECTRON CAPTURE IN THE INVESTIGATION OF THE INTERNAL BREMSTRAHLUNG FROM THE DECAY OF $^{59}\text{Ni}$

D. Berényi, G. Hock, A. Ménes, G. Székely, Cs. Ujhelyi and A. Zon

The internal bremsstrahlung spectrum from the non-unique second forbidden pure electron capture decay of  $^{59}\text{Ni}$  was investigated in a lime-store low background chamber using a 20 cm<sup>3</sup> Ge(Li) detector to search for the effects of the virtual electron capture in the spectrum-shape of internal bremsstrahlung.

Comparing the experimental data with the Cutkosky, Zon-Rapoport and virtual capture theory, the best fit was found for the Zon-Rapoport theory, and thus the virtual capture theory is not indispensable at the interpretation of the experiment.

Some additional results are also obtained in the present study. Thus, the  $\lambda$  value, the ratio of matrix elements  $\lambda=0,030\pm0,02$ , as well as the total disintegration energy,  $Q(^{59}\text{Ni}-^{59}\text{Co})=1074,2\pm\pm1,3$  keV have been determined. The existence of a positive beta branch was proved with the  $3\cdot10^{-2}$  estimated value of the branching.

The publication is in preparation.

## ELECTRON CAPTURE RATIOS IN THE DECAY OF $^{126}\text{I}$

E. Vatai and L. Andó

The L/K and  $\epsilon/\beta^+$  ratios are investigated in the first forbidden ( $2^- \rightarrow 2^+$ ) decay of I-126 using inner source scintillation technics. Preliminary results do not contradict to the decay to the 666.2 keV level or to the theoretical expectations for the 1420 keV level. Complete evaluation of experimental data, as well as control measurements are now under way.

## SUPERCONDUCTING MAGNETIC SYSTEM FOR NUCLEAR SPECTROSCOPIC APPLICATION

Tárkányi F., Novák D., Füle K.

ATOMKI Közlemények 16/4 (1974) 325-337.

A superconducting magnetic system was built to be used as an electron transporter in an in-beam conversion electron spectrometer. The magnetic characteristics of the system are described.

The field created by the two Nb-Ti coils in a bore of  $\varnothing$  4 cm and in a length of 2x9 cm, has an average field strength of 32 kOe, while its distribution along the axis guarantees that the magnetic mirror effect for the transported electrons will be small.

## EXCITATION OF LIGHT Hg NUCLEI IN THE DECAY OF Tl

T. Fényes, I. Mahunka, Z. Máté, R.V. Jolos\*, V. Paar\*\*

To be published in Nuclear Physics

Recent YASNAPP (Dubna) experimental results on the decay of light thallium isotopes ( $^{188, 189, 190, 191, 192, 193, 194, 195, 197}\text{Tl}$ ) are briefly reviewed. From the systematics of available experimental data on the excited states of light even and odd Hg nuclei general conclusions are drawn. New calculations have been performed for the energy levels and electromagnetic properties of light even Hg nuclei by coupling two valence-shell proton holes (cluster) to the quadrupole core vibration. The properties of light odd Hg nuclei have been calculated on the basis of the pairing plus quadrupole residual interaction model by coupling one neutron quasiparticle to the anharmonic quadrupole core vibration. These nuclei have also been considered by coupling a three-neutron-hole cluster to vibrations. The theoretical results are qualitatively similar in both representations and explain many experimental data.

---

\* Joint Institute for Nuclear Research, Dubna, USSR

\*\* Institute "Rudjer Boskovic", Zagreb, Yugoslavia

## INVESTIGATIONS FOR DETERMINING THE OPTIMUM MEASUREMENT GEOMETRY OF Si(Li) X-RAY SPECTROMETER

M. Kis-Varga and J. Bacsó

The analytical sensitivity of radioisotope excited Si(Li) detector X-ray spectrometer was investigated. The optimum source-sample-detector geometry was determined by measuring the effect of the sizes (diameter and thickness) of the sample, the source-sample and detector-sample distance as well as the effect of the thickness and diameter of the aperture of source-holder upon the intensity of fluorescent X-rays. Good agreement was found between the theoretically calculated and experimentally measured sensitivity in the atomic number region  $Z=20-40$ .

## THE DETERMINATION OF TRACE-ELEMENTS BY Si(LI) X-RAY SPECTROMETER IN CIGARETTES

J. Bacsó, G. Kalinka, M. Kis-Varga, Cs. Ujhelyi

The trace-element content of cigarettes was measured by radioisotope excited X-ray fluorescence method. The inorganic constituents in cigarette tobacco, dropped ash, cigarette paper and cigarette smoke condensate were determined in the atomic number region  $Z=19-82$ .

It was found that the substantial amount of trace-elements in tobacco was transferred into smoke.

## ON THE SELF-CONSISTENCY OF THE LANE MODEL

R. G. Lovas

Individual search has been performed for the parameters of the Lane potential by fitting two of the  $(p,p)$ ,  $(p,\bar{n})$  and  $(n,n)$  differential cross-sections for a selection of nuclei. The Lane potential obtained has been tested by a comparison with the cross-section of the third process. It is concluded that only the approach of fitting  $(p,p)$  and  $(p,\bar{n})$  is practicable, and the description of the  $(n,n)$  cross-section is satisfactory only if average proton potential is used and if the real and imaginary parts of the symmetry potential are not allowed to vary independently.

ROLAND EÖTVÖS UNIVERSITY

DEPARTMENT FOR ATOMIC PHYSICS

BUDAPEST

INVESTIGATION OF THE  $3/2^-$  770 keV SHORT-LIVED ISOMERIC STATE OF  $^{51}\text{Cr}$  EXCITED BY 14.7 MeV FAST NEUTRONS

F. Deák, S. Gueth, P. Kálmán and Á. Kiss  
Acta Phys. Hung. 37./1974/ 339.

The production of  $3/2^-$  770 keV short-lived isomeric state of  $^{51}\text{Cr}/n, 2n/$  reaction at 14.7 MeV neutron energy. The measured cross section, combined with that known for the whole  $/n, 2n/$  process from other experiments, was used to determine the spin-cut-off factor after deriving the isomeric ratio. The half-life of the  $3/2^-$  state was deduced as well.

EXPERIMENTAL INVESTIGATION OF THE NEUTRON-GAMMA COMPETITION IN 14.7 MeV FAST NEUTRON REACTIONS

F. Deák, S. Gueth, J. Inczédy and Á. Kiss  
Acta Phys. Hung.

The energy spectra of the evaporated neutrons from  $^{55}\text{Mn}$  and  $^{209}\text{Bi}$  targets were investigated at 14.7 MeV bombarding energy in order to learn about the probability of the  $/n, n\gamma/$  process at excitation energies, where the evaporation of the second neutrons was energetically allowed. The role of the gamma deexcitation proved to be negligible in the case of the Bi target, while the measurements on Mn provided evidence for considerable larger gamma competition than expected on the basis of the usual statistical assumptions.

DETERMINATION OF THE NITROGEN CONTENT OF THE ORGANIC  
COMPOUNDS BY MEANS OF FAST NEUTRON ACTIVATION ANALYSIS

F. Deák, S. Gueth, Á. Kiss and Cs. Sükösd

The aim of this work was to investigate the possibility of the adoption of activation analysis by 14 MeV neutrons for the determination of the nitrogen content in the organic compounds. The activity with 10 minutes half-life, produced in the  $^{14}\text{N}/n, 2n/^{13}\text{N}$  reaction at 14 MeV neutron energy, is suitable for the exact, fast determination of N content without destruction of the sample. The necessary weight of the samples are 1-5 g. The deviation of the determined N content is better than 10 %.

B.A.R.C.-831

GOVERNMENT OF INDIA  
ATOMIC ENERGY COMMISSION

PROGRESS REPORT ON NUCLEAR DATA ACTIVITIES  
IN INDIA - XI

Compiled by

M. Balakrishnan  
Indian Nuclear Data Group  
Nuclear Physics Division

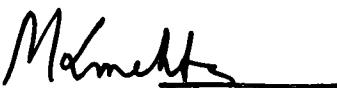
BHABHA ATOMIC RESEARCH CENTRE  
BOMBAY, INDIA  
1975

## I N T R O D U C T I O N

The eleventh progress report on Nuclear Data Activities in India covers the work done during the calendar year 1974. A part of the work reported here has been presented at the Nuclear Physics and Solid State Physics Symposium held at Bombay during December 1974 as well as some work done during the current year. Apart from the work done in the field of nuclear fission the major thrust of work in India is directed towards basic Nuclear Physics research both theoretical and experimental. The experiments predominantly involve charged particle reactions or level scheme studies. However during the current year a small programme has been started with a view to assess the feasibility for measuring neutron capture data on  $^{233}\text{Th}$  between 0.1 and 2 MeV to 5% accuracy. It is hoped to evolve this programme into a more extensive data measuring and evaluation programme for Thorium cycle data which may involve collaboration between a few laboratories in India as well as Bangladesh. A short summary of this preliminary work is given as items number 20, 21 and 22 under section A.

The total number of CINDA entries sent to the Nuclear Data Section of the International Atomic Energy Agency during the period of report is 15. The liaison activity with computer programme library (CPL) of the NEA was continued.

Among the new facilities, the installation of the 224 cm Variable Energy Cyclotron has progressed to a stage where beam trials are expected to start during December this year. The design of the 100 MeV thermal research reactor is frozen and the civil works have started.



(M.K. Mehta)

Convener,  
Indian Nuclear Data Group.

<u>I N S T I T U T I O N</u>	<u>P A G E</u>
A. Bhabha Atomic Research Centre, Bombay	132
B. Tata Institute of Fundamental Research, Bombay	149
C. Saha Institute of Nuclear Physics, Calcutta	155
D. Andhra University, Waltair	160
E. Banaras Hindu University, Varanasi	169
F. Birla Institute of Technology, Pilani	173
G. Burdwan University, Burdwan	175
H. Dibrugarh University, Assam	176
I. Indian Institute of Technology, Kanpur	177
J. Kurukshetra University, Kurukshetra	180
K. Marathwada University, Aurangabad	183
L. Physical Research Laboratory, Ahmedabad	184
M. Punjab University, Chandigarh	194
N. Punjabi University, Patiala	198
O. Reactor Research Centre, Kalpakkam	201
P. University of Delhi, Delhi	202
Q. University of Madras, Madras	205

INDIAN NUCLEAR DATA GROUP

MEMBERS

- |                                |   |                                                                                            |
|--------------------------------|---|--------------------------------------------------------------------------------------------|
| 1. M. Balakrishnan(Secretary): |   | Nuclear Physics Division<br>*BARC.                                                         |
| 2. B.B. Baliga                 | : | Saha Institute of Nuclear<br>Physics, 92 Acharya Prafulla<br>Chandra Road, Calcutta - 9.   |
| 3. V.C. Deniz                  | : | Experimental Reactor Research<br>Section, BARC.                                            |
| 4. A.S. Divatia                | : | Variable Energy Cyclotron<br>Project, Calcutta.                                            |
| 5. S. Gangadharan              | : | Analytical Chemistry Division<br>BARC.                                                     |
| 6. S.B. Garg (Co-opted)        | : | Reactor Engineering Division<br>BARC.                                                      |
| 7. M.C. Joshi "                | : | Department of Physics,<br>University of Bombay,<br>C.S.T. Road, Kalina,<br>Bombay 400 029. |
| 8. S.S. Kapoor                 | : | Nuclear Physics Division<br>BARC.                                                          |
| 9. M.K. Mehta (Convener)       | : | Nuclear Physics Division<br>BARC.                                                          |
| 10. S.K. Mitra (Co-opted)      | : | Tata Institute of Fundamental<br>Research, Homi Bhabha Road,<br>Bombay - 400 005.          |
| 11. M.P. Navalkar "            | : | Neutron Physics Section<br>BARC.                                                           |
| 12. B.P. Rastogi               | : | Theoretical Reactor Physics<br>Section, BARC.                                              |
| 13. N.S. Satya Murthy          | : | Nuclear Physics Division<br>BARC.                                                          |
| 14. M. Srinivasan              | : | Neutron Physics Section<br>BARC.                                                           |

---

\* Bhabha Atomic Research Centre,  
Trombay, Bombay 400 085.

A. BHABHA ATOMIC RESEARCH CENTRE, BOMBAY 400 085

1. Analytic Distorted Waves for DWBA Calculations -

N.K. Ganguly and D.K. Srivastava - In the computation of T matrix for reaction channels the required distorted waves are generated by numerically integrating the scattering equation. In case a finite range interaction is used the requirement on the computer time for T matrix evaluation becomes prohibitive. To circumvent this difficulty some attempts have been made by a number of workers<sup>1)</sup>.

It is shown that an analytic scattering function can be obtained by expanding it in terms of the product of a plane wave and the value of the  $\psi$  -function at the scattering center and its derivatives. Analytic expression for a square-well potential and comparison of the elastic scattering cross-section obtained in this fashion with the results of exact calculation is presented.

The convergence of the series-expansion of the scattering  $\psi$  -function and its implication for the general DWBA analysis of reaction mechanism is studied.

1) R.T. Janus and I.E. Mc Carthy, Phys. Rev. C10C(1974)1041 and references therein.

2. Effect of Stripping Channel on Energy Dependence of Deuteron

Optical Potential - S. Pal, D.K. Srivastava, N.K. Ganguly and S.N. Mukherjee\* - Coupled-channel calculation has been done for

---

\* Physics Dept., Banaras Hindu University, Varanasi.

$^{48}\text{Ca}$ , coupling the elastic and p-stripping channel at five energies of the incident deuteron, e.g. 5.0, 7.2, 10.0, 13.0 and 16.0 MeV. The stripping cross-sections are in good agreement with experimental data. The calculated elastic scattering cross-sections fit the experimental values qualitatively.

Coupling of reaction channels is expected to remove energy dependence of the optical potential used in the elastic channel excepting the intrinsic one. In case of  $^{48}\text{Ca}$ , the energy gap between  $0^+$  g.s. and  $2^+$  first excited state being large (3.83 MeV), the coupling of the most probable stripping channel is expected to remove most of the energy dependence. This was investigated by fitting the coupled-channel prediction for the elastic scattering cross-section with a conventional optical model search code. The nature of the energy dependence of the d- $^{48}\text{Ca}$  optical potential is similar mainly for the imaginary part as obtained by other workers in the case of  $^{40}\text{Ca}$  both by coupled-channel analysis and analysing elastic scattering data.

3. Consistent Microscopic and Phenomenological Analysis of Composite Particle Optical Potential - Sheela Mukhopadhyay\*, D.K. Srivastava, N.K. Ganguly - A microscopic calculation of composite particle optical potential has been done using a realistic nucleon-helion interaction and folding it with the density distribution of the targets. The second order effects were simulated by introducing a scaling factor which was searched

---

\* Ph.D. Student

on to reproduce the experimental scattering results. Composite particle optical potential was also derived from the nucleon-nucleus optical potential. The second order term was explicitly treated as a parameter. Elastic scattering of 20-MeV- $^3\text{H}$  on targets ranging from  $^{40}\text{Ca}$  to  $^{208}\text{Pb}$  have also been analysed using phenomenological optical model. Agreement of these results with above calculations verified the consistency of the microscopic theory. But the equivalent sharp radius calculated with n-helion interaction was observed to be smaller than phenomenological value. This was attributed to the absence of saturation effects in the density-independent interaction used. Saturation has been introduced by a density dependent term of the form  $(1 - c f^{2/3})$ , where  $f$  is the compound density of the target helion system.

#### 4. Assymetry Dependence of Proton Optical Potential -

D.K. Srivastava, S. Mukhopadhyay\*, S. Pal and N.K. Ganguly - In the optical-model studies the half-value radius of nuclear potential is adopted to vary as  $A^{1/3}$ . However, it is known from various studies that at least in isotopic sequences, the half-value radius increases less rapidly than  $A^{1/3}$ . This is easily resolved by considering the concept of equivalent sharp radius<sup>1,2)</sup>. The proton elastic scattering data for 64,66,68-Zn at 30 MeV, for 64, 66,68-Zn at 50MeV, for 112,114,116,118,120,122,124-Sn at 30 MeV and 144,148,150,152,154-Sn at 50 MeV have been analysed using simple optical model, with above mentioned modification, with a view to know the isospin dependence of optical potential parameters,

\*Ph.D. Student

In addition to finding isospin dependence of parameters, the volume integral of imaginary potential per nucleon is found to vary linearly with the asymmetry parameter  $(N-Z)/A$ . This taken along with similar variation for  $Q$  value for  $(p,n)$  reactions may lead to better understanding of the imaginary potential.

- 1) W.D. Myers, Nucl. Phys. A204 (1973) 165
- 2) D.K. Srivastava, N.K. Ganguly and P.E. Hodgson, Phys. Lett. 51B (1974) 439

5. Study of the Reaction  $^{55}\text{Mn}(p,n)^{55}\text{Fe}$  from  $E_p = 1.35$  MeV to 5.4 MeV - S. Kailas, Y.P. Viyogi, S.S. Saini, S.K. Gupta, N.K. Ganguly, M.K. Mehta, A. Banerjee, S.S. Kerekatte - The total  $(p,n)$  cross-section for the reaction  $^{55}\text{Mn}(p,n)^{55}\text{Fe}$  was measured in 5keV steps using a  $^{55}\text{Mn}$  target ( $\sim 8$  keV thick for  $E_p = 3$  MeV) and a  $4\pi$ -geometry neutron counter, from  $E_p = 1.35$  MeV to 5.4 MeV. The excitation function exhibits a large number of resonances, some of which can be identified with the isobaric analogue states in the compound nucleus  $^{56}\text{Mn}$ . The excitation function averaged over 200 keV energy interval is analysed on the basis of optical model. Hauser Weshbach theory with Moldauer's modification is used to get the fit to the experimental data. The isobaric analogue resonance at  $E_p = 1.54$  MeV is analysed to get the spectroscopic factor.

6. Microscopic Approach to Back-bending Effects in  $^{158}\text{Er}$  and  $^{162}\text{Er}$  - M.R. Gunye - The recently observed high spin states in the rare earth nuclei are studied in a self-consistent variational approach with the angular momentum projected Hartree-BCS wavefunctions. The nuclear Hamiltonian employed in the present work consists of the pairing plus quadrupole interactions. The nuclear deformation  $B$ , the neutron pairing gap  $\Delta_n$  and the proton pairing gap  $\Delta_p$  are varied to obtain the minimum energy for each angular momentum state. Our results rule out the suggestion of a phase transition from a superconducting to a normal state at the critical angular momentum  $J \approx 12$ . On the other hand, our results favour the interpretation of the back-bending effect in terms of a two-band theory. It should, however, be pointed out that the pairing gaps  $\Delta_p$  and  $\Delta_n$  decrease with the increase in angular momentum  $J$ . The calculated energy spectra in  $^{158}\text{Er}$  and  $^{162}\text{Er}$  are in good agreement with the recent experimental data.

7. A Note on the Determination of Fragment Mass, Energy and Angular Distributions with a Double Gridded Ionisation Chamber - N.N. Ajitanand and S.S. Kapoor - Data recorded earlier<sup>1)</sup> event by event on magnetic tape with a double gridded ionisation chamber for the case of thermal and 2.2 MeV neutron induced fission of  $^{235}\text{U}$  has been used to investigate the detailed characteristics of observed fragment distributions at various angles with respect to the electric field direction of the chamber. The relation between the grid and collector pulse heights enabled an event by event

evaluation of the energy and angle of the fission fragments. The energy and mass distributions of the fragments emitted at different angles were then studied and it was found that these distributions are significantly distorted at angles near  $90^\circ$  due to target thickness effects. By considering the data at those angles where energy degradation effects are small, one is able to obtain the mass distributions at various angles in fast and thermal neutron fission. The fast neutron distribution is divided by the thermal neutron distribution at each angle to bring out any possible dependence of the mass asymmetry on the angle in fast neutron fission.

1) N.N. Ajitanand, R.K. Choudhary, S.R.S. Murthy, P.N. Rama Rao and S.S. Kapoor, Nucl. Phys. & Solid State Phys. (India) 16B, (1973).

8. Higher Isospin States in  $^{36}\text{Ar}$  through  $\alpha$  Particle Capture Resonances - D.R. Chakrabarty, M.A. Eswaran, H.H. Oza and N.L.

Ragoowansi - With a view to locating and studying the higher isospin states in the self-conjugate nucleus  $^{36}\text{Ar}$ , the excitation function in the reaction  $^{32}\text{S}(\alpha, \gamma)^{36}\text{Ar}$  has been obtained in the bombarding energy range,  $E_\alpha = 4.5$  to  $4.8$  MeV. An isotopically enriched  $^{32}\text{S}$  target of 10Kev thickness and a large volume NaI(Tl) scintillation detector for gamma rays were used. Two isolated resonances at  $E_\alpha = 4.53 \pm 0.01$  and  $4.69 \pm 0.01$  MeV have been located, corresponding to the excitation energy in  $^{36}\text{Ar}$  of  $E_{\text{ex}} = 10.67$  and  $10.82$  MeV respectively. The decay of these resonances have been determined as also the absolute strengths, to

be  $0.86 \pm 0.13$  eV and  $2.2 \pm 0.2$  eV respectively. Angular distribution at the  $E_{\alpha} = 4.69$  MeV resonance has also been measured. Based on these measurements, possible spin and isospin assignments of these resonances are discussed.

9. Resonance Spectroscopy of  $^{30}\text{Si}$  Nucleus in the Excitation Energy Range 14.276 MeV to 15.022 MeV. - L.V. Namjoshi\*, S.K. Gupta and M.K. Mehta - Excitation functions for the reaction  $^{26}\text{Mg}(\alpha, \alpha)^{26}\text{Mg}$  from 4.185 MeV to 5.145 MeV lab. energy measured at angles  $81^{\circ}$ ,  $118^{\circ}$ ,  $135^{\circ}$  and  $165^{\circ}$  have been analysed using R-matrix theory of nuclear reactions. The computer program MULTI coding the multi-level-multichannel expression for differential cross section has been used for the purpose. Shape analysis of the observed anomalies have resulted in identification of nine levels in the compound nucleus  $^{30}\text{Si}$ . The excitation energies and spins and parities of these levels are  $14.320(0^{+})$ ,  $14.376(0^{+})$ ,  $14.597(0^{+})$ ,  $14.647(2^{+})$ ,  $14.675(1^{-})$ ,  $14.718(3^{-})$ ,  $14.874(0^{+})$ ,  $14.918(3^{-})$  and  $15.022(4^{+})$  MeV. Tentative determination of total widths and partial widths for  $(\alpha, \alpha)$  channel have been made. The average cross section differs from Rutherford cross section by about 30% at all angles except at  $81^{\circ}$ . The average cross section could be fitted with optical model even though the incident energy is about 2 MeV below the Coulomb barrier.

---

\* NSTS Scholar.

10.  $^{19}\text{F}(\alpha, n)^{22}\text{Na}$  Reaction in the Energy Range 2.6 to 5.1 MeV -

M. Balakrishnan, S. Kailas, S.S. Kerekatte and M.K. Mehta - Absolute total cross section for the reaction  $^{19}\text{F}(\alpha, n)^{22}\text{Na}$  has been determined for the incident alpha energy range  $E_\alpha = 2.6$  to 5.1 MeV using thin target ( $\sim 6$  keV for 2 MeV alphas) and in fine steps of 5 keV. The excitation function shows some isolated resonances and also some cluster of states in  $^{23}\text{Na}$  in the energy of excitation 12.6 to 14.7 MeV. An average strength function is extracted for the alpha-widths in this energy range. The results are compared with existing similar data in this region, obtained from gamma ray information.

11.  $^{29}\text{Si}(\alpha, n)^{32}\text{S}$  Reaction near Threshold - M. Balakrishnan,

S. Kailas, S.S. Kerekatte and M.K. Mehta - The low energy neutron cross sections are interesting both from nuclear spectroscopy points and of astrophysical points. We have measured the reactions  $^{29}\text{Si}(\alpha, n)^{32}\text{S}$  just near the threshold in the energy range  $E_\alpha = 1.8$  to 2.5 MeV after reducing back ground effects substantially. The  $(n, \alpha)$  cross sections were obtained using reciprocity relations. The reaction shows some interesting structures of width around 80keV wide and the alpha width, neutron width and reduced widths have been extracted for these structures. The possible significances of there structures are discussed. The average alpha strength functions indicates an abnormal behaviour in this region.

12 Alpha Particle Trajectory Calculations in Spontaneous Ternary Fission of  $^{252}\text{Cf}$  and Studies of Scission Point Configurations -

R.K. Ghoudury and V.S. Ramamurthy - Three-point-charge model trajectory calculations have been carried out to search for possible scission configurations in spontaneous ternary fission of  $^{252}\text{Cf}$ . The distribution of fragment kinetic energies and alpha particle energies for various mass divisions were used as input. Three parameters were used to specify the scission configuration: the interfragment distance  $D$ , the distance of the alpha particle from the heavy fragment  $X$ , and the distance of the alpha particle from the fission axis  $Y$ . As different from similar earlier investigations, for each mass division, not only the most probable values of the parameters  $D, X$  and  $Y$  but also their variances have been obtained. It is shown that with these parameters as input, it is possible to explain most of the experimentally observed energy and angular correlations. An important conclusion arising out of the present investigations is that the alpha particles originate nearer to either one of the fragments.

13. Alpha Particle Trajectory Calculations in Spontaneous

Quaternary Fission of  $^{252}\text{Cf}$ . - S.K. Kataria - The trajectory calculations have been performed in an attempt to explain the energy and angular correlations between the two light charged particles (LCP) emitted in the spontaneous fission of  $^{252}\text{Cf}$ . Three possible emission mechanisms and scission configurations for LCP have been

tested with trajectory calculations and compared with the observed energy and angular correlations. The first hypothesis is that the two LCP are the result of breakup of  $^8\text{Be}$ . The second hypothesis is that the two LCP are produced in between the fragments near the axis of separation, simultaneously. The last hypothesis tested is that the two LCP are being emitted from the two fragments independent of each other. Only the last hypothesis predicts angular and energy correlation in agreement with the experimental results. From trajectory calculations for quaternary fission, many important conclusions have been reached regarding the emission mechanism of LCP.

14. Three Dimensional Correlations of Fragment Mass, Fragment Energy and Long Range Alpha Particle (LRA) Energy in the Fission of U-235 by Thermal Neutrons - D.M. Nadkarni, R.K. Chaudhury, S.R.S. Murthy, P.N. Rama Rao and S.S. Kapoor - To investigate in detail the various correlations between the energy and mass of fission fragments and LRA energy we have carried out a 3-parameter investigation in the thermal neutron fission of U-235. A back-to-back gridded ionization chamber was used to measure the energies of correlated fragments and the energy of coincident LRA was measured with semiconductor detectors. This setup ensured that events recorded are not restricted to any particular angle between fragments and LRA but cover all the angles. The data have been analysed to obtain total coulomb energy distributions in binary and

ternary cases. The average LRA energy was seen to decrease with asymmetry in mass division. One other new feature observed was the non-linear anticorrelation between  $E_k$  and  $E_\alpha$  and the dependence of this anticorrelation on the mass asymmetry. With these data scission parameters in ternary fission are derived by carrying out trajectory calculations.

15. Shape Mixing in  $^{184,186}\text{Hg}$  - C.V.K. Baba - Recent potential energy calculations on even Hg isotopes have shown that  $^{184,186}\text{Hg}$  are possibly deformed with two energy minima one each for oblate ( $\beta_2 = -0.14$ ) and prolate ( $\beta_2 = 0.28$ ) shapes. The quasi-rotational levels in these nuclei have been studied by heavy ion reactions at Berkeley and Chalk River. The salient features of these studies are (i) a deviation of the energy levels from a rotational sequence for  $I \leq 6$ ; the levels with higher spins showing a good rotational spectrum and (ii) the deviation of the  $4^+ \rightarrow 2^+$  and  $2^+ \rightarrow 0^+$ , E2 transition rates from the rotational value with  $\beta_2 = 0.28$ . These features of the spectra are explained on the basis of mixing of bands based on the oblate and prolate shapes. The results of a simple band mixing calculation are presented and they reduce the observed level spacings and  $B(E2)$  values.

16. Nuclear Structure Study of  $^{50}\text{V}$  by the  $^{50}\text{Ti}(p,n\gamma)^{50}\text{V}$  Reaction - S.K. Gupta, S. Saini, L.V. Namjoshi and M.K. Mehta - The information on gamma ray transitions, branching ratios, spins and parities of

low-lying levels of  $^{50}\text{V}$ , has been obtained by Ge(Li)-Ge(Li) coincidence measurements. Comparison of the experimental results has been made with the calculations using lowest seniority shell model wavefunctions.

18. On the Fundamental Representation of SU(3) Group - S.K. Gupta and I.V.V. Raghavacharyulu - In terms of Biedenharn basis it has been shown that the fundamental representation of SU(3) group is dependent only on one parameter. The expressions for the fundamental representation matrices have been derived in terms of this parameter. Gellmann-Nishijima representation turns to be one of the representations which is obtained by substituting different values for the parameter.

19; Spectra of Doubly Odd-Nuclei - S. Saini and S.K. Gupta - The energy levels of doubly odd nuclei like  $^{42}\text{Sc}$ ,  $^{48}\text{Sc}$  and  $^{50}\text{V}$  have been calculated. The two body residual interaction employed has been a schematic one consisting of a short range delta-function plus a long range quadrupole-quadrupole interaction. We have assumed neutron and proton seniorities to be good quantum numbers and used the lowest seniority wave-functions in all these calculations. The experimental spectra are satisfactorily fitted when the parameters of the interaction are suitably adjusted.

20. Measurement of Neutron Capture Cross Section on  $^{232}\text{Th}$

between 0.1 and 2 MeV - H.M. Jain, S.K. Gupta, R.P. Anand, R.N.

Jindal and M.K. Mehta - The capture cross sections on  $^{232}\text{Th}$  reported in the literature in the above energy range have errors of the order of 20%. There are large discrepancies between different sets of data. The earlier work was generally done by measuring the induced  $\beta$  activity of  $^{233}\text{Th}$ . In order to remove the discrepancy and as a check on the previous work it is proposed to measure the cross section with reduced errors. This would be done by measuring the intensity of a few delayed gamma lines emitted following the  $\beta$  decay. With the help of an accurately calibrated Ge(Li) detector this can be done to within less than 10% error. This would require the knowledge of the branching ratios for various gamma rays also to an accuracy better than 10%. Preliminary work to measure this branching ratios and relative photopeak efficiency has been started. A simultaneous irradiation of one thorium and one gold foil, both of 14 mm diameter, was done in a well thermalized neutron flux ( $\sim 10^9$  n/cm<sup>2</sup>/sec) at the CIRUS reactor at Trombay for 15 minutes. The gamma spectra of the irradiated were measured with a 27 cc Ge(Li) detector with resolution 3.3 keV FWHM at 662 keV. The ~~measured~~ intensities of seven different photopeaks ( 162, 169, 441, 448, 459, 670 and 678 keV) were extracted, and identified to be arising from the decay of  $^{233}\text{Th}$  as shown by their half life. The 459 and 670 keV gammas were found to be prominent. The photopeak efficiencies of the seven gammas will be measured relative to the 412 keV gamma from  $^{198}\text{Au}$ . The computer

program SAMPO was adapted to BESM-6 for fitting the multiple peaks.

Using the measured relative efficiencies and thermal neutron capture cross-section  $^{232}\text{Th}$  and  $^{197}\text{Au}$ , the branching ratios for the seven gammas will be calculated. These branching ratios and the known neutron capture cross-section  $^{197}\text{Au}$  will be used to measure the capture cross section for  $^{232}\text{Th}$  for higher energy neutrons. The capture cross section on gold is known to an accuracy of 3-4%. However absolute measurement is also planned where the neutron flux will be measured utilising a silicon surface barrier sandwich system which is being developed as described below.

#### 21. Neutron Spectrum and Flux Determination using Silicon

Surface Barrier Sandwich System - O.P. Joneja, J.C. Coachman

and M.P. Navalkar - Among several neutron detectors available, a silicon surface barrier sandwich system enclosing a suitable

radiating material can be effectively employed for finding neutron

spectrum as well as neutron flux. The radiating material

chosen for the purpose could be  $\text{He}^3$  or  $\text{Li}^6$ . The process of

detection involves neutron interaction with the radiating

material, resulting thereby in two charged particles moving

approximately in the opposite direction, which can be easily

detected by two separate detectors arranged in a sandwich geometry.

In order to establish one to one correspondance between neutron

energy and pulse height, the individual outputs are added up and in addition a coincidence unit is incorporated to avoid single particle events. The analyser output is to be corrected for energy dependent geometry effects, variation of cross-section with respect to energy and finally resolution correction because of finite resolution of the system under consideration. The leakage factors associated with geometry have been simulated by Monte-Carlo method whereas the desired point x-sections are suitably interpolated from the available nuclear data. As regards resolution correction, a special advancing matrix is constructed from the thermal response of the spectrometer which can be suitably operated on the cross-section vector to generate a new cross-section set. The resulting cross-section set would obviously contain the effect of resolution correction.

In order to determine the neutron flux for definite neutron energies produced from an accelerator, the resolution correction can be avoided in case the energy spread due to the finite solid angle is smaller than the resolution of the system. The neutron flux can then be evaluated from the counts under the peak and suitable leakage and cross-section correction. In order to measure neutron fluxes within the error of neutron cross-section for the reaction of interest, a high degree of accuracy is desired for identical properties of detectors as well as for finding the total number of radiating atoms in the system and defining the areas of the detector correctly.

All the electronics has been fabricated for this spectrometer and initial calibration, study of the detector

behaviour etc. are in progress.

22. Summary of the cross section work done in TRPS of Reactor Group - S.B. Garg - Thorium utilization in fast reactors gives rise to Th-233 which is very short lived, its half-life being 22 minutes. Th-233 affects the production of U-233 especially in high flux fast reactors when the capture reaction is taking place at a very rapid rate compared to its  $\beta$ -decay process. The cross-sections of Th-233 are, thus, important and these have not been measured at all.

To fill this void optical model was used to determine the total, elastic and compound nucleus formation cross-sections in the energy 0.1 MeV to 20.0 MeV. Channel theory of fission and dipole radiation theory were then used to estimate the fission and the capture cross-sections.

In addition to the above, following programmes have been pursued:

- (1) Evaluation of neutron cross-sections in the resolved and unresolved resonance regions:
  - (i) A computer code RESEND to evaluate the neutron cross-section, in the resolved and unresolved resonance regions was modified and commissioned on CDC-3600 computer. The code consists of two overlays and is based on single and multilevel Breit Wigner theory and Adler and Adler formalism in the resolved resonance region, and Lan and Lynn theory in the unresolved resonance region.

(ii) Cross-sections for Na, Fe, Cr, Ni, Th-232, Pu-233, U-233, U-234, U-235, U-236, Pu-238, Pu-239, Pu-240, Pu-241, Pu-242, Am-241, Am-243 and Cm-244 were evaluated in resonance regions with the resonance parameters taken from ENDF - data files and the point cross-sections thus generated were combined with the background corrections listed in ENDF-files. These cross-sections can, now, directly be used in generating the unbroadened dilute multigroup cross-sections for reactor physics studies.

(2) Generation of Legendre coefficients and Transformation matrices:

In reactor physics studies the Legendre coefficients are used in the ultrafine group treatment of the neutron propagation in order to calculate correctly the elastic transport and elastic removal cross-sections and therefore these coefficients are generated at thousands of energy points. The transformation matrices are calculated to transform these coefficients from CM to Lab system.

Using the updated scattering cross-section data from ENDF-files the Legendre coefficients have been generated at 1021 energy points in the energy range 0.4 eV to 10 MeV with a constant lethargy width of 1/60 for the nuclides B, C, N, Be, O, Na, Cr, Fe and Ni.

(3) Generation of multigroup cross-sections

To carry out the reactor physics studies multigroup cross-sections for fissile, fertile and structural materials have been generated in the energy range 0.2 eV to 15 MeV using the point cross-section data from ENDF-files. The discrete level, inelastic and (n,2n) scattering matrices have also been evaluated.

B. TATA INSTITUTE OF FUNDAMENTAL RESEARCH BOMBAY 400 005.

1. Internal Conversion Process and Core-Polarization g-Factors -

B.N. Subba Rao - Since 1959 there have been reported several measurements of the Nuclear structure (Penetration) effect in M1 Internal Conversion in non-deformed as well as deformed nuclei. Very few of these can be explained with the present day nuclear models. Where such explanations have been attempted, only the numerator of the penetration parameter  $\lambda$ , i.e. the penetration matrix element has been evaluated with the model, resulting in signless (absolute) magnitudes for  $\lambda$ . The  $l$ -forbidden M1 transitions are of special concern in (non-deformed) retarded M1 transitions and here an effective operator approach is employed to evaluate not only the core polarization g-factor,  $g_p$ , but also the penetration parameters,  $\lambda$ , with their sign. In order to keep track of phase conventions in the definition of nuclear matrix elements, the amplitudes of multipole mixing ratio,  $\delta(E2/M1)$ , are also evaluated. With such simultaneous comparison of  $\lambda$  and  $\delta$  from both experiment and theory, it is believed that a better picture emerges as to the nuclear structure information emerging from these penetration effect measurements. Odd-proton and odd-neutron  $l$ -forbidden M1 transitions in  $^{121}\text{Te}$ ,  $^{123}\text{Te}$ ,  $^{129}\text{I}$ ,  $^{133}\text{Cs}$ ,  $^{141}\text{Pr}$ ,  $^{143}\text{Pr}$ ,  $^{147}\text{Pm}$ ,  $^{149}\text{Pm}$ , ( $^{175}\text{Lu}$ ,  $^{181}\text{Ta}$ ),  $^{197}\text{Au}$ ,  $^{201}\text{Tl}$ ,  $^{203}\text{Tl}$ ,  $^{207}\text{Tl}$ , are considered in this work.

2. g Factor of the 635.4 keV  $7/2^+$  Level in  $^{171}\text{Tm}$  - S.B. Patel<sup>\*</sup>, P.N. Tandon and K.P. Gopinathan<sup>+</sup> - The 635.4 keV level in  $^{171}\text{Tm}$  fed in the  $\beta$  decay of the 7.5 h  $^{171}\text{Er}$  was recently identified unambiguously to be the  $7/2^+(404)$  Nilsson state from directional correlation studies of  $\gamma$  rays through that level<sup>1)</sup>. The half-life of this level was measured to be  $1.26 \pm 0.06$  nsec by delayed coincidence technique<sup>1)</sup>. Here we report the measurement of the g factor of this level using the perturbed angular correlation technique. The measurement was made using the 277.4 - 210.5 keV  $\gamma$ - $\gamma$  cascade in an externally applied magnetic field of 10.0kG. The results are:  $A_2 = 0.124 \pm 0.005$ ,  $R = 0.047 \pm 0.007$ , and  $\omega\tau = 0.160 \pm 0.023$ . Assuming Tm to be in the  $3^+$  ionic state after  $\beta$  decay of  $^{171}\text{Er}$ , the g factor is obtained to be  $0.36 \pm 0.06$ . This value is in good agreement with the Nilsson estimate ( $g = 0.41$ ) for this level.

\* Present address: Ramnarain Ruia College, Bombay

+ Present address: Reactor Research Centre, Kalpakkam,

1) K.P. Gopinathan and S.B. Patel, in Proc. Internat. Conf. Nucl. Phys., Munich, 1973, Vol. I, p 300.

3. Potential Energy Curves from the Strutinsky Prescription and from a Microscopic Approach - Y.S.T. Rao, C.S. Warke and S.K. Mukhopadhyay - Strutinsky shell correction method has been quite successful in getting potential energy curves for heavy nuclei. The more microscopic pairing-plus-quadrupole (PPQ) model as used

by Kumar and Baranger has been extremely successful in explaining the properties of medium heavy nuclei. Because of this reason, it is worth extending shell correction methods towards lighter mass region and PPQ model to heavier mass region and compare their results. We present results of both these methods in the neighbourhood of Os, Pt, Hg and W, and compare the deformation energy curves of these two methods. We discuss the significant differences and similarities in the predictions of these two methods and try to reconcile them.

4. Study of Isobaric Analogue States in  $^{64}\text{Zn}$  through Proton Capture by  $^{63}\text{Cu}$  - A. Roy, K.V.K. Iyengar and M.L. Jhingan -  
The reaction  $^{63}\text{Cu} (p, \gamma) ^{64}\text{Zn}$  has been studied in the proton energy range 1650-2750 keV using the Van de Graaff accelerator at B.A.R.C. Trombay. About 100 resonances were observed in the excitation function out of which the prominent ones at  $E_p = 1731, 1882, 2036, 2099, 2312, 2352, 2421$  and  $2479$  keV have been identified as analogues of the ground and low-lying excited states of  $^{64}\text{Cu}$ . The overall energy resolution was 2.5keV. The Coulomb displacement energy for the isobaric pair  $^{64}\text{Cu}-^{64}\text{Zn}$  has been deduced to be  $(9.63 \pm 0.01)$  MeV. The spectra of  $\gamma$ -rays and their angular distributions have been obtained at resonances corresponding to the analogue of the ground and first four excited states of  $^{64}\text{Cu}$ . The resonance strengths and the branching ratios for the  $\gamma$ -decay of the resonances will be presented. The M1 width of the  $\gamma$ -decay

from the resonance at 1731 keV to the ground state of  $^{64}\text{Zn}$ ,  $(0.20 \pm 0.04)$  eV, is in excellent agreement with the value 0.19 eV deduced from the log ft value of 5.3 of the  $\beta$ -decay of the parent analogue.

5. Measurement of Isotopic Neutron Capture Cross-Section for  
 $^{51}\text{V}$ ,  $^{63}\text{Cu}$ ,  $^{74,76}\text{Ge}$ ,  $^{75}\text{As}$ ,  $^{98,100}\text{Mo}$ ,  $^{104}\text{Ru}$ ,  $^{115}\text{In}$ ,  $^{128,130}\text{Te}$ ,  
 $^{140,142}\text{Ce}$ ,  $^{185,187}\text{Re}$  at  $E_n = (25 \pm 5)$  keV - R.P. Anand\*,

D. Bhattacharya, M.L. Dhingra and E. Kondaliah - We have measured the isotopic neutron capture cross-sections of a number of nuclei, the majority of which are fission products, at the neutron energy  $(25 \pm 5)$  keV. The neutrons have been obtained from the monoenergetic filtered neutron beam facility that we have developed at the reactor CIRUS, B.A.R.C. This gives a flux of  $\sim 10^5$  n/cm<sup>2</sup>/sec. over an area of 3" diameter.

We have employed the gamma-ray activation techniques which enables one to get the isotopic cross-section values directly. For improved accuracy, our measurements have been done relative to the corresponding thermal values. By this procedure we have been able to bring down the errors considerably in most of the cases. The 441 keV gamma-ray coming from  $^{127}\text{I}(n,\gamma)^{128}\text{I}$  has been used as a flux monitor.

The data has been analysed within the framework of Lane and Lynn's theory of neutron capture assuming the inelastic

\* NPD, B.A.R.C. Bombay.

processes to be negligible at this energy. The analysis yields the p-wave neutron strength functions.

6. An Anomaly in the Neutron Capture Cross-Section of  $^{198}\text{Au}$  at 25 keV - R.P. Anand\*, D. Bhattacharya and E. Kondaiah - The neutron capture cross-section of  $^{198}\text{Au}$  at 25 keV, derived from shell transmission or activation methods, is frequently referred to as a standard. However the divergence between the published values of this cross-section is as much as a factor of two. In both of the above mentioned methods, self-shielding and multiple scattering corrections play an important role in the final evaluation of the cross-section. We have made a detailed study of the problem at  $(25 \pm 5)$  keV neutron beam facility at the reactor APSARA, B.A.R.C. A stack of gold foils, with thin and thick foils alternately placed, was irradiated. The specific activity of the foils, when plotted against foil thickness, is found to fall sharply upto a thickness of  $150\text{mgms/cm}^2$  but then remains flat right upto a thickness of  $1700\text{mgm/cm}^2$ . The thickness of the thin foils used by us was  $50\text{mgm/cm}^2$ . This sharp fall suggests that possibly there is some prominent resonance in the gold cross section at this energy. Recently Schneider has seen an intermediate structure in the total cross-section of gold around 23 keV. Using this intermediate structure we are now able to explain the anomaly to a good extent.

7. Level Scheme of  $^{74}\text{As}$ . B. Lal, Y.K. Agarwal, S.M. Bharathi and C.V.K. Baba\* - The level scheme of  $^{74}\text{As}$  has been studied through the  $^{74}\text{Ge}(p,n)^{74}\text{As}$  reaction. Gamma-ray and internal conversion electron measurements were carried out using Ge(Li) detectors and a six gap electron spectrometer. The level scheme was established by gamma-gamma coincidence measurements. New levels at 372.7, 525.8, 532.8, 632.1, 731.6, 752.7, 758.3, 801.6, 902.9 and 1128.5 keV have been established. Lifetime measurements on some of the levels were also performed by gamma-electron delayed coincidence measurements. As a result, the half-life of  $26.8 \pm 0.5$  ns observed in the earlier work and attributed to a level at  $\sim 278$  keV has been found in the present work to correspond to a level at 258.9 keV. The half-lives of the 271.3 and 277.5 keV levels were measured to be  $1.0 \pm 0.1$  ns and  $< 0.3$  ns respectively. The reduced transition probabilities deduced from these measurements are compared with theoretical predictions, and the main configurations of a few levels are determined from this comparison.

---

\* N.P.D., B.A.R.C. Bombay.

C. SAHA INSTITUTE OF NUCLEAR PHYSICS, CALCUTTA.

1. Lifetimes of Excited Levels and Electromagnetic Transition Rates in  $^{130}\text{Te}$  - V.K. Tikku, H. Singh and B. Sethi - The

lifetimes of  $2153.0(7^-)$  and  $1819.3(6^+)$  keV levels in  $^{130}\text{Te}$  populated in the decay of isomers of  $^{130}\text{Sb}$  have been measured by the delayed coincidence technique using a time to amplitude converter. The results are:  $T_{\frac{1}{2}}(2153.0 \text{ keV}, ^{130}\text{Te}) = 116 \pm 6 \text{ nsec}$  and  $T_{\frac{1}{2}}(1819.3 \text{ keV}, ^{130}\text{Te}) = 9.0 \pm 0.4 \text{ n sec}$ . These results along with energy and intensity measurements of  $\gamma$ -transitions in  $^{130}\text{Te}$  reported earlier by us <sup>1)</sup> have been utilized to deduce the transition probabilities. The large hindrance ( $\sim 10^7$ ), observed for the  $333.7 \text{ keV } (2153.0(7^-) \rightarrow 1819.3(6^+)$  transition compared to the s.p. Weisskopf estimate strongly supports the suggestion that the  $2153.0 \text{ keV}$  level arises due to a coupling between two neutrons of type  $(2d_{3/2}^{-1}, 1h_{7/2}^{-1})_{7^-}$ . The results of the experimental lifetime of the  $1819.3(6^+)$  keV is compared with those obtained from two proton cluster core coupling model.

1) V.K. Tikku, H. Singh and B. Sethi, Nuclear Physics & Solid State Physics, (India) 16B (1973).

2. K-Capture Probability in the Decay of  $^{139}\text{Ce}(140 \text{ d})$

B.K. Dasmahapatra - The K-capture probability ( $P_K$ ) for the  $165.8 \text{ keV}$  state of  $^{139}\text{La}$  in the decay of  $^{139}\text{Ce}(140 \text{ d})$  is determined by a method recently developed by us (B.K. Dasmahapatra and P. Mukherjee, J. Phys. A7(1974) 388). In this method  $P_K$  is

determined from the analysis of the KX-ray gamma ray sum-peak observed with a high resolution (500 eV) X-ray detector in a close geometry set up. The value of  $P_K$  obtained is  $0.74 \pm 0.06$ . As the EC feeding to the 165.8 keV state is 100 % and it decays to the ground state through the 165.8 keV transition only, a measurement of the KX-ray intensity together with the use of known conversion coefficients of the 165.8 keV transition yield  $P_K = 0.72 \pm 0.04$ . Using the weighted average of  $P_K$  determined as above the mass difference between  $^{139}\text{Ce}$  and  $^{139}\text{La}$  is observed to be  $269 \pm 19$  keV in good agreement with the value  $275 \pm 15$  keV obtained from the mass adjustments.

3. Excited states in  $^{85}\text{Sr}$  from the Reaction  $^{85}\text{Rb}(p,n\gamma)^{85}\text{Sr}$  -

S.K. Basu - In-beam  $\gamma$ -ray measurements following the reaction  $^{85}\text{Rb}(p,n\gamma)^{85}\text{Sr}$  have been undertaken with a high resolution 32.2 c.c. co-axial Ge(Li) detector at a proton energy of 3.8 MeV. Both natural as well as enriched (99.5%) rubidium nitrate targets were used. To identify the  $\gamma$ -rays due to (p,n) reaction, spectra were taken with the proton beam de-graded in energy by mylar absorbers. The following  $\gamma$ -rays with energies (in keV): 193.9, 231.6, 238.7, 409.6, 504.5, 535.7, 546.7, 612.0, 698.2, 767.5, 788.0, 821.2, 914.0, 1030.5, 1262.0, 1323.8 and 1588.5 have been assigned to be from levels below 1.9 MeV excitation in  $^{85}\text{Sr}$ . Twelve levels are proposed to accommodate the observed transitions of which the levels at 785.9, 936.9, 1398.0 and 1588.5 keV have not been reported previously. The branching ratios for the

proposed levels are deduced and the level structure is discussed in the light of recent experimental<sup>1)</sup> and theoretical investigations<sup>2)</sup>.

1) S.K. Basu and A.P. Patro, To be published.

2) S.K. Basu and S. Sen, Nucl. Phys. A220 (1974) 580.

#### 4. Decay Schemes of the 9.7 H and 6.2 D Isomers of $^{196}\text{Au}$ -

R.K. Chattopadhyay, P. Bhattacharya, B. Sethi and V.K. Tikku -

The decay schemes of the 9.7 hour  $^{196\text{m}}\text{Au}$  and the 6.2  $\mu$   $^{196\text{g}}\text{Au}$

have been investigated with the help of high resolution X-ray

Ge(Li) and 32c.c. Ge(Li) detectors, using Laben 4096 channel

analyzer. The sources were produced by (n,2n) reaction on

specpure gold with 14 MeV neutrons. In the decay of  $^{196\text{m}}\text{Au}$

$\gamma$ -rays with energies of 30.6 and 50.5 keV have been detected

for the first time. The energies of these  $\gamma$ -rays are in

excellent agreement with the conversion electron studies of the

transitions in  $^{196}\text{Au}$  reported earlier. The  $\gamma$ -rays correspon-

ding to the 84.6 and 174.9 keV transitions in  $^{196}\text{Au}$  which were

not found by some of the earlier workers, have also been

observed. In the decay of  $^{196\text{g}}\text{Au}$ , it is found that the 1271 keV

level in  $^{196}\text{Pt}$  is also populated in addition to the other levels

reported in the literature. A 393 keV  $\gamma$ -ray de-exciting this

level has been detected. The existence of 326 keV transition

in  $^{196}\text{Pt}$  has been confirmed. Revised energies and intensities

of all observed transitions in  $^{196}\text{Pt}$ ,  $^{196}\text{Au}$  and  $^{196}\text{Hg}$  are given

and the decay schemes of  $^{196\text{m\&g}}\text{Au}$  based on these results are

studied.

5. Level Structure of  $^{147}\text{Pm}$ . - B.K. Sinha, S. Sen and

R. Bhattacharyya - Level properties of  $^{147}\text{Pm}$  have been studied from the decay of  $^{147}\text{Nd}$  (11.1 d). Experimental set up consists of a pair of XP 1021 photomultiplier tubes coupled to high resolution Bicron  $1\frac{1}{2}$  inches x 1 inch NaI(Tl) phosphors and an overlap type of TAC set up using avalanche transistor pulse shaper. For detection of  $\beta$  -rays, 1 inch x  $3/8$  inch NE 102 plastic phosphors are used. Typical time resolution using NaI(Tl) phosphors for the  $\text{Co}^{60}$  gamma rays is 600 ps. Mean life of the 91, 410 and 531 keV levels have been determined by measuring the time distribution of the coincidence events between 870 keV  $\beta$  -91 keV gamma rays, 275 - 319 keV gamma rays and (370 keV  $\beta$  -ray - 531 keV gamma ray respectively. Mean lives of these levels deduced from centroid shift method are  $\tau(91) = 3.80 \pm 0.04$  ns,  $\tau(410) = 201 \pm 20$  ps and  $\tau(531) \leq 10$  ps. Angular correlation of the 275-319 keV cascade has been remeasured with a view to clarify some anomalies in the previous results. Differential angular correlation measurement of the 319-91 keV cascade has also been undertaken. Experimental results are compared with theoretical calculations of the level structure of  $^{147}\text{Pm}$  using core-particle coupling model.

6. Spectroscopic Study of  $^{107,109}\text{Cd}$  excited States through

$^{107,109}\text{Ag}(p,n\gamma)$  Reactions - M.B. Chatterjee, B.B. Baliga and

R. Bhattacharyya - (p,n) reactions are known to excite both the

single particle states and collective states. Hence they are ideal to study the low-lying states of several nuclei where the Q-values are not too negative. The excited states of  $^{107,109}\text{Cd}$  have been observed from the  $^{107,109}\text{Ag}(p,n\gamma)$  reaction. In beam spectroscopic study of gamma ray singles have been carried out with the Ge(Li) detector varying the proton energy from 3.0 to 5.25 MeV in steps of 250 keV Van-de-Graaff accelerator of BARC. Energies and intensities of gamma rays have been measured. Some of the levels which were weakly populated in decay have been strongly excited in the reaction work. New gamma lines have been observed which were not reported in our decay works earlier. Further support for the existence of these lines have been obtained from the published works on (p,n) and (d,p) reactions. Discussions on various levels of  $^{107,109}\text{Cd}$  obtained from reaction data will be presented in the light of decay data of our earlier experiments and other published works in the literature.

D. ANDHRA UNIVERSITY, WALTAIR

1. K-Conversion Coefficients and K/L Ratios of 244 and 344 keV Transitions of Sm-152 & Gd-152 - J. Rama Rao, U.V. Chalpathi Rao, D.S. Reddy, K.L. Narasimham and V. Lakshminarayana - A 35 cc Ge(Li) and a 3 mm Si(Li) detector system has been calibrated for relative efficiency versus energy for gamma rays and conversion electrons in the energy range 100-800 keV. Using the system, the K-conversion coefficients and K/L ratios are measured for the 244 and 344 keV transitions of Sm-152, and Gd-152 respectively occurring in the decay of Eu-152. For the 344 keV transition good agreement is observed between the present results and theory. However, considerable deviation is noticed in the case of 244 keV transition of Sm-152.

2. Shape of the  $0 \rightarrow 0$  Beta Transition of  $^{166}_{110}$  and the Pseudo-Scalar Interaction - K. Venkata Ramaniah and K. Venkata Reddy - The beta spectrum shape of the  $0^- \rightarrow 0^+$  transition of 110-166 is studied after a subtraction of the  $0^- \rightarrow 2^+$  inner beta transition in coincidence with the 80 keV gamma ray, corrected for its shape, from the gross spectrum of 110-166. The measured shape factor is  $C(W) = k \left[ 1 - (0.131 + 0.003)/W \right]$  for an end point energy of  $1844 \pm 2$  keV. The present shape is well explained by the Nilsson model. An analysis employing exact formulation of Bhalla and Rose yield  $C_p/C_A = -2.5$  and the ratio of the axial vector matrix elements  $\lambda = -14$ . These results exclude the predictions of partially conserved axial vector current theory due to Tadic. The parameters obtained from the present work disagree with the

theoretical predictions of Rose and Osborn and Pearsson. The deviation of the  $0^- \rightarrow 0^+$  beta transition from  $\beta$ -approximation is explained as due to the peculiar combination of nuclear matrix element parameters.

3. Spectral Shapes of the Beta Decay Transitions  $1^- - 2^+$  and  $1^- - 0^+$  of the Re-188 Nucleus - K. Venkata Ramaniah and K.

Venkata Reddy - The beta spectral shapes of the non-unique first forbidden,  $1^- - 2^+$  and  $1^- - 0^+$  beta transitions in the decay of Re-188 are studied employing an intermediate image beta ray spectrometer, producing the isotope by neutron irradiation of 99.83% enriched Re-187 stable isotope. The shapes of these beta transitions were found to be essentially identical fitting into the shape factor of the form  $G(W)=k(1+aW)$  with  $a=0.123 \pm 0.023$  in the case of the  $1^- - 2^+$  beta transition for an end point energy of  $1962 \pm 2$  keV and  $a=0.110 \pm 0.0036$  in the case of  $1^- - 0^+$  beta transition for an end point energy of  $2120 \pm 2$  keV. The shape factor results are discussed in comparison with the Nilsson model in the single particle description. The  $\Lambda$  values for the two transitions are estimated from the present shape measurements through the Simm's relations using the theoretical and experimental nuclear matrix element parameters.

4. Nuclear Structure Effect in the K-conversion Process of the 223 keV Transition in Cs-133 - K. Venkata Ramaniah and K. Venkata Reddy - The highly retarded 223 keV transition in Cs-133 has been

investigated by determining the K-conversion coefficient of the 223 keV transition using the relative conversion electron intensity measured with an intermediate image beta ray spectrometer and the relative gamma ray intensity using a 35 c.c Ge(Li) detector through the intense 356 keV gamma transition. The K-conversion coefficient is obtained as  $\alpha = 0.092 \pm 0.01$ . The present K-conversion coefficient is used along with the published gamma-gamma correlation data on the  $\gamma_{80} \rightarrow \gamma_{223}$  cascade in a subsequent analysis for the penetration parameter. A value of  $+10 \pm 0.5$  is obtained for the penetration parameter agreeing very well with the theoretical value obtained by Church and Weneser for Z-55.

##### 5. Spectral Shape Measurements of the K-forbidden Beta

Transitions of Eu-152 and Eu-154 - K. Venkata Ramaniah, Rajan Mathews and K. Venkata Reddy - The K-forbidden beta transitions of Eu-152 and Eu-154 are studied in detail for their beta spectral shapes employing an intermediate image beta ray spectrometer. A detailed analysis in terms of  $C(W)/C_B$  vs  $W$  where  $C_B$  is the modified  $B_{ij}$  shape correction factor, for different values of  $D$  and  $W_0$  is made. The highest energy ( $3^- \rightarrow 2^+$ ) beta groups of Eu-152 and Eu-154 exhibit large deviations from statistical shapes and are well fitted into modified  $B_{ij}$  shapes with end point energies  $1481 \pm 2$  and  $1845 \pm 2$  keV. The value of  $D$  is  $6 \pm 1$  in the case of Eu-152. The present result yields  $Y^2 = 1.25 \pm 0.25$  in the case of Eu-154. An analysis of the experimental shapes using the

Nilson model configurations for the initial and final states, yielded that  $K'=1$  component is dominating the  $K$ -admixture of the initial states. The shape factor results are discussed combining with the beta-gamma angular correlation results due to different authors.

6. First-Forbidden Beta Transitions of  $^{42}\text{K}$  - B. Mallikarjuna Rao, C. Narasimha Rao, P. Mallikharjuna Rao and K. Venkata Reddy - The  $2^- \rightarrow 2^+$  beta transitions are one of the most interesting and complicated of the first-forbidden non-unique transitions, since all the six nuclear matrix elements operate in this beta transition. There are four earlier shape measurements of this transition. While the two earlier measurements report a shape consistent with  $\xi$ -approximation, Daniel and Andre independently report a deviation from the statistical shape. To clarify the situation further, a remeasurement of the shape of this transition employing an Intermediate-image focussing beta ray spectrometer was made in this work. The results are discussed on the basis of the present measurements and the nuclear matrix elements evaluated by other authors.

Small order deviations from the unique shape of the  $2^- \rightarrow 0^+$  transition are reported by Daniel et al. Eman et al and Abacasis et al have attempted to interpret these deviations theoretically. To substantiate the observations made by the above authors, a careful analysis of the spectral shape is made in this work.

7.  $3^- \rightarrow 4^+$  Beta Decay in  $^{140}\text{La}$  - P. Mallikharjuna Rao, C.

Narasimha Rao, B. Mallikharjuna Rao and K. Venkata Reddy - A detailed and systematic investigation of the shape of the  $3^- \rightarrow 4^+$  beta transition of  $^{140}\text{La}$  have been carried out employing an optimised Siegbahn-Slatis coincidence beta ray spectrometer. The experimental shape factor of this transition is weighted least-square fitted to a shape correction factor of the form

$$C(W) = k(1+aW+b/W+cW^2)$$

The applicability of various nuclear models like shell model and quasi-particle model, to describe the nuclear states involved in this transition, has been discussed. For a complete description of the characteristics of this beta transition in terms of

$\xi$ - approximation, CVC theory etc..., an evaluation of nuclear matrix elements NHE) combining the present shape measurement with the only other available beta-gamma angular correlation data has also been performed.

8. Beta Decay to the First  $2^+$  Excited State of  $^{42}\text{Ca}$  - B. Vema

Reddy, M.L. Narasimha Raju and D.L. Sastry - The directional correlation between non-unique first-forbidden 2 MeV beta and the 1.52 MeV gamma-ray in the decay of K-42 has been measured as a function of beta particle energy in the range 350 to 1850 keV employing a fast-slow scintillation assembly. Nuclear matrix elements governing the 2 MeV beta transition are extracted using the accurate formalism of Buhring that are modified by Simms.

The value of  $\lambda$ , the correction term in the expression of Damgaard and Winther for the vector matrix element ratio, is found to be  $1.17 \pm 0.37$ . Simple shell model configurations for the involved states in the transition could not explain the results on experimental matrix elements.

9. The First Forbidden 358 keV Beta Decay in Yb-175 - D.K.

Priyadarsini, M. Srinivasa Rao, B. Vema Reddy and D.L. Sastry - Beta-Gamma directional correlation measurements for the 358 keV beta and the following 114 keV Gamma cascade were carried out using a fast-slow Scintillation assembly. The measured anisotropy is

$$A = 0.1517 \pm 0.0430 \text{ at } E_{\beta} = 300 \text{ keV.}$$

An attempt is made to derive the matrix  $\phi$  elements consistent with the present  $\beta$ - $\gamma$  angular correlation and the beta spectrum shape of Rao. The Longitudinal polarisation is predicted and finally the results are discussed in the light of the Nilsson model wave functions for the Yb-175 nucleus.

10. Coupled Channel Calculations for Neutron Scattering from

U-235 - U. Satyanarayana and S. Ramamurthy - A coupled channel calculation has been done for inelastic scattering of neutrons from U-235 and the results are compared with the Hauser-Feschbach theory. The results are discussed.

11. Strong Absorption Model for Neutron Scattering from Th-232, U-235, U-238 and Pu-239 - U. Satyanarayana, S. Ramamurty and N. Lakshmana Das - Elastic and inelastic scattering of neutrons from Th-232, U-235, U-238 and Pu-239 have been calculated using strong absorption model. A computer program has been developed to do these calculations on IBM 1130. The differential cross section for elastic scattering has been calculated with and without the strong absorption condition; and there is a difference of about 0.5 barns per steradian which may be attributed to the simplifications made when strong absorption condition is included in the calculations. The radius parameter is quite different from that used in optical model calculations.

12. Cross-section for (n,2n) Reactions at 14 MeV - N.Lakshmana Das, C.V. Srinivasa Rao, B.V. Thirumala Rao, J. Rama Rao and V. Lakshminarayana - Activation cross-sections for the reactions Nd-142(n,2n)Nd-141g, Nd-146(n,2n)Nd-147, Gd-160(n,2n)Gd-161 and Er-162(n,2n)Er-163 have been determined at 14 MeV using a 35 c.c. coaxial Ge(Li) detector and the mixed powder technique. The finite size of the target samples and their self-absorption effects for gamma rays have been experimentally taken into account by calibrating the Ge(Li) detector for volume sources using the simulation technique. The measured cross-sections are compared with previous results using scintillation detectors and with various theoretical predictions.

13. Decay of W-187 - K. Subba Rao\*, P. Ila, K. Sudhakar, K.L. Narasimhan, K. Premchand and V.Lakshminarayana\*\* - The spectrum of gamma rays accompanying 24 hour decay of W-187 has been investigated with a calibrated 35 cc Ge(Li) detector. From the estimated relative photon intensities and the recent conversion electron intensity data, conversion coefficients of eleven transitions in Re-187 have been deduced. In particular, the internal conversion penetration parameter of the hindered 35 keV transition was deduced from the present value of the conversion coefficient. The experimental results are presented and discussed with respect to spin-parity assignment of levels of Re-187.

14. Gamma-Gamma Angular Correlation Studies in Os-188 - D.K. Priyadarsini, B.R. Sastry, V. Seshagiri Rao and D.L. Sastry - Gamma-Gamma directional correlation measurements between the 931-155, 478-155, (825+829)- 478 keV. cascades involving the states  $0^+$ ,  $2^+$ ,  $2^+$ ,  $0^+$ ,  $2^+$ ,  $(1^+, 2^+)$ ,  $2^-$  in Os-188 were performed employing a Ge(Li) - NaI(Tl) system available with the Nuclear Spectroscopy group, TIFR, Bombay. The final results are as follows:

$$A_2(478, 155) = -0.03534 \pm 0.01399$$

$$A_4(478, 155) = 0.9889 \pm 0.01987$$

$$A_2(931, 155) = 0.2171 \pm 0.0452$$

$$A_4(931, 155) = 1.449 \pm 0.0473$$

---

\*\* Present address: University of Groningen, Groningen, Netherlands.

\* Present address: Physics Department, Regional Engineering College, Warangal.

$$A_2 (824+829, 478) = 0.0003002 \pm 0.03679$$

$$A_4 (824+829, 478) = 0.2178 \pm 0.4999$$

The results on (478-155) keV Cascade show a quadrupole content  $Q_\gamma \geq 0.99$  for the 478 keV gamma transition. The experimental coefficient for the 931-155 keV Cascade are in accordance with the spin sequence  $0^+ - 2^+ - 0^+$ .

15. A Note on the Angular Momentum Analysis of the jj coupling Shell Model-III - A. Satyanarayana Rao - In previous notes<sup>1,2</sup> the angular momentum analysis in the  $(j)^2$  and  $(j)^n$  configurations was given an interpretation in terms of elementary solutions of homogeneous ultrahyperbolic equations of the normal type. In this note the results of (1) are extended by considering solutions of these equations by the method of separation of variables. Polynomial solutions are constructed in an explicit form with a mention of basic sets of homogeneous harmonic polynomials in several variables of related equations useful in a closed jj-coupling shell of identical particles in the j-orbit.

1. 'A note on the Angular Momentum Analysis of the jj-coupling shell model', Nucl. Phys. & Solid State Phys. (India) 15B (1972), 229-232.
2. "A note on the Angular Momentum Analysis of the jj-coupling Shell Model-II". Nucl. Phys. & Solid State Phys. (India) 16B (1973).

E. BANARAS HINDU UNIVERSITY, VARANASI

1. J-Dependence in (d,p) Reactions at Low Energy - S.N.

Mukherjee - The  ${}^2P_{3/2}$ - ${}^2P_{1/2}$  J-dependence in stripping angular distribution and the vector analyzing power for the (d,p) reaction in calcium isotopes at incident deuteron energy around 5.0 MeV has been studied by coupled channel method and DWBA and the results are compared with experiments. It is shown that a large portion of J-dependence is caused by the coupling of the stripping channel to the incident deuteron channel. The necessity of including the deuteron break-up channel and the deuteron-D state is stressed.

2. Sum Rules for  $\gamma$  (d,n) $\beta$  Reaction - R. Shyam and S.N. Mukherjee -

Levinger-Bethe sum rules for  $\gamma$  (d,n) $\beta$  reaction have been evaluated for realistic nucleon-nucleon forces with soft core. The bremsstrahlung weighted and integrated cross sections have been evaluated and the results are compared with experiments and those obtained employing Yale and Hamada-Johnson potentials with hard core. It is seen that the results are insensitive to the nature of the core.

3. Volume Integral of the Absorptive Part of Proton Optical

Potential - D.C. Agrawal - More than a decade ago Feshbach(1958) suggested that the volume integral of the potential is a better measure of the strength of the potential because it contains the effect of both the well depth and the geometry. The volume

integral of the real central potentials have been extensively studied recently, however, no such investigation has been reported so far regarding the absorptive part of the nuclear potential. Here we present the results of a detail investigation of volume integrals of the absorptive part of optical potential for protons with energies varying from 9.8 to 61.4 MeV from target nuclei in the mass range from 40 to 208. It is found that the total volume integral (sum of the surface and volume absorption terms) per particle ( $J/A$ ) of the absorptive part of the proton optical potential is a practically well-defined quantity, and independent of the mass number of the target nucleus. It is well known that the strength of the absorptive part of the optical potential increases with the increase of incident proton energy, since more inelastic channels get opened; however,  $J/A$  is found to be practically constant within the above incident proton energy.

#### 4. Back-Bending and Band-Crossing in $^{156}\text{Dy}$ - A.N. Mantri -

Experimental study of the ground and  $\beta$ -bands in deformed nuclei has been extended recently to very high spin states. Plots of  $J$  versus  $\omega^2$  yield back-bending curves for these states. One of the explanations put forward for back-bending feature is in terms of band-crossing. We have analysed the recent experimental results for  $^{156}\text{Dy}$  in terms of a simple-band-crossing model. Assuming the usual form of the rotation-vibration interaction, results for the interband-to-intraband  $B(E2)$  ratios from such a calculation are

compared with the available experimental results. The nature of the intersecting bands is also analysed.

##### 5. Physically Consistent Fermi Gas Model for Nuclear Level

Densities - A.K. Jain and P.C. Sood - The conventional formulation of the Fermi gas model for calculating nuclear level densities gives correct results only over a limited energy range, defined by the experimental neutron resonance data; its predictions come out far too low at excitations near the ground state and too high for excitations above 15 MeV. A modification of the model known as the back shifted Fermi gas model - yields a better agreement by treating the model parameters 'a' and ' $\Delta$ ' as free, while keeping the spin cut-off parameter related to the rigid body moment of inertia as before. However, in this formulation one no longer has the straight forward identification of 'a' and ' $\Delta$ ' with the level density parameter and the gap parameter, derivable both from the conventional approach to experimental data and the Strutinsky type calculations. We suggest that the anomaly is related to the energy dependence of the moment of inertia and proceed as follows. The gap parameter ' $\Delta$ ' is fixed from the experimental pairing energies, and the level density parameter 'a' is determined from experimental resonance data using the rigid body estimate for the spin out-off parameter  $\sigma$ . Taking 'a' and ' $\Delta$ ' to be energy independent, the fits to low energy levels of these nuclei are obtained by varying  $\sigma$ . The results so obtained are used to discuss the energy variation of

partial wave can be solved exactly. However separable expansion for the Perey-Buck potential will be in fact an infinite series and difficult to obtain. Similarly the solution of the Schrodinger equation for the local optical potential with Saxon-Wood type radial form can be solved only numerically. In view of this we construct a single rank separable potential which will replace the local potential in optical model. We achieve this by approximating the local potential by a set of square well potentials and then constructing an equivalent one-term nonlocal separable potential for the latter for each partial wave for a given energy. The orbital angular momentum dependence of this potential comes from Bessel function of order  $(\ell + \frac{1}{2})$ . The usual parameters of the optical potential can be retained in this method to facilitate the least square calculation of the cross-section. Numerical calculations are carried out to illustrate this method.

G. BURDWAN UNIVERSITY, WEST BENGAL

1. Pairing Vibrations in Zirconium Isotopes - M.K. Ghosh\* and B.C. Sawanta - The Zirconium isotopes span an interesting region around the mass number A-90. The stable isotope  $^{90}\text{Zr}$  has a closed neutron subshell. The modified random phase approximation (MRPA) has been applied to study pairing vibrations in Zirconium isotopes. Pairing correlations in the ground state and the excited states of Zirconium isotopes have been calculated and compared with experimental results. For ground to ground state transitions our results are in good agreement with the experimental ones. The predicted excited '0' pairing-vibrational states of Zirconium isotopes, however, occur at energies somewhat higher than those observed experimentally by Flynn et al<sup>1)</sup>.

1. E.R. Flynn, J.G. Berry and A.G. Blair, Nucl. Phys. A218, 285 (1974).

---

\*Present address: Mosul University, Iraq.

H. DIBRUGARH UNIVERSITY, ASSAM

1.  $O^{18}$  Energy Levels from a Realistic N-N Potential - A.K. Deka and P. Mahanta - Nuclear calculations during the last few years have shown that soft core realistic potentials are more suitable than the potentials with ideal hard cores. N-N potential being a basic tool for nuclear structure investigation the search for a good realistic finite N-N potential would continue for some time. In the present work the reference spectrum and separation methods as developed by Kuo and Brown are used to calculate the shell model energy levels of  $O^{18}$ . We use a finite N-N realistic potential<sup>1)</sup> having good fit to the phase shift data. Calculations show great improvement over those resulting from use of bare matrix elements reported previously and low lying levels are almost the same as obtained from the hard core Hamada-Johnston potential obtained by Kuo and Brown without core polarisation. Moreover, the charge dependancy of the potential seems not to be important in the present work.

I. INDIAN INSTITUTE OF TECHNOLOGY, KANPUR

1. Generalised Rotationally Invariant Core (RIC) Model - A Two Mass-point Approach - V.R. Prakash - A generalised RIC

model for rotational-vibrational spectra of deformed even-even nuclei of ellipsoidal shape in the rare-earth region has been proposed by incorporating many important features of various macroscopic models proposed earlier. The two mass-point model<sup>1)</sup> and the governor model<sup>2)</sup> moments of inertia are obtained on the basis of the proposed model with appropriate limiting values of the radius of the RIC. Also, the model moment of inertia goes to zero for spherical nuclei, thus giving no rotational spectra for such nuclei. A quantum mechanical treatment of the model on the basis of the two mass-point concept, is expected to give results which are in better agreement with experiments.

1) V.R. Prakash, B.M. Bahal and V.K. Deshpande, Can. J. Phys. 51, 2474 (1973).

2) L.E.H. Trainor and R.K. Gupta, Can. J. Phys. 49, 133 (1971).

2. Measurement of Fast Neutron Scattering and Total Cross

Sections of  $^{141}\text{Pr}$  - R. Singh and H.H. Knitter\* - The differential elastic neutron scattering cross sections of  $^{141}\text{Pr}$  were measured at incident neutron energies of 1.2, 1.7 and 1.9 MeV in the angular range between 25 to 150 degrees. The 3 MeV Van-de-Graaff

\* J.N.R.C., C.B.N.M., Geel, Belgium.

machine at C.B.N.M., Geel was used to obtain proton pulses of width 1 ns at 1 MHz repetition rate and a  $495 \mu\text{g}/\text{cm}^2$  TiT target for producing neutrons. The measurements were made with flight paths of 1.43 m at the incident neutron energies of 1.2 and 1.7 MeV and 2.3 m at 1.9 MeV. The over all time resolution was about 2.5 ns. At 1.7 MeV the differential inelastic neutron scattering cross sections corresponding to  $Q = -1122$  keV, and at 1.9 MeV the ones corresponding to  $Q = -1122$ , and  $Q = -1295$  keV were also determined. In a transmission experiment, the total cross section was measured between 0.50 and 2.42 MeV. The total and differential cross sections were calculated using the nuclear optical model. The calculated results were compared with the experimental data.

### 3. Gamma Decay in Proton Capture Reactions in $^{48}\text{Ti}$ - H.R.

Prabhakara and G.K. Mehta - In  $1f_{7/2}$  nuclei the compound nuclear states reached by proton capture reactions using low energy accelerators are still observable as isolated resonances, some of which can be identified as isobaric analogue resonances having simple structure. In  $^{48}\text{Ti}$  at proton energies 1.387 MeV and 1.564 MeV, 8.115 and 8.289 MeV levels are excited respectively in  $^{49}\text{V}$ . None of these are known to be analogue resonances. The resonance at 1.564 MeV has a simpler decay scheme as compared to the one at 1.387 MeV. The decay properties of these resonances will be discussed.

4. On the Anticorrelation in LRA Fission - B. Krishnarajulu and G.K. Mehta - The experimentally observed anticorrelation between the average total fragment kinetic energy ( $E_F$ ) and the alpha energy ( $E_\alpha$ ) could be of considerable importance in determining the correct set of initial values of, and correlations between, the initial parameters in trajectory calculations on LRA fission.

It is observed that this anticorrelation can be reproduced by fixing the value of the initial interfragment distance,  $D$ . However, in doing so it is not possible to explain some asymptotic distributions, e.g. the angular distribution of the alpha particles; unless one assumes a correlation between  $D$  and the point of emission of the alpha particle,  $X_0$ . The exact nature of this correlation has not been determined as yet.

We have also studied the anticorrelation as a function of the mass ratio,  $R$ .

J. KURUKSHETRA UNIVERSITY, KURUKSHETRA

1. Calculated Cross-Sections, Energy and Angular Distributions of Ni-58 Reactions with 14 MeV Neutrons - B.S. Wadhwa and R.K.

Mohindra - The direct and compound nucleus cross-sections of the type  $(n,p)$ ,  $(n,n')$ ,  $(n,a)$ ;  $(n,n'p)$ ,  $(n,2n)$ ,  $(n,n'a)$ ,  $(n,pn')$  and  $(n,an')$  have been computed using a diffused edge optical model potential at 14.0 and 14.8 MeV (Lab.). Some of our previous cross-sections have been modified and corrected<sup>1)</sup>. The spin dependence, shell and pairing energy effects in various level density formulae have been considered. Newton's shell dependent level density formula with slight modification of effective  $(2j+1)$  values gives better agreement for primary and secondary emissions.

Angular distributions in the reactions  $(n,p)$ ,  $(n,n')$  and  $(n,a)$  have also been computed using Newton's shell dependent level density formula with dependence on spin and spin cut off parameter<sup>2)</sup>. The calculated energy and angular distributions of  $(n,p)$  and  $(n,a)$  show fairly good agreement with the recent experimental data<sup>3,4)</sup>.

1) Wadhwa and Mohindra, Proc. Nucl. Phys. and Solid State Phys.

Symp., India, 15B (1972) 139.

2) Douglas and MacDonald, NuclPhys.13(1959) 382.

3) Alvar, Nucl Phys. A 195 (1972) 289.

4) Khan et al., Nucl. Phys. A 202 (1973) 123.

2. Statistical Analysis of Neutron Reduced Widths - H.C.

Sharma and Ram Raj and N. Nath - The  $\chi^2$ -distribution of neutron reduced widths of a large number of nuclides is studied and the associated degree of freedom ( $\nu$ ) for each nucleus obtained. It is found that  $\nu$  varies from nucleus to nucleus and could have a value different from unity used in the literature for the estimation of (n,n') reaction yields. It is further noticed that the inclusion of statistical weight factor ( $g$ ) in the analysis affects the  $\chi^2$ -distribution significantly. The statistical procedure for dealing such a  $\chi^2$ -distribution with varying degrees of freedom is studied.

3. Neutron Shell Effects and Systematics of (n,2n) cross sections at 14.7 MeV - B.S. Wadhwa and R.K. Mohindra -

The existence of shell effects in (n,2n) cross sections around 14 MeV has been controversial<sup>1,2)</sup>. With the availability of recent systematized (n,2n) cross section data<sup>3)</sup> at 14.7 MeV, it was considered worthwhile to reinvestigate the possible systematics including the existence of shell effects. The systematics have been undertaken with respect to (N-Z)/A, Q-values,  $B(n)_{\text{Comp}}$  and neutron number, 'N'. It is found that in some of these plots closed shell nuclei with N=20, 28 and 50 show some evidence of shell effects while N=82 and 126 do not give any indication. The careful analysis of  $\sigma$  (n,2n) vs (N-Z)/A in the vicinity of N=28 and 50 shows that magic nuclei N=28 have a distinctively slower rise than their

non-magic neighbouring nuclei and also at  $N=50$ , there is lower trend. The discrepancy in the heavy mass region is evidently due to the overwhelming effect of the neutron excess over the coefficient of magicity.

An empirical relation between  $\sigma(n, 2n)$  and  $(N-Z)^2/A$  has been worked out which predicts results within  $\pm 15\%$ , for nuclei in the mass region  $A \geq 110$ .

- 1) P. Hille, Nucl. Phys, A 107 (1968) 49.
- 2) S.M. Qaim, Nucl. Phys. A 185 (1972) 614.
- 3) Z.T. Body, Atom. En. Rev. 11(1973).

K. MARATHWADA UNIVERSITY, AURANGABAD

1. Levels of  $^{29}\text{P}$  from the  $^{28}\text{Si}(p,p'\gamma)^{28}\text{Si}$  Reaction - R.G.

Kulkarni - The gamma rays were produced by inelastic scattering of protons by the first excited state of  $^{28}\text{Si}$  at 1.78 MeV. A 3 in. x 3 in. NaI(Tl) crystal was used to detect the gamma rays. Excitation curves for the 1.78 MeV gamma rays have been measured in the proton energy range from 4.6 to 5.0 MeV. Resonances were observed at  $E_p = 4.69, 4.89$  and  $4.95$  MeV. At 4.69 and 4.89 MeV, the angular distributions of the 1.78 MeV gamma rays were measured. By comparison with theory, the corresponding compound levels of  $^{29}\text{P}$  at 7.26 and 7.45 MeV were assigned spins and parities to be  $5/2^+$  and  $5/2^-$ , respectively.

2. Coulomb Excitation of Levels in  $^{53}\text{Cr}$  - R.G. Kulkarni and P.N.

Patarwale - The excited states of  $^{53}\text{Cr}$  were investigated by means of Coulomb excitation using 5.5 to 7.2 MeV  $\alpha$ -particle projectiles. The de-excitation gamma rays were studied with the aid of a 25 cm<sup>3</sup> high-resolution Ge(Li) detector. Six excited states in  $^{53}\text{Cr}$  were populated by direct E2 excitation up to an excitation energy of 2322 keV. Energy level measurement with an accuracy of  $\pm 2$  keV and B(E2) values obtained (in units of  $e^2\text{fm}^4$ ) are as follows: 564 keV,  $100.0 \pm 0.5$ ; 1006 keV,  $115.6 \pm 0.8$ ; 1287 keV,  $253.7 \pm 1.8$ ; 1539 keV,  $28 \pm 2$ ; 1970 keV,  $195.4 \pm 5.2$ ; 2322 keV,  $147.8 \pm 5.3$ . The measured B(E2) values are compared with the predictions of a Core-excitation model of de-Shalit.

L. PHYSICAL RESEARCH LABORATORY, AHMEDABAD

1. Spontaneous Fission Spectrum of Curium - 248 M.N. Rao -

The mass-yield distributions in the spontaneous fission of  $\text{Cm}^{242,244}$ ,  $\text{Pu}^{244}$ ,  $\text{Cf}^{252}$  and in the neutron induced fission of  $\text{Cm}^{245}$  and  $\text{Cf}^{249}$ , determined by radiochemical, mass-spectrometric and other methods in different laboratories are studied in detail to deduce the spontaneous fission spectrum of  $\text{Cm}^{248}$  with particular reference to the fine structure in the heavy fragment mass-peak. The yields are normalized to mass number 132. The fission xenon (and krypton) spectra determined mass-spectrometrically in a special group of extra-terrestrial samples, known as carbonaceous chondrites (whose composition is similar to that of our Sun) are compared with the laboratory-deduced spontaneous fission spectrum for  $\text{Cm}^{248}$ . This study points out that lighter actinides show fine structure effects in their mass-yield spectra whereas it is not so with the heavier ones. The significance of the difference in the mass-spectra of now-extinct nuclides,  $\text{Pu}^{244}$  and  $\text{Cm}^{248}$  for understanding the nucleosynthesis-processes which contributed to our solar system materials are briefly discussed.

2. Structure of  ${}^8\text{B}$  with Projected Multi-Major Shell Hartree-Fock Calculations - V.B. Kamble, S.B. Khadkikar and D.R. Kulkarni -

Major shell-mixing calculations are carried out in the configuration space of first four major shells within the framework of Hartree-Fock (H-F) theory for the  ${}^8\text{B}$  nucleus incorporating centre

of mass motion and Coulomb corrections Axial symmetry is assumed. The interaction used is the realistic interaction obtained by Sussex group directly from the experimental phase-shifts. Good angular momentum states have been projected from the H-F solution to explain some of the properties of this nucleus, viz. the energy levels, magnetic dipole moment and the electric quadrupole moment. Preliminary band-mixing calculations for the bands  $k=1$  and  $k=2$  are also carried out. Energy levels and the magnetic dipole moment are compared with the experimental data and the agreement is found to be fair. The electric quadrupole moment has been theoretically predicted. The results are also compared with other theoretical calculations.

3. A Shell-Model Calculation of Ga<sup>74</sup> - D.P. Ahalpara and K.H. Bhatt-The low-lying energy levels of Ga<sup>74</sup> are studied by simple shell-model calculation in which it is assumed that a proton hole in orbit  $2p_{3/2}$  is coupled with neutrons in  $2p_{1/2}$  and  $1g_{7/2}$  orbits. The negative-parity states are assumed to arise from the configuration  $\pi(2p_{3/2}^{-1}) \nu[(2p_{1/2})^2(1g_{7/2})^3]$  while the positive parity states are assumed to arise from the configuration  $\pi(2p_{3/2}^{-1}) \nu[(2p_{1/2})^1(1g_{7/2})^+]$  The neutron-neutron effective interaction needed for the calculation was taken from the experimentally observed  $(1g_{7/2}^{-1} 1g_{9/2})$  multiplet in Nb<sup>90</sup>. To get the proton-neutron interaction, surface-delta interaction was used where the strength of the interaction was adjusted to fit the  $(1g_{9/2})^2$  multiplet obtained through the particle-hole to particle-particle

transform of  $(1g_{9/2}^{-1} 1g_{9/2})$  multiplet in  $Nb^{90}$ . The recently observed<sup>2)</sup> low lying states of  $Ga^{74}$  are  $4^{-}, 3^{-}, 1^{+}$ . The model described above gives  $4^{-}$  as the ground state and  $3^{-}$  as the first excited state.

1) Nucl. Phys. A187, 161 (1972), Y. Yoshida, M. Ogawa, T. Hattori, H. Taketani, H. Ogata and I. Kumabe.

2) Phys. Rev. C9, 2252 (1974), J. Van Klinken and L.M. Taff.

#### 4. Intermediate Coupling Model Description of Zinc Isotopes -

J.J. Dikshit and B.P. Singh\* - The properties of the negative parity states of  $^{65}Zn$  and  $^{69}Zn$  are investigated in the frame work of the intermediate coupling in the unified vibrational model. In the model, a quasineutron is coupled to an anharmonically vibrating core. The neighbouring even-even (A-1) isotope is considered as a core. Observed properties of the core nucleus is used to describe its anharmonicities. The model as applied involves only few free parameters. Energy levels, electromagnetic transition rates, life times, static moments etc. have been calculated. The results of present calculations have been compared with experimental results. Drastic changes in electromagnetic properties of the isotopes are very well accounted for. Also, the model predicts the quadrupole moments of first  $2^{+}$  states of  $^{64}Zn$  and  $^{66}Zn$ . The experimental values should be close to -0.08 barn and -0.09 barn respectively. Further comments on the results for  $^{69}Zn$  will be made.

\* Indian Institute of Geomagnetism, Bombay.

5. Spectral Distribution Study of Nuclei in fp-Shell - R. Haq and J.C. Parikh - Systematics of nuclei in the beginning of fp-shell are investigated using the spectral distribution method of French. The centroid energies and widths for various distributions are evaluated using the interaction of Kuo with the modification suggested by McGrory et al. The two moment distributions are used to determine ground state energies fractional occupancy of the single particle orbits for ground states and low lying spectra of various nuclei in this shell. The results are compared with the deformed configuration mixing calculations of Dhar et al. Bearing in mind the accuracy and limitations of the method, the binding energies of nuclei are given well despite the large variations in the dimensionalities of the spaces that we are working with. We observe however that as the spaces encountered become larger one needs to do a finer averaging. We have also investigated the goodness of Wigner SU(4) symmetry in these nuclei. The mixing of various SU(4) representations near the ground state provide a measure of symmetry mixing and the substantial admixture in most of the cases show that it is badly broken, largely due to the single particle spin orbit coupling.

6. On a New Explanation of the Coriolis Kinking Effect in Deformed Odd-Even Nuclei - S.K. Sharma and K.H. Bhatt - Experimental spectra of deformed odd-A nuclei do not exhibit a purely rotational spectrum. According to the collective

rotational model of Bohr and Mottelson, a large part of the deviation of the spectrum from a rotational sequence comes from the coriolis coupling between the odd particle and the core. This coupling gives rise to the so-called kinking effect in which the energy levels of odd-A nuclei can be separated into two groups of states with opposite  $(J+1/2)$  parity, say  $3/2, 7/2, 11/2 \dots$  and  $5/2, 9/2, 13/2 \dots$ . In the present paper we show explicitly, in the framework of a schematic model in which a collective set of levels for the proton group are coupled to a similar set of levels for the neutron group, that such a feature in the spectra of even-odd deformed nuclei results from the higher multipoles ( $Q^4, Q^4, Q^6, Q^6$  etc.) of the effective interactions operative in these nuclei.

7. A Microscopic Study of the Even-Even Nickel Isotopes in the 2p-1f Shell - S.K. Sharma - The even-even Ni isotopes have earlier been extensively studied within the theoretical framework provided by the various approximate methods such as those involving quasi-particles, as well as in the (exact) shell-model scheme, in the configuration space consisting of only the  $2p_{3/2}, 1f_{5/2}$  and  $2p_{1/2}$  orbits, with the nucleus Ni56 as an inert core. Though the problem of core-excitations (with respect to the Ni56 core) has also been tackled by including some of the np-nh (with  $n \leq 4$ ) excitations in the diagonalization space, it has still not been possible to account for the spectra of the low-lying states in a completely microscopic and parameter-free manner. In this paper,

the Nickel, isotopes are studied in the framework of the Projected HFB method within the complete 2p-1f shell space. The effective interaction employed is a slightly modified version of the Kuo-Brown effective interaction for the 2p-1f shell. This interaction has earlier been shown to reproduce qualitatively the observed  $B(E2)(0 \rightarrow 2)$  systematics for Cr and Fe isotopes. The present calculation yields quite satisfactory results for the low-lying  $J=0,2,4$  and 6 states in Ni isotopes, The electric quadrupole transition probabilities for the states in the ground state band are also computed.

8. On the Structure of Low-lying Levels in Ni<sup>56</sup> - S.K. Sharma -  
A traditional shell-model calculation for the nucleus Ni<sup>56</sup> in the configuration space of the complete 2p-1f shell is impossible for various reasons. It is necessary to resort to some kind of truncation or approximation while making a choice of the shell-model basis. Various theoretical schemes, often contradictory, have been proposed, in a number of calculations carried out recently, depending on the approximations employed as well as owing to rather arbitrary choices of the (unknown) parameters as, for example, the spherical single-particle energies and the two-body effective interaction. In the present work it is shown that it is possible to describe the low-lying states in Ni<sup>56</sup> in a simple way in terms of the two HF states obtained by carrying out calculations with a slightly modified version of the Kuo-Brown

interaction for the 2p-1f shell. The theoretical spectrum consisting of the spherical HF state, the two 1particle-1hole states with  $J=2$  and  $J=4$  and the states obtained by angular momentum projection from the deformed, excited HF solution, is in quite good qualitative agreement with the observed spectrum upto about 6 MeV.

9. On the Low-lying Levels in Fe-52 - S.K. Sharma - An attempt is made to provide a microscopic description of the low-lying excited levels in the nucleus Fe-52, within the frame-work of the projected HF and projected HF-BCS prescriptions in the configuration space consisting of the 2p-1f shell orbits. Deformed HF calculations, carried out by employing an effective interaction obtained by a small modification of the Kuo-Brown effective interaction for the 2p-1f shell, are seen to give rise to two HF minima for Fe-52. The excited HF solution is found to occur at 3.3 MeV relative to the lowest-energy solution. Whereas the excited HF solution is unstable towards the onset of pairing correlations, the one pertaining to the ground state is seen to be quite stable. An improved escription of the excited states in Fe-52 is thus obtained by carrying out an HF-BCS calculation. States with good angular momentum are projected from the lowest-energy HF as well as the excited HF-BCS intrinsic states. The theoretical (positive parity) spectrum thus obtained compares very well with the experiments upto about 6 MeV excitation. Static quadrupole moments  $O_2^+$  and the reduced transition

probabilities  $B(E2) (J \rightarrow J')$  for the low-lying states are computed.

10. On the Structure of the Low-lying  $0^+$  states in Ni-56 in a Three-Dimensional Caricature Space - S.K. Sharma - The purpose of this paper is to demonstrate that the ground as well as the first excited  $0^+$  states in the nucleus Ni-56 are predominantly of Zero-particle Zero-hole (op-oh) and 4p-4h nature with respect to the  $|(1f_{7/2})^{16} J=0 \rangle$  core. First we carry out the deformed HF calculations in the complete 2p-1f space. A slightly modified version of the Kuo-Brown two-body interaction is used and the single-particle energies are taken from Ca-41 spectrum. It is noted that the excited HF solution is almost 4p-4h with respect to the ground state. The energy variances  $\sigma^2 (= \langle H^2 \rangle - \langle H \rangle^2)$  for the two HF states is then computed. Next, a 3x3 Hamiltonian matrix is constructed in the "caricature" space consisting of the basis states with op-oh, 2p-2h and 4p-4h configurations. The HF energies and the variances provide information about the two diagonal and the two off-diagonal matrix-elements. A set of values ranging from several MeV above it are taken for the average position of all the (2p-2h)  $J=0, T=0$  states. The results show that ground state in Ni-56 is dominantly a op-oh state and the first excited state is mostly of 4p-4h nature.

11. Binding Energy Systematics in 1f-2p Shell Nuclei - A.K. Dhar

D.R. Kulkarni and K.H. Bhatt - Binding energy (B.E.) systematics has been studied in the framework of deformed configuration mixing formalism for the isotopes of Ti(A=44-52), V(A=47,51), Cr(A=48,52), Fe(52,54) and Ni(56), using the modified Kuo-Brown interaction and  $^{42}\text{Ca}$  single particle energies. Contribution to B.E. arising from two particle-two hole excitation within fp shell have been estimated through second order perturbation calculation. The experimental and theoretical values, in general are in good agreement. Deviations in B.E. for higher mass nuclei indicate the modification in T=0 part of the chosen effective interaction.

12. Shape Indeterminacy and Spectrum of  $^{51}\text{V}$  - A.K. Dhar, S.B.

Khadkikar, D.R. Kulkarni and K.H. Bhatt - The deformed configuration mixing calculations performed in the framework of projected Hartree Fock (HF) formalism lead to the indeterminacy of ground state shape for the nucleus  $^{51}\text{V}$ . Multiple HF solutions of almost-equal deformation ( $\approx 10/b^2$ ) have been obtained within about 0.5 MeV of each other. This indicates lack of collectivity at shell closure. Because of the dominance of (f7/2) configuration in the low-lying states of  $^{51}\text{V}$ , except for the lowest J=3/2 and 9/2 states, large overlaps are obtained for the states projected from the above intrinsic states. The observed low-lying J=3/2 and 9/2 states of  $^{51}\text{V}$  are found to belong dominantly to the oblate and prolate K=3/2

intrinsic states respectively. The calculated spectra and  $B(E2)$  values are in good agreement. As in other  $N=28$  nuclei, besides the low-lying states of small intrinsic deformation, a band of states belonging to a highly deformed prolate intrinsic state is likely to exist quite low in the spectrum of  $^{51}\text{V}$ .  $B(E2)$  values for transitions between these highly deformed states have been calculated.

13. Collective States in  $^{48}\text{V}$  - A.K. Dhar, D.R. Kulkarni and K.H. Bhatt - The structure of the low-lying collective states in  $^{48}\text{V}$  has been studied in the framework of deformed configuration mixing formalism. For the ground state band of states, the reduced electric quadrupole transition probabilities have been calculated. The structure of the negative parity band of states observed recently in ( $^{16}\text{O}$ , pn) reaction is shown to be consistent with the description of a proton excitation from the  $d_{3/2}$  state to the fp shell space. The observed values of the moment of inertia parameter  $S=57.3$  keV and the intrinsic electric quadrupole moment of 0.79b of the negative parity band of states are in very good agreement with the corresponding estimated values of 56.9 keV and 0.82b respectively.

M. PUNJAB UNIVERSITY, CHANDIGARH

1. Conversion Coefficient Measurements in  $^{144}\text{Pr}$ ,  $^{192}\text{Pt}$  and  $^{192}\text{Os}$ .

Nirmal Singh, S.S. Bhati, Punjar Dass and P.N. Trehan - K- and L-conversion lines' intensities have been measured in  $^{144}\text{Pr}$ ,  $^{192}\text{Pt}$  and  $^{192}\text{Os}$  using a double focusing beta ray spectrometer of TIFR, Bombay. In addition, gamma ray intensities have been measured in  $^{144}\text{Pr}$  using a Ge(Li) detector. From these studies, K- and L-shell conversion coefficients of various transitions in  $^{144}\text{Pr}$ ,  $^{192}\text{Pt}$  and  $^{192}\text{Os}$  have been calculated. The existence of 1055keV level in  $^{192}\text{Pt}$  has been confirmed and a spin  $2^+$  has been confirmed for the 1090 keV level in  $^{192}\text{Pt}$ . The multipolarities of 196, 308 and 604 keV transitions in  $^{192}\text{Pt}$  and 488 keV transition in  $^{192}\text{Os}$  were found to be  $M1+(99.0\pm 0.5)\%E2$ ,  $M1+(96.5\pm 0.5)\%E2$ ,  $M1+(79\pm 7)^5\%E2$  and  $M1+(94\pm 2)\%E2$  respectively. The multipolarities and ' $\delta$ ' values of these transitions agree well with the theoretical estimates from Kumar and Barangar model. A new level at  $804(0^{+1})$  keV has been proposed on the basis of this model to account for the existence of 314.8 keV transition (multipolarity  $M1(87\pm 3)\%E2$ ) which can be fitted between 804 and 489 keV levels.

2. Magnetic Moments via Single-Particle Transfer Reactions -

Ashwani Kumar and R.K. Bansal - Non energy weighted multipole sum rules have been used to derive explicit relationship between the magnetic moment of the target state and the one-particle transfer strengths. One version of the relationship demands, from a single

transfer reaction experiment, complete spectroscopic information about both the isospin-bands of states of the residual nucleus, which the experimentalist usually finds very difficult to obtain. Another version requires a single experiment to furnish information only about one isospin-band of states but one has to do now two experiments-one pickup and one stripping - on a given target state, to be able to calculate its magnetic moment. This latter version has been used to calculate ground state magnetic moments of  $F^{19}$ ,  $Ti^{47}$ ,  $V^{51}$ ,  $Y^{89}$ ,  $Nb^{93}$ ,  $Pb^{207}$  and  $Bi^{209}$  from the available experimental data. The calculated values compare reasonably well with the known magnetic moments. It has been emphasized how the calculation of magnetic moment serves as a check on the accuracy of the measured strengths, especially the distribution of total strength to the various J-states populated via particle transfer to a particular orbit.

### 3. Two-particles and Two-holes-core excitation Effects -

S. Shelly and R.K. Bansal - The formalism for calculating the effects of two-particles and two-holes excitations accompanied by the isospin excitations of the target nucleus on the structure of the final nucleus states obtained via single proton transfer has been presented. The target considered has a neutron filled orbit outside a doubly closed shell inert core and the proton is added to one of the empty orbits. The energies, wave functions and spectroscopic factor have been

calculated for 3/2 excited states of  $^{49}\text{Se}$  nucleus and 5/2 excited states of  $^{61}\text{Cu}$  nucleus using some standard two body interactions.

A comparison of the present results with those obtained by taking into account only the already known isospin excitations of the core indicates that the two-particles two-holes excitation of the target results in many more,  $\ell=1$  and  $\ell=3$  states in the  $^{49}\text{Se}$  and  $^{61}\text{Cu}$  spectra respectively than allowed otherwise. Experiments seem to confirm such a trend.

4. Level Structure Studies in  $^{160}\text{Dy}$  - S.S. Bhati, Nirmal Singh, Punjar Dass and PN. Trehan - Energy and intensity measurements of various gamma rays in  $^{160}\text{Dy}$  have been done using a Ge(Li) detector. In addition gamma-gamma angular correlation studies of ten cascades were done in  $^{160}\text{Dy}$  using a Ge(Li) - NaI(Tl) fast coincidence set-up. These cascades are 299-966, 299-879, 197-87, 962-87, 879-87, 215-962, 296-(879)-87, 215-(962)-87, 299-(682)-197 and 215-(765)-197 keV. Out of these 215-(962)-87 and 215-(765)-87 keV cascades have been attempted for the first time. The multipolarities of 197, 215, 299, 879 and 962 keV gamma rays were found to be  $E2+(2\pm 2)\%M3$ ,  $E1+(2\pm 2)\%M2$ ,  $E1+(0.5\pm 0.5)\%M2$ ,  $M1+(99.5\pm 0.5)\%E2$  and  $M1+(98\pm 1)\%E2$  respectively. The reduced E1 and E2 transition probabilities of various transitions in  $^{160}\text{Dy}$  have been compared with unified model calculations. This comparison shows that 1264 keV state belongs to K=2 gamma

vibrational band, while 1286 and 1399 keV states are either K=0 or K=2 states and 1358 keV state is either K=0 or K=1 state.

5. Level structure studies in  $^{99}\text{Tc}$ ,  $^{140}\text{Ce}$  and  $^{147}\text{Pm}$ . S.S. Bhati, Nirmal Singh, Punjar Dass and P.N. Trehan - Energy and intensity measurements with considerable precision have been done in  $^{99}\text{Tc}$ ,  $^{140}\text{Ce}$  and  $^{147}\text{Pm}$  using a 8 c.c. Ge(Li) detector in conjunction with ND-1100 multichannel analyser. The technique of Gehrke et al<sup>1)</sup> was used for energy and efficiency calibration. The accuracy obtained in energy and intensity measurements were of the order of 0.05 keV and 3-5% respectively. With this accuracy, it was possible to improve upon the previous values of energies and intensities. In addition, gamma ray coincidence spectra were taken in  $^{140}\text{Ce}$  and  $^{147}\text{Pm}$  using a Ge(Li)-NaI(Tl) fast-coincidence set-up. On the basis of single's as well as coincidence studies, the existence of 312 keV gamma ray in  $^{147}\text{Pm}$  has been confirmed. Also, the existence of 722 keV level in  $^{147}\text{Pm}$  has been confirmed. The 298 keV gamma ray proposed by H. Singh et. al has not been observed in the present study.

1) R.J. Gehrke, R.L. Heath and J.E. Cline, Nucl. Inst. and Methods 91 (1971) 349.

N. PUNJABI UNIVERSITY, PATIALA

1. Some Internal Conversion Puzzles - H.S. Sahota - Despite large number of attempts to explain the nature of the 279, 191 and 192 keV transitions in  $^{203}\text{Tl}$ ,  $^{197}\text{Au}$  and  $^{114}\text{In}$  respectively they have remained puzzles. In the case of 279 keV transitions in  $^{203}\text{Tl}$  nuclear penetration effects were involved so that an agreement for mixing ratios obtained from L-subshell ratios, electron gamma directional correlations and coulomb excitation measurements could be found. Later measurements of gamma linear polarisation-gamma directional correlations gave a much smaller value for  $\delta$ . The resonance fluorescence results for  $\delta$  were also in favour of a smaller value. For the 191 keV transition in  $^{197}\text{Au}$  the K-conversion coefficient and subshell ratio measurements yield a penetration parameter of  $\lambda = 5 \pm 2$ . The sign of  $\lambda$  obtained from the theoretical calculations is negative while the numerical value is 4, in agreement with above. For the 192 keV E4 transition in  $^{114}\text{In}$  the k as well as the L subshell conversion coefficients are smaller by nearly 30%. Although the nuclear penetration effects are usually associated with the lower multiple order transitions yet it becomes necessary in this case to consider their presence to explain the internal conversion process of this transition.

2. Spin Assignment to 42ms. state of  $\text{In}^{114}$  from the Isomeric cross section Ratios - K.G. Garg and C.S. Khurana - The isomeric

cross-section ratio measurements are a very useful method of investigating the angular momentum effects in nuclear reactions. The isomeric ratio may yield information of spin dependence of nuclear level densities in the final nucleus which is characterized by a spin cut-off parameter  $\sigma$ . In this paper firstly the analysis has been carried out for  $\text{Sc}^{45}(n,2n)\text{Sc}^{44}$  reaction where a value of 0.483 has been obtained for the theoretical value of isomeric cross-section ratio which is in agreement with experimental ones existing in the literature<sup>1,2,3,4</sup>). Also a value of  $\sigma = 3.5$  is obtained which is same as that of given in reference<sup>1</sup>). Secondly, we have employed this technique of comparison of the experimental cross-sectional ratios with the theoretical ones performed for  $\sigma = 3$  to assign a value of spin = 8 to the 42ms state of In <sup>114</sup> nucleus. Weisskopf estimates<sup>1</sup> for the photon transition probabilities also strongly support this spin value.

- 1) J. Karolyi and J. Csikai, Nucl. Phys. A112 (1968) 234.
- 2) S.K. Mukherjee et. al., Proc. Phys. Soc. London, 77A(1967)508.
- 3) J.R. Preswood and B.P. Bayhurst, Phys. Rev. 121(1961)1438.
- 4) L.A. Rayburn, Phys. Rev. 122(1961)168.

### 3. Double Coriolis Coupling in Odd-Odd Deformed Nuclei - S.D.

Sharma and V.P. Garg - Double Coriolis coupling is expected to play an important role in the study of spectra, static moments and transition probabilities of odd-odd nuclei in bands with  $k=0^+$  and  $1^+$ . Odd-even shift observed in case of these bands is

expected to be useful to understand the nature of nuclear forces as only the tensorial forces are likely to explain the odd-even shift. As the first step, the effect of double coriolis coupling on the moments of inertia of deformed odd-odd nuclei is studied. The computed results are compared with the experimental reports.

4. Coriolis Coupling Effects on the Magnetic Moments of Odd-A and Odd-odd Nuclei - V.P. Garg and S.D. Sharma - Bohr and

Mottelson's symmetric core model was extended to the case of odd-A nuclei by Chi & Davidson and further to odd-odd nuclei by Sharma and Davidson. The model consists of rotating core inert to vibrations and odd nucleon (s) moving in deformed harmonic oscillator potential well (s) with L.s and 1.1. terms. The odd-nucleon (s) is (are) taken according to single particle Nilsson orbitals. The total Hamiltonian consists of rotational part, Nilsson's Hamiltonian (s) for odd nucleon (s), (and the residual particle interaction for odd-odd nuclei). Jagdev and Sharma reported coriolis coupling effect on Moments of Inertia of odd-A and odd-odd nuclei. They also reported magnetic moment of these nuclei without configuration mixing. In the present study, coriolis coupling (which accounts for  $k=\pm 1$  mixing) has been used to calculate magnetic moments of some of deformed odd-A and odd-odd nuclei. (The effect of double Coriolis coupling is used for the states with  $K=0^{\pm}, 1^{\pm}$ ). The results are found in better agreement with experimental reports.

O. REACTOR RESEARCH CENTRE, KALPAKKAM

1. Evaluation of Fission Width of  $1+$  Spin State and Updating of Intermediate Resonance Parameters Based on Double Humped Fission Barrier Model for PU-239 - S. Ganesan - An accurate knowledge of fission width of  $J=1+$  spin state is important and attractive for many reasons. After reviewing the theoretical and experimental work done earlier, on the analysis of intermediate structure in the fission cross section of PU-239 and specially the generation of intermediate resonance parameters based on Weigmann's formulation of Strutinsky's need for updating the intermediate resonance parameters as any other basic neutron nuclear data is updated. Starting from the latest recommended values of the ratio of capture to fission cross section for PU-239, we evaluate by adjustment, a set of fission width values for  $1+$  spin state corresponding to the observed variations in alpha values. Using these values of fission widths we obtain a set of 37 intermediate resonance parameters using which one can generate reliable widths of  $1+$  spin state for any energy region below 10 keV.

P. UNIVERSITY OF DELHI

1. Is  $\Lambda C^{12*}$  a Strangeness Analogue State?-Swapna Banerjee and N. Panchapakesan - Strangeness analogue states are coherent superposition of particle-hole states where the particle and neutron hole occupy identical orbits. We discuss the possibility of  $\Lambda C^{12*}$  state being a strangeness analogue state in the framework of alpha particle model. We first discuss  $C^{12*}$  in this model using equilateral triangle configuration. This is done with three different N-N potentials; those of Volkov, Gillet and Brink-Boeker. The radius and separation of the alpha clusters are determined knowing the binding energy of  $C^{12}$ . The same wavefunction is taken to describe  $\Lambda C^{12*}$  in which one cluster has a  $\Lambda$ -particle in it instead of a nucleon. With this wavefunction the  $\Lambda$ -N potential which gives the observed binding energy is calculated. This  $\Lambda$ -N potential is expressed in terms of an equivalent soft potential which has a volume integral about 30% to 50% more than that obtained from the study of light hypernuclei. The idea of strangeness analogue state is thus seen to be consistent with the alpha particle model.

2. Pion Condensation and the Presence of Nucleon Resonances in Nuclear Matter - N. Panchapakesan - The presence of mesons like pions inside the nucleus has been a matter of study for a long time. Recently it has been suggested that the pion could be in a resonant state with the nucleon and be present as a nucleon resonance  $\Delta$  of mass 1236 MeV. The attractive interaction of the pion and nucleon in p-wave has also led to the suggestion that a

condensate of coherent pions of same momenta may be formed in dense systems. We study the interaction of pions in nuclear matter with the static model. Following Bethe, we use the theory of refractive index and the requirement of unitarity. We conclude that the pions, if condensed, must be necessarily in a resonant state with the nucleon forming a  $\Delta$  resonance. The critical density for appearance of the resonance is shown to be  $\sim 0.074$  baryons  $F^{-3}$  much lower than the nuclear matter density of  $\sim 0.16$  baryons  $F^{-3}$ . The presence of resonances in nuclei should, therefore, play a significant role in nuclear physics.

### 3. Magnetic Moment of the Deuteron in the Presence of Nucleon

Resonances - N. Panchapakesan and R. Venkataraman - Magnetic moment of the Deuteron  $M_d$ , includes the intrinsic magnetic moment of Nucleons and the orbital magnetic moment. The amount of  ${}^3D$  state present is fixed by the Quadrupole moment and is taken to be about 7%.  $M_d$  is calculated to be 0.8400nm, below the experimental value of 0.8573nm and the difference is attributed to mesonic effects. One way of taking mesonic effects into account is to consider the Physical Nucleon to be a superposition of Nucleon and a  $\Delta$  resonance.  $\Delta$  has a mass of 1236 MeV and Spin 3/2 and Isospin 3/2. Bethe has shown that the width of  $\Delta$  increases with Nuclear density. We calculate the probability of the presence of  $\Delta$  and calculate the

contribution of  $\Delta$  to the magnetic moment. We take the  $\Delta_s$  to be also in the  ${}^3S$  or  ${}^3D$  states. We obtain a value of 0.8644nm which is more than the experimental value. The result depends on the Nuclear density and hence on the Deuteron wavefunction. We present values for two possible models.

#### 4. Nuclear Structure Studies through Proton-Hole State Formation -

R.S. Kaushal and S.K. Monga - In order to understand the nuclear structure properties, we consider the formation of a real proton-hole state in nuclear matter by doorway mechanism and investigate the spreading widths of the hole states thus formed in relation to the particle-hole energy gap parameter ( $\Delta$ ) and the saturation nuclear density ( $k_F$ ). Our calculations with rank two N-N separable potential of Monga's type show that the  ${}^1S_0$  free two-body force when inserted in the Bethe-Goldstone equation is strongly over repulsive in producing the widths of the expected magnitude. Our results, which are in agreement with others' investigations too, are further confirmed by detailed analysis using different values of the parameters  $\Delta$  and  $k_F$  for the nuclear matter.

Q. UNIVERSITY OF MADRAS

1. Asymmetry and Polarization of the Recoil Nucleus in the

Reaction  $\mu^- + {}^{12}\text{C} \rightarrow {}^{12}\text{B} + \nu_\mu$  - V. Devanathan and P.R.

Subramanian - Expressions for the resultant polarization of  ${}^{12}\text{B}$

nuclei recoiling in the experimental arrangement of Louvain-

Saclay Collaboration<sup>1)</sup> are derived. How these polarizations are

related to the average polarization  $P_N$ , the longitudinal polariza-

tion  $P_L$  and the asymmetry parameter  $\alpha$  is investigated. The

experiment consists of two parts. In the first (second) part,

the polarization of the nuclei recoiling into the forward(backward)

hemisphere is preserved whereas it is destroyed in the backward

(forward) hemisphere. Of the three quantities  $\alpha$ ,  $P_N$  and  $P_L$

only  $P_N$  and  $P_L$  can be found directly. It is proved that  $\alpha - 2 P_L$

$= 1$  and this relation is independent of nuclear models and

coupling constants of the muon capture interaction<sup>2)</sup>. Using this

relation,  $\alpha$  can be found. It is found that  $\alpha$ ,  $P_N$  and  $P_L$  are

sensitive to the  $g_p/g_A$  ratio but insensitive to the nuclear model

used.

1) For measurements on average polarization, see A. Possoz et al,

Phys. Lett. 50B (1974) 438.

2) P.R. Subramanian and V. Devanathan, Phys. Rev.C. to be published.

2. Cascade Process in Muon Capture: Gamma-Neutrino Angular

Correlations - V. Devanathan and P.R. Subramanian - A nuclear

cascade process resulting from muon capture and subsequent de-excitation by gamma emission is considered. The gamma ray yield is expressed in terms of certain observable correlations involving the three vectors - the gamma ray momentum  $k$ , the neutrino momentum  $\vec{\nu}$ , and the muon polarization  $\vec{P}$ . We have investigated the process  $^{16}\text{O}(0^+, \text{g.s.}) \xrightarrow{\mu^-} ^{16}\text{N}(1^-, 392\text{keV}) \xrightarrow{\gamma} ^{16}\text{N}(0^-, 120 \text{keV})$ . The angular correlation coefficients are independent of  $g_P/g_A$  but sensitive to  $g_A/g_V$  and nuclear structure. We have used the single particle j-j coupling shell-model and the Gillet and Vinh Mau wave functions. Simple relations independent of nuclear models and coupling constant of the muon capture interaction are obtained between nuclear recoil asymmetry  $\alpha$  and the angular correlation coefficients. Measurements of correlation coefficients, therefore, give one a handle to find  $\alpha$  and hence present an alternative to ~~other~~ efforts in the field<sup>1)</sup>.

1) A. Possoz et al., Phys. Lett. 50B (1974) 438.

Previous reports published by the Indian Nuclear Data  
Group (INDG) :-

1.	A.E.E.T./NP/10	Progress report on Nuclear Data activities in India-I	1964
2.	A.E.E.T. - 227	Nuclear Data measuring facilities in India	1965
3.	A.E.E.T. - 228	Progress report on nuclear data activities in India-II	1965
4.	A.E.E.T. - 267	Progress report on nuclear data activities in India-III	1966
5.	A.E.E.T. - 305	Progress report on Nuclear data activities in India-IV	1967
6.	B.A.R.C. - 401	Progress report on Nuclear data activities in India-V	1969
7.	B.A.R.C. - 474	Progress report on Nuclear data activities in India-VI	1970
8.	B.A.R.C. - 553	Progress report on Nuclear data activities in India-VII	1971
9.	B.A.R.C. - 614	Progress report on Nuclear data activities in India-VIII	1972
10.	B.A.R.C. - 695	Progress report on Nuclear data activities in India-IX	1973
11.	B.A.R.C. - 770	Progress report on Nuclear data activities in India-X	1974



TEHRAN UNIVERSITY NUCLEAR CENTRE

REPORT OF RESEARCH AND EDUCATIONAL ACTIVITIES

1971 - 1973

Vienna, August 1975

C O N T E N T

1- Introduction.....	211
2- Activities.....	211
A- Education.....	211
B- Services.....	213
C- Research.....	213
3- List of Publications.....	216

## I N T R O D U C T I O N

Tehran University Nuclear centre (T.U.N.C) was established in 1959 in order to supply and develop means to utilize this important and new form of energy, i.e. Nuclear energy, in various fields, such as science, Agriculture, Medicine and industry.

T.U.N.C., is functionally administered by a Directorate, assisted by advisory and coordinating committees. Its budget which includes the salary of the employees, expenses for performing research activities, and other educational and laboratory expenses is included in the Tehran University budget. There are a total of 40 scientists in T.U.N.C all with doctoral degree from abroad. Major research Facilities at T.U.N.C. include a 5 M.W. pool type research reactor, a 3 MeV. Van De Graaf, a 6000 curies cobalt source and research laboratories such as: Nuclear physics, Nuclear Electronics, Radiochemistry, Activation Analysis, Radiobiology, Food preservation and Carbon Dating.

## A C T I V I T I E S

### A-EDUCATION

#### 1- Academic Courses:

- a) Participation in teaching graduate and under graduate courses at different colleges in Tehran University.
- b) Master of Science degree in Nuclear Science in three different majors of Nuclear physics, Nuclear chemistry and Radiobiology with cooperation

of Science Faculty, Tehran University.

- c) Master of public Health degree in Health physics with cooperation of Faculty of Public Health of Tehran University and World Health Organization.

## 2- Training Courses

Tehran University Nuclear centre organizes annually a Radioisotope course to familiarize participants from Tehran University and other national organizations on the use of radioisotopes in Science, Industry, Agriculture and Medicine. Special Courses in Health physics and radiation protection are held regularly in T.U.N.C.

International and regional courses are also organized at T.U.N.C with assistance of such organization as International Atomic Energy Agency, Food and Agricultural organization, World Health Organization and Central Treaty Organization.

Name of the course & seminar and symposium	Date	No. of participants
1- Ninth Radioisotope course.	29 May 29 June 1971.	22
2- Second course in Health physics.	3 Oct.-7 Nov. 1971.	23
3- Seminar on utilization of nuclear power reactor in Iran	11-14 Dec. 1972	60
4- IAEA. International Symposium on irradiation facilities for research reactors.	6-10 Nov. 1972	110 (24 countries).
5- Training course for administration Staff of Nuclear Power Reactor.	23 Dec. 1972 -6 Jan. 1973	8
6- Training course for technical Staff of Nuclear Power Reactor.	23 Dec. 1972 -10 Jan. 1973	14
7- Tenth Radioisotope course.	20 May-15 June 1973.	21
8- First Advanced course in Health physics.	8 May-8 June 1973.	18
9- Eleventh Radioisotope course	9 June-9 July 1973.	21

B-SERVICES:

This includes services in radiation protection (film badge, dosimetry, area monitoring, repair of electronic equipments and consultation and assistance to various institutions to train their administrators and employees in the use and safe handling of radioactive materials. This activity is presented by T.U.N.C. on request of any organization in need of it.

C-RESEARCH:

The research projects at T.U.N.C are conducted in the various research section of the centre. Following are the titles of research projects which are being carried out at present.

- 1- Reactor power measurement using N-16 Activity.
- 2- Reactor power measurement using fluctuations of the neutron detector.
- 3- Neutron spectrum measurement in TARR core and at beam port D.

- 4- Track recording of charged particles in organic materials.
- 5- Construction of wire scanning system and thermal neutron flux distribution measurement using DY-Al and gold foils.
- 6- Investigation on abrasion of piston rings using Iranian motor oils.
- 7- Radiation damage, by proton, on ionic crystals.
- 8- Study of Colour Centres in  $\gamma$ -irradiated monocrystal of BaClF.
- 9- Radioisotope production and Quality Control.
- 10-  $\gamma$ -Ray Polymerization of methacrylic acid in Presence of water and N.N. dimethyl formamide.
- 11- Grafting of acrylic acid onto polyvinyl chloride by direct radiation methods.
- 12- Preparation of wood polymer composite by ionizing radiation.
- 13- Uranium and Thorium measurement in Iranian rocks.
- 14- Trace elements in archeological samples measured by activation analysis technique.
- 15- Radiocarbon dating of archaeological samples .
- 16- Measurement of radionuclides and trace elements in Iranian sea water.
- 17- Non destructive neutron activation analysis of atmosphere pollutants utilizing Ge-(Li)- $\gamma$ -ray detectors.
- 18- Measurement of trace elements in Iranian cigarette smokes by neutron activation analysis.
- 19- Dosimetry of Natural radioelements in the air.
- 20- Determination of Iodine in eggs by neutron activation analysis and study of possibility to increase iodine in egg by nutrition behavior.

- 21- Radiation effects on amino acids and peptides.
- 22- Effect of cyclohexamide on Salt uptake.
- 23- Effect of different levels of phosphours on salt tolerance in Iranian varieties of barley.
- 24- Chemical analysis of Iranian Caviar.
- 25- Pasteurization of Salmonella and E. Coli contaminated caviar by  $\gamma$ -radiation.

List of The papers published by T.U.N.C. Academic Staff

1971 - 1973

A-PHYSICS:

- 1- B. Parsa, A. Ashari, L. Goolvard, and Y.M. Nobar, 1971 Decay Scheme of 2.7th  $^{92}\text{Sr}$ , "Nuclear physics, A125, 629-640.

ABSTRACT:

Gamma rays emitted in the decay of 2.71 h  $^{92}\text{Sr}$  have investigated with a Ge(Li) detector. Sources were prepared by Separating Sr from fission products. A total of 10  $\gamma$ -rays were attributed to the decay of  $^{92}\text{Sr}$  in a complex spectra with interferences from  $^{91}\text{Sr}$  and  $^{92}\text{Y}$ . Gamma coincidences in the decay of  $^{92}\text{Sr}$  were observed with a NaI(Tl)-Ge(Li)- setup. The decay scheme of  $^{92}\text{Y}$  excited states at 241.4, 892.8, 953.3 and 1383.9 KeV. The observed level structure is compared with previously reported predictions based on effective interaction calculations. The value for the half-life of  $^{92}\text{Sr}$  was determined to be  $2.71 \pm 0.01$  h.

RADIOACTIVITY  $^{92}\text{Sr}$  (from  $^{235}\text{U}$  (n, fission); measured  $E_{\gamma\gamma}$ ,  $\gamma\gamma$  coin,  $T_{1/2}$  deduced log ft.  $^{92}\text{Y}$  deduced levels, J.X. Ge(Li) and NaI(Tl) detectors.

- 2- M. Yuste, M. Rahmani, D. Jumeau. L. Taurel and J. Badoz, 1973, "E.S.R. Study of  $\text{U}_2$  Centres in Ba ClF". J. Phys. C. Solid State phys., 6, 3167-3173.

ABSTRACT:

An X Irradiation, at 78 K, of a BaClF crystal containing  $\text{OH}^-$  ions leads to the formation of hydrogen atoms in interstitial sites ( $\text{H}_1^0$  or  $\text{U}_2$

centres) thermally stable below  $T \sim 100K$ . The magnetic properties of the  $U_2$  centres are compared with those observed in the case of  $U_2$  centres in NaCl crystal. The thermal stability is studied and compared with those of the  $U_2$  and  $U_3(H_3^O)$  centres in NaCl.

3- M. Rahmani, "Etude des Centres Colores qui apparaissent dans le mono cristal de BaClF irradié aux rayons - X a  $295^0 K$  et de leurs Cinétiques de formation", 1973, Bull. Faculty of Science, Tehran Univ. Vol 4, No. 5

RESUME:

Les bandes fines a 308 nm et 288 nm dans le cristal non irradié sont les resultats des transitions excitoniques des impuretes  $OH^-$ .

Dans le cristal irradié a  $295^0K$ , la bande a 550 nm et la bande double a 440 nm mesurées a  $78^0K$  sont attribuable respectivement aux centres  $F(F^-)$  et  $F(Cl^-)$ .

La cinotique de formation des centres  $F(F^-)$  est plus grande que celle de  $F(Cl^-)$ .

B. Nuclear Technology

- 1- A. Afshar -Bakeshloo, 1971, "prospect, of Nuclear power plant in Iran"  
Economic Integregation of Nuclear power Station in Electrical power  
Systems, 619, IAEA, Vienna.

ABSTRACT:

Iran, with an area of 1,65 million Km<sup>2</sup> and a population of about 26.5 million, is very rich in fossil-fuel resources. The total amount of oil, natural gas, and coal reserves in the country are estimated to be approximately 6000 million tons, 300 trillion ft<sup>3</sup>, and 100 million tons, respectively. The potential hydro power is estimated at about 30 billion KWh/yr. In addition, because of the suitable latitude in south Iran, there is the possibility of using solar energy. Promising uranium ore deposits are also reported in some parts of Iran. Because Iran has had no need for nuclear raw materials, prospection has proceeded rather slowly. Thus information about the uranium resources of the country is very limited at present. However, in a country such as Iran, which is undergoing a process of rapid industrialization, both future demand and supply of power are subject to wide uncertainties. So the forecast of power demand and supply vary within much wider limits than in highly - industrialized countries. The electrical utility in Iran is under the Government. The country is divided into 10 electrical zones, each supplied by several units. At the end of 1969 the total installed capacity was 1313 MW(e).

Details of the forecast future power demand and type of units for all the zones for 20 years (up to 1987) are presented. Net generation is expected to be 9574 MW(e) in 1987. This figure reflects the development of industry according to Government plans. The estimated specifications for the required stations are included. Figures are given for the energy exchange between the electrical zones. Also, price information on oil and coal are presented. The existing percentages of total capacity in hydroelectric (35%), steam (33%), diesel (22%) and natural gas (10%) power stations will be by 1987 respectively 68%, 25%, nil and 7%. Recently, the Government has been interested in studying the economic feasibility of nuclear power for the future in Iran. This subject is under study, but the paper gives some very preliminary estimates of the probable size of a nuclear power plant. It is concluded that a UNIT of 500 MW(e) nuclear power would be desirable in 1980 for an area that is far away from the fuel resources and also close to the industrial load centre.

- 2- A. Afshar-Bakeshloo, N. Farivar-Sadri, H. Panahandeh, H. Parnianpour, A. Pazirandeh, M. Sarram, 1972, "Peaceful uses of Nuclear Energy and prospects of Nuclear power in Iran", Peaceful uses of Atomic Energy, Vol. 6, 455 IAEA, Vienna.

ABSTRACT:

The first step towards the utilization of nuclear energy for peaceful purposes was initiated by the establishment of the Tehran University Nuclear Center. The 5-MW research reactor at Tehran University went critical in November 1967 and has been fully operational since May 1970.

The research reactor is used for research and educational purposes and also for the production of radioisotopes. At present, the main emphasis in peaceful uses of nuclear energy in Iran is put on the utilization of nuclear power plants for production of electricity; therefore this paper will deal with this subject.

Iran, with an area of 1.65 million square kilometers and a population of about 29 million, is very rich in fossil fuel resources. The estimated resources of oil, natural gas, and coal in the country are approximately  $70 \times 10^9$  barrels,  $214 \times 10^{12}$  ft<sup>3</sup>, and  $4.55 \times 10^9$  tons, respectively. Information regarding the price of oil, gas, and coal is presented. Hydro potential is also estimated to be about  $30 \times 10^9$  kWh/yR.

Due to a suitable latitude in the south of Iran, there is the possibility of utilizing solar energy; uranium ore deposits have been reported in some parts of the country. Because Iran has had no need for nuclear raw materials, prospecting has proceeded rather slowly. Thus, information about the uranium resources in the country is very limited at the moment. However, in a country such as Iran, which is undergoing a process of rapid industrialization, both future demand and supply of power are subject to wide uncertainties.

Iran is divided into 10 electrical zones, each one supplied by several units. At the end of September 1970, the total installed capacity was 1330 MW(e). Forecast details for the future power demand for the type of units for the period up to 1987 are presented. Net generated power in 1987 is expected to be 9547 MW(e). This figure reflects, to large extent, the country's industrial development according to Government plans. The distribution of the total existing electric power stations is 35% hydro, 33% steam, 22% diesel, and 10% gas. The respective figures for 1987 are predicted to be 68, 25, 0 and 7%.

Recently the Government initiated a feasibility study for utilization of nuclear power for future energy demands. A very preliminary study has shown that a 500-MW(e) nuclear power plant would be desirable in about 1980.

3- M. Sarram and N. Farivar - Sadri, 1973, "Irradiation Facilities at the Tehran University Research Reactor", Irradiation Facilities for Research Reactors, 385, IAEA, Vienna.

ABSTRACT;

IRRADIATION FACILITIES AT THE TEHRAN UNIVERSITY RESEARCH REACTOR.

The Tehran University Research Reactor is a 5-MW pool type, light-water moderated, heterogeneous solid fuel reactor. Initial criticality was achieved in November 1967 and 5-MW operation was reached in January 1968.

The reactor, being a typical research reactor, has the standard experimental and irradiation facilities such as beam tubes, thermal column, pneumatic rabbit system. In addition, the reactor has a dry gamma room and dry neutron irradiation chamber. The design features of these irradiation facilities are presented in detail. In addition, the installation of various experimental facilities which are under study are discussed.

4- M. Sarram, 1973, "The Current Safety philosophies for Design and Operation of Nuclear power plants", Principles and standards of Reactor Safety, IAEA - SM - 169/1.

ABSTRACT:

Experience has shown that the current safety philosophies practised in the design of nuclear power plants and their operations are more than adequate; however one must always plan for additional safety measures. One of the main problems to be considered in evaluating the safety of a power plant is the reactor structural design, in particular the containment. The current containment systems constructed for thermal power plants may be classified as pressure containment, and multiple containment systems. Salient design features of the multiple containment system and its safety philosophies are presented. Another main problem encountered in the design of power plants is the philosophy of secondary safety systems. The importance of a secondary safety system such as emergency cooling comes into the picture when one considers the following figures for energy releases in a typical PWR, 185 MW(e), Maximum Hypothetical Accident, with 20% concept of stretch; nuclear excursion:  $2 \times 10^7$  Btu, chemical reactions:  $10^7$  Btu, decay heat:

$3 \times 10^7$  Btu and stored energy in coolant:  $10^8$  Btu, which is an order of magnitude higher than others. The paper also presents other standard limits for risk evaluation, safety measures to be used for design of nuclear power plants.

5- H. Karami and A. Afshar-Bakeshloo, 1970, "The Age of  $^{241}\text{Am}$ -Be Neutrons in  $\text{H}_2\text{O}$ ", Bulletin of Tehran University Nuclear Center, Vol 2, No. 1.

ABSTRACT:

The neutron age for non-fission source  $^{241}\text{Am}$ -Be neutrons was measured in  $\text{H}_2\text{O}$ . The age was evaluated from the second moment of the slowing down distribution at the 1.458 ev. resonance of Indium and then the value of for thermal neutrons (0.025 eV) are obtained. The age is found to be  $97.8 \text{ Cm}^2$ .

6- M.R. Hamidian and A. Pazirandeh, 1973, "Gamma Dosimetry in the Tehran University Research Reactor Core." Atomkern Energie, Vol. 22, 67-68.

ABSTRACT:

The Radio-photo-Luminescence (RPL) property of some materials can be utilized for dosimetry purposes. In the present work the FD-R1-1 glass dosimeter, 1 mm diameter and 6 mm long made by Toshiba was used. First the glass dosimeter was calibrated using Victoreen Chamber.

The neutron sensitivity of dosimeter was determined by using dysprosium foil, for absolute flux measurement, and covered glasses with Cd and Sn the sensitivity was determined to be  $1 \text{ rem} = 10^9 \text{ n Cm}^{-2} \text{ S}^{-1}$ .

The heating up the dosimeter up to 400 °C was studied and the sensitivity of heated and unheated glasses are compared. The experimental results show that the FD-R1-1 glass loses about 10% of its dose after 10 minutes being at 200 °C, about 50% at 320 °C and 100% at 400 °C for the same heating time.

The sensitivity of the fission chamber, used for start-up the reactor, to gamma was studied. Experimental results show that the fission neutrons, travelled 30 cm in water.

Gamma dose distribution inside the fuel element of the reactor during operation and shut down was studied and compared to the neutron flux distribution.

7- A. PAZIRANDEH, and C.B. Besant 1973, "Measurement of Fission Ratios in zero Power Reactors" British Nuclear Energy Society II, 377.

ABSTRACT:

Fission rate ratios of  $^{238}\text{U}$  relative to  $^{235}\text{U}$  have been measured in the University of London reactor CONSORT by detecting the fission product gamma activity from irradiated uranium foils. It was necessary to utilize a time-dependent calibration factor to relate the gamma activity ratio to the true fission ratio. Possible systematic errors in the technique have been investigated in detail. The technique has been used by other laboratories for measurements in fast reactors and so the neutron spectrum dependence of parameters, such as the time-dependent calibration factor, has been examined.

It has been found that the calibration factor can change by 6% in going from a typical thermal reactor spectrum to a typical fast reactor spectrum. The overall systematic error in fission rate measurements has been reduced to 1.5%. Comparisons between experimental  $^{238}\text{U}/^{235}\text{U}$  fission ratios and predictions using the GMS-I code have also been made.

8- M. Kasari, H. Panahandeh, A. Pazirandeh and S. Bozorg-Cami, 1973, "Farah-Abad gas line test using a radionuclide". Kerntechnik, 9,424-425.

ABSTRACT:

The test was carried out successfully and no obstruction was found in the pipe. This experiment shows that this type of non-destructive testing is very cheap and fast and can be utilized in many similar cases.

9- Y.M. Nobar, Dj. Moghimi, and Z. Brzezinski, "A New Solid State Safety Amplifier For Reactor Control", Accepted by Kerntechnik.

ABSTRACT:

A new transistorized safety amplifier has been designed and constructed for the T.U.N.C. research reactor. The new unit will replace the present one using vacuum tubes and relays. The input signals for the safety amplifier come from two ionization chambers. Each ionization chamber actuates three memory circuits which they operate under a majority voting procedure. Furthermore, each ionization chamber simultaneously actuates the memory circuit of the other by cross coupling. Consequently, reactor scrams will mostly result from faults of nuclear origin, and not of electronic failures.

Ease of serving, exchangeability of components, subassemblies and the suitable size are the other advantages of the new system,

10- S. Farrokhi, Dj. Moghimi, R. Nahavandi, M. Pichevar and B. Delaunay, 1972, Le van de Graaff de 3 MeV du centre Nucleaire de Tehran. B.I.S.T. Commessaria at l'energie atomique. No. 172, 65-70.

ABSTRACT:

A 3 MeV horizontal van de Graaff has been installed in the Tehran Nuclear Centre. 400 $\mu$  A of 3 MeV hydrogen beam, 50 $\mu$  A of 3 MeV proton beam, and 100 $\mu$  A of 3 MeV electron beam have been obtained. This operation is briefly described.

C- Chemistry

I- M. Kasrai and A. U. Maddock, 1970, "Chemical Effects of Nuclear Transformations in Alkali Chlorides. Part II. Analytical problems with sulphur - 35 "J. Chem Soc., A 1105,

ABSTRACT:

<sup>35</sup>S released in an alkali chloride matrix is present in four chemically distinguishable forms. An analytical procedure enabling one to determine their proportions is described. Evidence is given that the four products. Sulphide, thiocyanate, sulphite, and sulphate, separated in the process are derived from four different lattice entities.

2- M. Kasrai, A. U. Maddock, and J.H. Freeman, 1971, "Chemical Effects of Nuclear Transformations in Alkali Chlorides. Part III. Behaviour of Ion Implanted <sup>35</sup>S "Trans. Faraday Soc., 67, 2108.

ABSTRACT:

The valence distribution of ion implanted  $^{35}\text{S}$  in sodium chloride has been investigated and the influences of pre-bombardment of the crystal with O, S and Cl measured. The effects of pre- or post-irradiation of the crystals with  $\gamma$  radiation and of thermal annealing combined with these treatments have been examined. A small part of the  $^{35}\text{S}$  penetrates deeply into the crystal, giving a supertail to the distribution. This phenomenon is attributed to interstitial diffusion and the valence distribution of this sulphur has been measured.

3- M. Kasrai, A.G. Maddock, and I.S. Suh, 1973, " $^{35}\text{S}$  in Doped Alkali Chloride;  $\text{CN}^-$ ,  $\text{SH}^-$ , and  $\text{S}^{\equiv}$  Doping", Presented in the 7th International Hot Atom Chemistry Symposium, Julich, W. Germany Sept., 10 - 14.

ABSTRACT:

The influence of  $\text{CN}^-$ ,  $\text{SH}^-$  and  $\text{S}^{\equiv}$  anionic doping of hydroxide-free sodium chloride on the initial distribution and the annealing characteristics of  $^{35}\text{S}$  produced by the (n,p) reaction in the crystals has been investigated. The analytical procedure allowing the determination of four forms of  $^{35}\text{S}$  developed earlier has been used. The doping leads to spectacular differences in behaviour and provides further evidence of the role of V centres in the formation of the  $^*\text{SO}_3^{\equiv}$  and  $^*\text{SO}_4^{\equiv}$  precursors.

4- M. Kasrai and M. Raie, 1973, "The State of  $^{35}\text{S}$  in Doped Crystals of Alkali Chlorides", Presented in the 7th International Hot Atom Chemistry Symposium, Julich, W. Germany, Sept. 10-14.

ABSTRACT:

It has been shown that when neutron irradiated alkali chloride crystals are dissolved in carrier solution containing  $\text{CN}^-$  ions, a fraction of  $^{35}\text{S}$  appears as  $\text{CNS}^-$  ions. This fraction has been attributed to the presence of atomic sulphur in the lattice. In order to examine the effect of  $\text{CN}^-$  ion in the lattice, samples of potassium chloride have been doped with various concentrations of potassium cyanide. After the irradiation samples were analysed for  $\text{S}^-$ ,  $\text{CNS}^-$ ,  $\text{SO}_3^-$  and  $\text{SO}_4^-$ .

The results show that the  $\text{SO}_3^-$  and  $\text{SO}_4^-$  proportions in the doped crystals are generally low (less than 10%) and as the mole fraction of  $\text{CN}^-$  ion is increased the  $\text{CNS}^-$  proportion is also increased. There is an evidence to show that not all atomic sulphur in the lattice is converted to  $\text{CNS}^-$  but some still remains as atomic. Photo and thermal annealing of doped crystals show an increase in the  $\text{S}^-$  fraction mainly at the expense of the  $\text{CNS}^-$  fraction. The results of KCN doping and HCN doping have been compared. In the latter case it is presumed that an  $\text{OH}^-$  impurity is replaced by the the  $\text{CN}^-$  ion.

These results are interpreted on the basis of disappearance of usual type of V centres in the doped crystals and the formation of a new type of centres, "CN" centres, which are less oxidizing entities.

5- G. Marino, L. Valente, R.A.W. Johnstone, F. Mohammadi-Tabrizi. and G.C. Sodini, 1972, "N-Methylation of peptides", J.C.S. Chem.Comm., 357.

SUMMARY

A method for the N-methylation of peptides (amide bonds) is described and preferred conditions are suggested whereby all amino-acid

residues except arginine react without prior modification.

6- Z. Khalkhali, B. Parsa and B. Parsa, 1972, "Measurement by Non-Destructive Neutron Activation Analysis of Bromine Concentration in the Secretions of Nursing Mothers, "Nuclear Activation Techniques in the Life Sciences, IAEA-SM-157/26, 461 Vienna.

ABSTRACT:

A study was made of secretional pathways of bromine in nursing mothers. Ten nursing subjects were given a dose of 0.5g Br/ 50 Kg weight, and the changes in the bromine concentration in their plasma, milk, sweat and urine were measured over a period of one week. Activation analysis of the collected samples was performed by irradiation at the Tehran University Research Reactor in a thermal flux of  $2 \times 10^{13} \text{ n cm}^{-2} \text{ s}^{-1}$  for a period of 1 h. The irradiated samples were analysed by a Ge(Li) detector and an 800-channel analyser. The bromine concentration in the plasma and observed body secretions reached its maximum after 48 h. In the case of plasma it then fell giving a biological half-life of about 4 d and later levelled off to a longer decay period. Bromine concentration in urine tended to become steady after the 48-h peak. In the case of milk a sharp decline with a biological half-life of about 3 d followed the observed peak in the second day. A similar situation was obtained with sweat where the excretion of bromine was mainly in the first few days. Measurement of bromine concentration in the plasma and body secretions various individuals revealed that those with higher standards of living had a bromine concentration about three times greater than that of people

with low living standards. This is most probably due to the different dietary conditions. It was concluded that the bromine has a cumulative effect in the body. By comparison, the tissues have a higher bromine binding capacity than the plasma components. The high rate of bromine excretion in the milk suggests a significant poisoning route in case of mothers who breast-feed their newborn infants and take bromine compounds as medication.

- 7- M. Razeghi and B. Parsa, 1973, "The Determination of Microimpurities in Quartz Samples by the Radioactivation Method of Analysis, "Radiochemical and Radioanalytical Letters, 13, 95, .

ABSTRACT:

Seventeen elements at trace levels have been determined by - neutron activation analysis in a quartz sample. Na, K, Sc, Mn, Fe, Co, Zr, Nb, Sb, Cs, La, Eu, Yb, Hf, Ta, Au and Th have been determined by a nondestructive technique using a high resolution Ge/Li/ detector.

- 8- Z. Abedinzadeh and B. Parsa, 1973, "Determination of Trace Elements in the Iranian Cigarette Tobacco by Neutron Activation Analysis, "Journal of Radioanalytical Chemistry, Vol. 14, No. 1, 139.

ABSTRACT:

The concentration of 24 trace elements in the tobacco of two different brands of Iranian cigarettes. "Zarrin" and "Oshnoo", has been measured. by neutron activation analysis employing a high-resolution

Ge(Li) detector. These elements are: Na, K, Sc, Cr, Mn, Fe, Co, Zn, Se, Br, Rb, Ag, Sb, Cs, Ba, La, Ce, Sm, Eu, Tb, Hf, Au, Hg and Th.

9- Z. Abedinzadeh and B. Parsa, "Instrumental Neutron Activation Analysis of Iranian Wines", Bull. Faculty of Science, Tehran Univ., 42,4, No. 2.

ABSTRACT:

Instrumental neutron activation analysis employing a high-resolution lithium drifted germanium  $\gamma$ -ray detector has been used to identify some of the trace elements in two different brands of Iranian wine, "Velvet" and "1001". This was carried out by irradiating the wine samples in the Tehran University Research Reactor at a flux of  $2 \times 10^{13} \frac{\text{neutrons}}{\text{cm}^2 \text{ -- Sec}}$  for periods which ranged from 15 minutes to 4 hours. The irradiated samples were then analyzed at suitable periods with a 40 cm<sup>3</sup> Ge(Li) and an 800-channel analyzer. A total of 10 elements have been identified employing this technique. These include Na, K, Sc, Cr, Mn, Fe, Co, Br, Rb, and Zn.

10-B. Parsa and S.S. Markowitz, "Determination of Lead in Atmospheric Air and in Aluminum by <sup>3</sup>He-Induced Nuclear Reactions", LBL-1901, June 1973 (to be published in the Analytical Chemistry).

ABSTRACT:

Helium-3 activation analysis has been applied to develop a very sensitive means of trace lead analysis. The procedure involves the bombardment samples with <sup>3</sup>He particles to induce  $\text{Pb} + {}^3\text{He} \rightarrow {}^{207}\text{Po}$  reaction on lead isotopes.

The 992-KeV  $\gamma$ -ray of 5.84-hr  $^{207}\text{Po}$  is used as the "signal" for lead determination. Only milligram amounts of sample are required. The excitation function for the production of  $^{207}\text{Po}$  from the reaction of  $^3\text{He}$  with lead of natural isotopic composition is presented. If necessary, destructive analysis may be carried out, and a radiochemical separation procedure to plate polonium onto a silver foil is discussed. The accuracy of the measurement is about 3 to 5% for comparative analysis. For absolute determinations the error is estimated to be 9-12%. Under reasonable irradiation and counting conditions, the detection limit is approximately  $50 \text{ pg/cm}^2$  corresponding to 0.5 ppb in a matrix  $100 \text{ mg/cm}^2$  thick.

11-B. Parsa and S.S. Markowitz, "The Half-Life and the Decay Branching Ratio of  $^{207}\text{Po}$ ", LBL-1902, June 1973, to be published in the Journal of Inorganic and Nuclear Chemistry).

ABSTRACT:

$^{207}\text{Po}$  was produced via  $^3\text{He}$  activation of lead samples. Polonium was chemically separated from the irradiated targets. Measurements were performed with Ge(Li) and surface-barrier type  $\alpha$  counters. The decay of the 992-KeV  $\gamma$ -ray of  $^{207}\text{Po}$  was followed and a half-life of  $350.3 \pm 4.1 \text{ min}$  (or  $5.84 \pm 0.07 \text{ hrs}$ ) was obtained for  $^{207}\text{Po}$ . The  $\alpha$ -decay branching of  $^{207}\text{Po}$  was measured to be  $0.0210 \pm 0.0018\%$ .

12-A. Owlya and F. Fakhr-Vaezie, 1973 "Determination of Selenium in Astragalus Sp. (by Neutron Activation Analysis). Bull. Faculty of Science, Tehran University, Vol. 5, No.2.

ABSTRACT:

A report from veterinary faculty indicated that within 15 days more than 68 sheeps were found dead by eating a plant called "Gavan". Later on, sample of this plant was sent to T.U.N.C. for analysis. Clinical evidence showed that the poisoning has been possibly due to the presence of selenium in plant. This element could not be determined by chemical method, because of its low concentration in the sample. Activation analysis technique which is a very sensitive method for the determination of trace elements in biological and nonbiological materials is being used for this study.

In this work this particular element was determined in the sample by nondestructive neutron activation analysis, using a high resolution Ge(Li) detector. After a decay period of one month radionucleids with short and intermediate half lives die out. Then photopeaks of selenium 75 with half-life of 120 days is easily characterized. The 0.265 and 0.280 MeV peak of selenium-75 are used for this determination. The result of the several experiments showed the existance of  $513 \pm 32$  ppm. of selenium in the plant samples which is above the permissible dose of this element. In this study we did not determined the other trace elements in the sample.

13- A. Owlya, F.FAKHR-Vaezi and B. Parsa, 1974 "Determination of the Trace Element levels in Iranian Margarine by Neutron Activation Analysis", Radiochem., Radioanal. Letters. 16/6/355-362.

ABSTRACT:

By means of neutron activation analysis the concentration levels of trace elements in Iranian Margarines were studied. A high resolution

γ-ray spectrometer has been used to identify the radionuclids in irradiated "Shah-Passand" and "Ghoo" samples of Margarine. A total of 13 elements at trace levels have been determined by this technique. They include Cl, Mn, Na, K, Br, La, Au, Cr, Fe, Cs, Sc, Zn, and Co.

14-A. Mahdavi, 1970, "Instrumental Neutron Activation Analysis Of Some Rock Forming Minerals". Bull. Faculty of Science, Tehran University, No. 3, 24-30.

ABSTRACT:

Rock forming minerals from an "Oslo essexite" from Ranviksholman, Oslofjorden and a Larvikite from Malberget, Tjøm, have been analysed using NaI (Tl) detector, by instrumental neutron activation analysis. In addition, a Norwegian geochemical reference sample apatite from Odegarden, Balm, and an apatite from Knipan (Ljosland) were analysed.

15- A. Mahdavi, 1971 "Antimony Contents of some Oslo Essexites", Bull. Faculty of Science Tehran Univ. Vol. 3, No. 2.

ABSTRACT:

The antimony content of ten Rock samples and two minerals (biotite and pyroxene) from Oslo essexites determined by neutron activation, range from 0.03 to 0.35 p.p.m. The highest figures were from two rock samples higher in sulfide Minerals. Which are believed to carry most of the antimony.

The rock samples come from Viksfjell volcanic neck, Hedland area; the two mineral samples were separated from an essexite rock sample from ranviksholment.

- 16- A. Mahdavi and C.H. Bovington, 1972, "Neutron Activation Analysis of some Obsidian Samples from archeological and Geological Sites in Iran" , Journal of British Institute for Persian Study, Vol. 10.

ABSTRACT:

Obsidian is a volcanic glass which occurs in restricted sites. Cutting tools and other objects made from this material were used by prehistoric man and are found in many prehistoric archaeological Sites. It is possible to characterize and relate archaeological and geological samples in terms of their trace element composition. In the present work we have analysed a number of excavated and source samples for their Na and Mn content. The analysis were carried out by neutren Activation. The results indicate an obvious relation between source samples and -- archaeological Samples, and suggest a pre-hystoric obsidian trade rout from central Anatabia and lake van area to Hassanlu, Sosa and Fars.

- 17- C.H. Bovington, A. Mahdavi, S. Dessaunettes, and R. Masoumi, 1972, "Radio-carbon Date of some Carbonate Concentrations and Surrounding Soil Sample", Bull. Faculty of Science, Tehran Univ. Vol. 4

ABSTRACT:

A preliminary study on the relative radiocarbon ages of calcium carbonate in the surrounding soil has been jointly carried out by the Soil Institute of Iran and the Radiocarbon Laboratory of Tehran University Nuclear Centre.

Samples of concretions and surrounding soil were collected from different locations and the results obtained are based on the 5730 years half life  $C^{14}$ . Benzene synthesis and liquid scintillation were used for this study.

Samples came from Chazvin and Shiraz area. The ages obtained ranges from 10381-15527 years. Both soil carbonates and concretion give near identical ages.

- 18- C.H. Bovington and R.Masoumi, 1972. "Tehran University Nuclear - Centre Radiocarbon List I. Radiocarbon 14, 456.
- 19- C.H. Bovington, A. Mahdavi, and R. Masoumi, 1973, "Tehran University Nuclear Center: Radiocarbon Dates II", Radiocarbon, Vol.15 No. 3.

ABSTRACT:

Ages reported in this date list are calculated using the Libby half life of  $5568 \pm 30$  years with 1959 as the standard year of reference; results are quoted in years B.C. and A.D./B.C. time scale .

Since much of our work involves correlations with material in an historical context in Mesopotamia it is important that the reader considers the implications of using 5730 years as the half-life of  $C^{14}$  and the corrections proposed by Ralph and Michael (1969) and other to allow for discrepancies between radiocarbon ages and calendrical ages.

All samples were examined for plant rootlets and other foreign matter, treated with 3M HCl, 3M NaOH, and de-ionized water. The contemporary - reference used is 0.95 of the specific activity of NBS oxalic acid.

- 20- C. Bovington, A. Mahdavi and R. Massoumi, 1973, Radiocarbon evidence for a chronology for S.W. Iran, from the mid fourth to mid third Millenia B.C. Accepted by ISMEO, East and West.

ABSTRACT:

Attempt has been made to review the radiocarbon evidence for S.W. Iran and related sites and its consistency with typological evidence.

Considerable confusion exists in many circles about the relationship between "Radiocarbon age" and true or calendrical Age. The correction Terms proposed by Ralph and Michael, permit a conversion of radiocarbon to calendrical age, sufficiently accurate for the purpose of the establishment of a reasonable chronology in S.W. Iran from the mid IV to mid 111<sup>rd</sup> Millenia B.C. evidences for the periods at Shar Sokhte, tape Yahya, Namazga, and Mundigak have been considered and the suggested chronology for this periods does not seem to be in variance with typological evidence.

BILOGY.

- 1- F. Didehvar, 1971, "The phosphorus Fertilization of Alfalfa (*Medicago sativa*". Bull. Faculty of Science, Tehran Univ., Vol. 2, No. 4, 25.

Part I:

Phosphorus uptake from top dressing with Ammonium phosphate.

The percentage of P in the plant derived from fertilizer estimated from the measurements of P<sup>32</sup> ranged from 22-30 per cent on the older Crop.

Part II.

The effect of different methods of cultivation on the uptake

of shesphate by newly seeded Alfalfa. The results suggest that under experimental Condition disc ploughing and deeper placement of fertilizer was beneficial to alfalfa in the early stages of growth and maturity.

Part III.

The effect of different methods of cultivation on the uptake of phosphours by alfalfa and Barly. overall results suggest that the fertilizer may be least efficiently distributed after chisel ploughing but that the magnitude of the difference can be much affected by condition.

- 2- F. Didehvar, A. Myers and L. Watson 1971, "Growth of the Wheat Leaf (*Triticum aestivum*)", Bull. Faculty of Science, Tehran University, Vol. 3, No. 3, 9.

ABSTRACT:

The wheat leaf in the early stages of growth consists only of a blade which grows from the base; when the blade is completed the ligule forms and from this time no more growth of the blade can be observed. The sheath then develops proximally to the ligule, its base being the last part to mature. There is a single basal (intercalary) meristem, throughout the period of growth of leaves.

- 3- F. Didehvar, 1972, "Absorption of  $^{32}\text{P}$  phosphate by Alfalfa (*Medicago sativa*) from Various Depths of Soil", Bull. Faculty of Science, - Tehran Univ. Vol. 4, No. 2 100.

ABSTRACT:

The results presented here suggest that effectiveness of any given method of placing the fertilizer depends on the time of the year.

Shallow placement of fertilizer is more effective earlier in the year and deeper incorporation is more effective later.

- 4- N. Rouhanizadeh and Zh. Khalkhali, 1971, "Evaluation Biochimique de la propriete radioprotectrice du "Shirkhesht", Radioprotection 6, 279.

In order to investigate the radioprotective action of "Shirkhesht", a non toxic natural substance, a biochemical evaluation of the DNP complex in irradiated animals has been made both with and without administration of "Shirkhesht". The sensitivity of the DNP complex to irradiation has also been investigated. The results so far confirm:

- the considerable change of the DNP complex in the irradiated tissues,
- "Shirkhesht" appears to have quite a considerable radioprotective action (25-30%) with the main advantage of being administrated orally.

- 5- N. Rouhanizadeh, L. Riazi, A. Owlya, and Zh. Khalkhali, 1973, "Preparation of  $^{113m}\text{In}$  - Ferric Hydroxide Macroaggregate For Lung Scanning", IAEA/SM-171/13.

The aim of this work was to prepare  $^{113m}\text{In}$  - labelled iron hydroxide macroaggregate with pH and particle size suitable for lung scanning. The aggregate was prepared by mixing the required amount of  $\text{FeCl}_3$  with  $^{113m}\text{In}$  followed by the addition of  $\text{NaCl}$  and co-precipitation of  $^{113m}\text{In}$  with  $\text{Fe}^{+++}$  ions. The final pH was adjusted by gelatine solution and 0.1 N  $\text{HCl}$ . The prepared aggregates were then analysed for activity, pH and particle size and injected into rats. The distribution of activity in the lungs,

liver and blood was investigated using scintillation counting.

It was found that the grade and concentration of gelatine and the PH of the solution at the precipitation step are the most significant factors affecting the quality of the macroaggregate.

- 6- M. Raie and N. Rouhanizadeh, 1972, "Uptake of  $^{32}\text{P}$  in Different Organs of Caspian Sea Fish", Bull. Faculty of Science, Vol. 4, No. 2.

ABSTRACT:

IN VITRO phosphorus absorption in all organs of sturgeon, was higher than white fish. This may be due to the physiological and structural differences between the two fish, the higher absorption.

Seen in the white fish in the in vivo case, may possibly be due to the higher rate of growth and earlier maturation of the white fish(27). The higher phosphorus uptake by kidney in both in vivo and in vitro can be attributed to the particular structural features and vital functions of the organ. Similar results were obtained by Anderzej and Iysak (17).

In order to investigate further details of phosphorus absorption by different organs of the two fish, differential absorption ratios of phosphorus was measured. Autohistoradiography of liver and other tests showed that the strugeon fish in general absorbed more phosphorus than the white fish.

- 7- N. Rouhanizadeh, S. Samii et ZH. Khalkhali, 1973. Degradation des desoxyribopolynucleotides dans les tissus Lymphatiques du Rat Apres Irra-

diation et action Radioprotectrice du Shirkhesht. Radioprotection, Vol. 8, No. 4,

ABSTRACT:

The aim of this work was to study the radioprotective action of a natural substance "Shirkhesht". This was performed by a simple biochemical evaluation of the DNP complex of the irradiated animals prior and after application of "Shirkhesht". The sensitivity of the DNP complex of the irradiated lymphoid tissues has also been investigated. We concluded that: Considerable changes occur in the DNP complex of the irradiated animals. Shirkhesht appears to moderate these changes to an appreciable extent.



CURRENT RESEARCH IN NUCLEAR PHYSICS, SOLID STATE PHYSICS

AND THEIR APPLICATION IN ACTIVATION ANALYSIS IN IRAQ

FOR 1970-1971

(These are preliminary results and are to be published soon).

The (n, $\gamma$ ) group activities within the physics Department  
of Nuclear Research Institute - Iraqi Atomic Energy Comm-  
ission for the years 1970 - 1971

This group utilizes one of the reactor channels as a source of neutron and its work is mainly in the (n, $\gamma$ ) field. However, a new setup is being completed to study neutron inelastic scattering on various isotopes. The group is equipped with a 4096 channel analyzer & two Ge(Li) detector of 30 and 15cc. Also an 8"x12" NaI(Tl) detector for anticoincidence measurements and anticompton experiments.

The group had been completed and are going to complete the following researches and works during 1970 and 1971.

1. Measurement of the Reaction  $^{35}\text{Cl}(n,\gamma)^{36}\text{Cl}$  using a Three-Crystal Pair & Anti-Compton Spectrometer.

J.D.Jafar, A.A.Abdulla, N.H.Al-Quraishi, M.S.Alwash, J.Kaifosz, M.A.Khalil, M.H.Al-Kaissy & Z.Kosina.

The Cl(n, $\gamma$ ) reaction was investigated and the energies and intensities of 190 resolved  $\gamma$ -rays are reported.

A three-crystal NaI-Ge pair and anti-compton spectrometer was used. A computer programme useful in the automatic analysis of  $\gamma$ -ray spectra is briefly described.

A boot-strap technique generated a self-consistent energy calibration and the binding energy of  $^{36}\text{Cl}$  was determined to be  $8580.7 \pm 1$  KeV.

The appearance of single and double escape peaks in addition to photopeaks above pair production threshold will complicate the  $\gamma$ -ray spectrum even further and may cause ambiguities in its interpretation. It is essential to use pair spectrometers for accurate high energy measurements of  $\gamma$ -transitions.

In this present work a high efficiency three crystal NaI-GeNaI pair spectrometer has been used in an investigation of the  $(n,\gamma)$  spectrum from natural chlorine.

The intensity of the 25mm extracted neutron beam from the thermal column of the IRT-2000 was  $1.5 \times 10^8$  n/sec at the target position. The three crystal pair spectrometer consists of a splitting annular Na(Tl) crystal 12" long x 8" in diameter with 2" central through-hole. The two halves are optically isolated and each is viewed by six 2" EMI 9656 photomultiplier tubes of high quantum efficiency 28%. The central detector is a 10CC coaxial Ge(Li) crystal mounted at the end of a long right-angle arm extending from a chicken-feed type LN<sub>2</sub> dewar vessel. The measured energy resolution (fwhm) of one crystal half was 10.6% for Cs<sup>137</sup> and 8% and 7.5 for the Co<sup>60</sup> lines. The resolution of the Ge(Li) detector was 3 KeV for Co<sup>60</sup> (1.33 MeV).

The coincidence efficiencies with energy restriction on the annihilation pair can be high, from 20-25% of the double escape peak area in the single spectrum may be collected in the coincidence mode. The high-energy data (above 2047.1 KeV) were taken with the pair spectrometer in a single run of 22 hours. The electronic arrangement permits simultaneous accumulation of data in the two operating modes when two multichannel analyzers are available.

The results were analyzed by an IBM 1130 computing system. A special programme was written for the automatic analysis of  $\gamma$ -ray spectra where the whole spectrum is plotted, smoothed and peaks located. Then the whole spectrum was divided into intervals for fitting and normalized discrete gaussian shape weighting function was used. After this the energies and intensities of  $\gamma$ -rays were determined.

The results were found to be in satisfactory agreement with those of Groshev et al. for the commonly observed lines. The results are listed in Table (1).

Table 1

Gives the energies and their intensities from  $^{35}\text{Cl}$  (n, $\gamma$ )  $^{36}\text{Cl}$

<u>No.</u>	<u>Energy</u>	<u>Intensity</u>	<u>No.</u>	<u>Energy</u>	<u>Intensity</u>
1	8580.7	3.91	51	4752.2	0.13*
2	7792.1	10.38	52	4730.2	0.76
3	7415.4	11.52	53	4684.5	0.05
4	6979.2	2.46	54	4617.6	0.31
5	6953.3	0.16*	55	4588.1	0.29
6	6894.6	0.08*	56	4549.1	0.66
7	6870.2	0.08*	57	4526.1	0.48*
8	6646.0	0.01*	58	4519.1	0.18*
9	6628.9	4.55	59	4459.2	0.10
10	6620.9	8.97	60	4441.3	1.20
11	6544.9	0.16	61	4416.0	0.34
12	6487.4	0.19	62	4355.8	0.17
13	6423.3	0.33	63	4299.0	0.46
14	6380.4	0.27	64	4282.2	0.05
15	6341.9	0.16	65	4207.0	0.19
16	6268.6	0.44	66	4191.6	0.10
17	6112.0	23.82	67	4165.4	0.08
18	6087.8	1.25	68	4139.4	0.38
19	6051.0	0.05	69	4128.5	0.14
20	5957.5	0.29	70	4112.8	0.06
21	5904.0	1.38	71	4083.4	0.86
22	5778.9	0.15	72	4019.3	0.07*
23	5756.6	0.10*	73	4055.5	0.63
24	5734.8	0.48	74	4042.2	0.07
25	5716.2	6.15	75	4029.0	0.17
26	5704.4	0.50*	76	3999.9	0.14
27	5634.7	0.07	77	3981.7	(1.40)
28	5604.8	0.48	78	3963.6	0.40
29	5585.7	0.58	79	3917.0	0.11
30	5518.5	1.98	80	3862.4	0.06*
31	5474.7	0.10	81	3823.8	1.97
32	5372.4	0.06	82	3775.1	0.19
33	5262.8	0.13	83	3750.5	0.36
34	5247.8	0.64	84	3737.3	0.20
35	5205.8	0.26	85	3708.0	0.18*
36	5151.9	0.18*	86	3697.4	0.14*
37	5143.8	0.09*	87	3661.4	0.22
38	5125.0	0.04	88	3665.5	0.28
39	5110.7	0.09	89	3625.8	0.15*
40	5079.1	0.17	90	3613.6	0.08*
41	5018.8	0.51	91	3604.7	0.36*
42	4991.0	0.20*	92	3600.6	0.43*
43	4980.8	4.09	93	3588.8	(0.74)
44	4954.5	0.10*	94	3518.9	0.12*
45	4945.5	1.22	95	3567.2	0.30*
46	4886.4	0.08	96	3561.9	0.90*
47	4846.3	0.04	97	3549.3	0.09*
48	4830.4	0.23	98	3514.4	0.06*
49	4816.1	0.19	99	3502.2	0.49
50	4758.7	0.14*	100	3470.0	0.15

Table 1 (Cont.)

<u>No.</u>	<u>Energy</u>	<u>Intensity</u>	<u>No.</u>	<u>Energy</u>	<u>Intensity</u>
101	3460.7	0.07*	153	2296.0	0.28
102	3429.3	0.84	154	2263.1	0.16*
103	3415.1	0.08*	155	2247.4	0.13*
104	3375.0	0.65	156	2241.1	0.16*
105	3367.1	0.08*	157	2234.1	0.32 <sup>1</sup>
106	3350.6	0.17	158	2210.9	0.32
107	3333.2	0.84	159	2191.7	0.24
108	3316.5	0.25	160	2169.3	0.62
109	3294.3	0.07	161	2124.6	0.32
110	3273.5	0.04*	162	2110.2	0.26
111	3267.7	0.09	163	2094.8	0.81
112	3250.8	0.21	164	2063.7	0.45*
113	3245.0	0.11*	165	2058.0	0.82*
114	3212.5	0.07*	166	2047.1	0.50
115	3201.5	0.11	167	1959.9	10.03
116	3161.8	0.09*	168	1951.7	16.25
117	3152.2	0.06*	169	1625.9	0.19
118	3135.3	0.11	170	1610.1	3.16
119	3116.5	0.92	171	1513.7	0.27
120	3106.6	0.11*	172	1394.7	0.15
121	3095.2	0.07*	173	1327.6	0.92
122	3087.1	0.08*	174	1204.3	0.30
123	3062.1	3.97	175	1165.0	24.40
124	3027.7	0.07*	176	1131.6	1.61
125	3016.3	1.02*	177	788.0	23.35
126	3002.1	0.76	178	633.0	0.33
127	2994.9	0.93	179	609.5	0.23
128	2975.3	1.44	180	596.0	0.90
129	2953.7	0.18*	181	517.1	27.20
130	2896.3	0.48	182	436.2	0.90
131	2877.5	0.29*	183	357.6	0.07
132	2864.4	0.73	184	337.8	0.09
133	2845.9	0.88	185	325.3	0.17
134	<del>2811.4</del>	0.45	186	291.9	0.31
135	2801.1	1.01	187	252.2	0.13
136	2754.4	(0.96)	188	197.0	0.41
137	2740.0	0.14*	189	173.8	0.37
138	2711.9	0.09	190	138.1	0.37
139	2677.0	1.56			
140	2648.8	0.28			
141	2623.7	0.58			
142	2593.2	0.11			
143	2538.7	0.33			
144	2529.1	0.27			
145	2492.7	0.79			
164	2470.7	0.90			
147	2432.2	0.21			
148	2420.4	0.63			
149	2397.2	0.17			
150	2385.8	0.12			
151	2330.8	0.22			
152	2316.9	0.87			

- 1) Asterisks indicate poor estimate for the intensity due to complex line shapes.
- 2) Intensities in parentheses have a slight contamination from known <sup>24</sup>Na lines.

2. Cascade De-excitation of p-levels in Even-Odd Nuclei with  $21 \leq A \leq 41$  after Thermal Neutron Capture.

J.D.Jafar, M.A.Khalil, Fawzia A.H. & A.M.Demidov.

It is observed that the majority of p-levels with a large neutron width  $\sigma^2(2J + 1)$  also have the largest reduced transition probability  $(I/E^3)$  when decaying into the single-particle level  $2s_{1/2}$  neutron state. However, for  $2p_{1/2}$  levels and other p-levels higher than  $2p_{3/2}$  the largest reduced transition probabilities are observed for de-excitation into the  $2p_{3/2}$  state. This enhanced M1 strength in comparison with E1 transitions, in the decay of p-levels, results from the predominantly single-particle character of p-states and the relatively simple nature of the M1 transitions involved where only the spin-orbit coupling is affected while the nuclear core undergoes slight re-arrangement. For example, in  $^{29}\text{Si}$  the matrix elements of M1 transitions from the  $2p_{1/2}$  level nearly equals the single-particle estimate, whereas the E1 transition into the  $2s_{1/2}$  state is only  $5.5 \times 10^{-3}$  of the single-particle value. Table (2) gives the radiation width of p-levels.

Table 2 Radiation Widths of p-levels

Nucleus	Level Energy MeV	Transition Energy MeV	Type of Transition	Experiment		Theory
				eV	W.U	eV
$^{29}\text{Si}$	4.93	4.93	E1	0.52	$6.9 \cdot 10^{-3}$	75
$^{29}\text{Si}$	6.33	6.33	E1	0.91	$5.5 \cdot 10^{-3}$	166
$^{29}\text{Si}$	6.33	1.41	M1	0.051	0.9	0.057
$^{41}\text{Ca}$	2.47	0.52	M1	$9 \cdot 10^{-4}$	0.35	$2.7 \cdot 10^{-3}$
$^{41}\text{Ca}$	2.47	2.47	E2	$9 \cdot 10^{-6}$	$1.2 \cdot 10^{-2}$	$7.5 \cdot 10^{-4}$
$^{41}\text{Ca}$	2.47	0.46	E1	$10^{-7}$	$10^{-3}$	$7.5 \cdot 10^{-2}$

Gamma Rays From Thermal Neutron Capture in Si<sup>30</sup> & S<sup>34</sup>

J.D.Jafar, A.A.Abdulla, N.H.Al-Quraishi, M.S.Alwash,  
M.A.Khalil & A.M.Demidov.

Gamma radiation from the reactions Si<sup>30</sup>(n,γ)Si<sup>31</sup> and S<sup>34</sup>(n,γ)S<sup>35</sup> was measured with a Ge(Li) spectrometer. All the observed γ-transitions can be placed in the decay schemes of Si<sup>31</sup> and S<sup>35</sup> except the 4093 KeV in Si<sup>31</sup>.

The neutron binding energy is 6588.4 ± and 6986.4 ± 0.3 KeV for Si<sup>31</sup> and S<sup>35</sup> respectively.

The γ-ray spectra from thermal-neutron capture in enriched S<sup>34</sup> reported here, had not been previously measured. And only about two or three of the strongest γ-transitions in Si<sup>31</sup> and S<sup>35</sup> have been identified in previous studies of thermal neutron capture in natural targets.

In this work the energies and intensities of γ-transitions in Si<sup>31</sup> and S<sup>35</sup> are listed. The decay scheme for S<sup>35</sup> was constructed, on the basis of energy levels identified in the (d,p) reaction. Primary transitions to the ground or first excited states were not observed.

In table (3), Report Ph-9, 1970, the absolute intensities I<sub>γ</sub> and the reduced transition probabilities, I<sub>γ</sub>/E<sup>3</sup> are listed for primary M1 transitions feeding 2S1/2 and 1d3/2 one-particle and one-hole states for eight nuclei with odd neutrons in the mass range A=21-41.

Given the ratio of the reduced primary transition  
B(M1)  
Probabilities ----- . The Weisskopf single-particle estimate for this ratio is=  
B(E1)  
0.028 for nuclei with A≈30. This reduction in the transition probability suggests that "Channel capture" is important in these reactions. The partial radiative width should then be proportional to E<sup>2</sup> and not to E<sup>3</sup> as this was predicted by Lane and Lynn, due to the dependance of the transition matrix elements on the level depth relative to the capture state in channel capture. For this reason the partial radiative width was calculated for two cases :

When width is assumed to be proportional to  $E^3$  and to  $E^2$  respectively. Table 4, Report Ph-9, 1970, gives the ratio of reduced transition probabilities feeding  $2P_{3/2}$  and  $2P_{1/2}$  levels.

It may be concluded that this data lends further support to the importance of the channel capture mechanism in the processes under consideration.

Tables (5,6) gives the energies and their intensities for both reactions.

Table 3

INTENSITY & RELATIVE PROBABILITY OF M1 TRANSITION FROM THE CAPTURE STATE TO  $1d_{3/2}$  &  $2S_{1/2}$  LEVELS

Primary transition to $1d_{3/2}$ or $1d_{3/2}^{-1}$ state				Primary transition to $2S_{1/2}$ or $2s_{1/2}^{-1}$ state			
Nucleus	$E_x$ (MeV)	$I_\gamma$ %	$\frac{B(M1; 1/2^+ \rightarrow 3/2^+)}{B(E1; 1/2^+ \rightarrow 3/2^+)} \%$	$E_x$ (MeV)	$I_\gamma$ %	$\frac{B(M1; 1/2^+ \rightarrow 1/2^+)}{B(E1; 1/2^+ \rightarrow 3/2^-)} \%$	$B_n$ (MeV)
$^{21}\text{Ne}$				2.79	3.1	0.33	
$^{25}\text{Mg}$	0.976	0.4	0.6	0.584	1.8	0.12	7.33
$^{29}\text{Si}$	1.273	8	1.3	0	2.4	0.25	8.48
$^{31}\text{Si}$	0	1	0.14	0.752	<0.4	<0.08	6.59
$^{33}\text{S}$	0	2.3	1.1	0.842	3.8	2.25	8.64
$^{35}\text{S}$	0	<0.1	<0.05	1.572	<1.6	<1.8	6.99
$^{37}\text{Ar}$	0	10.1	1.4	1.410			8.79
$^{41}\text{Ca}$	2.01	1.0	2.7	2.571	2.2	10	8.36

Average = 1.0

Average = 2.1

Average without  $^{41}\text{Ca}$  = 0.8

Table 4

RATIOS OF REDUCED TRANSITION  
PROBABILITIES FEEDING  $2P_{3/2}$  AND  $2P_{1/2}$  LEVELS

Nucleus	$\frac{(I_{\gamma} / E_{\gamma}^3)_{2P_{1/2}}}{(I_{\gamma} / E_{\gamma}^3)_{2P_{3/2}}}$	$\frac{(I_{\gamma} / E_{\gamma}^2)_{2P_{1/2}}}{(I_{\gamma} / E_{\gamma}^2)_{2P_{3/2}}}$
$^{29}\text{Si}$	1.5	0.86
$^{31}\text{Si}$	3.0	1.26
$^{33}\text{S}$	1.7	0.9
$^{35}\text{S}$	3.1	1.3
$^{37}\text{Ar}$	1.8	1.05
$^{41}\text{Ca}$	2.0	1.2

TABLE 5  
GAMMA RAYS FROM THE  $^{30}\text{Si} (n, \gamma) ^{31}\text{Si}$  REACTION

This work			Beard et al. <sup>1</sup>	
$E_{\gamma}^a)$ (KeV)	$E_R^b)$ (KeV)	Intensity <sup>c)</sup>	E (KeV)	Intensity
752.44 ± 0.15	0.01	100	753.0 ± 1.0	1.1
1306.1 ± 0.3	0.03	18	1307 ± 2	0.081
1695.6 ± 0.5	0.05	2.3	1694.8 ± 1.0	0.032
1837.3 ± 0.8	0.07	2.6		
2204.6 ± 0.8	0.08	12	2206.9 ± 0.6	0.11
2316.7 ± 1.0	0.09	2.8		
2781.1 ± 0.15	0.13	66	2781.0 ± 0.2	0.77
3054.76 ± 0.16	0.16	71	3055.0 ± 0.4	0.73
3534 ± 1.0	0.22	≈5	3534.0 ± 1.0	0.022
3630.7 ± 0.4	0.23	6.3	3630.2 ± 0.3	0.076
4382 ± 2	0.33	1.7	4381.5 ± 0.4	0.018
4529.3 ± 0.3	0.36	14	4528.3 ± 0.2	0.13
4903 ± 1	0.42	<1.0	(4902)	<0.007
6587.6 ± 0.8	0.8	1.1	6588.7 ± 0.4	0.018

a) Except for the 4903 KeV, all the  $\gamma$ -rays listed have been included in the level scheme for  $^{31}\text{Si}$ .

b)  $E_R$  is the recoil-energy correction.

c) Number of  $\gamma$ -rays per 100 neutron captures in  $^{30}\text{Si}$ .

TABLE 6  
 GAMMA RAYS FROM THE  $^{34}\text{S} (n,\gamma) ^{35}\text{S}$  REACTION

$E_{\gamma}^a$ (KeV)	$E_R^b$ (KeV)	Intensity $c)$
646.9 ± 0.5	0.00	0.7
775.5 ± 0.15	0.00	19.5
908.1 ± 0.3	0.01	0.5
1572.15 ± 0.1	0.03	39
1839 ± 1	0.05	3.6
2022.8 ± 0.2	0.06	12
2082.65 ± 0.1	0.06	18
2347.5 ± 0.1	0.08	54
2555.9 ± 0.4	0.09	3.4
2614.3 ± 0.3	0.10	1.3
2796.6 ± 0.5	0.11	6.1
3184.3 ± 0.2	0.15	7
3331.08 ± 0.15	0.16	7.8
3390.86 ± 0.2	0.17	5.5
3802 ± 0.3	0.21	3.6
4189.6 ± 0.3	0.26	1.9
4268.4 ± 0.7	0.27	0.4
4638.4 ± 0.2	0.32	56
4903.4 ± 0.3	0.36	3.2
4963.2 ± 0.5	0.37	2.6
6078.2 ± 1.0	0.50	0.3

a) All the  $\gamma$ -rays listed have been included in the level scheme for  $^{35}\text{S}$ .

b)  $E_R$  is the recoil-energy correction.

c) Number of  $\gamma$ -rays per 100 neutron capture in  $^{34}\text{S}$ .

Gamma Rays from Thermal Neutron Capture in

Se<sup>75</sup>, Se<sup>78</sup>, Se<sup>81</sup>, Mo<sup>97</sup>, Mo<sup>99</sup> and Mo<sup>101</sup>.

M.A.Khalil, M.R.Ahmed, S.A.Al-Najar,  
A.M.Demidov, F.A.Hussian & Kh.I.Shakarchi.

The study of Se<sup>75</sup>, Se<sup>78</sup>, Se<sup>81</sup>, Mo<sup>97</sup>, Mo<sup>99</sup> and Mo<sup>101</sup> decay schemes by the thermal neutron capture method carried out by utilizing Ge(Li) detector and 4096 channel analyzer and the channel No: 1 on the (IRT-2000). The isotopes of Se<sup>78</sup>, Se<sup>81</sup>, Mo<sup>97</sup>, Mo<sup>99</sup> were studied before by other groups, but not accurately. Their intent was to study the low and high energy portions of the spectra, i.e. below 3MeV and above 6MeV. That portion of the spectrum lying between 3 and 6 MeV was not studied before because of the difficulties that usually arise in analysing the spectrum associated with the overlapping of photopeaks with single and double escape peaks. The great complexity of the spectrum in the medium energy range above the pair production threshold causes many ambiguities in identifying the "pure" photopeaks and furthermore misinterpretation of the experimental results. More than 50 new  $\gamma$ -lines were found from the results of our experiments & we introduction about 20 new levels in the decay scheme. Also we determined the binding energy values and the intensity of all  $\gamma$ -transitions observed. The decay scheme for each of Se<sup>75</sup>, Se<sup>78</sup>, Se<sup>81</sup>, Mo<sup>97</sup>, Mo<sup>99</sup> & Mo<sup>101</sup> isotopes were constructed. The spectrum calibration utilizing Cl, Si for calibration the standard sources <sup>36</sup>Cl, <sup>29</sup>Si, <sup>203</sup>Hg, <sup>137</sup>Cs, <sup>60</sup>Co, <sup>57</sup>Co & <sup>22</sup>Na were used. Gain and Zero stabilization techniques were employed and the overall spectral resolution (FWHM) over 24 hours was approximately 3.5 KeV for E=1MeV and 8KeV at E=7 MeV. The IBM-1130 computer at the Engineering College was utilized for sorting out the decay schemes and calculating the energy levels for each isotope.

To simplify the techniques of solving the problems of mixing between the peaks in the spectrum of Se and Mo isotopes pair spectrometer can be employed. This technique attenuate the contribution of  $\gamma$ -energies which are not created by pair production. This method was not employed because of the lack of material and the very small cross sections of Se and Mo isotopes.

Fast Neutron Inelastic Scattering Facility at the  
IRT-2000.

A.A.Abdulla, M.R.Ahmed, S.A.Al-Najar, M.A.Al-Amily  
Kh.I.Shakarchi.

Inelastic Scattering of Fast Neutrons :-

The nuclear physics group planned to study the feasibility of the inelastic scattering of fast neutrons using neutron filters for the reduction of capture reactions. Using an extracted beam and Ge(Li) detector we expect that gamma-ray de-excitation, following neutron inelastic scattering, can be readily identified, and that such type of nuclear reactions provided by pile neutrons will involve a large amount of separated isotopes, available at this time.

Introduction :-

In this field of research only two experiments were done: The first by Donahue in 1961 who used an extracted beam and NaI(Tl) detector in angular correlation measurements. The second by Nichole and Kennet (1971), who used Ge(Li) detectors for studying in-core inelastic scattering experiments. They also used neutron filters.

It was decided here to provide such experiments using 30cc coaxial Ge(Li) detector and 4096 channel analyzer, and the channel number (8) was chosen for this purpose.

Filters :

0.5mm Cd, 40mm Pb and 10mm B<sub>4</sub>C filters, Pb stainless steel collimators were installed into the channel gate and the extracted beam was of the same dimension of the last collimator (about 25mm). The beam was allowed to pass through series of filters outside the channel gate to achieve further exclusion of the thermal & resonance components. These filters were made of B<sub>4</sub>C and Cd plates of different thicknesses, taking into consideration that other materials such as paraffine and lead may also be used as filters. The filter-box and collimator 20mm in diameter which was used to collimate the filtered beam, were enclosed together inside a "Shielding block" made in the form of an iron container filled with paraffine and heavily loaded with iron and adjacently placed to the reactor wall. The filter-box together with the steel box plugged in, which was filled with paraffin and iron as a continuation of the shielding block, was equipped with a pulley to make possible the process of changing the different filters under investigation.

Set-up of the facility :

The detector shielding assembly was made of three layers 5cm Fe, 8cm paraffin with B<sub>4</sub>C and 10cm Pb. A cylinder of LiH 20mm in diameter and 10cm in length was plugged into the hole made in the detector shield to project additionally the detector crystal against the scattered fast neutrons.

Calculations :

Calculations were carried out to determine the expected distribution of the neutron spectrum after transmission through different filters of different thicknesses. Also the rise of the temperature in the first filter exposed to neutrons and gamma-rays was calculated.

Primary Results :

More than 30  $\gamma$ -rays due to  $\text{Nb}^{93}(n,n'\gamma)\text{Nb}^{93}$  reaction were detected and related to the excitation of the energy levels : (743.9), (808.5), (978.8), (1082.5), (1296.7), (1485), (1501), (1684.6), (1911.5), (1968.4) (KeV).

The Solid State Group activities within the Physics Department of  
Nuclear Research Institute - Iraqi Atomic Energy Commission for  
The years 1970 - 1971

The solid State Group is equipped with a 4-circle Neutron diffractometer and a 4-circle X-Ray diffractometer.

The main work which has been done and carried out so far could be summarised as :

1. After finishing the commissioning and bringing the Neutron diffractometer into working condition. The immediate work carried out was testing of all systems of the N.D. (Monochromator, detection system, and programming control system). The work include measuring of the :-
  - a- Rocking curves of the monochromator at different Bragg angles.
  - b- Stability and plateau of the two detection systems (monitor and main channels).
  - c- Automatic operation and reproducibility.
2. The evaluation of the various diffractometer parameters for the powder diffraction. A Nickle powder has been used as a standard sample. The whole pattern of Nickle is registered for different collimation conditions in order to determine the resolution and intensity by using different soller slits collimators. Effects of fuel elements arrangements on flux in horizontal channel No. 6 were determined.
3. Three powder samples of MgO isotopes ( $\text{Mg}^{24}\text{O}$ ,  $\text{Mg}^{25}\text{O}$ ,  $\text{Mg}^{26}\text{O}$ ) has been investigated in order to evaluate the scattering cross section of each isotopes seperately. In addition to these three isotopes, MgO natural has been investigated also. This study has been shown that the diffraction maximum intensities with odd Millers's indices are significantly less than these with even indices. This indicates that the sign of the coherent scattering amplitudes are positive. The values at the wavelength  $\lambda=1.02 \text{ \AA}$  are :  $b^{24}\text{Mg}=0.547 \pm 0.018$ ,  $b^{25}\text{Mg}=0.362 \pm 0.014$ ,  $b^{26}\text{Mg}=0.489 \pm 0.015$ . And thus the values for the natural mixture of magnesium isotopes will be equal to  $0.523 \pm 0.017$ , which is in good agreement with formerly measured values.

At present the Solid State group is engaged in determining the thermal neutron spectrum of the horizontal channel (no.6) using the Lead Single Crystal which is mounted in the Neutron diffractometer as monochromator.

Expansion of this unit will be in the direction of the Magnetic structure studies which will be materialised by the installation of a cryostat and magnet and therefore extending the work to a temperature at or even below the temperature of liquid helium (4.2°K).

#### X-Ray Diffraction :

Since the commissioning of the Hilger and Watts single crystal diffractometer, the intention has been to carry our work complementary to the Neutron diffraction. This was materialised in determining the percentage of  $Mg(OH)_2$  in the three isotopes of MgO,  $Mg^{24}O$ ,  $Mg^{25}O$ ,  $Mg^{26}O$  by quantitative X-Ray diffraction phase analysis. The direct method suggested by Alexander and Klug with some modification which were later used to study their coherent amplitude scattering by neutron diffraction.

Amongst the work that was carried out by this group is the evaluation of the various diffractometer parameters and also the application of quantitative phase analysis to metallic and Inorganic materials.

At present, preliminary studies are being made to make use of the diffractometer in the calculation of absorption coefficients from metallic spherical and cylindrical single crystals. Future plans include the extension of quantitative phase analysis to ternary and quaternary systems and also the application of X-rays in particle size determination of powders and colloidal solutions.

Expansion of this unit will be materialised by the installation of a second X-Ray generator with vertical tube stand, this generator will provide stable X-Ray to many cameras that are available both in the chemistry and physics department.

The Activation Analysis Group activities within the Physics  
Department of Nuclear Research Institute - Iraqi Atomic Energy  
Commission for the years 1970 - 1971

The activation analysis laboratory is well-equipped to handle both routine analysis & research work. The equipment presently includes 30cc Ge(Li) detector, 2048-channel analyser, fast pneumatic transport system, and a number of NaI detectors and counting systems.

Research continues to occupy the major portion of the available operation time of the measuring facilities in this group. A variety of research projects were undertaken in the last year, and some of them have been brought to a successful conclusion while others are at the developmental stages. Abstracts of the published papers are included in Section B.

A. Services

The group also performs a number of service analyses for the other departments of the Institute and for outside agencies. During the last year the group analysed over 1,300 service samples for the following :

- 1- Dept. of Geology,  
Dept. of Chemistry,  
Dept. of Isotope Production  
of the Nuclear Research Institute.
- 2- National Minerals Company,  
Dora Oil Refineries,  
Dept. of Geological Survey,  
University of Baghdad,  
and the Army Chemical Laboratories.

B. Research

Below is a list of the research projects completed during the last year or in progress :

Completed :

- 1- " The activation analysis of uranium and thorium and their mixtures by delayed neutron detection method. " by E.T.George, G.I.Barisov, G.Y.Al-Shahery and M.Al-Abbasi.

The analysis of fissile isotopes of  $^{235}\text{U}$ , and  $^{232}\text{Th}$  were carried out in the IRT-2000 reactor using delayed neutron detection technique. An automatic vacuum pneumatic transporter was used with two channels of irradiation: bare and cadmium covered. Pressurized  $^3\text{He}$  detector was used for neutron counting.

The results of the quantitative determination of uranium in several reference samples (IAEA standards) and the limit of sensitivity of the method are presented.

Two methods of the quantitative determination of fissile elements in two component mixtures (with known and unknown total mass of fissile elements) are described. For a mixture of  $^{235}\text{U}$  and  $^{238}\text{U}$  the range of the determined weight ratios of  $^{235}\text{U}$  and  $^{238}\text{U}$  under both methods is found. For a mixture of  $\text{U}_{\text{nat}}$  and  $\text{Th}$  the range of the weight ratios of  $\text{U}_{\text{nat}}$  and  $\text{Th}$  under their unknown total mass is found, as well as the limit of sensitivity of the method for thorium under the zero content of uranium.

- 2- "Determination of trace elements in Iraqi crude oils via NAA". by Hussain A'-Shahristani and M.Al-Atyia.

The trace elemental composition of crude oil from the various Iraqi oil fields has been studied. The instrumental neutron activation analysis technique was used. The method neither requires chemical separation nor pre-or post-concentration of trace elements by ashing. High resolution Ge(Li) detector permitted the simultaneous multi-elemental determination of V, Al, Mn, and Na.

The vanadium concentrations remained quite constant within the same reservoir but varied remarkably among reservoirs of different geological ages. The vanadium concentration ranged from 1.6-109 ppm. Manganese generally followed the same trend as vanadium with its concentration varying from

less than 0.15 to 1.6 ppm. Sodium and aluminum concentrations varied from one sample to another even within the same reservoir. Concentrations ranged from 5-55 ppm and from less than 25-1050 ppm for aluminum and sodium respectively.

- 3- "Determination of some elements in the sediments of Iraqi rivers by INAA" by E.T.George and M.J.Al-Atyia.

In this work many sediment samples from the Iraqi rivers were analyzed for geological purposes, using INAA. The  $\gamma$ -rays were detected and analyzed using a high-resolution 30 cm<sup>3</sup> Ge(Li) detector and ND-2048 channel analyzer. The elements determined are: Na, Mg, Al, Ca, Ti, V, Mn, Sc & Hf.

Using 3 sec. irradiation, 20 sec. delay and 10 sec. counting Sc and Hf were successfully determined by their isotopes <sup>46m</sup>Sc (T<sub>1/2</sub>=20 sec.) & <sup>179m</sup>Hf (T<sub>1/2</sub>=19 sec.)

The method used in this analysis was simple, non-destructive, fast and quite sensitive.

- 4- "Vertical Migration of oil in the Northern Iraqi oil fields: vanadium concentration evidence".

by Hussain Al-Shahristani and M. J. Al-Atyia.

A study was made to determine the vanadium concentration in oil samples representing the various pay horizons of all the Iraqi Oil fields.

Variations of vanadium content of oils from different pays were measured to establish the history of migration and accumulation of these oils.

The vanadium content of oil from different fields varies drastically from 1.6 to 109 ppm whereas the vanadium content of oils drawn from different wells in the same pay is remarkably constant. In the Kirkuk field, oil from Lower/Middle Cretaceous reservoirs contains 45 ppm V compared to

26 ppm V for oil from the overlying Oligocene/Lower Miocene reservoirs. In the Zubair field, oils from the second, third and fourth pays contain 57, 15 and 2 ppm V respectively.

The path of migration of oil in the northern Iraq oil fields is clearly reflected by the vanadium concentration variation. The results indicate that oil in Northern Iraq originated during the Lower/Middle Cretaceous, and has migrated vertically to the Tertiary reservoirs where it is found now.

5- "Determination of Uranium Content in Geological Samples by Neutron Activation".  
by M.R.Ahmed, A.A.Abdulla and G.Y.Al-Shahery.

Samples were irradiated in the IRT-2000 research reactor at the Nuclear Research Centre. The decay rate of  $^{239}\text{Np} \rightarrow ^{239}\text{Pu}$  was measured and compared with a standard of known uranium content. Two techniques were applied; in the first method a Ge(Li)  $\gamma$ -ray spectrometer of high resolution was used to measure the  $\gamma$ -ray spectrum from this decay. In the second scintillation counters were placed in coincidence for detecting two-step cascade  $\gamma$ -rays from the same decay. The results from both techniques were in satisfactory agreement.

6- "Measurement of Neutron and Gamma field Parameters on Irradiation Position of Vacuum Pneumatic Transporter System".  
by E.T.George, G.I.Borisov, G.Y.Al-Shahery, M.A.Al-Abbasi, O.K.Zhuravlev.

A system of vacuum pneumatic transporters was assembled and the tubes inserted into the IRT-2000 reactor through a horizontal channel. The system is described in short, listing basic technical characteristics. Given are the data of the measurements of neutron and gamma field parameters on the irradiation positions of the pneumatic transporters.

In Progress :

- 7- "Determination of Arsenic in Iraq tobacco via NAA",  
by H.Al-Shahristani and A. Romaya.

Two methods are under development to measure exceedingly small quantities of arsenic in tobacco samples.

The first involves chemical separation and the second is instrumental using coincidence technique.

- 8- "Investigation of some problems of spectral interferences when analyzing geological samples".  
by E.T.George and M.Al-Atyia

During the measurement of activated geological samples, a number of compound peaks are observed. This study has been undertaken to resolve these peaks and particularly the 511 KeV.

- 9- "Determination of cadmium in foods",  
by H.Al-Shahristani and S.Is'hac

A technique is being developed to determine cadmium concentrations in local foods. Cadmium is initially absorbed on anion exchange resins and its radioactive indium daughter-product is washed away and counted.

- 10- "Determination of elements with very short half lives produced by (n, $\gamma$ ) and (n,n') reactions",  
by H.Al-Shahristani, E.T.George, M.Al-Atyia and K.Abbas.

Radioactive elements with half-lives ranging from sub-second to few seconds are being investigated using a fast pneumatic transport system and synchronised counting facility.

CURRENT RESEARCH IN NUCLEAR PHYSICS, SOLID STATE PHYSICS

AND THE EXPERIMENTAL NUCLEAR PHYSICS IN IRAQ

FOR 1972-1974

(These are preliminary results and are to be published soon).

The Solid State Group Activities within the  
Physics Department of Nuclear Research  
Institute, Iraqi Atomic Energy Commission  
for the Years 1972-1974

Solid state physics group utilizes double axis neutron diffractometer to identify crystal structures for different alloys and materials and to measure diffraction parameters of irradiated samples. An X-ray diffractometer is used by the group for crystal and powder studies of various materials.

1. Specifications and parameters of Iraqi Atomic Energy Commission Diffractometer.

G.Al-Shahery, A.Abul-Khail, F.A.Amin, A.Al-Naimi, A.Al-Saji, V.F.Petronin, M.G.Zemlyanov.

The equipment parameters were determined using Ni powder as standard control sample. Effects of fuel elements/cn flux in horizontal channel employ-  
arrangements  
ed were determined. The report also includes methods of calculating the various parameters involved. A brief description of the neutron diffractometer is also included.

Table 1. Shows results of the measurements of the rocking curves at different Bragg angles for different Beam Narrowers.

$2\theta$	Beam Narrower mm	Peak intensity C/10 sec.	FWHM degree
$15^\circ$	10 x 10 mm	1562	0.4 $^\circ$
	30 x 30 mm	46496	0.7 $^\circ$
$24^\circ$	10 x 10 mm	11010	0.4
	30 x 30 mm	400056	0.55
$90^\circ$	10 x 10 mm	3671	0.4
	30 x 30 mm	145670	0.45

The experimental statistical distribution of counts in regions of  $N \pm \sqrt{N}$  and  $N \pm 2\sqrt{N}$  are shown in the following table.

Mode of statistics	Theoretical value	Experimental values	
		main dete	monitor
$N \pm \sqrt{N}$	0.680	0.514	0.750
$N \pm 2\sqrt{N}$	0.954	0.950	0.965

TABLE 2. Effect of control rods on flux

No. of observation	Count/10sec	AR cm	RR <sub>1</sub> cm	RR <sub>2</sub> cm	Note
1	469821	10.5	23.4	23.4	
2	469236	20	22.5	25	AR Variable Compensated by RR <sub>1</sub> while RR <sub>2</sub> constant.
3	469036	19	22.5	25	
4	450661	25	22	25	
5	450228	24.5	22	25	
6	436894	30	21.2	25	
7	435635	29.8	21.2	25	
8	425492	35	20.4	25	
9	418473	40	19.9	25	
10	413352	45	19.4	25	
1	450521	25	21.5	25	
2	450431	25	22.6	24	
3	459957	25	23.8	20	
4	467664	25	25.8	17	
5	465603	25	27.8	14	
6	465641	25	31.7	10	
7	462745	25	33.9	0	
8	432629	25.5	14.5	30	
9	413011	25	8.1	35	

TABLE 3A- Effect of control rods on flux per cm length

AR influence inside Reactor core in cm	Flux variation integrated intensity %	Flux variation per one cm of AR %	Note
1-20 cm	1.382	0.133	RR <sub>2</sub> constant while compensated by RR <sub>1</sub>
20-35 cm	8.2	0.503	
35-45 cm	2.24	0.213	
Total (1-45) cm	11.82	0.749	

TABLE 3B

RR <sub>2</sub> influence inside reactor core in cm	Flux variation integrated intensity %	Flux variation per one cm of RR <sub>2</sub> %	Note
1-18	1.086	0.1195	AR constant while RR <sub>2</sub> compensated by RR <sub>1</sub>
18-35	9.80	0.544	
35-40	1.66	0.326	
Total (1-40)	12.54	0.989	

N n/n	AR cm	RR <sub>1</sub> = RR cm	I/I <sub>max</sub>	N n/n	AR cm	RR <sub>1</sub> = RR <sub>2</sub> cm	I/I <sub>max</sub>
1	10	27	1.00	17	33.3	21	0.933
2	16.2	27	0.992	18	37.4	21	0.921
3	23	27	0.976	19	71.2	17.5	1.00
4	28.2	27	0.952	20	20.5	17.5	0.994
5	33.2	27	0.936	21	23.5	17.5	0.986
6	38.3	27	0.940	22	27.5	17.5	0.966
7	13	24	1.0	23	32	17.5	0.954
8	15.8	24	0.978	24	36	17.5	0.934
9	22.5	24	0.976	25	39.9	17.5	0.928
10	29	24	0.960	26	20.1	13	1.00
11	36	24	0.952	27	21	13	0.992
12	38.7	24	0.944	28	22.8	13	0.984
13	11.5	21	1.00	29	24.5	13	0.975
14	16.3	21	0.987	30	26.3	13	0.967
15	22.2	21	0.970	31	29	13	0.959
16	26.8	21	0.952	32	32	13	0.951
				33	13	35	0.944
				34	13	39.5	0.934

TABLE No. 5 - Integrated Intensity of Different Bragg Reflections.

hkl	Experimental intensity count Absolute scale	Theoretical intensity $P/I_C \times 10^{24}$	$I_C \times 10^{24}$	$I_0$ count /cm <sup>2</sup> per 8 min.	Experimental relative intensity	Theoretical relative intensity	Residual factor R for all
111	7722.2	1.451495	17103.62	1.2482936	100	100	0.00285
200	4312.8	0.25307	17041.92	1.2437905	0.552	0.560	
220	4242.8	0.249852	16981.25	1.2393625	0.549	0.553	
311	6016.65	0.361788	16630.31	1.213744	0.779	0.801	
222	1886.95	0.110419	17088.99	1.2472.258	0.244	0.245	
400	872.6	0.052212	15633.64	1.1410083	0.126	0.138	
331	3606.30	0.210236	17153.57	1.2519391	0.467	0.466	
420	3094.2	1.202057	15312.74	1.1175877	0.400	0.447	

Mid value

16610.255

1.21286961

0.00285

TABLE No. 5- Ratio of Intensity to FWHm for Different Collimeters.

Collim. of experiment Planes (hkl)	Collimation condition I Pattern A Fig. (14)	Collimation condition II Pattern B Fig. (14)	Collimation condition III Pattern C Fig. (14)	Ratio of intensity and FWHU'S in Arbitrary Scale
hkl	$I_A$ FWHU <sub>A</sub>	$I_B$ FWHU <sub>A</sub>	$I_C$ FWHU <sub>C</sub>	$I_A : I_B : I_C$ $F_A : F_B : F_C$
111	49.4    1.4°	17.0    0.7°	12.8    0.55°	1 : 0.344 : 0.259    1 : 0.5 : 0.393
311	39.2    1.5°	12.6    1.15°	10.5    1.1°	1 : 0.322 : 0.269    1 : 0.78: 0.737
222	12.5    1.5°	4.0    1.25°	3.2    1.2°	1 : 0.320 : 0.251    1 : 0.83: 0.8

2. The Neutron Coherent Scattering Amplitudes for Magnesium Isotopes.

A.Al-Saji, A.Abul-Khail, F.A.Amin, A.Al-Naimi, G.Y.Al-Shahery, V.F.Petrunin, M.G.Zemlyanov.

The neutron coherent scattering amplitudes for the three stable isotopes' of Magnesium i.e.  $^{24}\text{Mg}$ ,  $^{25}\text{Mg}$ ,  $^{26}\text{Mg}$  has been studied by neutron diffraction technique using four-circle neutron diffractometer. The three isotopes were prepared in an oxide powder form, and the investigation was done on each isotope separately and so was the calculation.

TABLE 1 - Isotopic Composition of Samples

No.	Name	isotope content in percent		
		$^{24}\text{Mg}$	$^{25}\text{Mg}$	$^{26}\text{Mg}$
1	$^{24}\text{MgO}$	98.5	.9	.6
2	$^{25}\text{MgO}$	4.3	92.0	3.7
3	$^{26}\text{MgO}$	11.4	1.3	87.3

TABLE 2 - Impurities of the Samples

No.	Name	impurities													
		Ba	K	Na	Ca	Fe	Al	Si	Cr	Ni	Cu	Mn	Pb	Sn	Sr
1	$^{24}\text{MgO}$	006	006	002	003	002	003	003	006	002	002	003	015	002	006
2	$^{25}\text{MgO}$	02	002	002	013	002	002	002	002	002	002	002	002	026	002
3	$^{26}\text{MgO}$	006	002	002	063	002	002	003	002	002	002	003	003	002	006

3. Thermal-Neutron Coherent Scattering Amplitudes and Cross Sections of Lead Isotopes.

B.Aladdin, M.Sarsam, E.Ajaj, A.Abdullah, A.Abul-Khail, M.G.Zemlyanov.

The thermal neutron coherent scattering amplitudes and cross sections for lead samples of the natural isotopic mixture and of a mixture enriched with 204, 206, 207 and 208 isotopes were determined. The samples used in the measurements were made in cylindrical form by cold pressing, thus dispensing with aluminium containers. The determination of the constants involved the determination of the Zero angle position of the main detector, the incident neutron wavelength, the experimental constant, the neutron beam distortion by the sample, and the angular distribution of elastically scattered neutrons.

TABLE 1. The Isotopic Composition of the Samples.

Sample No.	Isotopic composition, %			
	204	206	207	208
1	1.48	23.6	22.6	52.3
2	47.90	23.7	11.6	16.8
3	-	87.9	8.8	3.3
4	0.2	3.0	83.3	13.5
5	-	0.3	1.0	98.7

TABLE 2. The Content of other Various Elements in the Isotopic Samples.

Sample No.	Impurities, %												
	Na	Ca	Mg	Fe	Al	Si	Ni	Cu	Bi	Zn	Ag	Sb	Sn
1	0.0006	0.0011	0.0005	0.0007	0.0014	0.0020	0.0005	0.0016	0.0003	<0.001	<0.00005	-	-
2	0.0006	<0.0003	0.0005	0.0002	0.0005	0.0009	<0.0003	0.0002	-	0.0003	<0.00005	-	-
3	<0.00005	0.0005	<0.00004	0.0005	0.0008	0.0015	<0.0003	0.0003	-	0.0007	<0.00005	<0.001	0.00007
4	0.004	-	0.005	0.0004	0.0004	0.0008	0.0005	0.0003	0.00006	<0.0005	0.00005	-	-

TABLE 3. The Characteristics of the Used Samples.

Sample No.	Diameter mm.	Height mm.	Weight gm.	Exp. density $\rho$ gm/cm <sup>3</sup>	Theoretical density $\rho_0$ gm/cm <sup>3</sup>	Relative density $\rho/\rho_0$	Density of isotope nucleus, nuclei/cm <sup>3</sup> , x 10 <sup>23</sup>			
							204	206	207	208
1	11	26.0-6	30.191	11.143	11.347	0.982				
2	11	27.305	29.012	11.180	11.253	0.994	0.1570	0.0774	0.0377	0.0544
3	11	27.935	29.815	11.231	11.290	0.995	0	0.2884	0.0287	0.0197
4	11	11.977	12.237	10.725	11.341	0.952	0.000533	0.00946	0.2615	0.04221
5	11	28.037	30.446	11.293	11.390	0.992	0	0.000990	0.00329	0.3228

TABLE 4. The Ratios between Integrated Intensities for Some Reflection of Pb-Powder.

reflex (hkl)	Pb (powder)	Pb rod (rotating)
111	1	1
200	0.52	0.51
220	0.46	0.46
(311+222)	0.85	0.87

TABLE 5. The Results of the Measurements and the Average Wavelength of Neutrons Incident on the Sample.

N	(hkl)	$\lambda_{exp}$	$\lambda_{average}$
1	111	1.022926	1.0223
2	200	1.022204	
3	220	1.022024	
4	311	1.022091	
5	222	1.022254	

6. The Integrated Intensities of Scattered Neutrons.

hkl	Integrated intensities		$\frac{I_{hkl}}{V} \times 10^{-24}$
	$P_{hkl}$ (experimental)	$P_{hkl}$ (theoretical)	
111	14660.922	14729.105	1413.822
200	3176.812	3202.944	1399.384
220	3033.728	3230.943	1354.316
311	12057.615	11952.479	1341.971
222	3704.062	3651.736	1353.221
400	1995.909	2064.301	1264.885
331	6038.931	7020.255	1250.254
420	5335.850	5699.373	1213.738
422	5897.084	5716.177	1229.467

TABLE 7. The Expected Values of the Background from the Container.

hkl	values of B.G. for Aluminium container	
	calculated from (220)	calculated from K constant
111	1664.791	2215.757
200	919.676	1241.396
220	856.833	1161.733
311	1183.809	1610.159
222	355.703	404.385
400	187.487	256.482
331	602.999	827.376
420	564.204	775.146
422	444.171	613.050
511,333	506.150	701.072
440	151.229	210.702

TABLE 8. The Transmission Measurements for all Pb and Ni. Samples.

Sample	$\mu_k$	
	Calculated	Observed
204 Pb	0.207	0.195
206 Pb	0.181	0.183
207 Pb	0.193	0.189
208 Pb	0.178	0.178
Pb (natural)	0.182	0.181
Ni (natural)	0.412	0.400

TABLE 9.  
Natural Lead The Observed and Calculated Integrated Intensities for Natural Lead.

$hkl$	Integrated Intensities		$(I_{hkl}/K)10^{-12}$
	$P_{hkl}$ (experimental)	$P_{hkl}$ (theoretical)	
111	10140.914	9832.581	3.650135
200	5102.767	5350.635	3.441435
220	4658.954	4713.257	3.249703
311	5933.386	6228.761	3.013106
222	1970.751	1339.437	3.134152
400	952.080	909.301	2.869709
311	2723.584	2802.437	2.614117
420	2482.263	2578.244	2.552575
422	1981.472	1901.692	2.461532
511,333	2004.712	2056.367	2.248944

TABLE 10  
The Observed and Calculated Integrated Intensities  
for Pb<sup>204</sup>

Pb-204

hkl	Integrated Intensities		$(I_{hkl}/K) 10^{-12}$
	$P_{hkl}$ (experimental)	$P_{hkl}$ (theoretical)	
111	9465.325	9007.189	3.515426
200	5011.177	4907.121	3.399675
220	4439.023	4310.400	3.161967
311	6023.034	5691.107	3.026274
222	1939.148	1690.075	3.098861
400	815.173	829.433	2.646678
331	2692.596	2553.707	2.590625
420	2574.404	2348.640	2.590625
422	2016.613	1730.008	2.475044
511,333	1008.039	1868.924	2.128593

TABLE 11  
The Observed and Calculated Integrated Intensities for  
Pb<sup>206</sup>

Pb-206

hkl	Integrated intensities		$(I_{hkl}/K) 10^{-12}$
	$P_{hkl}$ (experimental)	$P_{hkl}$ (theoretical)	
111	9255.136	8596.415	3.429259
200	4572.389	4654.767	3.212172
220	3947.530	4066.611	2.951918
311	5623.411	5354.466	2.894724
222	1945.808	1581.867	3.071546
331	2498.234	2385.871	2.470565
420	2492.052	2198.271	2.521717
511,333	1697.431	1735.862	2.041503

TABLE 12  
The Observed and Calculated Integrated Intensities for Pb<sup>207</sup>

hkl	Integrated intensities		$(I_{hkl}/K)10^{-12}$
	$P_{hkl}$ (experimental)	$P_{hkl}$ (theoretical)	
111	5766.329	5710.723	3.89017
200	3257.127	3094.615	3.88599
220	2549.736	2660.516	3.39763
311	3651.431	3456.441	3.34053
222	1030.841	1014.814	3.20345

TABLE 13  
The Observed and Calculated Integrated Intensities for Pb<sup>208</sup>

hkl	Integrated intensities		$(I_{hkl}/K)10^{-12}$
	$P_{hkl}$ (experimental)	$P_{hkl}$ (theoretical)	
111	8136.951	7642.196	3.219937
200	4014.559	4175.055	3.006165
220	3674.006	3708.111	2.941980
311	5227.039	4936.384	2.785190
222	1730.304	1463.670	2.882341
400	810.912	729.561	2.603236
331	2354.899	2264.690	2.393921
420	2251.555	2093.645	2.393922
422	1607.477	1555.584	2.183513
511,333	1669.754	1694.422	2.021347

TABLE 14. The Corresponding Cross-Section for the free Atom and the Bound Atom.

Sample	$\delta_{\text{free}}$ barns	$\delta_{\text{bound}}$ barns
204 Pb	11.483000	11.59509
206 Pb	10.021300	10.118817
207 Pb	11.163500	11.271611
208 Pb	9.902950	9.998427
Pb(natural)	10.237960	10.336941

4. The Performance of Neutron Diffractometer on the Comparison of Two Monochromators Crystals.

B. Aladdin, E.Ajaj, A.Abul-Khail & M.G.Zemlyanov.

The performance of a neutron diffractometer is influenced by a number of parameters that should be rigorously investigated. Among these parameters are the neutron flux distribution at the sample and the dependence of F.W.H.M. for Bragg reflections on monochromator angle and angular divergence of collimators. This investigation was directed at fixing the suitable parameters and the comparison of two single crystals one made of pyrolytic graphite and the other made of lead to be used as monochromators.

TABLE (1) Comparison of the two Monochromators Crystals Lead and Graphite

Type of monochromator	$2\theta_m$	Reactor Power MW	Time of measurement SEC	Integrated Intensity	Angular Divergence of collimators			Position of Beam limiting device		
					1	2	3	1	2	3
C	18	1.8	10	87813	30'	30'	30'	10x10	10x10	10x10
Pb	24	1.8	10	22000	30'	30'	30'	10x10	10x10	10x10

TABLE (2) The Chosen Combination of Angular Divergences

Combination	Angular Divergence		
	1st Collim	2nd Collim	3rd Collim
1	30'	Hollow	30'
2	30'	"	20'
3	20'	"	30'

The (n, $\gamma$ ) group activities within the  
Physics Department of Nuclear Research  
Institute - Iraqi Atomic Energy Comm-  
ission for the years 1972 - 1974

The (n, $\gamma$ ) group of this Department studies the problems of nuclear spectroscopy and nuclear structure by measuring spectra of  $\gamma$ -rays from the inelastic scattering of reactor fast neutrons.

The measurements are conducted on rare elements and separated isotopes. The latter are supplied by the Kurchatov Atomic Energy Institute (Moscow) within the frame work of co-operation between the two Institutes.

The  $\gamma$ -spectra obtained are processed on an IBM 1130 Computer to calculate level populations in the (n,n', $\gamma$ ) reaction with the aid of the Hauser-Feshbach statistical model.

The results of the measurements are to be published in the form of an atlas divided in to three parts. Results of the separated-isotopes studies are intended for publication in scientific journals. Work is also underway to apply (n,n', $\gamma$ ) spectroscopy for the determination of element composition of various samples using 30 cm<sup>3</sup> Ge(Li) detector and 4096 channel analyzer.

New experimental set up is now being constructed for measuring the angular distribution of  $\gamma$ -rays from these reactions.

1.  $\gamma$ -Rays from the  $\text{Se}^{74}(n,\gamma)\text{Se}^{75}$  Thermal-Neutron Reaction.

M.R.Ahmed, M.A.Khalil, F.A.Hussein and A.M.Demidov.

Spectrum of  $\gamma$ -rays from the  $(n,\gamma)$  thermal-neutron reaction has been measured, using a Ge(Li) spectrometer. Energies and intensities for 152  $\gamma$ -lines of the spectrum have been determined. A diagram of  $\gamma$ -transitions of  $\text{Se}^{75}$  has been made.

Table 1.

Isotopic composition and isotope contribution to thermal-neutron capture by  $\text{Se}^{74}$  sample.

Isotope	74	76	77	78	80	82
Isotope abundance in the sample, %	40.9	8.1	4.7	13.1	27.1	6.1
Contribution to neutron-capture cross-section, %	69	23	6.7	0.2	0.6	0.4

Table 2.

Energies and intensities for  $\gamma$ -rays of  $\text{Se}^{75}$

$E_{\gamma}$ , KeV	$I_{\gamma}$ , %	Position in the diagram of $\gamma$ -transitions; level energies , KeV
7909.2 (20)	0.20 (10)	C-111.6
7734.2 (10)	35 (5)	C-286.6
7441.7 (12)	0.93 (20)	C-579.4
7398.6 (12)	0.57 (15)	C-622.7
7173.2 (15)	0.33 (10)	C-847.3
7130.8 (12)	0.28 (8)	C-890.5
7064.2 (10)	1.0 (2)	C-956.8
7007.3 (10)	1.7 (4)	C-1013.5
6841.4 (15)	0.21 (7)	C-1179.8
6827.2 (10)	1.0 (3)	C-1193.8
6437.8 (10)	3.5 (5)	C-1583.4
6317.9 (15)	0.15 (5)	C-1703.0
6224.5 (10)	1.9 (4)	C-1776.6
6214.2 (15)	0.28 (8)	C-1806.2
6131.3 (10)	0.48 (10)	C-1889.8
6082.5 (15)	0.80 (20)	C-1938.0
6071.4 (15)	0.19 (6)	C-1949.0
6043.5 (12)	0.34 (8)	C-1976.8
5906.4 (15)	0.22 (7)	C-2114.5
5859.1 (10)	0.69 (12)	C-2162.0
5766.2 (15)	0.20 (6)	C-2254.5
5755.0 (12)	0.45 (8)	C-2265.0
5569.5 (10)	1.4 (3)	C-2452.6
5461.5 (10)	0.96 (20)	C-2559.6
5428.8 (12)	0.59 (12)	C-2592.3
5420.0 (12)	0.44 (10)	C-2601.1
5397.3 (10)	0.48 (10)	C-2623.8
5339.7 (12)	0.41 (10)	C-2681.4
5289.5 (10)	0.61 (12)	C-2731.6
5246.3 (12)	0.43 (10)	C-2774.8
5220.8 (15)	0.21 (7)	C-2800.3
5139.0 (10)	0.62 (12)	C-2882.1

Cont. Table 2.

1	2	3
5086.2 (15)	0.61 (15)	C-2934.9
4064.5 (15)	0.30 (8)	C-2956.6
4992.1 (15)	0.41 (10)	C-3029.0
4922.6 (10)	1.1 (3)	C-3098.5
4875.1 (10)	0.87 (20)	C-3146.0
4844.8 (10)	0.64 (15)	C-3176.3
4817.3 (15)	0.21 (7)	C-3203.8
4803.6 (15)	0.18 (6)	C-3217.5
4756.1 (10)	0.76 (15)	C-3265.0
4692.0 (10)	1.2 (2)	C-3329.1
4687.0 (10)	1.0 (2)	C-3334.1
4632.0 (15)	0.29 (8)	C-3389.1
4563.6 (10)	1.1 (2)	C-3457.5
4487.6 (15)	0.31 (8)	C-3533.5
4463.0 (15)	0.24 (7)	C-3558.1
4438.8 (12)	0.59 (10)	C-3582.3
4416.0(15)	0.21 (7)	C-3605.1
4406.7 (12)	0.52 (10)	C-3614.4
4339.1 (10)	0.68 (10)	C-3682.0
4162.8 (10)	0.70 (10)	C-3858.3
4019.6 (15)	0.47 (10)	C-4001.5
4009.5 (10)	0.97 (15)	C-4011.6
3953.2 (15)	0.38 (10)	
3903.0 (15)	0.30 (9)	
3732.7 (10)	0.40 (10)	
3562.7 (10)	0.54 (10)	
3522.4 (10)	0.60 (10)	
3339.0 (10)	0.28 (8)	
3306.8 (8)	0.42 (10)	
3191.5 (8)	0.29 (7)	
3185.6 (8)	0.26 (7)	
2972.1 (10)	0.35 (8)	
2941.6 (10)	0.31 (8)	
2672.2 (15)	0.21 (7)	
2651.5 (10)	0.26 (7)	
2633.3 (8)	0.20 (7)	

Cont. Table 2.

1	2	3
2405.2 (7)	0.23 (7)	
2277.0 (8)	0.15 (5)	
2214.0 (5)	0.48 (10)	
2153.4 (6)	0.47 (10)	2265.0-111.6
2135.2 (6)	0.39 (10)	
2086.8 (10)	0.28 (8)	
2072.8 (10)	0.22 (7)	
2037.0 (10)	0.35 (8)	
2022.2 (8)	0.39 (8)	
1934.7 (8)	0.32 (8)	
1882.3 (8)	0.26 (7)	
1812.2 (8)	0.30 (8)	
1694.6 (10)	0.14 (5)	1806.2-111.6
1677.3 (7)	0.40 (10)	
1556.6 (7)	0.23 (7)	
1515.6 (5)	0.85 (15)	
1490.0 (5)	0.40 (10)	1776.6-286.6
1467.0 (8)	0.18 (6)	
1448.8 (5)	0.26 (8)	
1436.1 (5)	0.41 (10)	
1366.6 (8)	0.25 (7)	
1244.9 (5)	0.26 (7)	
1224.1 (5)	0.59 (10)	2114.5-890.5
1179.8 (7)	0.10 (5)	1179.8-0
1144.5 (5)	3.0 (6)	
1127.9 (10)	0.10 (5)	
1101.7 (8)	0.16 (6)	1949.0-847.3
1082.3 (8)	0.16 (6)	1193.8-111.6
1048.5 (8)	0.21 (7)	1938.0-890.5
1023.7 (5)	0.48 (8)	
1004.0 (3)	0.95 (15)	1583.4-579.4
978.6 (3)	1.4 (3)	
962.2 (3)	1.9 (4)	
952.1 (3)	1.1 (3)	
930.2 (5)	0.20 (7)	
925.8 (10)	0.24 (8)	

Cont. Table 2.

1	2	3
920.6 (10)	0.20 (8)	1583.4-664.1; 2114.5-1193.8
912.8 (3)	1.5 (4)	
897.6 (3)	0.74 (10)	
890.5 (10)	0.50 (10)	890.5-0
873.8 (8)	0.38 (10)	
859.4 (4)	0.41 (8)	859.6-0
847.3 (6)	0.26 (7)	847.3-0
839.7 (3)	3.0 (7)	
812.5 (6)	0.18 (6)	1703.0-890.5
797.0 (7)	0.13 (5)	1976.8-1179.8
789.1 (3)	0.78 (10)	
781.1 (6)	0.09 (3)	
770.4 (3)	0.57 (10)	
748.7 (10)	0.40 (10)	
733.7 (2)	3.2 (5)	
701.7 (8)	0.17 (5)	
675.96 (20)	2.0 (4)	2452.6-1776.6
669.1 (3)	0.21 (7)	956.8-286.6
658.0 (3)	0.41 (8)	
634.9 (6)	0.09 (4)	
627.71 (20)	0.86 (15)	
610.4 (10)	6.0 (10)	
585.5 (5)	0.4 (2)	1013.5-428.0
573.0 (4)	1.1 (2)	859.6-286.6
551.5 (8)	0.16 (5)	664.1-1116.6 ; 2265.0-1703.0
516.3 (3)	3.0 (6)	1179.8-664.1
490.8 (5)	0.81 (15)	
467.8 (5)	0.06 (3)	579.4-111.6
461.0 (5)	0.14 (5)	
445.3 (4)	0.19 (6)	
431.8 (5)	2.2 (5)	859.6-428.0
428.0 (3)	3.5 (6)	428.0-0
405.6 (8)	0.06 (3)	
400.8 (6)	0.12 (4)	As <sup>75</sup>

Cont. Table 2.

1	2	3
377.52 (20)	3.0 (5)	664.1-286.6; 956.8-579.4
349.44 (20)	0.77 (12)	1013.5-664.1
340.3 (10)	0.21 (6)	
319.2 (10)	1.0 (3)	
316.1 (10)	1.0 (3)	428.0-111.6
309.3 (8)	0.15 (5)	
292.81 (15)	7.2 (10)	579.4-286.6; 956.8-664.1
286.61 (10)	75 (10)	286.6-0
264.65 (10)	1.0 (2)	As <sup>75</sup>
211.61 (10)	1.1 (2)	
191.4 (3)	0.24 (6)	
141.0 (4)	5 (2)	428.0-286.6
136.6 (3)	1.5 (7)	As <sup>75</sup>

2.  $\gamma$ -Rays' from the  $\text{Se}^{77}(\text{n},\gamma)\text{Se}^{78}$  Thermal-Neutron Reactions.

M.R.Ahmed, M.A.Khalil, S.Al-Najar and A.M.Demidov.

A spectrum of  $\gamma$ -rays from the  $\text{Se}^{77}(\text{n},\gamma)\text{Se}^{78}$  thermal-neutron reaction has been measured with the help of a Ge(Li)-spectrometer. Energies and intensities have been determined for 124  $\gamma$ -lines of the spectrum. A diagram of  $\gamma$ -transition of the  $\text{Se}^{78}$  nucleus is discussed.

Table 1.

Isotopic Composition and Isotope Contribution to Thermal-Neutron Capture by  $\text{Se}^{77}$  - Sample.

Isotope	74	76	77	78	80	82
Isotope Abundance in the Sample %	0.3	4.7	68.1	9.9	13.9	3.1
Contribution to Neutron-Capture Cross-Section, %	0.5	12.1	86.8	0.1	0.3	0.2

Table 2.

Energies and Intensities for  $\gamma$ -Ray of  
Se<sup>78</sup>

$E_{\gamma}$ , KeV	$I_{\gamma}$ , %	Position in the diagram of $\gamma$ -transitions
(10496,5)	---	
9882,9 (15)	13.0 (20)	C-613.9
9188.0 (15)	7.3 (10)	C-1308.9
8998.3 (15)	0.24 (4)	C-1499.0
8738.4 (20)	0.05 (2)	C-1759.3
8501.6 (12)	2.3 (3)	C-1996.3
8168.2 (15)	2.5 (4)	C-2327.7
8160.3 (20)	1.9 (3)	C-2335.4
7959.4 (12)	0.6 (2)	C-2538.0
7814.9 (15)	0.11 (3)	C-2683.2
7743.7 (10)	0.55 (8)	C-2753.5
7657.7 (10)	0.61 (8)	C-2839.4
7598.6 (10)	0.37 (6)	C-2898.5
7490.9 (10)	0.96 (12)	C-3005.9
7309.9 (20)	0.33 (5)	C-3187.4
7254.8 (15)	0.53 (7)	C-3242.4
7208.2 (10)	1.9 (3)	C-3289.2
7113.1 (10)	0.93 (15)	C-3383.4
7048.8 (15)	0.41 (6)	C-3448.5
6974.9 (12)	0.58 (3)	C-3522.4
6905.2 (10)	0.89 (12)	C-3592.1
6873.0 (12)	0.45 (5)	C-3624.3
6810.6 (10)	0.88 (12)	C-3686.7
6498.7 (10)	1.3 (3)	C-3999.3
6460.0 (10)	0.54 (7)	C-4037.3
6343.8 (15)	0.21 (5)	C-4152.5
6315.5 (10)	1.4 (3)	C-4181.8
6244.1 (10)	1.1 (2)	C-4253.2
6153.8 (15)	0.30 (10)	C-4343.5
6133.1 (15)	0.39 (10)	C-4364.2
6108.3 (15)	0.42 (15)	C-4389.0
6046.5 (10)	1.0 (2)	C-4451.1
6026.6 (12)	0.50 (10)	C-4470.7
5967.5 (15)	0.22 (5)	C-4529.8

Cont. Table 2.

1	2	3
3439.7 (7)	0.74 (15)	
3385.0 (8)	0.78 (15)	3383.4-0
3280.5 (8)	0.71 (15)	
3220.9 (10)	0.58 (12)	4529.8-1308.9 ?
3184.8 (8)	0.18 (4)	
2873.8 (8)	0.84 (15)	4181.8-1308.9
2769.5 (6)	0.88 (15)	3383.4-613.9
2674.9 (8)	1.2 (2)	3289.2-613.9
2509.3 (10)	0.40 (10)	
2476.5 (10)	0.55 (10)	
2392.0 (7)	1.0 (2)	3005.9-613.9
2284.6 (6)	1.3 (2)	2898.5-613.9
2240.8 (10)	0.20 (5)	4923.2-2683.2
2199.9 (8)	0.61 (12)	
2162.8 (6)	0.82 (12)	
2034.0 (6)	0.65 (12)	
1995.9 (15)	2.5 (4)	1996.3-0
1924.0 (5)	1.7 (3)	2538.0-613.9
1894.9 (7)	1.2 (3)	
1851.5 (7)	0.70 (15)	
1748.4 (8)	0.40 (10)	4645.0-2898.5
1721.5 (8)	0.9 (3)	2335.4-613.9
1713.8 (6)	1.9 (8)	2327.7-613.9
1672.0 (8)	0.10 (3)	3999.3-2327.7
1652.8 (7)	0.33 (10)	
1552.7 (8)	0.16 (6)	4451.1-2898.5
1530.2 (5)	0.98 (15)	2839.4-1308.9
1382.5 (5)	1.7 (3)	1996.3-613.9
1377.8 (8)	0.35 (10)	
1373.5 (8)	0.32 (10)	2683.2-1308.9
1339.1 (4)	1.2 (2)	4722.7-3383.4
1309.0 (3)	9.3 (15)	1308.9-0
1293.8 (5)	0.20 (5)	
1240.8 (3)	3.1 (5)	1854.7-613.9
1229.3 (7)	0.35 (7)	2538.0-1308.9
1145.4 (5)	2.2 (3)	1759.9-613.9

Cont. Table 2.

1	2	3
5945.0 (12)	0.54 (8)	C-4552.4
5878.5 (12)	0.14 (3)	C-4618.3
5852.4 (15)	0.20 (5)	C-4645.0
5812.9 (15)	0.95 (20)	C-4684.5
5774.7 (10)	0.42 (10)	C-4722.7
5682.8 (10)	0.18 (5)	C-4814.6
5615.5 (15)	0.29 (8)	C-4881.9
5574.2 (15)	0.20 (5)	C-4923.2
5498.1 (15)	0.50 (10)	C-4999.3
5436.6 (15)	0.14 (4)	C-5060.4
5369.3 (10)	0.65 (12)	C-5128.1
5333.4 (12)	0.23 (5)	
5252.4 (15)	0.19 (5)	
5156.1 (15)	0.22 (5)	
5107.8 (15)	0.18 (5)	
4985.9 (15)	0.15 (4)	
4961.9 (15)	0.18 (5)	
4856.4 (12)	0.19 (5)	
4810.8 (15)	0.18 (5)	
4689.5 (15)	0.20 (5)	
4626.2 (15)	0.29 (7)	
4500.8 (15)	0.24 (6)	
4452.6 (10)	0.62 (12)	
4446.2 (15)	0.50 (10)	
4391.5 (15)	0.10 (3)	
4376.8 (15)	0.10 (3)	
4338.0 (10)	0.51 (10)	
4285.3 (15)	0.22 (5)	
4262.9 (10)	0.26 (5)	
4141.2 (15)	0.34 (6)	
4096.3 (15)	0.28 (6)	
4071.2 (10)	0.40 (8)	4684.5-613.9
4033.1 (15)	0.34 (6)	
3855.1 (8)	0.41 (7)	
3631.7 (10)	0.40 (7)	
3476.9 (10)	0.20 (5)	

Cont. Table 2.

1	2	3
1080.2 (6)	0.61 (10)	1694.1-613.9
1026.5 (8)	0.36 (8)	2335.4-1308.9
1019.1 (8)	0.38 (8)	2327.7-1308.9
1011.6 (8)	0.40 (8)	4253.2-3242.4
1006.5 (8)	0.53 (10)	
960.9 (10)	0.14 (5)	4343.5-3383.4
888.3 (8)	3.3 (10)	1503.2-613.9
885.1 (8)	4.2 (10)	1499.0-613.9
843.2 (4)	0.60 (10)	2839.5-1996.3
840.4 (5)	0.18 (6)	3522.4-2683.2
828.6 (4)	0.96 (15)	2327.7-1499.0
743.6 (6)	0.24 (7)	
695.0 (2)	17.1 (30)	1308.9-613.9
687.6 (3)	3.6 (6)	1996.3-1308.9
651.9 (5)	0.31 (10)	
613.9 (2)	76 (10)	613.9-0
545.4 (4)	2.31(4)0	1854.7-1308.9
497.8 (5)	0.50 (10)	1996.3-1499.0
355.2 (3)	0.20 (4)	2683.2-2327.7

3. Gamma-Spectra of  $\text{Mo}^{97}$ ,  $\text{Mo}^{99}$  and  $\text{Mo}^{101}$  from Thermal-Neutron Capture.

M.R.Ahmed, M.A.Khalil, S.Al-Najar and A.M.Demidov.

Spectra of  $\gamma$ -rays from thermal-neutron capture in  $\text{Mo}^{96}$ ,  $\text{Mo}^{98}$  and  $\text{Mo}^{101}$  have been measured, using a Ge(Li)-spectrometer. Energies and intensities of the  $\gamma$ -lines isolated from the spectrum have been determined. Diagrams of  $\gamma$ -transitions of  $\text{Mo}^{97}$  and  $\text{Mo}^{99}$  nuclie have been made.

Table 1.

Isotopic composition of samples (P), isotope contributions to thermal-neutron capture by samples (Q), and cross-sections of thermal-neutron capture by Mo-isotopes ( $\gamma$ )

Sample	Isotope	92	94	95	96	97	98	100
$\text{Mo}^{96}$	P	0.7	0.8	2.5	87.2	5.7	2.3	0.8
	Q	<0.1	-	23.6	67.9	8.1	0.2	0.1
$\text{Mo}^{98}$	P	<0.2	<0.2	0.9	1.3	1.4	95.1	1.3
	Q	<0.3	-	40.3	4.9	9.5	44.0	0.8
$\text{Mo}^{100}$	P	1.1	1.3	1.5	1.9	1.7	3.8	88.7
	Q	<0.9	-	46.9	4.9	8.0	1.3	38.1
	$\delta$	<0.3	-	$14.5 \pm 0.5$	$1.2 \pm 0.6$	$2.2 \pm 0.7$	$0.15 \pm 0.20$	$0.20 \pm 0.05$

Table 2

Energies and intensities for  $\gamma$ -rays of  $\text{Mo}^{97}$

$E_{\gamma}$ , KeV	$I_{\gamma}$ , %	$E_{\gamma}$ , KeV	$I_{\gamma}$ , %
6141.2 (12)	0.30 (10)	1618.6 (4)	0.4 (15)
6100.4 (10)	0.32 (10)	1516.0 (4)	0.35 (10)
5305.1 (8 )	0.52 (12)		
5063.0 (10)	0.40 (10)	1284.8 (3)	0.90 (20)
4657.7 (12)	0.27 (8 )	1268.5 (5)	0.33 (10)
4543.1 (8 )	1.5 (3 )	1265.2 (2)	1.2 (2 )
4473.7 (12)	0.12 (4)	1118.0 (5)	0.36 (10)
4323.1 (15)	0.16 (5)	1091.9 (5)	2.1 (6)
4309.0 (8 )	0.33 (10)	1024.0 (3)	0.50 (10)
4256.9 (12)	0.24 (8)	1008.5 (5)	0.65 (10)
4243.1 (15)	0.33 (10)	897.9 (5)	0.25 (10)
4178.7 (12)	0.35 (10)	888.3 (5)	0.35 (10)
4027.8 (8 )	0.80 (20)	720.5 (3)	11 (3)
3813.1 (10)	0.72 (20)	679.6 (2)	5.1 (10)
2578.7 (10)	0.36 (10)	658.3 (2)	0.90 (25)
2512.9 (5)	0.52 (12)		
2278.3 (7)	0.40 (12)	481.0 (2)	21 (4)
2198.4 (5)	0.33 (10)	407.2 (2)	3.2 (8 )
2152.4 (5)	0.44 (12)	352.4 (4)	0.22 (7)
		238.4 (2)	1.5 (3)
		118.6 (8)	0.8 (3)

Table 3.

Energies and intensities for  $\gamma$ -rays of Mo<sup>99</sup>

$E_{\gamma}$ , KeV	$I_{\gamma}$ , %
5926.5 (10)	2.5 (8)
5576.4 (10)	2.3 (8)
5020.5 (15)	1.7 (6)
4902.2 (10)	1.8 (6)
4461.0 (10)	1.4 (5)
3996.0 (10)	2.8 (7)
3333.1 (10)	1.6 (5)
1100.8 (8)	5.0 (12)
928.7 (4)	2.3 (6)
674.1 (4)	2.5 (7)
656.0 (3)	2.1 (6)
631.8 (2)	6.7 (12)
548.9 (3)	0.8 (3)
534.3 (3)	3.8 (8)
525.6 (2)	4.4 (8)
450.9 (2)	5.5 (10)
427.6 (3)	2.3 (6)
385.5 (3)	0.8 (3)
351.0 (10)	16 (5)
273.0 (10)	0.4 (2)
264.1 (2)	5.2 (10)
253.3 (10)	11 (3)
174.8 (7)	6 (2)
139.8 (15)	10 (4)
97.6 (2)	35 (8)

Table 4

Energies and intensities for  $\gamma$ -rays of  $\text{Mo}^{101}$

$E_\gamma$ , KeV	$I_\gamma$ , %	Radiative isotope
5381.5 (15)	0.7 (3)	
5267.0 (15)	1.9 (6)	
5103.0 (12)	8.2 (20)	
4881.6 (15)	1.3 (4)	
4555.8 (15)	0.9 (3)	
4386.3 (12)	3.5 (9)	
4221.4 (12)	2.0 (6)	
4104.7 (10)	6.0 (12)	
4047.2 (10)	2.1 (6)	
3949.4 (10)	3.5 (9)	
2089.5 (6)	2.1 (5)	$\text{Tc}^{101}$
2041.3 (5)	2.6 (6)	$\text{Tc}^{101}$
2032.9 (5)	9.5 (20)	$\text{Tc}^{101}$
1841.6 (6)	2.9 (7)	
1673.6 (6)	2.1 (6)	$\text{Tc}^{101}$
1542.8 (7)	1.5 (4)	
1532.7 (5)	7.0 (15)	$\text{Tc}^{101}$
1355.7 (7)	1.1 (3)	$\text{Tc}^{101}$
1345.6 (7)	1.4 (4)	$\text{Tc}^{101}$
1304.8 (5)	2.7 (7)	
1251.0 (5)	4.0 (10)	$\text{Tc}^{101}$
1160.1 (5)	3.6 (9)	$\text{Tc}^{101}$
1059.2 (10)	1.0 (3)	
1032.0 (6)	0.7 (2)	

$E_{\gamma}$ , KeV	$I_{\gamma}$ , %	Radiative isotope
1012.4 (3)	13 (4)	Tc <sup>101</sup>
972.6 (3)	3.4 (9)	
967.0 (10)	1.3 (4)	Tc <sup>101</sup>
934.4 (3)	3.0 (8)	Tc <sup>101</sup>
877.4 (3)	2.6 (7)	Tc <sup>101</sup>
833.9 (8)	3.0 (10)	Tc <sup>101</sup>
810.9 (10)	0.86 (30)	
714.4 (5)	6.2 (10)	Tc <sup>101</sup>
590.9 (2)	17 (4)	Tc <sup>101</sup>
584.1 (3)	1.9 (5)	
561.3 (5)	3.0 (8)	
545.0 (2)	5.5 (10)	Ru <sup>101</sup>
540.0 (10)	0.8 (3)	
535.4 (2)	6.6 (10)	Mo <sup>100</sup>
506.1 (2)	10 (2)	Tc <sup>101</sup>
398.5 (3)	1.5 (3)	Tc <sup>101</sup>
378.8 (3)	0.56 (15)	
365.5 (5)	0.7 (2)	
306.5 (2)	90.3	Ru <sup>101</sup>
294.4 (2)	10 (2)	Tc <sup>101</sup>
276.0 (4)	7.3 (15)	
237.2 (2)	11 (2)	
212.1 (4)	1.4 (4)	
191.8 (2)	21 (4)	Tc <sup>101</sup>
184.7 (3)	1.7 (4)	Ru <sup>101</sup>
180.4 (3)	13 (3)	
157.8 (3)	7 (2)	
127.4 (2)	2.7 (6)	Ru <sup>101</sup>

P R O G R E S S   R E P O R T

July 1975

The relevant nuclear research to INDC in Israel during the last year was continued according to the outline given in the consolidated Progress Report for 1974 (INDC(SEC)-42/L).

The experimental work was concentrated mostly in four main subjects:

Neutron and reactor physics studies

Nuclear fission studies

Gamma scattering measurements

Reactions with accelerated particles.

The major experimental facilities consisted of a 5 MW swimming pool uranium enriched reactor at the Soreq Nuclear Research Centre, a 26 MW Heavy Water Tank-Type natural uranium reactor at the Negev Research Centre, a 6 MeV Tandem, type EN accelerator and a 3 MeV Van-de-Graaf accelerator at the Weizmann Institute of Science, Rehovoth--this in addition to other experimental laboratory facilities based on nuclear spectroscopy and associated equipment. A considerable work was done, as well in theoretical nuclear studies.

Brief abstracts of the work carried out during the last year, both published and unpublished, are given in the following section, listed according to the laboratories.

T E L - A V I V   U N I V E R S I T Y

Theoretical Nuclear Physics Group

The main areas of interest are:

Isobaric Analog Resonances, Coulomb Energies, Giant Resonances in Nuclei, Pion-Nucleus Interactions, Hartree-Fock Theory, Nuclear Fission and Fusion, Generalized Approximative Procedures in the Many Body Problem, Weak and Electromagnetic Interactions of Nuclei, Hypernuclei.

MULTI-DETERMINANTAL HARTREE-FOCK THEORY

G. Shadmon and I. Kelson  
(Nucl. Phys., to be published)

Systematic generalizations of the independent particle approximation are introduced. Functionals which describe the qualities of these approximations are defined and investigated. Appropriate equations, obtained by applying the variational principle, are derived and methods of their solution are outlined. The concept of the Hartree-Fock self-consistent Hamiltonian is generalized.

SPACE AVERAGING TECHNIQUES OF DETERMINANTAL MEASURES

I. Kelson and G. Shadmon  
(Journal of Math. Phys., to be published)

Techniques for evaluating approximate space-averages of determinantal measures are discussed. The concept of Combinatorial Structure Diagrams is introduced and investigated.

CHARGED PARTICLE DIAGNOSTICS OF LASER PRODUCED PLASMA

I. Kelson and S. Yankielowicz  
(Nucl. Inst., to be published)

The use of charged particles from thermonuclear reactions as a diagnostic tool of high density pellets is suggested and the range of its applicability investigated. A phenomenological relation between  $\langle \rho r \rangle$  and the median energy of the protons in the D-D reaction is obtained.

INTERPRETATION OF COLLECTIVE HYPERNUCLEAR STATES  
PRODUCED BY STRANGENESS-EXCHANGE REACTIONS

N. Auerbach and A. Gal

(Physics Letters 48B, 22, 1974)

The concept of Strangeness Analog Resonance may not be useful for describing low momentum transfer strangeness exchange reactions on nuclei. A band of collective excitations is expected where the lowest and most enhanced one is invariably around 10 MeV above hypernuclear ground state.

CORE POLARIZATION AND COULOMB DISPLACEMENT ENERGIES

N. Auerbach

(Nuclear Physics A229, 447, 1974)

A systematic study of the core polarization correction to Coulomb displacement energies is carried out. A zero range density independent and density dependent force is used to calculate this correction in  $A = 16$ ,  $A = 40$  and  $A = 208$  regions. It is found that the core polarization correction does not increase the Coulomb displacement energies and, therefore, cannot resolve the existing discrepancy between theory and experiment. Moreover, when the mean square radius of the excess neutron distribution is decreased the core polarization correction to the Coulomb energy becomes attractive and cancels the gain resulting from the direct Coulomb term.

Hence, it is concluded that the discrepancy cannot be resolved even when the excess neutron distribution has an anomalously small radius. It is also pointed out that when the core polarization term is added the discrepancy is almost equal in mirror nuclei with a single hole in the  $N = Z$  core and those with a single particle outside the same core. Evidently, additional charge asymmetric corrections are required to resolve the discrepancies in Coulomb displacement energies.

ANALOG SPIN WAVE FUNCTIONS AND SPREADING WIDTHS  
OF ISOBARIC ANALOG RESONANCES

W.M. MacDonald and N. Auerbach

(Physics Letters 53B, 425, 1975)

The coupling of the isobaric analog state (IAS) to the giant isovector monopole state has been shown by Mekjian and Auerbach to dramatically affect

the calculation of the spreading width. We show that the inclusion of this coupling is equivalent to a new definition of IAS as an eigenstate of analog spin in which each proton radial wave function is distorted relative to the corresponding neutron radial wave functions by the central Coulomb field.

ISOBAR MIXING AND COULOMB DISPLACEMENT ENERGIES IN NUCLEI

N. Auerbach

(Physics Letters 53B, 417, 1975)

It is pointed out that because of the electromagnetic mass splitting of members of a nucleon isobar multiplet (such as the  $\Delta_{33}$ ), admixtures of this isobar in nuclei may lead to substantial corrections in Coulomb displacement energies.

THE ABC EFFECT IN THE REACTION  $NN \rightarrow d\pi\pi$

I. Bar-Nir, T. Risser and M.D. Shuster

(Nuclear Physics, in press)

A simple peripheral model for the reaction  $NN \rightarrow NN\pi\pi$  is extended to the reaction  $NN \rightarrow d\pi\pi$ . Predictions for the differential and total cross sections are compared with recent experiments. The enhancement of the deuteron recoil-momentum spectrum near the  $\pi\pi$  threshold (ABC effect) is well reproduced.

Experimental Nuclear Physics Group

Research Subjects

- 1) Study of the prompt p-decay following  $\pi^+$  and  $\pi^-$  bombardment of several nuclei.
- 2) Study of  $\alpha$ -emission following  $\pi^-$  bombardment of several nuclei.
- 3) Single pion charge exchange ( $\pi^+, \pi^0$ ) measurements on light nuclei.
- 4) The reactions ( $\pi^+, \pi^+n$ ) and ( $\pi^-, \pi^-n$ ) on  $C^{12}$  and  $N^{14}$ .
- 5) Study for design of  $\pi^0$  spectrometer.
- 6) Elastic- and inelastic scattering of high energy electrons on the even isotopes of Sm.
- 7) The study of giant resonances excited by electrons, measured in coincidence with neutrons (proposal).
- 8) Coulomb excitation of giant resonances by heavy ions.
- 9) Measurement of parity forbidden  $\alpha$ -decay.
- 10) Direct reactions  $Zr^{92}(d, \alpha)Y^{90}$ ,  $Zr^{96}(d, \alpha)Y^{94}$ ,  $Zr^{91}(d, He^3)Y^{90}$ ,  $Mo^{95}(p, d)Mo^{94}$  and  $Mo^{97}(p, d)Mo^{96}$ , for nuclear structure purposes.
- 11) Study of unbound isobaric analog states and their subsequent decay: ( $He^3, d$ ) on the Cu-isotopes.
- 12) Measurement of anisotropy in the decay of the IAS in  $Cu^{61}$ .

THE  $(\pi^{\pm}, \pi N)$  KNOCKOUT REACTIONS ON  $C^{12}$   
FROM 30 TO 90 MeV

J. Alster, D. Ashery, S. Cochavi, M.A. Moinester, A.I. Yavin and M. Zaider  
Phys. Rev. 8C, 2039 (1973))

The cross sections for the knockout reactions  $C^{12}(\pi^{\pm}, \pi^{\mp}n)C^{11}$  and  $C^{12}(\pi^{\pm}, \pi^{\pm}n + \pi^0p)C^{11}$  were measured over the energy range of 30 to 90 MeV by an activation method, and compared to existing calculations. In this energy range, the ratio  $\sigma(\pi^{-}C^{12})/\sigma(\pi^{+}C^{12})$  of the cross sections is 2 to 3 times smaller than the corresponding ratio for pions on nucleons, contrary to the expectations of the impulse approximation. Such a behaviour has previously been known only near the energy of the (3,3) resonance.

PION CHARGE EXCHANGE REACTIONS

M. Zaider, J. Alster, D. Ashery, N. Auerbach, S. Cochavi, M.A. Moinester  
J. Warszawski and A.I. Yavin  
(High Energy Physics and Nuclear Structure, Ed. G. Tibell, 219 (1973)).

Published calculations and data for pion single charge-exchange are presented and lead to some open questions. We report the results of measurements of the cross section for the reactions  $^{13}C(\pi^{\pm}, \pi^0)^{13}N$  and  $^{11}B(\pi^{\pm}, \pi^0)^{11}C$  over the energy range of 30 to 90 MeV by an activation method. The data for  $^{13}C$  correspond solely to the excitation of the ground state analog. The excitation curve for  $^{13}C$  is flat, in disagreement with available predictions for analog state transitions, using either plane-wave or non-local optical potentials, but can be explained by a local optical potential.

INTERACTION OF POSITIVE AND NEGATIVE PIONS  $^{27}Al$  AND  $^{28}Si$

D. Ashery, M. Zaider, Y. Shamai, S. Cochavi, M.A. Moinester, A.I. Yavin and J. Alster  
(Phys. Rev. 32, 943 (1974))

The interaction of 25, 70 and 100 MeV positive pions and of 70 MeV negative pions with  $^{27}Al$  and  $^{28}Si$  was studied by the detection of  $\gamma$  radiation emitted from residual nuclei formed in the reaction. Large cross sections for the removal of "a"

clusters were found for both nuclei and both pion charges. Very different behavior is observed for the two target nuclei with respect to both one and three nucleon removal. A large difference is observed in the population of mirror states in  $^{27}\text{Al}$  and  $^{28}\text{Si}$  by respective proton and neutron removal from  $^{28}\text{Si}$ . A large asymmetry is observed between the cross sections for the  $(\pi^-, \pi^- p)$  and  $(\pi^+, \pi^+ n)$  on  $^{28}\text{Si}$  leading to the same mirror states. The ratio of  $\pi^+$  to  $\pi^-$  cross sections for proton knock-out is about a third of the value predicted by a simple impulse approximation.

$(\pi^\pm, \pi N)$  KNOCKOUT REACTIONS ON  $^{14}\text{N}$  FROM 50 TO 90 MeV

M. Zaider, J. Alster, D. Ashery, S. Cochavi, M.A. Moinester and A.I. Yavin  
(Phys. Rev. 10C, 938 (1974))

The cross sections for the knockout reactions  $^{14}\text{N}(\pi^-, \pi^- n)^{13}\text{N}$  and  $^{14}\text{N}(\pi^+, \pi^+ n + \pi^0 p)^{13}\text{N}$  were measured over the energy range of 50 to 90 MeV by an activation method. The ratio of the cross sections  $(\pi^{14}\text{N})/\sigma(\pi^{12}\text{C})$  at 70 and 90 MeV for both  $\pi^+$  and  $\pi^-$  is in good agreement with the similar ratio from high energy (p,pn) reactions on the same targets. This is consistent with a quasi-free pion-nucleus knockout picture. However, the ratio  $\sigma(\pi^{-14}\text{N})/\sigma(\pi^{+14}\text{N})$ , found to be about a third of the free pion-nucleus ratio, is in disagreement with the simple impulse approximation model.

STUDY OF THE  $^{91}\text{Zr}(d, ^3\text{He})^{90}\text{Y}$  REACTION

S. Cochavi, S. Gilad, M.A. Moinester, J. Alster, M. Buenerd and P. Martin  
(Nucl. Phys. A293, 73 (1974))

The  $^{91}\text{Zr}(d, ^3\text{He})^{90}\text{Y}$  reaction was studied at a deuteron energy of 28 MeV. Angular distributions were measured from  $13^\circ$  to  $47^\circ$ ;  $\ell_p$  values and transition strengths were determined by DWBA analysis. The angular distributions for the  $(\pi p_{p/2})(\nu d_{5/2})$  doublet (g.s. and .20 MeV state) exhibit the characteristic  $\ell = 1$  shape. States at 1.42, 1.57, 1.64, and 1.81 MeV were also populated strongly in the  $(d, ^3\text{He})$  reaction; the 1.42, 1.57 and 1.81 levels contain  $\ell = 1$  transition strength and are most likely members of the  $(\pi p_{3/2}^{-1})(\nu d_{5/2})$  multiplet. The 2.03 MeV state has a characteristic  $\ell = 3$  angular distribution and is suggested to be the only member of the  $(\pi f_{5/2}^{-1})(\nu d_{5/2})$  sextet to be unambiguously

observed in this study, most probably the  $5^-$  or  $4^-$  member. The members of the  $(\pi g_{9/2})(\nu d_{5/2})$  sextet were populated weakly (less than 100  $\mu\text{b}/\text{sr}$ ) in this reaction.

STUDY OF THE (p,d) REACTION ON  $^{95}\text{Mo}$  AND  $^{97}\text{Mo}$

S. Cochavi, A. Moalem, D. Ashery, J. Alster, G. Bruge and A. Chaumeaux  
(Nucl. Phys. A211, 21 (1973))

The reactions  $^{95,97}\text{Mo}(p,d)^{94,96}\text{Mo}$  were studied at a proton energy of 26 MeV. Angular distributions were measured from  $11^\circ$  to  $40^\circ$  and compared with distorted wave born approximation calculations;  $\ell$  values and spectroscopic factor were extracted for the low-lying states of  $^{94}\text{Mo}$  and  $^{96}\text{Mo}$ . The angular distributions of these states have a characteristic  $\ell = 2$  shape. The ratios of the summed spectroscopic factors to the  $0^+$ ,  $2^+$ , and  $4^+$  states are in good agreement with the  $(2d_{5/2})^n$  neutron configurations. The  $2^+$  strength is strongly fractionated in both  $^{94}\text{Mo}$  is split among two states, whereas in  $^{96}\text{Mo}$  it is concentrated in the second  $4^+$  state.

STUDY OF THE  $^{92,96}\text{Zr}(d,\alpha)^{90,94}\text{Y}$  REACTIONS

S. Gilad, S. Cochavi, M.A. Moinester, J. Alster, M. Buenerd and P. Martin  
(Nucl. Phys. A233, 81, 1974)

The hole-hole structure of  $^{94}\text{Y}$  was studied via the reaction  $^{96}\text{Zr}(d,\alpha)^{94}\text{Y}$  and compared to the particle-hole structure of  $^{90}\text{Y}$ , which was populated by the reaction  $^{92}\text{Zr}(d,\alpha)^{90}\text{Y}$ . The deuteron beam energy was 28 MeV. Angular distributions of both reactions were obtained for the prominent lines. New states of  $^{94}\text{Y}$  were observed at 0.44, 1.17, 1.39, 1.53, 1.82, 1.90, 2.17, 2.33, 2.46 and 2.77 MeV. Our data are consistent with the previous reported  $2^-$  assignment of the ground state, and we suggest  $J^\pi = 3^-$  for the 0.44 MeV state, these being members of the  $(\pi 2p_{1/2}, \nu d_{5/2}^{-1})$  doublet. The 1.17 state is suggested to be a member of the  $(\pi p_{3/2}^{-1}, \nu d_{5/2}^{-1})$  multiplet. The Q-value of the  $^{96}\text{Zr}(d,\alpha)^{94}\text{Y}$  reaction was measured to be  $7.609 \pm 0.020$  MeV. The reaction  $^{94}\text{Zr}(d,\alpha)$  was performed at two angles. Several new states of  $^{92}\text{Y}$  were observed at 0.31, 0.78, 1.03, 1.31, 1.49, 1.69 and 1.89 MeV.

ISRAEL ATOMIC ENERGY COMMISSION

A GENERALIZED PERTURBATION THEORY AND VARIATIONAL PRINCIPLE FOR MULTIPLE RATIOS OF LINEAR AND BILINEAR FUNCTIONALS<sup>(1)</sup>

E. Greenspan

Variational principles and a generalized perturbation theory for single ratios of linear or bilinear functionals were recently published by Stacey<sup>(2)</sup>.

The present work extends Stacey's formulation to more general functionals having the form of a product of an arbitrary number of ratios of linear flux functionals and of bilinear functionals. Nuclear systems which are described by the homogeneous or the inhomogeneous Boltzmann equation were considered. The computational strategy and effort required for applying the generalized perturbation theory and variational principle to a multiple ratio were considered and a possible application of the new formulation was described.

REFERENCES:

1. Greenspan, E., Nucl. Sci. Eng., in press.
2. Stacey, Jr., W.M., J. Math. Phys. 13, 1119 (1972)

AN APPROXIMATION TO THE STATIONARY NEUTRON TRANSPORT EQUATION-SIMILAR TO THE P<sub>n</sub> APPROXIMATION

M. Lemanska

The neutron flux in slab geometry was obtained in the form

$$\phi(x, \mu) = f(x) - \mu \frac{df(x)}{dx} + \mu^2 \frac{d^2 f(x)}{dx^2} + \dots + (-1)^{\nu} \mu^{\nu} \frac{d^{\nu} f(x)}{dx^{\nu}} + \dots \quad (1)$$

where the function  $f(x)$  is the solution of

$$f = c \left\{ f + \frac{1}{3} \frac{d^2 f}{dx^2} + \frac{1}{5} \frac{d^4 f}{dx^4} + \dots + \frac{1}{2\nu+1} \frac{d^{2\nu} f}{dx^{2\nu}} + \dots \right\} \quad (2)$$

Then

$$f = c \left\{ f + \frac{1}{3} \frac{d^2 f}{dx^2} \right\} \quad (3)$$

was used as an approximation to calculate the critical thickness of several assemblies in slab geometry. The results are better than those obtained by the P<sub>1</sub> approximation as may be seen in Table 1.

TABLE 1  
Critical half-thicknesses of an infinite slab  
(in mean free paths)

c	Exact <sup>(1)</sup>	P <sub>1</sub> <sup>(1)</sup>	P <sub>3</sub> <sup>(1)</sup>	P <sub>5</sub> <sup>(1)</sup>	Present work	S <sub>2</sub> code
1.02	5.6655	5.839	5.663	5.672	5.795	5.754
1.05	3.3002	3.488	3.319	3.307	3.454	3.374
1.10	2.1134	2.309	2.135	2.121	2.274	2.198
1.20	1.2893	1.485	1.318	1.298	1.427	1.390
1.40	0.7366	0.919	0.779	0.75	0.806	0.845
1.60	0.5120	0.680	0.559	0.530	0.522	0.619

REFERENCE:

1. Bell, G.I. and Glasstone S., Nuclear Reactor Theory, Van Nostrand-Reinhold, New York, 1970, p. 97.

EXACT SOLUTION OF THE P<sub>1</sub> TIME-DEPENDENT EQUATIONS WITH TIME-DEPENDENT CROSS SECTIONS FOR SLAB AND SPHERICAL GEOMETRY<sup>(1)</sup>

M. Lemanska and Y. Menning\*

The P<sub>1</sub> approximation to the time-dependent neutron transport equation with time-dependent cross sections for slab and spherical geometry was solved using the generalized Lie series technique. The variables were separated in the solution obtained, the radial part of which consists of the zero and first spherical moments of the stationary angular flux. In this way the discretization was obtained in the time variable only.

REFERENCE:

1. Lemanska, M. and Menning, Y., Z. Angew. Math. Phys. 25, 433 (1974)

ON THE ESTIMATION OF ERRORS IN REACTOR THEORY

Y. Ronen

A larger scope for the functional analysis method for error estimation<sup>(1,2)</sup> was obtained by introducing L<sub>1</sub> space to the calculations<sup>(3)</sup>. The advantages of introducing the L<sub>1</sub> space are the possible close estimation of errors, and a simplification of the calculations. Introduction of the L<sub>1</sub> space to reactor physics problems also gives some meaning to the interpretation of errors, because this is the natural space for reactor theory problems.

---

\*Swiss Federal Institute for Reactor Research, Würenlingen, Switzerland

The method was illustrated by some examples<sup>(4)</sup> dealing with the multi-group diffusion equation, where errors in eigenvalues and in fluxes are estimated and compared with the actual errors.

REFERENCES:

1. Ronen, Y., Nucl. Sci. Eng. 47, 195, (1972)
2. Ronen, Y., Nucl. Sci. Eng. 52, 147, (1973)
3. Ronen, Y., Atomkeroenergie 21, 183, (1973)
4. Ronen, Y., Nucl. Sci. Eng. 54, 467 (1974)

APPLICATION OF TWO-DIMENSIONAL SPLINE THEORY TO THE SPHERICALLY SYMMETRIC TRANSPORT PROBLEM<sup>(1)</sup>

L. Finkelstein and A.D. Krumbein

The non-conservation form of the spherically symmetric, energy-dependent transport equation was simulated in a manner which can be solved exactly by a biquadratic spline. The spline was then calculated by a one-step explicit formula. The results obtained thus far, (critical parameters and integrated fluxes), are in excellent agreement with one-speed, one-layer bench mark problems<sup>(2)</sup>. The cases compared ranged from  $c=1.6$ , the largest value found in nature, to  $c=1.02$ , where  $c$  is the average number of neutrons emerging from a collision<sup>(2)</sup>.

The merits of the method are: exact representation of the sources within the framework of splines, simplicity of the numerical algorithm, and reasonably short computing times.

Multistep formulas have been tried for a cubic-quadratic spline and were found to be unstable even for diminishing steps.

REFERENCES:

1. Finkelstein, L. and Krumbein, A.D., Trans. Amer. Nucl. Soc. 18, 166 (1974)
2. Bell, G.I., and Glasstone, S., Nuclear Reactor Theory, Van Nostrand-Reinhold, New York, 1970, p. 101.

TWO-DIMENSIONAL NUMERICAL TRANSPORT BY THE METHOD OF CHARACTERISTICS

L. Finkelstein and M. Segev

A little exploited method of solution of the neutron transport equation is to write its leakage term in the form of a full derivative, replace the source term by a sequence of iteratively defined sources, and then solve numerically along the characteristics (straight lines) of the differential operator.

Considerable computational savings which the method provides can be realized

only if

- a) a sufficiently simple and accurate cubature formula for the two-dimensional source integral is available, and
- b) the numerical solution of the ordinary differential equations along the characteristics can be obtained using relatively large steps.

Our approach to the cubature formula is to divide the surface of the directional sphere into a given number<sup>f</sup> of equally shaped subsurfaces in a way such that a characteristic crosses the centrum of each subsurface. This discretizes the directions of the angular fluxes. Any directional flux is then represented by a one-dimensional spline along its characteristic. This permits large integration steps.

The above method was applied to finite cylinders, infinite cylinders, spheres and slabs. We used one and six energy groups, and also six and eight directions in the cubature formula.

The results were compared with data from bench marks and also experimentally measured systems. The relative errors in  $k_{\text{eff}}$  were of the order of  $10^{-2}$  for six directions in the cubature formula, and a fraction of  $10^{-3}$  for the eight direction formula. The cases compared ranged from  $c=1.6$ , the largest value found in nature, to  $c=1.02$ , where  $c$  is the average number of neutrons emerging from a collision.

An additional advantage of the method is algorithmic simplicity, which permits easy programming.

#### VARIANCE REDUCTION IN DYNAMIC MODELS FOR PARTICLE TRANSPORT SIMULATION

M. Goldstein and B.P. Zeigler\*

A new formulation of the Monte Carlo method for dynamic models of three dimensional particle transport within a homogenous medium was made<sup>(1)</sup>. A "basic model" was defined using the standard Monte Carlo procedure. Then two variance reduction techniques, statistical weighting and exponential transform, were formulated by alterations in the basic model, so as to produce so-called "biased models". Each biased model was formally shown to produce the same estimate of the parameter of interest (detector response) as the basic model. This was done using methods of comparison of dynamic models derived from system theory. It was also shown that the two variance reduction techniques reduce the running time of the problem significantly.

#### REFERENCE:

1. Goldstein, M., NRCN-354, 1973.

---

\* University of Michigan, Ann Arbor, Michigan, U.S.A.

PARAMETRIC REPRESENTATION OF THE SHIELDING FACTOR CURVES

Y. Gur and S. Yiftah

The self-shielded multigroup cross section set can be divided into two parts: a) infinitely diluted cross sections and scattering matrix elements, which are constants, and b) self-shielding factors (ssf) of two continuous variables (temperature and background cross section). As the ssf are tabulated curves, the user must interpolate between given values and to date there is no single or even accepted solution to the problem of interpolation. Current methods were reviewed<sup>(1)</sup> and found to be either complicated or inaccurate (or both).

Parametric representation is a natural means of representing a curve. Two new methods for a parametric representation of the temperature dependent ssf curve were developed<sup>(1)</sup>, one of which was found to fit the data very well. That representation is obtained as follows. Write:

$$\log(\sigma_0) = A \operatorname{arctanh} [mf(\sigma_0) + n] + D$$

where  $f(\sigma_0)$  is the shielding factor for the background cross section,  $\sigma_0$ . Temperature dependence as well as indexes specifying reaction type and group number are omitted. As  $\operatorname{arctanh}(x)$  is defined in the domain  $-1 \leq x \leq 1$  and the shielding factor curve has values in the range  $f(0) \leq f(\sigma_0) \leq 1$ , we choose  $m$  and  $n$  so that

$$\begin{aligned} m + n &= 1 \text{ for the upper limit of } f(\sigma_0) \\ mf(0) + n &= -1 \text{ for the lower limit of } f(\sigma_0) \end{aligned}$$

by which  $m = 2/[1 - f(0)]$  and  $n = 1 - 2/[1 - f(0)]$ .

Denote

$$C = 1 - f(0)$$

and obtain

$$\log(\sigma_0) = A \operatorname{arctanh} \left[ \frac{2}{C} f(\sigma_0) + 1 - \frac{2}{C} \right] + D$$

Any pair of points  $[\sigma_0, f(\sigma_0)]$  defines  $A$  and  $D$  which, together with  $C$ , completely define the shielding factor curve to be

$$f(\sigma_0) = 1 - \frac{C}{2} \left[ 1 - \tanh \frac{\log(\sigma_0) - D}{A} \right]$$

As  $A$ ,  $C$ , and  $D$  are temperature dependent, and  $\log[f(\sigma_0)]$  is linear in  $\log T$ , a set of six parameters  $[A(T_1), C(T_1), D(T_1), A(T_2), C(T_2), D(T_2)]$  completely defines  $f(\sigma_0, T)$ .

As different pairs of points belonging to the same curve gave different values for  $A$  and  $D$ , a best-fit search in the ranges of  $A$  and  $D$ , found by taking

all possible pairs of each curve, was tried<sup>(1)</sup> and best A and D values to represent the curve were obtained.

More recently, we calculated A and D by each possible pair of points  $[\sigma_0, f(\sigma_0)]$ . It was found that there always exists at least one pair whose A and D are good parameters for the representation of the entire curve. Moreover, we found that the pair [10, f(10)] and [100, f(100)] yields good representations of the entire set of shielding factor curves of  $^{235}\text{U}$  (better than 2%),  $^{238}\text{U}$  (better than 1.5% for  $\sigma_0 \leq 100$ , and better than 7% in the entire range),  $^{239}\text{Pu}$  (better than 1% for  $\sigma_0 \leq 100$ , better than 5% in the entire range), and  $^{241}\text{Pu}$  (better than 1.5% for  $\sigma_0 \leq 100$  and better than 6% in the entire range), while the pair [100, f(100)] and [1000, f(1000)] yields good parametric representation of the entire set of shielding factor curves of  $^{240}\text{Pu}$  (better than 5% for  $\sigma_0 \leq 1000$  and better than 20% in the entire range), and of  $^{242}\text{Pu}$  (better than 10% in the entire range). Also, for different temperatures, the deviations of the same  $f(\sigma_0)$  factor were in the same direction and roughly the same percent, which reduces the influence of the deviations on the Doppler coefficient. In the range of importance for fast reactor calculations (above 500 eV), the fit is very good (much better than 1%) for all isotopes, reaction types, temperatures, and background cross sections with the pair [10, f(10)] and [100, f(100)]. Thus, instead of calculating many values per curve and representing the shielding factor curve as a table, one can calculate only three values per curve and represent each curve by three parameters per temperature.

A nuclear system representing a large power reactor was calculated with shielding factors obtained from the parametric representation based upon [10, f(10)], and [100, f(100)] and then calculated with exact shielding factors. Very good agreement was found, as may be seen in Table 2.

TABLE 2  
 $k_{\text{eff}}$  and Doppler coefficient of the Intercomparison-8<sup>(3)</sup> nuclear system  
calculated with approximated and exact shielding factors

Temp. °K	$k_{\text{eff}}$			Doppler coef x 10 <sup>6</sup>		
	300	900	1500	600	900	1200
Parametric representation	.92244	.91512	.91223	.022125	.010305	.004386
Exact	.92254	.91517	.91228	.022293	.010358	.004383

REFERENCES:

1. Gur, Y., and Yiftah, S., IA-1295, 1974.
2. Gur, Y., and Yiftah, S., Trans. Amer. Nucl. Soc. 19, 391 (1974)
3. Okrent, D., ANL-7120, 1965.

## SELF-SHIELDED GROUP CONSTANTS FOR FAST REACTOR CALCULATIONS<sup>(1)</sup>

Y. Gur, S. Yiftah, M. Segev and L. Gitter

Two identically generated sets of self-shielded 26-group constants were computed by the code system developed here. The infinitely diluted cross sections and scattering matrix were computed by NANICK<sup>(2)</sup> and its modified version NAKED<sup>(4)</sup> from ENDF/B-III<sup>(3)</sup> tapes and the KEDAK<sup>(5)</sup> library, respectively. The shielding factors were generated by NASIF<sup>(6)</sup> from ENDF/B-III tapes and by its modified version NASIFK from the KEDAK file.

The outputs of NANICK and NASIF (ENDF/B-III based data) and of NAKED and NASIFK (KEDAK based data) were combined into two libraries for fast reactor calculations. Elements included in the libraries are H, C, O, Na, Cr, Fe, Ni, <sup>235</sup>U, <sup>238</sup>U, <sup>239</sup>Pu, <sup>240</sup>Pu, <sup>241</sup>Pu and <sup>242</sup>Pu.

Nuclear systems were calculated, and comparative analyses performed<sup>(7-10)</sup>. The differences in the cross sections obtained from different files were studied and a list of cross sections having  $k_{eff}$  sensitive to this difference is given in Table 3, in decreasing order of importance.

TABLE 3

Sensitivity list for  $k_{eff}$  in order of importance

- |                                                              |
|--------------------------------------------------------------|
| 1. Pu-239 fission cross section in the range 1 to 100 keV    |
| 2. U-238 capture cross section in the range 1 to 1000 keV    |
| 3. Pu-239 capture cross section in the range 1 to 100 keV    |
| 4. U-238 inelastic cross section in the range 10 to 1000 keV |
| 5. U-235 fission cross section in the range 50 to 1000 keV   |
| 6. U-238 elastic cross section in the range 10 to 10,000 keV |
| 7. Pu-239 $\bar{\nu}$ in the range 1 to 3000 keV             |
| 8. Fe $\bar{\nu}$ in the range 10 to 10,000 keV              |

A comparison between plutonium and uranium cross sections is given in Table 4.

### REFERENCES:

1. Gur, Y., Yiftah, S., and Segev, M., IA-1291, 1973.
2. Gur, Y., TNSD-R/419, Appendix No. 5.
3. Drake, M.K., (Ed.), BNL-50274, 1970.
4. Gitter, L., and Gur, Y., in: IA-1262, 1972, p. 29.
5. Woll, D., KFK-880, 1968.
6. Gur, Y., and Yiftah, S., IA-1292, 1973.
7. Yiftah, S., Gur, Y., Segev, M., and Gitter, L., in: Nuclear Data in Science and Technology, IAEA, Vienna, 1973, Vol. II, p. 75.
8. Yiftah, S., Gur, Y., Segev, M., and Gitter, L., Trans. Israel Nucl. Soc. 1, 6 (1973)
9. Yiftah, S., Gur, Y., Segev, M., and Gitter, L., in: Proc. of Int. Symp. on Phys. of Fast Reactors, Tokyo, 1973, Vol. 3, p. 1479.
10. Segev, M., Yiftah, S., Gur, Y., and Gitter, L., Nucl. Sci. Eng. 55, 103 (1974)

TABLE 4  
Pu and U cross sections from ENDF/B-III and KEDAK

Group	Lower energy (eV)	Upper energy (eV)	Uranium-235 fission		Uranium-238 capture		Plutonium-239 fission	
			ENDF/B-III	KEDAK	ENDF/B-III	KEDAK	ENDF/B-III	KEDAK
1	6.500E+06	1.050E+07	1.577E+00	1.620E+00	5.898E-03	6.873E-03	2.184E+00	2.069E+00
2	4.000E+06	6.500E+06	1.074E+00	1.187E+00	1.049E-02	1.186E-02	1.699E+00	1.724E+00
3	2.500E+06	4.000E+06	1.207E+00	1.282E+00	2.333E-02	2.672E-02	1.901E+00	1.865E+00
4	1.400E+06	2.500E+06	1.289E+00	1.304E+00	5.791E-02	6.592E-02	2.021E+00	1.956E+00
5	8.000E+05	1.400E+06	1.210E+00	1.219E+00	1.227E-01	1.444E-01	1.745E+00	1.708E+00
6	4.000E+05	8.000E+05	1.164E+00	1.183E+00	1.217E-01	1.335E-01	1.607E+00	1.607E+00
7	2.000E+05	4.000E+05	1.288E+00	1.317E+00	1.265E-01	1.382E-01	1.512E+00	1.495E+00
8	1.000E+05	2.000E+05	1.510E+00	1.525E+00	1.693E-01	1.898E-01	1.542E+00	1.529E+00
9	4.650E+04	1.000E+05	1.849E+00	1.796E+00	2.679E-01	2.855E-01	1.668E+00	1.579E+00
10	2.150E+04	4.650E+04	2.295E+00	2.222E+00	4.913E-01	4.699E-01	1.789E+00	1.688E+00
11	1.000E+04	2.150E+04	3.129E+00	2.787E+00	7.187E-01	7.273E-01	2.125E+00	1.898E+00
12	4.650E+03	1.000E+04	3.913E+00	3.790E+00	9.694E-01	1.036E+00	2.451E+00	2.276E+00
13	2.150E+03	4.650E+03	5.543E+00	5.167E+00	1.297E+00	1.241E+00	3.200E+00	2.886E+00
14	1.000E+03	2.150E+03	7.922E+00	7.436E+00	1.854E+00	2.257E+00	4.954E+00	3.744E+00
15	4.650E+02	1.000E+03	1.199E+01	1.120E+01	3.534E+00	3.710E+00	9.003E+00	7.361E+00
16	2.150E+02	4.650E+02	1.689E+01	1.653E+01	4.486E+00	4.701E+00	1.256E+01	1.249E+01
17	1.000E+02	2.150E+02	2.307E+01	2.022E+01	1.841E+01	1.949E+01	1.875E+01	1.744E+01
18	4.650E+01	1.000E+02	3.304E+01	3.012E+01	1.628E+01	2.169E+01	5.574E+01	5.483E+01
19	2.150E+01	4.650E+01	4.339E+01	4.033E+01	6.426E+01	8.134E+01	1.895E+01	1.836E+01
20	1.000E+01	2.150E+01	5.453E+01	4.810E+01	1.142E+02	1.121E+02	9.180E+01	9.501E+01
21	4.650E+00	1.000E+01	5.502E+01	4.996E+01	1.535E+02	1.749E+02	3.615E+01	3.809E+01
22	2.150E+00	4.650E+00	1.693E+01	1.759E+01	6.845E-01	6.583E-01	1.057E+01	1.100E+01
23	1.000E+00	2.150E+00	3.081E+01	3.383E+01	4.915E-01	4.938E-01	2.213E+01	2.328E+01
24	4.650E-01	1.000E+00	6.234E+01	6.169E+01	5.795E-01	5.880E-01	7.648E+01	8.914E+01
25	2.150E-01	4.650E-01	1.429E+02	1.541E+02	7.834E-01	8.048E-01	1.377E+03	1.515E+03

## PRACTICAL PREPROCESSED NUCLEAR DATA FILES FOR FAST REACTOR CALCULATIONS

Y. Gur and S. Yiftah

Basic nuclear data libraries, such as ENDF/B-III, are used today for the generation of multigroup cross section sets. Since the multigroup sets are determined by calculating the weighted averages of the cross section curves, knowledge of the weighting function within each group is required. In principle, this function is not only dependent on the specific reactor, but is also a function of position in the reactor. With existing codes and methods the weighing function in the Bondarenko type library is not iterated, since each time the weighing function is changed, a code that handles the basic data library and consumes much computer time must be run.

A new method that enables the user to obtain effective, self-shielded multigroup cross section sets averaged over any desired weighting function in a few computer seconds from a preprocessed library, without reference to the basic data library, was developed<sup>(1)</sup>. The preprocessed library is only 2-3 times as large as a Bondarenko type library and may be generated using existing codes.

A family of functions with terms into which any weighting function can be expanded is used. Group averages of each cross section with respect to terms of the family and a set of shielding factors form the preprocessed library. Two families of functions,  $f_n(E)$ , are considered, and two methods are given for the expansion of  $W(E)$  into each series of  $f_n(E)$ . Nuclear parameters obtained via these methods were compared with the same parameters obtained using the exact weighting function (SNEAK flux) to check the methods. Very good agreement was found.

A preprocessed compact library of ENDF/B-III materials is available, upon request, from the authors.

### REFERENCES:

1. Gur, Y., and Yiftah, S., IA-1293, 1974

## COMPARATIVE ANALYSIS OF AMERICAN AND GERMAN NUCLEAR DATA FILES FOR THE CALCULATION OF FAST FISSION REACTORS

S. Yiftah, Y. Gur, M. Segev and L. Gitter

The main sources of nuclear data for fast reactor calculations are the American ENDF/B-III, the German KEDAK, the British UKNDL and the Russian evaluated nuclear data files. Every country uses its own evaluated files and code package to obtain the physics parameters of the designed reactors and the question being

asked is whether these physics parameters would remain the same had another source been used as an input for the calculation.

A code package named NANICK, which handles both ENDF/B-III and KEDAK via the same algorithm generating multigroup-self-shielded neutron cross section sets and calculates physics parameters of nuclear systems, was completed and used to calculate a number of fast nuclear systems and critical experiments in a spherical approximation. These calculations are used as a tool for detecting discrepancies between nuclear data from different files.

It was shown<sup>(1-3)</sup> that ENDF/B-III and KEDAK predict different physics parameters for fast reactors. A perturbation analysis of these discrepancies has led to the identification of significant differences between KEDAK and ENDF/B-III cross sections. These differences are mainly in the fission and capture cross sections of Pu-239, in the capture and inelastic cross sections of U-238, and in the huge Na resonance. Viewing file differences as the reflection of the experimental state of the art, and based on a goal of 1% accuracy in  $k_{\text{eff}}$  prediction, the needed accuracy in cross section measurements was determined.

#### REFERENCES:

1. Yiftah, S., Gur, Y., Segev, M., and Gitter, L., in: Nuclear Data in Science and Technology, LAEA, Vienna, 1973, Vol. II, p. 75.
2. Yiftah, S., Gur, Y., Segev, M., and Gitter, L., in: Trans. Israel Nucl. Soc. p. 8 (1973)
3. Yiftah, S., Gur, Y., Segev, M., and Gitter, L., in: Proc. of Int. Symposium on Physics of Fast Reactors, Tokyo, 1973, Vol. 3, p. 1479.

#### EVALUATION OF NUCLEAR DATA FOR ACTINIDE ISOTOPES

M. Caner and S. Yiftah

A survey was made of isotopes from U to Cm for which a new nuclear data evaluation might be of interest. The factors affecting the choice of a given isotope were:

- a. which isotopes influence fast breeder reactor economics<sup>(1-3)</sup>.
- b. which evaluations are available<sup>(4,5)</sup>, and which isotopes are included in the ENDF/B and UKNDL files<sup>(5)</sup>.
- c. which experimental data are available<sup>(4-13)</sup>. Here we were interested in seeing if there were more recent data than those in the last available evaluation, and if there was enough information to perform optical model and statistical theory calculations.

d. for which isotopes were requests for new nuclear data measurements made by reactor physicists<sup>(14)</sup>. Here, in particular, we examined the new experimental data to see if they satisfied the requests.

In the light of the above considerations an evaluation of the isotopes  $^{238}\text{Pu}$ ,  $^{241}\text{Am}$ , and  $^{244}\text{Cm}$ <sup>(15)</sup> was begun.

$^{238}\text{Pu}$  is an alpha-emitter and is important as a heat source; it has found application in power supplies in space and in heart pacemakers.  $^{241}\text{Am}$  has potential uses as a heat source (through alpha-ray emission), as a gamma-ray source and as a target for  $^{242}\text{Cm}$ .  $^{244}\text{Cm}$  is used as a target material for the production of  $^{252}\text{Cf}$  and as a heat source. The above mentioned isotopes are economically significant, since they reduce the price of reprocessed nuclear fuel.

#### REFERENCES:

1. Ottewitte, E.H., NBS-299, Vol. I, 1968, p. 415.
2. Seelmann-Eggebert, E., Kerntechnik 10, 425 (1971)
3. Seaborg, G.T., et al., in: Peaceful uses of At. Energy, IAEA, Vienna 1972, Vol. 7, p. 487.
4. CINDA 72, Vol. 2, IAEA, Vienna, 1972.
5. Newsletter Bull. CCDN-NW/14, 1972.
6. Lederer, C.M., et al., "Table of Isotopes", 6th ed., John Wiley & Sons, N.Y., 1968.
7. Ellis, Y.A., and Wapstra, A.H., Nuclear Data Sheets B3, B3-2-1 (1969)
8. Ellis, Y.A., Nuclear Data Sheets B4, 543, 581, 635, 683 (1970)
9. Schmorak, M.R., Nuclear Data Sheets B4, 561, 623, 661 (1970)
10. Ellis, Y.A., Nuclear Data Sheets B6, 257 (1971)
11. Artna-Cohen, A., Nuclear Data Sheets B6, 225, 287 (1971)
12. Ellis, Y.A., Nuclear Data Sheets B6, 539, 621 (1971)
13. Artna-Cohen, A., Nuclear Data Sheets B6, 577 (1971)
14. RENDA 72, INDC (SEC)-27/L, IAEA, Vienna, 1972.
15. Caner, M., and Yiftah, S., TNSD-R/430, 1973, Appendix 2.

#### A NEW EVALUATION OF NUCLEAR DATA FOR PLUTONIUM-240, 241, 242<sup>(1)</sup>

M. Caner, S. Yiftah, B. Shatz\* and R. Meyer\*

The isotopic composition of the plutonium produced as a by-product in thermal reactors, which is to serve as fuel for fast reactors, may be typically in the following range: Pu-239, 50-65%; Pu-240, 20-25%; Pu-241, 10-15%; Pu-242, 5-10%. This means that for a typical 1000 MWe fast reactor fueled with about three tons of plutonium, almost half, or 1.5 tons, may consist of higher plutonium isotopes. This emphasizes the importance of having data files which reflect the latest available experimental information and evaluated data for these isotopes. Current data files for Pu-240, Pu-241 and Pu-242 are based on data prior to the following dates: KEDAK, 1967; ENDF/B-III, 1968 for Pu-240, 1970 for Pu-241, 1967 (with resonances revised in 1971) for Pu-242.

---

\* Kernforschungszentrum, Karlsruhe, Federal Republic of Germany

New experimental data are available on resonance parameters and fission cross sections. In addition, there are new measurements of the total and scattering cross sections of Pu-240 in the keV range.

A new evaluation of nuclear data for Pu-240, Pu-241 and Pu-242, based on the new experimental information and nuclear model calculations, has been performed by us<sup>(2-4)</sup>. The numerical data have been incorporated into the new KEDAK file.

In the present work we have reviewed the most significant nuclear data for Pu-240, 241, 242 and compared them with the ENDF/B-III file and with our previous 1967 evaluation forming part of the KEDAK file. Discrepant data and parts of the evaluations based on nuclear model calculations are emphasized.

#### REFERENCES:

1. Caner, M., Yiftah, S., Shatz, B., and Meyer, R., in: Proc. of Int. Symposium on Physics of Fast Reactors, Tokyo, 1973, Vol. 2, p. 683.
2. Caner, M., and Yiftah, S., IA-1243 (1972)
3. Caner, M., and Yiftah, S., IA-1276 (1973)
4. Caner, M., and Yiftah, S., IA-1275 (1973)

#### NASIF: CODES FOR COMPUTING GROUP SHIELDING FACTORS FROM RESONANCE PARAMETERS

Y. Gur and S. Yiftah

Four versions of NASIF, computer codes for calculating group shielding factors from resonance parameters, have been completed.

Version 1 is a fully automatic code for computation from ENDF/B-III tapes<sup>(1)</sup>. This version treats an entire ENDF/B-III tape in one run. It is automatic in the sense that the user is not required to be familiar with the contents of the basic data library. Only the identifying numbers of the isotopes whose shielding factors are to be computed are needed. In this version the integration of the cross section is performed with only three resonances (i.e. the resonance nearest the energy point and one resonance on each side of it) contributing to the computed cross section.

Version 2 differs from version 1 in that the number of "side" resonances is specified by the user (as input data, up to 12 "side" resonances from each side are permitted). If one "side" resonance is requested the results are identical to those of version 1.

Version 3 differs from version 2 in that the central and one "side" resonance contribute to the calculated cross section in the integration, while the contribution of the wings of 11 "side" resonances from each side is collapsed

into a parabola. This version yields results identical to those of version 2 with 12 "side" resonances, yet is as quick as version 1 in computing group shielding factors<sup>(2)</sup>.

Version 4 computes shielding factors from KEDAK resonance parameters.

Versions 2, 3 and 4 read basic data from cards either punched from ENDF/B-III tapes or prepared from KEDAK data in the ENDF/B-III format.

Table 5 shows result obtained by the three ENDF/B-III versions.

TABLE 5

<sup>239</sup>Pu fission self-shielding factors in two groups in the range of resolved resonances, at 300°K, and for a background of 10 b

Group	Energy range (eV)	Number of side resonances (Version 2)						Version 3
		1	2	3	4	9	12	
1	100-215	0.367	0.380	0.391	0.397	0.404	0.406	0.406
2	46.5-100	0.232	0.243	0.248	0.252	0.259	0.260	0.260
Time on IBM/370 (sec)		10	13	16.5	20	34.2	44.5	10

REFERENCES:

1. Gur, Y. and Yiftah, S., IA-1292, 1973.
2. Gur, Y. and Segev, M., Trans. Amer. Nucl. Soc. 19, 173 (1974)

THE HASHOV CODE

A.D. Krumbein

A program, HASHOV, was written in FORTRAN IV for use on the 370/165 IBM computer. It combines the Hansen exponential transformation method<sup>(1)</sup> for the solution of the space-time dependent diffusion equation in one space dimension, with certain advantageous features of the SHOAV<sup>(2)</sup> code. These include the capability of calculating cross section mixing and shielding factors, temperature feedback and several forms of reactivity insertion. Steady-state xenon and xenon feedback routines have also been included.

The code has been successfully checked against the results of prompt excursion problems originally analyzed by Yasinsky and Henry<sup>(3)</sup>.

REFERENCES:

1. Andrews II, J.B. and Hansen, K.F., Nucl. Sci. Eng. 31, 304 (1968)
2. Saphier, D. and Yiftah, S., IA-1217 (1971)
3. Yasinsky, J.B. and Henry, A.F., Nucl. Sci. Eng., 22, 171 (1965)

THE ROLE OF DISCRETE RESIDUAL LEVELS IN EVAPORATIVE DE-EXCITATION OF COMPOUND NUCLEI\*

L. Segal and J. Gilat

In statistical model calculations particle evaporation from excited nuclei is usually represented by:

$$R_{\mu}(E_c, J; E_f, j, s) = \frac{1}{h} \frac{\rho(E_f, j)}{\rho(E_c, J)} \sum_{S=|j-s|}^{j+s} \sum_{\ell=|J-S|}^{J+S} T_{\mu\ell}(\epsilon)$$

where  $R_{\mu}(E_c, J; E_f, j, s)$  is the rate of emission of particle  $\mu$  (of spin  $s$ ) from a nucleus with an excitation energy  $E_c$  and angular momentum  $J$  to form a residual nucleus with an excitation energy  $E_f$  and angular momentum  $j$ ;  $\rho(E_c, J)$  and  $\rho(E_f, j)$  are respectively the level densities of the initial and residual nuclei;  $h$  is Planck's constant and  $T_{\mu\ell}(\epsilon)$  is the transmission coefficient for the inverse process, i.e. the reaction of particle  $\mu$  with an orbital angular momentum  $\ell$  and energy  $\epsilon$  ( $\epsilon = E_c - E_f - B$ ;  $B$  is the binding energy of particle  $\mu$  in the initial nucleus) on the residual nucleus.

In most calculations this form is assumed to be valid even at low excitation energies (or near yrast), where the levels of the residual nucleus can no longer be described by a smooth level density function  $\rho(E_f, j)$ . For a more realistic description of the excited nucleus one should use individual discrete levels, the spacing of which decreases with increasing excitation energy until they merge smoothly into a continuous level density function.

Such a model was incorporated into the spin dependent evaporation code GROGI 2<sup>(1)</sup>. The resulting new code (named GGL) was then applied to the calculation of cross sections and particle spectra for the reactions  $^{62}\text{Ni}(p, p')^{62}\text{Ni}$ ,  $^{62}\text{Ni}(p, \alpha)^{59}\text{Co}$ ,  $^{59}\text{Co}(\alpha, \alpha')^{59}\text{Co}$  and  $^{59}\text{Co}(\alpha, p)^{62}\text{Ni}$ , at 18.06 MeV excitation energy of the  $^{63}\text{Cu}$  compound nucleus. Results of the calculations were compared with experimental data, recently obtained by Miller and Jaffe. Good agreement between theory and experiment was achieved for very reasonable choices of input parameters. Miller and Jaffe<sup>(2)</sup> proposed (partial)

---

\*Based on the thesis submitted by L. Segal to Bar Ilan University in partial fulfillment of the requirements for an M.Sc. degree in chemistry.

conservation of isospin in these reactions, to explain some discrepancies between their measurements and conventional spin dependent statistical calculations. When we analyze the data with our improved and more realistic model, we find no evidence for such isospin conservation.

REFERENCES:

1. Gilat, J., USAEC Report BNL-50246 (T-580), 1970.
2. Jaffe, G.M., COO-3122-3, 1, 1972.

HIGH PRECISION STUDIES ON THE LEVEL SCHEME OF  $^{80}\text{Se}$  BY THE RESONANT-SCATTERING METHOD<sup>(1)</sup>

H. Szichman

The energies and reduced strengths of the  $\gamma$ -rays following deexcitation of the 7818.9 keV highly excited level in  $^{80}\text{Se}$  reached by the  $(\gamma, \gamma')$  reaction were measured using a nickel capture  $\gamma$  source. The level scheme deduced for this nucleus was given. Measurements of the angular distributions of the scattered radiation permitted the assignment of spin values for most of the low-lying levels in this nucleus. Parity determinations were made comparing the reduced strengths with the statistics of known E1 and M1 transitions.

REFERENCE:

1. Szichman, H., Phys. Rev. C 8, 1429 (1973)

E1, M1, E2 AND M2 WIDTHS OF TRANSITIONS FROM BOUND LEVELS EXCITED BY THE  $(\gamma, \gamma')$  REACTIONS<sup>(1)</sup>

R. Moreh, A. Wolf, O. Shaha1, and J. Tenenbaum

A comparison was made between the E1 and M1 transition strengths from bound levels populated by the  $(\gamma, \gamma')$  reaction with the same data from unbound levels obtained via the  $(n, \gamma)$  reaction. It was shown that there is a clear increase in the M1 strength nuclei near closed shells. The E2/M1 ratios were found to be of about the same magnitude as the Weisskopf estimate, while the M2/E1 ratios were enhanced by a factor of  $10^3$ .

REFERENCE:

1. Moreh, H., Wolf, A., Shaha1, O., and Tenenbaum, J., in: Int. Conf. on Photonuclear Reactions and Applications, CONF-730301-P1, 1973, p. 293.

COMMENT ON M2-E1 MIXING OBSERVED IN  $(\gamma, \gamma')$  REACTIONS<sup>(1)</sup>

R. Moreh, A. Wolf and O. Shaha1

It was shown that the effect of overlapping resonances in the photo-excitation process of a  $(\gamma, \gamma')$  reaction is very small. The influence of this effect on the angular distributions of the inelastic transitions and hence on the M2/E1 mixing ratios was found to be negligible.

REFERENCE:

1. Moreh, R., Wolf, A., and Shaha1, O., Phys. Rev. C 8, 401 (1973)

TOTAL RADIATIVE WIDTH OF BOUND NUCLEAR LEVELS EXCITED BY THE  $(\gamma, \gamma')$  REACTION<sup>(1)</sup>

R. Moreh, A. Wolf, O. Shaha1 and J. Tenenbaum

The total radiative widths of bound nuclear levels, at an excitation energy around 7 MeV, as a function of  $A$  were presented. These widths were measured by employing self-absorption, temperature variation of the scattering cross section and absolute cross section measurements. By comparing the present results with the widths of unbound levels from  $(n, \gamma)$  work, it was shown that the radiative widths are continuous across the  $(\gamma, n)$  threshold for these nuclei.

REFERENCE:

1. Moreh, R., Wolf, A., Shaha1, O., and Tenenbaum, J., in: Int. Conf. on Photonuclear Reactions and Applications, CONF-730301-P1, 1973, p.295.

ELASTIC AND RAMAN SCATTERING OF PHOTONS FROM  $^{238}\text{U}$  (1)

T. Bar-Noy and R. Moreh

The results of measuring the elastic and Raman scattering cross sections for 7 discrete photo energies between 7.9 and 11.4 MeV were given. It was shown that by making slight changes in the parameters of the dipole resonance of  $^{238}\text{U}$ , the measured scattering of the cross sections are found to be in fair agreement with predictions of the simple rotator model.

REFERENCE:

1. Bar-Noy, T., and Moreh, R., in: Int. Conf. on Photonuclear Reactions and Applications, CONF-730301-P1, 1973, p 319.

DELBRUCK SCATTERING OF 7.9 MeV PHOTONS<sup>(1)</sup>

R. Moreh and S. Kahane

The elastic scattering cross section of 7.9 MeV photons by U and Th was measured in the angular range  $25^\circ - 140^\circ$ . It was shown that at this energy the forward elastic scattering is due almost entirely to Delbruck

scattering. The results are systematically lower by >50% than the calculated values. Good agreement with theory was obtained only after excluding the contribution of the real part of the Delbruck scattering amplitude.

REFERENCE:

1. Moreh, R., and Kahane, S., Phys. Lett. 47B, 351 (1973)

AN AUTOMATIC COMPTON POLARIMETER FOR GAMMA ENERGIES IN THE RANGE 5-10 MeV<sup>(1)</sup>

B. Arad and H. Szichman

A linear polarization analyzer based on a NaI Compton polarimeter and mini-computer was developed. Its use in photonuclear experiments and its reliability and advantages as compared with similar polarimeters were considered. Polarization measurements of the ground state transition from the 8.496 MeV level in <sup>90</sup>Zr show that the transition is M1, indicating a positive parity for this level.

REFERENCE:

1. Arad, B., and Szichman, H., Nucl. Instrum. Meth. 117, 355 (1974)

GAMMA DOSIMETER BASED ON USE OF A NE226 SCINTILLATOR

B. Divon, S. Eckhouse and M. Etzion

A gamma-radiation detector based on the use of a 2"x3" NE226 scintillator and a 56 AVP photomultiplier was tested as a dosimeter for relatively low  $\gamma$  dose rates in the presence of fast neutrons. The light output of the NE226 scintillator, as obtained for <sup>60</sup>Co gamma rays, was measured to be about 30% of that of the NE102A scintillator having similar dimensions and light collection efficiency. The sensitivity of the detector was also measured as a function of the  $\gamma$ -ray energy. Relative sensitivities to gamma rays from <sup>60</sup>Co, <sup>137</sup>Cs, <sup>22</sup>Na and the <sup>19</sup>F(p,  $\alpha$ )<sup>16</sup>O reaction were found to be equal to the relative calculated energy absorption coefficients, within experimental error. As an example, the relative measured sensitivity of the NE226 scintillator to 1.25 MeV  $\gamma$ -rays from <sup>60</sup>Co and 6.5 MeV  $\gamma$ -rays from <sup>19</sup>F(p,  $\alpha$ )<sup>16</sup>O is 1.77, as compared with 1.71 for the NE102A scintillator. The sensitivity to 14 MeV neutrons from the (D,T) reaction was also measured, and it was found that the relative sensitivity of the NE226 and NE102A scintillators is about 0.1. It was concluded that the relative sensitivity to 1.25 MeV  $\gamma$ -rays and 14 MeV neutrons of the NE226 dosimeter is about 1.5 : 1.

A WATER CERENKOV DETECTOR FOR THE DETECTION OF GAMMA RADIATION IN THE PRESENCE OF FAST NEUTRONS

S. Eckhouse, B. Divon and M. Shaanan

A water Cerenkov detector was evaluated as a gamma radiation detector having a low relative sensitivity to fast neutrons. Water was chosen as the medium due to its good transmission in the UV range. The photon production per unit volume and unit  $\gamma$  flux at energy E, in a wavelength range  $\lambda_1$  and  $\lambda_2$  is:

$$(1) \quad N(E) = A \left[ \frac{1}{\lambda_1} - \frac{1}{\lambda_2} \right] \int_{T_{th}}^{T_{max}(E)} \frac{d_e \sigma(E, T)}{dT} I(\beta(T)) dT$$

where  $\frac{d_e \sigma(E, T)}{dT}$  is the Compton differential cross section for electron production at energy T. T varies between the Cerenkov threshold and the Compton edge, and A is a constant.  $I(\beta(T))$  is defined by:

$$(2) \quad I(\beta(T)) = \int_{\beta_{th}}^{\beta(T)} \left( 1 - \frac{1}{n^2 \beta^2} \right) \frac{\beta^3}{(1-\beta^2)^{3/2}} \left( \frac{dE}{dx} \right)^{-1} d\beta$$

where  $\beta_{th}$  is the value of  $\frac{v}{c}$  at the Cerenkov threshold, n is the index of refraction, and  $\frac{dE}{dx}$  is the stopping power of electrons in water.

Figure 1 illustrates the calculated results in the interval  $2000\text{\AA} < \lambda < 7000\text{\AA}$ . These results were verified experimentally by measuring the relative sensitivities at known gamma energies. The detector was constructed of a 2" diam by 6" high cylindrical container viewed by a 56 UVP photo-multiplier. The sources used were  $^{60}\text{Co}$ ,  $^{24}\text{Na}$  and the  $\text{F}^{16}(\text{p}, \alpha)\text{O}^{16}$  reaction at 3 MeV proton energy. The proton source was the Van de Graaff accelerator located at the Weizmann Institute. The measured relative sensitivities are summarized in Table 1.

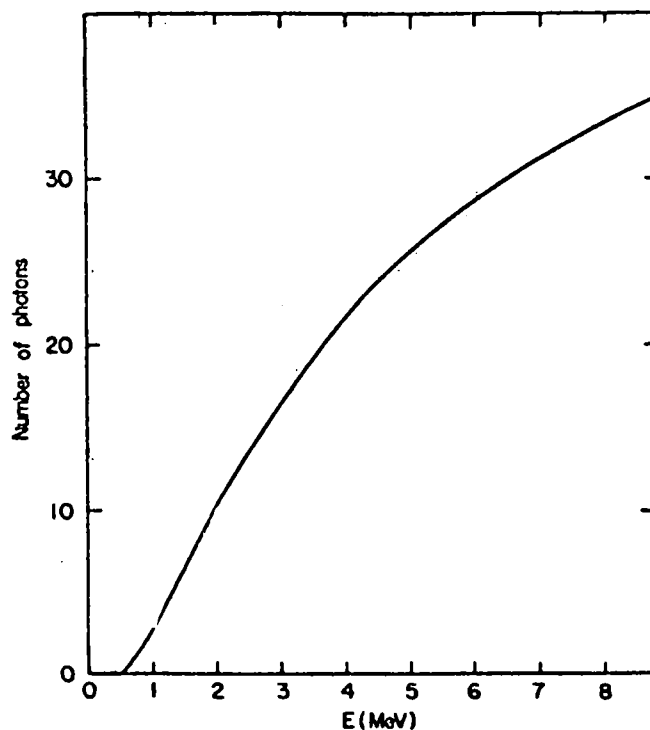


Fig. 1

The number of photons in the wavelength interval  $2000 \text{ \AA} \leq \lambda \leq 7000 \text{ \AA}$  produced by a flux of  $1 \gamma/\text{cm}^2$  in  $1 \text{ cm}^3$  of water as a function of gamma energy

TABLE 1

Relative measured and calculated sensitivities

Source	Energies (MeV)	Sensitivity per unit disintegration	
		measured	calculated
$^{60}\text{Co}$	1.17 1.33	1	1
$^{24}\text{Na}$	1.37 2.75	2.38	2.26
$^{16}\text{F}(p,\alpha)^{16}\text{O}$	6 7	5.8	5.46

The sensitivity of the detector to neutrons was calculated taking into account the production of  $\gamma$ -rays by neutrons through reactions on  $^{16}\text{O}$ . This sensitivity to 14 MeV neutrons was also measured using the (D,T) reaction and found to be less by a factor of  $\sim 1.5$  than the sensitivity to 1.25 MeV  $\gamma$ -rays from  $^{60}\text{Co}$  whereas the calculated sensitivity differs by a factor of  $\sim 4$ . This discrepancy seems to be due to the reaction  $^{16}\text{O}(n,p)^{16}\text{N}$ , where the  $^{16}\text{N}$  decays by  $\beta^-$  emission.

A SYSTEMATIC ODD-EVEN EFFECT IN THE INDEPENDENT YIELD DISTRIBUTIONS OF NUCLIDES FROM THERMAL NEUTRON FISSION OF  $^{235}\text{U}$  (1)

S. Amiel and H. Feldstein

A detailed analysis of experimental fission yield data was found to exhibit a systematically consistent odd-even effect in the independent yield distributions of the nuclides in thermal neutron fission of  $^{235}\text{U}$ . The odd-even effect in the element yield distribution for elements at the fission peaks appears as a sawtooth structure, in which the amplitudes between the enhanced even-Z yields and the less favored odd-Z yields are  $\pm 22\%$  of the mean values. The elements examined constitute 75% of the fission yield.

The distribution of the isotopic yields in many cases was found to have a sawtooth pattern superimposed on a gaussian-like shape, where the amplitudes between the high even-N and low odd-N values are on the average  $\pm 8\%$  of the mean values. This effect seemed to be unresolved at the light peak nuclides while it was pronounced at the heavy peak nuclides.

The isobaric dispersions were studied in 24 mass chains (14 at the heavy mass peak and 10 at the light peak) and were found to follow the general pattern of a gaussian with widths varying between 0.45 and 0.8 charge units. The detailed description of the isobaric dispersion is represented by a sawtooth structure fluctuating with amplitudes of  $\leq 30\%$  around a constant width gaussian in which the even Z nuclides are consistently enhanced. The only appearance of a significant closed shell effect is observed in  $^{134}\text{Te}$ .

The fact that the neutron pairing effect in the yields as compared with that of the protons is much smaller is attributed to the evaporation of neutrons during the de-excitation of the fragments, a process which is responsible for "washing out" of part of the original neutron pairing effect in the primary fragment formation in fission.

The experimental and "normal" (i.e., calculated by Wahl) independent yields of the elements formed in fission are presented in Table 2.

TABLE 2  
Independent yields of complementary elements (Z, 92-Z)  
in thermal neutron fission of <sup>235</sup>U

Elements	Exp. yield, %	"Normal" yield, %	$\frac{(\text{Exp. yield} - \text{"Normal" yield})}{\text{"Normal" yield}} \times 100^*$
As-Pr	1.2±0.1	1.4	-(14.3±7.1)
Se-Ce	4.3±0.3	3.6	+(19.4±8.3)
Br-La	5.9±0.4	7.6	-(22.4±5.3)
Kr-Ba	15.2±0.3	12.7	+(20.0±2.4)
Rb-Cs	11.7±0.5	15.1	-(22.5±3.3)
Sr-Xe	19.8±1.0	16.0	+(23.7±6.2)
Y-I	11.9±1.0	15.8	-(24.7±6.4)
Zr-Te	18.2±0.6	14.7	+(23.8±4.1)
Nb-Sb		9.1	
Mo-Sn		2.9	
	$\Sigma=88.2\pm1.4$		

\*Average deviation from normal distribution ±(22.0±5.4)%

The present set of experimental data indicates the relative importance of the individual properties of the fragments versus the collective behavior of the fissioning nucleus, as described by the calculations of deformations of shell-corrected liquid drop potential energy surfaces. One is also led to conclude that nucleon transfer, apparent from the different charge densities of the fragments, takes place before scission and that at scission there is a smaller probability of breaking pair configurations, consistent with energy considerations.

REFERENCE:

1. Amiel, S., and Feldstein, H., 3rd Symposium on Physics and Chemistry of Fission, Rochester, N.Y., August 1973. Vienna IAEA, 1974, Vol. 2, p 65-94, IAEA/SM-174/25.

### STATUS OF DELAYED NEUTRON DATA<sup>(1)</sup>

S. Amiel and T. Izak-Biran

The available delayed neutron data were reviewed. Since a few of the  $P_n$  values were measured directly, we attempted to calculate  $P_n$  values on the basis of experimentally measured delayed neutron yields and the recently determined fission yields<sup>(2)</sup>. The contribution of the individual precursors to delayed neutron groups and total delayed neutron emission in thermal fission of  $^{235}\text{U}$  was compared with experimental measurements. The fit seems satisfactory, but to obtain better accuracy the  $P_n$  values will be recalculated based on newer values of thermal and fast fission yields for  $^{235}\text{U}$  and  $^{233}\text{U}$  to be determined shortly.

#### REFERENCES:

1. Amiel, S., and Izak-Biran, T., IAEA Panel on Fission Product Nuclear Data, Bologna, 1973.
2. Amiel, S., and Feldstein, H., 3rd Symposium on Phys. and Chem. of Fission, Rochester, N.Y., August 1973. Vienna IAEA, 1974, Vol.2, p 65-94, IAEA/SM-174/25.

### ON THE DETERMINATION OF FRACTIONAL FISSION YIELDS FROM THE CHEMICAL REACTION YIELDS IN THE GAS PHASE<sup>(1)</sup>

Z.B. Alfassi\* and S. Amiel

The determination of fractional fission yields from the measured chemical yields of gaseous phase reaction products of fission fragments was studied in view of the kinetic theory of reactions of hot atoms. In order to have a linear dependence of the hot reactions yields on the reactant concentration it is suggested that reactants and moderators be used. These have a similar effect on the decrease of the energy of the hot atom ( $\alpha_r = \alpha_m$ ). For halogen atoms, it is suggested that methane be used as a reactant and not methyl halide.

#### REFERENCE:

1. Alfassi, Z.B., and Amiel, S., Inorg. Nucl. Chem., in press.

### ON-LINE STUDY OF GASEOUS FISSION PRODUCTS: RAPID TRANSFER TECHNIQUES<sup>(1)</sup>

H. Feldstein and S. Amiel

The time required for a mass separated fission product to reach the collector may be considered to be composed of the time required to leave the fission source (by diffusion, emanation or recoil), the transfer time, and the

---

\* Ben-Gurion University of the Negev, Beer-Sheva

mean residence time in the ion source. Since it is difficult to analyze each of these components separately, a number of transfer functions were derived for different configurations of target, transmission line and ion source, at different gas flow conditions, and the contribution of each stage to the overall delay was evaluated.

An adequate knowledge of the transfer time function is required for independent fission yield determinations in on-line mass separation studies, since the apparent yield of the separated fission product counted at the collector must be corrected for the decay occurring during the transfer from the irradiated target (especially in the case of short-lived isotopes) and for the decay of precursors in the target during irradiation and transfer.

REFERENCE:

1. Feldstein, H., and Amiel, S., in: Proc. of the 8th International EMIS Conference on Low Energy Accelerators and Mass Separators, Skovde, Sweden, June 1973, p.420.

A VERSATILE INTEGRATED TARGET-SURFACE IONIZATION SOURCE FOR ON-LINE ISOTOPE SEPARATIONS<sup>(1)</sup>

S. Amiel, Y. Nir-EI, M. Shmid, A. Venezia and I. Wismontsky

An integrated target-ion source designed to function both for negative and positive surface ionization was constructed. A large area target consisting of graphite foils coated with uranium is placed inside an heated chamber and exposed to a thermal neutron beam. The fission products diffuse out of the target chamber and pass through an heated tantalum guide tube, where they undergo ionization and are extracted into the mass separator (SOLIS). In the case of negative surface ionization, where halogens are separated, the intense electron emission is deflected by a small magnet placed near the exit of the ionization tube. The temperatures of the target and ionization chamber are controlled separately to optimize speed of separation, selectivity and ionization efficiencies. Diffusion time, efficiency and specificity as functions of the temperatures and dimensions were studied.

Collection and decay of activities were obtained for masses 92, 142 with positive surface ionization, and for masses 136-138 with negative surface ionization. The experimental surface ionization efficiencies were found in general agreement within a factor of 10 with the predicted values (e.g. 0.03% for I at  $\sim 1400^{\circ}\text{C}$  and  $>1\%$  for Rb).

both the values of the wave function and the normal component of the gradient of the wave function on the absorbing sphere. The solution to both boundary value problems separately is presented. The reflection from the absorbing sphere is treated and new formulae are derived. The differential and total cross sections of the described models are analyzed.

#### Zeros of the Scattering Amplitude in the Complex Angle Plane

A. Gersten

Nuclear Physics, A219, 317 (1974).

The possibility of reconstructing the scattering amplitude with the aid of the zeros in the complex  $\cos \theta$  plane of the differential cross section is considered. The reconstruction process is demonstrated in two examples. The location of the zeros of the scattering amplitude is examined for the strong absorption and optical models. It appears that there exists a correlation between the position of the zeros and the strength of the absorption.

#### Matrix Padé Approximants of the Nucleon-Nucleon Interaction

A. Gersten and Z. Solow

Phys. Rev., D10, 1031 (1974).

The matrix Padé approximants (with  $16 \times 16$  matrices) and the scalar Padé approximants (with  $4 \times 4$  matrices) of the nucleon-nucleon S-matrix elements are calculated for total angular momentum  $J \leq 4$  and for laboratory kinetic energy up to 425 MeV. The calculations are based on one- and two-pion exchanges of the pseudoscalar interaction. The coupling constant  $g$  is the only parameter of the interaction for which a value, consistent with experimental results  $g/4\pi = 15$  is assumed. A simplified calculational scheme and formalism are presented. In order to interpret the results properly we give estimates of which energy regions we expect the one- and two-pion exchanges to be significant. For these energy regions we found that the matrix Padé approximants

describe quite well the nucleon-nucleon interaction and give better approximation to the experimental data as compared to other methods of unitarization. The fact that in the framework of quantum field theory it is possible, even in limited energy regions, to give a reasonable description of the nucleon-nucleon scattering, give us more confidence in the pseudoscalar interaction as the fundamental interaction of nucleons and pions.

#### Regions of the Two-Nucleon Force

A. Gersten

Phys. Rev., C10, 1640 (1974).

Using an approximate Bethe-Salpeter equation approximate values were obtained for the partial wave contributions of the two and three pion exchange ladder diagrams. With these results the region hypothesis of the two-nucleon force was tested for this model. No definite region structure was observed for the S and part of the P and D waves ( $^3P_0$ ,  $^3P_1$ ,  $^3P_2$ ,  $^3D_1$ ,  $^3D_3$ ). A definite region structure was observed for other waves, but it was impossible to locate common (to all partial waves) radii for the outer and intermediate regions of this model of the two-nucleon interaction.

#### Einstein's Equivalence Principle. An Explicit Statement and its Derivation from Special Relativistic Presymmetry

Y. Avishai and H. Ekstein\*

Comm. of Math. Phys., 37, 193 (1974).

We propose a statement of the observable implications of the equivalence principle that is precise and general rather than allusive and illustrative. This statement is derived from previously formulated principles of special relativistic presymmetry. The substantial identity of our result with Einstein's curved-space formulation is exhibited.

\*Argonne National Laboratory.

### The Angular Dependence of a Broad Peripheral Resonance State

R.C. Fuller\* and Y. Avishai

Nuclear Physics, A222, 365 (1974).

We discuss the angular dependence of the shape-elastic resonance wave function for a state so broad decay occurs before the ions orbit the interaction region. In the shadow of the interaction region the nonstationary angular dependence is described by a Legendre function for complex angular momentum  $P_{\alpha}(\cos\theta)$ . In the lit region the same state has the angular dependence  $e^{-i\pi\alpha}P_{\alpha}(-\cos\theta)$ . After presenting theoretical arguments which show the necessity of using these different analytic continuations in the shadow and lit regions to states of complex angular momentum, we show, by way of illustration of the theoretical argument, results for a strong absorption model introduced several years ago by Austern.

\*University of Heidelberg.

### Test of the Validity of the Adiabatic Approximation in Scattering Theory

Y. Avishai and A.S. Rinat\*

Physics Letters B (in press).

Exact solutions for the scattering of a fast projectile  $x$  on deuterium are compared with various versions of the fixed scatterers approximation. The content of the approximations for a nucleon and a different projectile is discussed. The calculations show the approximate agreement of angular distributions in forward direction and the amount of disagreement in the backward hemisphere. In the case of nucleon scattering the importance of nucleon exchange, neglected in the FSA, is explicitly demonstrated. As expected, the quality of the tested approximations rapidly improves with diminishing mass ratio  $M_X/M_N$ .

\*Weizmann Institute of Science.

**Solution of the Three Body Problem with Inverse Square Potentials**

Y. Avishai

Jour. Mathematical Physics (in press).

The three body problem with two body inverse cube forces is solved by separation of the variables into an angular and a radial one. The angular equation is an integrodifferential one, which can be solved by splines, while the radial one is Bessel's.

**A Model of Black Nucleus**

Y. Avishai

Contributed paper, International Conference on Heavy Ion Scattering, Heidelberg.

A model of strongly absorptive nucleus based on geometrical optics is presented. The angular distribution at large angles is similar to that of the optical model. Unitarity is preserved, but the partial wave S matrix is finite for small angular momenta.

Simultaneous Heating and Temperature Measurements by an Infrared Laser Beam

Y.J. Kaufman\* and A. Gersten

Applied Optics (in press, 1975).

A method of simultaneous heating and temperature measuring by means of an ir CO<sub>2</sub> laser is proposed and tested. The proposed method is relatively simple and direct. In this experiment the temperature on the beam axis is a function of the beam intensity, the beam radius and the absorber mixture is measured. A good agreement is obtained between the experimental results and theoretical predictions based on the level scheme and the physical characteristics of the absorber. The temperature measurement proposed in the present paper is an additional experimental tool in investigating excitation processes in the ir region.

\*Technion - Israel Institute of Technology.

The Relativistic Pseudopotential Equation for Multichannel Baryon-Baryon Scattering

A. Gersten, P.A. Verhoeven\* and J.J. de Swart\*

Nuovo Cimento (in press 1975).

The approximation to the Bethe-Salpeter equation of Blankenbecler and Sugar and Logunov and Tavkhelidze is applied to the multichannel spin -  $\frac{1}{2}$  baryon-baryon interactions. Formulas for the one-boson-exchange potentials are given. It is discussed how to use the formalism when some or all channels are closed.

\*Institute for Theoretical Physics, University of Nijmegen, Nijmegen, The Netherlands.

### Kinematic Perturbation in the Three Body Problem

Y. Avishai

Phys. Rev. (in press 1975).

The mixed derivatives that appear in the three body Schrödinger equation (when written in terms of interparticle distances) are treated as a perturbation. The following results are obtained:

- a)  $B_3 \geq 3B_2$ , where  $B_n$  is the  $n$  body binding energy.
- b) For harmonic oscillator potential the calculated binding energy falls within 3% of the exact one.

Numerical results for attractive square well and exponential potentials are presented.

### Nuclear Physics and Spectroscopy

#### Study of the Energy Levels of $^{62}\text{Ni}$ Using the $(\gamma, \gamma')$ Reaction

R. Moreh, A. Wolf<sup>+</sup>, I. Jacob<sup>+</sup> and A. Nof<sup>+</sup>

Nucl. Phys., A224, 86 (1974).

Elastic and inelastic scattering of monochromatic photons were used for studying nuclear energy levels in  $^{62}\text{Ni}$ ; the photons were produced by thermal neutron capture in iron. The energy of the resonance level in  $^{62}\text{Ni}$  was 7646 keV. The angular distributions of the elastic and two inelastic lines were measured and the corresponding level spins determined. The parity of the resonance level was found to be odd using polarization measurements.

<sup>+</sup> Nuclear Research Center, Negev.

## Study of Nuclear Levels of $^{139}\text{La}$ in the 7.28 MeV Region Using a New Gamma Monochromator

I. Jacob<sup>†</sup>, R. Moreh and A. Wolf<sup>†</sup>

Int. Symp. on Neutron Capture Gamma Ray Spectroscopy, Petten, p. 177 (1974).

A lead target which resonantly scatters the 7.279-MeV line of neutron capture  $\gamma$  rays of iron was used as a source of variable energy  $\gamma$  radiation. Variation of the angle of the resonantly scattered beam between  $60^\circ$  and  $120^\circ$  permits an energy variation,  $\Delta E = 275$  eV, below the resonant energy. In  $^{139}\text{La}$ , a transmission experiment using a  $^{139}\text{La}$  absorber have yielded 3 dips in the above angular range. The values of  $g\Gamma_0$  of these levels, and the nuclear level spacing in  $^{139}\text{La}$  are deduced.

<sup>†</sup>Nuclear Research Center, Negev.

## Nuclear Photoexcitation

R. Moreh

Review talk presented to the International Symp. on Neutron Capture  $\gamma$ -Ray Spectroscopy, Petten, Holland (1974).

The various methods of nuclear photoexcitation using neutron capture gamma rays are reviewed. In particular, the photoexcitation of nuclear levels in the continuum region and the study of Delbruck scattering and nuclear Raman scattering are discussed. In addition, the photoexcitation by the method of random overlap and also by varying the photon energy either by nuclear scattering or by Compton scattering are illustrated in detail.

### Study of the Temperature Effect of Resonantly Scattered Capture $\gamma$ Rays

R. Moreh, O. Shahal<sup>†</sup> and I. Jacob<sup>†</sup>

Nucl. Phys., A228, 77 (1974).

The temperature effect of resonantly scattered capture  $\gamma$  rays was studied critically in the temperature range 4.2°K - 520°K in  $^{208}\text{Pb}$  and in the range 4.2°K - 670°K in  $^{62}\text{Ni}$ . The gamma source was produced by thermal neutron capture in iron; the energy of the  $\gamma$ -line scattered by  $^{208}\text{Pb}$  is 7.279 MeV and by  $^{62}\text{Ni}$  is 7.646 MeV. The observed variation with temperature of the scattered intensity from Ni was found to be in good agreement with Lamb theory using a single Debye temperature,  $\theta_D = 420^\circ\text{K}$ , throughout the whole temperature range. In the case of Pb, the agreement with Lamb theory using  $\theta_D = 104^\circ\text{K}$  was not as good, and a deviation from theory was observed in the temperature range 30° - 70°K; this deviation is discussed.

<sup>†</sup>Nuclear Research Center, Negev.

### Photoexcitation of the Giant Dipole Resonance in $^{181}\text{Ta}$ and $^{237}\text{Np}$

T. Bar-Noy<sup>†</sup> and R. Moreh

Int. Symp. on Neutron Capture Gamma Ray Spectroscopy, Petten, p. 181 (1974).

The elastic and inelastic (Raman) photon scattering from  $^{181}\text{Ta}$  and  $^{237}\text{Np}$  for energies between 8.5 and 11.4 MeV are measured. At 11.4 MeV, the results agree well with predictions of the simple rotator model (SRM) and the dynamical collective model (DCM) of the giant dipole resonance (GDR). At lower energies, the theoretical cross sections are obscured by the relatively large contribution of Delbruck scattering where the real amplitudes are not known accurately.

<sup>†</sup>Nuclear Research Center, Negev.

Study of the Giant Dipole Resonance of  $^{232}\text{Th}$  and  $^{238}\text{U}$  Using Elastic and Raman Photon Scattering

T. Bar-Noy<sup>+</sup> and R. Moreh

Nuclear Physics, A229, 417 (1974).

Differential cross sections for elastic and Raman scattering of photons from  $^{232}\text{Th}$  and  $^{238}\text{U}$  targets were measured. Eight photon energies in the range 7.9 - 11.4 MeV were used and were obtained from thermal neutron capture in Fe, Cr, Cu and Ni. Angular distribution of the elastic and Raman scattered radiation from  $^{232}\text{Th}$  was measured. The results are compared with calculations of the simple rotator model and the dynamical collective model of the giant dipole resonance after incorporating the effect of Delbruck scattering.

<sup>+</sup>Nuclear Research Center, Negev.

Study of the  $^{65}\text{Cu}$  Energy Levels Using the  $(\gamma, \gamma')$  Reaction

R. Moreh, O. Shahal<sup>+</sup> and J. Tenenbaum<sup>+</sup>

Int. Symp. on Neutron Capture Gamma Ray Spectroscopy, Petten, p. 173 (1974).

Elastic and inelastic resonance scattering of photons was used for studying the energy levels of  $^{65}\text{Cu}$ . The  $\gamma$  source was obtained from thermal neutron capture in Cr. The spins of the resonance levels at 8484- and 7939-keV were found to be 1/2 and 5/2 respectively. The partial and total radiative widths of the 8484-keV level were measured and found to be  $\Gamma = (0.33 \pm 0.03)\text{eV}$ ,  $\Gamma_0/\Gamma = 0.90 \pm 0.05$ .

<sup>+</sup>Nuclear Research Center, Negev.

Nuclear Radiation and Physics

An Analytic Expression for the Gamma Ray Self Absorption in the Perpendicular Axes Configuration

Y.S. Horowitz, S. Mordechai and A. Dubi

Nuclear Instruments and Methods 124, 313 (1975).

An analytic expression for the self absorption of gamma rays emitted from a point source on the face of a cylindrical absorber is constructed. The symmetry axis of the absorber makes an angle of  $90^\circ$  with the symmetry axis of the detector.

Photoneutron Reactions in  $^{18}\text{O}$

Y.S. Horowitz, J.D. Allan<sup>†</sup>, J.W. Jury<sup>†</sup>, R.G. Johnson\*, K.G. McNeill\* and J.G. Woodsworth\*

Canadian Journal of Physics (in press).

Photoneutron energy spectra from  $^{18}\text{O}$  have been measured by time-of-flight spectroscopy at bremsstrahlung endpoint energies from 11 MeV to 18 MeV in 1 MeV steps to obtain the  $(\gamma, n_0)$  and  $(\gamma, n_1)$  differential cross sections. The ground state photoneutron cross section contains at least 8 major resonances in the region from 9 to 17 MeV and has an average value of 100  $\mu\text{b}/\text{sr}$ . The cross section to the first excited state of  $^{17}\text{O}$  contains only two major resonances, at 11.4 MeV and 14.4 MeV; and the average cross section in the region from 11 to 16 MeV is about 40  $\mu\text{b}/\text{sr}$ . Of particular interest is a resonance at 14.4 MeV which appears to reflect a simple excitation of one of the valence neutrons to the  $2P_{3/2}$  state. Analysis of the  $(\gamma, n_0)$  and  $(\gamma, n_1)$  cross sections for this continuum state leads to estimates of the configuration amplitudes of the  $2S_{1/2}$  and  $1d_{5/2}$  components of this state to be  $0.62 \pm 0.06$  and  $0.78 \pm 0.08$  respectively and the ratio of the  $(2S_{1/2})^2$  to  $(1d_{5/2})^2$  amplitudes in the ground state of  $^{18}\text{O}$  to be  $0.39 \pm 0.02$ .

<sup>†</sup>Department of Physics, Trent University.

\*Department of Physics, University of Toronto.

THE WEIZMANN INSTITUTE OF SCIENCE

Department of Nuclear Physics

**RECOIL DISTANCE LIFETIME MEASUREMENTS  
OF THE LOWEST  $2^+$  AND  $4^+$  STATES OF  $^{18}\text{O}^\dagger$**

Z. BERANT, C. BROUDE, G. ENGLER and D. F. H. START <sup>††</sup>  
*Physics Department, Weizmann Institute of Science, Rehovot, Israel*

Received 15 March 1974

**Abstract:** Using the recoil-distance method, mean lives of  $3.58 \pm 0.18$  ps and  $24.8 \pm 1.3$  ps have been measured for the 1.98 MeV,  $2^+$  and 3.56 MeV,  $4^+$  states in  $^{18}\text{O}$ .

**THE MAGNETIC MOMENT OF THE  $4^+$ , 3.55 MeV LEVEL OF  $^{18}\text{O}^\dagger$**

Z. BERANT, C. BROUDE, S. DIMA <sup>††</sup>, G. GOLDRING  
M. HASS, Z. SHKEDI, D. F. H. START <sup>†††</sup> and Y. WOLFSON  
*Department of Nuclear Physics, The Weizmann Institute of Science, Rehovot, Israel*

Received 4 June 1974  
(Revised 30 September 1974)

**Abstract:** The magnetic moment of the  $4^+$ , 3.55 MeV level of  $^{18}\text{O}$  has been determined to be  $|g| = 0.62 \pm 0.10$  in a perturbed angular correlation measurement on nuclei recoiling into gas and vacuum. Analysis of the recoil-into-gas data using the Abragam-Pound model agrees with analysis of the recoil-into-vacuum data using a model for the electronic ensemble described in a previous communication. The value of the  $g$ -factor shows the  $4^+$  wave function to consist mainly of the  $d_{5/2}^2$  configuration.

**NUCLEAR DEFORMATIONS FROM INELASTIC  $\alpha$ -SCATTERING  
ON RARE EARTH NUCLEI AT ENERGIES NEAR THE COULOMB BARRIER**

W. BRÜCKNER, D. HUSAR, D. PELTE and K. TRAXEL  
*Max-Planck Inst. für Kernphysik and I. Physikalisches Inst. der Universität Heidelberg, Heidelberg,  
Germany*

and  
M. SAMUEL and U. SMILANSKY <sup>†</sup>  
*The Weizmann Institute of Science, Rehovot, Israel*

Received 24 May 1974

**Abstract:** Alpha particles in the energy range of 10-20 MeV and scattered at various angles were used to excite the  $0^+$ ,  $2^+$ ,  $4^+$  members in the ground state bands of  $^{152}\text{Sm}$ ,  $^{154}\text{Sm}$  and  $^{186}\text{W}$ . The measured excitation probabilities for bombarding energies below the Coulomb barrier were analyzed in the framework of Coulomb excitation theory. The resulting matrix elements of the E2 and E4 multipole operators were interpreted in terms of charge deformation parameters  $\beta_{\lambda=2,4}^c$ . The cross sections for higher energies were analyzed in terms of the deformed optical potential and resulted in potential deformation parameters  $\beta_{\lambda=2,4}^p$ . The two sets of deformation parameters show the same general trend of variation with target mass number. Still, significant differences are observed in some particular cases.

ELASTIC SCATTERING OF  $^3\text{He}$  AND  $^4\text{He}$   
AT INCIDENT ENERGIES NEAR THE COULOMB BARRIER

Y. EISEN<sup>†</sup>, E. ABRAMSON, G. ENGLER<sup>††</sup>, M. SAMUEL, U. SMILANSKY and Z. VAGER  
*The Weizmann Institute of Science, Rehovot, Israel*

Received 22 August 1974

**Abstract:** The elastic scattering of  $^3\text{He}$  and  $^4\text{He}$  from Zr, Mo, Cd, and Te isotopes is studied at incident energies near the Coulomb barrier. Marked differences are observed between the excitation curves of  $^3\text{He}$  and  $^4\text{He}$ . These differences are shown to be due to a large surface absorption in the  $^3\text{He}$  scattering. A systematic study of the size parameters deduced from the present and other  $^4\text{He}$  experiments shows deviations from the  $A^{1/3}$  law for nuclei near closed neutron shells.

Structure of States in the Mass-90 Region by  $(p,p'\gamma)$

Angular Correlation at the lowest  $5/2^+$  Analogue Resonances

N. Cue<sup>†</sup>, I. Plessner, Z. Vager and G.F. Wheeler<sup>††</sup>

The Weizmann Institute of Science, Rehovot

and

Department of Physics, State University of New York

at Stony Brook, N.Y. 11790<sup>\*</sup>

**Abstract:** Angular correlations between inelastically scattered protons leading to the  $2^+$  and in some cases the  $4^+$  states of even even nuclei in the mass 90 region, and subsequent  $2^+ \rightarrow 0^+$   $\gamma$ -rays were measured. Analogue resonances corresponding to the lowest  $5/2^+$  of odd nuclei were observed. The data was analysed using a method which takes into account compound nuclear enhancement. Relative decay partial amplitudes of the analogue resonances were deduced.

Nuclear Reactions between Oxygen Isotopes\*

D. Kalinsky, D. Melnik, U. Smilansky, N. Trautner and B.A. Watson<sup>†</sup>

Department of Nuclear Physics, The Weizmann Institute of Science

Rehovot, Israel

Y. Horowitz and S. Mordechai

Department of Physics

Ben Gurion University of the Negev

Beer Sheva, Israel

and

G. Baur and D. Pelte

Max Planck Institut für Kernphysik

ABSTRACT

Elastic, inelastic and neutron transfer cross-sections in the systems  $^{16}\text{O} + ^{17}\text{O}$ ,  $^{16}\text{O} + ^{18}\text{O}$  and  $^{17}\text{O} + ^{18}\text{O}$  have been measured at c.m. energies between 12-16 MeV and angles between  $60^\circ$ - $125^\circ$ . Two position sensitive detectors in coincidence were used to perform simultaneous measurements of the various outgoing channels. The data have been analysed with particular attention to the contributions of exchange effects.

**Spectrum of protons in fission of  $^{252}\text{Cf}$**

A. Gavron

*Nuclear Physics Department, The Weizmann Institute of Science, Rehovot, Israel*

Y. Gazit

*Nuclear Physics Department, Soreq Nuclear Research Center, Yavneh, Israel*

(Received 28 September 1973)

The spectrum of protons in fission of  $^{252}\text{Cf}$  has been measured using an improved collimation technique, which eliminates a large part of the background. The most probable proton energy was determined to be  $7.8 \pm 0.2$  MeV and the spectrum full width at half-maximum,  $6.1 \pm 0.3$  MeV. The number of protons emitted per long range  $\alpha$  particle is  $(1.6 \pm 0.1) \times 10^{-2}$ .

## SHELL MODEL FOR $N = 49$ NUCLEI

R. GROSS and A. FRENKEL

*The Weizmann Institute of Science, Rehovot, Israel*

Received 1 October 1974

The behavior of  $N = 49$  nuclei is examined in terms of a model based on a  $^{88}\text{Sr}$  core with a  $1g_{9/2}$  neutron-hole. Effective interactions between  $1g_{9/2}$  neutrons and  $1g_{9/2}-2p_{1/2}$  protons are determined from the spectra of  $^{88}\text{Y}$ ,  $^{89}\text{Zr}$ ,  $^{90}\text{Nb}$  and  $^{91}\text{Mo}$ . Close agreement is obtained also with experimental level spacings of  $^{92}\text{Tc}$  and  $^{93}\text{Ru}$ , as well as binding energies.

## A NEW SEMI-CLASSICAL THEORY FOR MULTIPLE COULOMB EXCITATION

S. LEVIT and U. SMILANSKY

*Department of Physics, The Weizmann Institute of Science, Rehovot, Israel*

and

D. PELTE

*Erstes Physikalisches Institut der Universität Heidelberg, Heidelberg, Germany*

Received 12 August 1974

A uniform semi-classical approach based on the classical limit of Feynman's path-integral representation is applied for the case of multiple Coulomb excitation. The resulting excitation probabilities are compared with those obtained from the conventional semi-classical treatment and also with the results of the full quantum mechanical coupled channels treatment.

## Dynamic single-particle effects in fission

Y. Boneh

*Nuclear Research Center, Negev, Beersheva, Israel,  
and Weizmann Institute of Science, Rehovot, Israel*

Z. Fraenkel

*Weizmann Institute of Science, Rehovot, Israel*

(Received 20 March 1974)

We calculate for a model nucleus the single-particle excitations in the transition from the saddle point to the scission point in the fission process. The model nucleus consists of a square well potential of finite depth filled with noninteracting "protons" and "neutrons." At every stage of the transition between the saddle point and scission point the shape of the potential surface is equal to the surface of the fissioning nucleus as predicted by the liquid-drop model but the depth of the potential is held constant. The rate of change of the nuclear surface is assumed to be equal to that predicted by the dynamical liquid-drop-model calculations of Nix. It is found that for this time scale there is a small probability for the particles to be raised to levels above the potential well and thus be emitted from the nucleus. The calculated number of emitted neutrons and protons is in qualitative agreement with the experimental results for the emission of scission neutrons and protons. However, there is a large energy transfer from the collective to the single-particle degrees of freedom and hence the transition cannot be considered adiabatic for this time scale. The inclusion in the model of a residual interaction is expected to reduce both the number of particles emitted and the energy transfer from the collective to single-particle degrees of freedom, thus making the transition more nearly adiabatic.



PROGRESS REPORT TO INDC

ON

NUCLEAR DATA ACTIVITIES

PAKISTAN INSTITUTE OF NUCLEAR SCIENCE & TECHNOLOGY  
P.O. NILORE, RAWALPINDI

JULY 1975

1. Inelastic Scattering of Neutrons from  $^{128}\text{Te}$  and  $^{130}\text{Te}$

Energy spectra of 14.7 MeV neutrons inelastically scattered from enriched isotopes of  $^{128}\text{Te}$  and  $^{130}\text{Te}$  have been taken at angles of  $30^\circ$ ,  $37^\circ$  and  $40^\circ$ . Energies of neutrons have been measured by the time of flight method using the associated particle technique with a flight path of 2 metres and time resolution of 1.25 nano-seconds per metre. It was not possible to resolve the ground states of  $^{128}\text{Te}$  and  $^{130}\text{Te}$  from their first excited states (at about 750 keV). Some groups of inelastically scattered neutrons have been observed corresponding to the energy levels in the range 4 to 10 MeV. Measurements of the total cross-sections of  $^{128}\text{Te}$  and  $^{130}\text{Te}$  at 14.7 MeV neutron energy have also been made. The data are being analysed using appropriate computer programmes.

2. Thermal Neutron Capture in even A Neodymium Isotopes

Work was continued on the study of the  $\gamma$ -rays produced as a result of thermal neutron capture in even A neodymium isotopes. The analysis of the  $^{142}\text{Nd}(n, \gamma)^{143}\text{Nd}$  data has been finalised and 344  $\gamma$ -rays have been assigned to  $^{143}\text{Nd}$ . A revised decay scheme for this nucleus based on the singles and coincidence data has been constructed which consists of 43 excited states and incorporates 173 of the  $\gamma$ -rays representing more than 80% of the total observed intensity. Many of these levels have been observed for the first time.

Final analysis of the  $^{144}\text{Nd}(n, \gamma)^{145}\text{Nd}$  data is also in progress. Computer analysis of the previously collected  $^{\text{nat}}\text{Nd}(n, \gamma)$  data has been completed. Moreover, measurements have been made to obtain the spectrum of gamma rays in the energy range 0.1 to 5.8 MeV produced in the reaction  $^{146}\text{Nd}(n, \gamma)^{147}\text{Nd}$ . These data are now being processed.

3. The  $^{170}\text{Er}(n, \gamma)^{171}\text{Er}$  Reaction

Work has been started on the measurement of  $\gamma$ -rays emitted in the neutron capture in enriched  $^{170}\text{Er}$  and natural Er targets.

4. In-Beam Neutron Activation Analysis

Non-destructive elemental analysis of stainless steel and iron ore samples has been carried out using neutron capture gamma rays. It has been shown that the use of low energy gamma rays, ranging from 0.2 to 1.4 MeV, helps considerably in reducing the time of analysis. The problems of congestion of peaks due to compton continuum and the double and single escape peaks in this region of the spectrum has been overcome by using the Ge(Li) detector in conjunction with a NaI(Tl) annulus in anti-compton mode. A paper on the work is to appear in J. Radioanal. Chem. 27 (1975) 115. Work has also been initiated to determine the protein content in cereals using the  $^{14}\text{N}(n, \gamma)^{15}\text{N}$  reaction.

5. Gamma Ray-Fission Fragment Energy Correlation Measurement in Spontaneous Fission of  $^{252}\text{Cf}$

The data processing of gamma ray-fission fragment energy correlation measurements for the spontaneous fission of  $^{252}\text{Cf}$  has been completed and analysis is in progress. The following gamma ray lines belonging to the ground state rotational bands have been observed.

Isotope	Energy
$^{106}\text{Mo}$	171.7 keV ( $2^+ \rightarrow 0^+$ )
$^{102}\text{Zr}$	151.9 keV ( $2^+ \rightarrow 0^+$ )
$^{100}\text{Zr}$	212.7 keV ( $2^+ \rightarrow 0^+$ )
$^{108}\text{Ru}$	242.3 keV ( $2^+ \rightarrow 0^+$ )
$^{110}\text{Ru}$	240.8 keV ( $2^+ \rightarrow 0^+$ )
$^{112}\text{Ru}$	236.8 keV ( $2^+ \rightarrow 0^+$ )

Half lives and B(E2) values of the transitions are being calculated. The variation of isotopic yields with total kinetic

energy of the fragment is presently being looked into.

Experimental preparations are also in progress for the following measurements :

- i) X-ray,  $\gamma$ -ray coincidence measurements in the spontaneous fission of  $^{248}\text{Cm}$ .
- ii)  $\gamma$ -ray-fission fragment energy correlation measurements in the spontaneous fission of  $^{248}\text{Cm}$ .

#### 6. Phonons in $\text{K}_{.5}\text{Rb}_{.5}\text{I}$

The phonons in alkali halides of KI and RbI have been previously studied by the technique of inelastic scattering of slow neutrons. It was of interest to find the phonon frequencies in mixed alkali-halide single crystals. A single crystal of  $\text{K}_{.5}\text{Rb}_{.5}\text{I}$  of about 1 cm diameter and 5 cm length has been used on the Triple-axis Neutron Spectrometer and phonons measured using the spectrometer in the constant Q-mode. The phonons were measured in the three symmetry directions 100, 110 and 111 and the frequencies of the phonons in these directions were found to be approximately in between those of the KI and RbI separate crystals. This is an interesting information about phonons in mixed alkali halides. An other aspect of studying the shell-model application to disordered alloy systems has also been looked into and the force constants determined. The work on this project has been completed and will soon be sent for publication.

#### 7. Debye-waller factors of KBr

Debye-waller factor is a useful parameter of a crystal. This can be determined from the measurement of the two axis neutron diffraction pattern of a powder sample. The diffraction peaks in a two-axis experiment contain considerable amount of Thermal Diffuse Scattering (TDS) for which theoretical corrections have to be applied in order to find the correct Debye-Waller factors. A technique has been developed whereby the diffraction

pattern is taken in a three-axis mode of the Triple-axis Spectrometer. The diffraction peaks thus observed contain almost negligible amount of the TDS. Hence Debye-Waller factors thus determined from the three-axis diffraction pattern are accurate. Using the KBr powder sample the Debye-Waller factors have been determined from the observed three-axis diffraction pattern. The B values determined by this technique are

$$B_k = 2.67 \text{ \AA}^2$$

$$B_{Br} = 2.33 \text{ \AA}^2$$

#### 8. Neutron Diffraction from cellulose-I

Unit cell of cellulose-I has been a subject of study for the past several years by X-ray diffraction and electron diffraction methods. However the unit cell dimensions determined by X-ray diffraction were half of those determined by the electron diffraction method. It was therefore interesting to investigate this controversy of cellulose-I by a different technique using the neutron diffraction method. Our results obtained by this method support the results of the electron diffraction technique.

Work of a similar nature on cellulose-II is in progress.

#### 9. Gaussian Approximation for Phonon Frequency Distribution Function of PuO<sub>2</sub> and UO<sub>2</sub>

The phonon frequency distribution function for PuO<sub>2</sub> and UO<sub>2</sub> has been approximated by a one-parameter Gaussian distribution. By comparing the limiting forms of the specific heat and the Debye-Waller factor calculated with this approximate distribution function with the corresponding limiting values of these quantities in the Debye model, the value of the parameter is found to vary inversely as the temperature T. The constant of proportionality is found to be of the order of Debye's temperature.

Values of the parameter for  $\text{UO}_2$  are calculated from its Debye's temperature and its experimental data on Debye-Waller factor, Debye's temperature and specific heat. The value of the parameter is also calculated for  $\text{PuO}_2$  from its specific heat data.

PUBLICATIONS

1. Total Cross-Section Measurements with a Neutron Generator.  
S. Mubarakmand, M. Ahmad, M. Anwar, M.S. Chaudhry.  
Nuc. Inst. & Meth. 115 (1974) 345
2. Neutron Diffraction Studies of the Unit Cell of Cellulose-I  
M.M. Beg, J. Aslam, Q.H. Khan, N.M. Butt, S. Rolandson,  
Amin Uddin Ahmad  
J. Polymer Phys. (Letters Edition) 12 (1974) 311
3. Precise Energies of Gamma Rays from Thermal Neutron Capture  
in Nitrogen.  
A.F.M. Ishaq, A.M. Khan, M. Anwar-ul-Islam, M.R. Najam  
Nucl. Inst. & Meth 121 (1974) 193
4. Debye Waller Coefficient of KCl by Powder Neutron Diffraction  
Method  
M.M. Beg, J. Aslam, N.M. Butt, Q.H. Khan, S. Rolandson  
Acta Crystallographica A30 (1974) 662
5. Gaussian Approximation for Phonon Frequency Distribution  
Function for  $\text{PuO}_2$  and  $\text{UO}_2$   
Abdullah Sadiq  
J. Nucl Sci. & Tech 12 (1975) 275
6. Thermal Neutron Capture in  $^{142}\text{Nd}$ .  
J.A. Mirza, A.M. Khan, M. Irshad, H.A. Schmidt, A.F.M. Ishaq,  
M. Anwar-ul-Islam  
Proc. 2nd Int. Symp. on Neutron Capture Gamma Ray Spectroscopy and  
Related Topics, held at Petten, the Netherland from Sept. 2-6, 1974.
7. The  $^{144}\text{Nd}(n, \gamma)^{145}\text{Nd}$  Reaction  
M.R. Najam, A.F.M. Ishaq, M. Anwarul Islam, A.M. Khan, J.A. Mirza  
Proc. 2nd Int. Symp. on Neutron Capture Gamma Ray Spectroscopy and  
Related Topics, held at Petten, the Netherland from Sept. 2-6, 1974.



INSTYTUT BADAŃ JĄDROWYCH  
ИНСТИТУТ ЯДЕРНЫХ ИССЛЕДОВАНИЙ  
INSTITUTE OF NUCLEAR RESEARCH

R A P O R T  
IBJ1502/I/PL/A

PROGRESS REPORT ON NUCLEAR  
DATA RESEARCH IN POLAND  
MAY 1974 - APRIL 1975

COMPILED BY  
A. MARCINKOWSKI

WARSZAWA 1975

### Editor s Note

This progress Report on nuclear data research in Poland /May 1974 - April 1975/ contains only information on research, which is closely related to the activities of the International Data Committee of the International Atomic Energy Agency in the field of charged particles and neutron physics. It does not include any information about other nuclear research as for example the use of neutrons for solid state physics studies.

The individual reports are not intended to be complete or formal, and must not be quoted in publications without the permission of the authors.

### Uwagi od wydawcy

Raport ten zawiera informacje o badaniach w zakresie fizyki jądrowej średnich energii przeprowadzonych w Polsce /maj 1974 - kwiecień 1975/ i związanych z działalnością Komitetu Danych Jądrowych Międzynarodowej Agencji Energii Atomowej.

Pominięto wyniki badań w innych dziedzinach fizyki jądrowej, w tym również badań w zakresie fizyki ciała stałego przy użyciu neutronów.

Poszczególne prace zawierają wstępne omówienie wyników badań nie wyczerpujące poruszanych tematów i nie powinny być cytowane bez zgody autorów.

Замечания от редакции

Этот сборник содержит сообщения о проведенных в Польше в период от мая 1974 до апреля 1975 исследованиях в области физики средних энергий, связанных с деятельностью Комитета по Ядерным Данным Международного Агенства Атомной Энергии. В данные не включены результаты исследований с области применения нейтронов в физике твердого тела. Эти доклады не являются полными и не рекомендуется ссылаться на них без согласия авторов.

CONTENTS

1. Differential Cross Sections of $^9\text{Be}/n$ , $\alpha / ^6\text{He}$ Reaction at 12.2, 14.1 and 18.0 MeV	361
2. Differential Cross Sections for the $/n, \alpha /$ Reactions Induced by 14 and 18 MeV Neutrons in $^{149}\text{Sm}$ , $^{171}\text{Yb}$ and $^{173}\text{Yb}$ Nuclei	364
3. Cross Sections for Fast Neutron Induced Reactions on $^{111}\text{Cd}$ and $^{112}\text{Cd}$ Isotopes	371
4. Study of Proton Inelastic Scattering on Magnesium Isotopes at 9.1 MeV	373
5. The Investigation of $^{158}\text{Eu}$ Decay	387
6. Levels in $^{130}\text{Ba}$ Fed from $^{130}\text{La}$ Decay	393
7. High-Spin Excited States and Evidence for Particle-Core Coupling in the N=83 Nuclei $^{145}\text{Sm}$ and $^{147}\text{Gd}$	397
8. High-Spin States in $^{144}\text{Nd}$ Observed in the $/\alpha, 2n/$ Reaction	400

DIFFERENTIAL CROSS SECTION OF  ${}^9\text{Be} (n, \alpha) {}^6\text{He}$  REACTION

AT 12.2, 14.1 AND 18.0 MeV

S. Burzyński, K. Rusek, W. Smolec, I. M. Turkiewicz,

J. Turkiewicz and P. Zuprański

The  ${}^9\text{Be} (n, \alpha) {}^6\text{He}$  reaction was studied with a telescopic system. Previous measurements at 14.1 MeV [1] have been repeated and extended to include the differential cross sections for the transition  ${}^9\text{Be} (n, \alpha_1) {}^6\text{He}$  leading to the first excited state of  ${}^6\text{He}$ . The differential cross sections have been measured at neutron energies of 12.2, 14.1 and 18.0 MeV. The results are presented in tables shown below. Data are in the c.m. system. The cross section errors are only statistical.

TABLE I

$E_n = 12.2 \text{ MeV } {}^9\text{Be}(n, \alpha_0) {}^6\text{He}$

$\vartheta$ [deg]	$2\Delta\vartheta$ [deg]	$d\sigma/d\Omega$ [mb/sr]	$\Delta d\sigma/d\Omega$ [mb/sr]
9.	8.5	0.46	0.15
17.	8.0	0.28	0.28
20.7	7.5	0.94	0.22
29.	7.5	1.50	0.32
39.	7.0	1.10	0.23
56.9	7.0	2.00	0.32
74.	7.0	2.87	0.43
90.7	6.0	1.93	1.17
117.2	7.0	0.34	0.61
136.5	7.0	1.77	0.35
147.6	7.5	1.82	0.29
156.7	8.0	2.23	0.25
161.7	8.0	2.57	0.25
170.0	8.5	4.13	0.30

TABLE II

$E_n = 12.2 \text{ MeV } {}^9\text{Be}(n, \alpha_1){}^6\text{He}$

$\theta$ [deg]	$2 \Delta \theta$ [deg]	$d\sigma/d\Omega$ [mb/sr]	$\Delta d\sigma/d\Omega$ [mb/sr]
9.	8.5	6.92	0.45
17.	8.0	7.32	0.54
20.7	8.0	6.75	0.45
29.	7.5	7.63	0.62
39.	7.0	6.12	0.51
56.9	7.0	3.45	0.41
74.	6.5	6.2	0.93
90.7	6.0	5.89	2.05

TABLE III

$E_n = 14.1 \text{ MeV } {}^9\text{Be}(n, \alpha_0){}^6\text{He}$

$\theta$ [deg]	$2 \Delta \theta$ [deg]	$d\sigma/d\Omega$ [mb/sr]	$\Delta d\sigma/d\Omega$ [mb/sr]
10.5	10.0	0.31	0.15
15.8	9.5	0.46	0.12
27.0	9.0	0.35	0.16
39.0	8.5	0.59	0.13
51.0	8.0	1.23	0.14
62.9	7.5	1.28	0.15
74.0	7.0	1.53	0.20
85.3	6.5	1.16	0.21
96.0	6.0	1.46	0.57
129.5	6.5	0.61	0.29
139.5	7.0	1.00	0.23
149.0	8.0	1.11	0.11
158.5	9.0	1.81	0.13
167.5	9.5	2.44	0.15
172.	10.0	3.28	0.18

TABLE IV

$E_n = 14.1 \text{ MeV } {}^9\text{Be}(n, \alpha_1){}^6\text{He}$

$\theta$ [deg]	$2\Delta\theta$ [deg]	$d\sigma/d\Omega$ [mb/sr]	$\Delta d\sigma/d\Omega$ [mb/sr]
10.5	10.0	5.05	0.24
15.8	9.5	5.09	0.21
27.4	9.0	4.58	0.21
39.6	8.5	3.71	0.22
51.6	8.0	3.75	0.20
63.8	7.5	4.01	0.18
75.1	7.0	2.48	0.23
86.4	6.5	2.42	0.51
97.2	6.0	1.79	0.66

TABLE V

$E_n = 18.0 \text{ MeV } {}^9\text{Be}(n, \alpha_0){}^6\text{He}$

$\theta$ [deg]	$2\Delta\theta$ [deg]	$d\sigma/d\Omega$ [mb/sr]	$\Delta d\sigma/d\Omega$ [mb/sr]
10.5	9.5	0.12	0.06
15.8	9.0	0.12	0.12
27.0	9.0	0.14	0.04
39.0	8.5	0.20	0.04
51.0	8.0	0.32	0.05
62.9	7.5	0.22	0.06
74.0	7.0	0.40	0.08
139.5	8.0	0.18	0.04
149.0	8.5	0.37	0.04
158.5	9.0	0.58	0.04
167.5	9.0	0.54	0.06
172.0	9.5	0.63	0.05

TABLE VI

$$E_n = 18.0 \text{ MeV } {}^9\text{Be}(n, \alpha) {}^6\text{He}$$

$\psi$ [deg]	$2\Delta\psi$ [deg]	$d\sigma/d\Omega$ [mb/sr]	$\Delta d\sigma/d\Omega$ [mb/sr]
9.7	9.0	2.23	0.10
15.8	8.5	2.53	0.21
27.3	8.5	2.83	0.12
39.5	9.0	2.05	0.08
51.5	8.5	1.88	0.13
63.6	7.5	1.65	0.14
74.8	7.0	1.71	0.19

1. Progress Report on Nuclear Data Research in Poland,  
May 1973 - April 1974

DIFFERENTIAL CROSS SECTIONS FOR THE  $(n, \alpha)$  REACTIONS  
INDUCED BY 14 AND 18 MeV NEUTRONS IN  ${}^{149}\text{Sm}$ ,  ${}^{171}\text{Yb}$  AND  
 ${}^{173}\text{Yb}$  NUCLEI

L. Głowacka, M. Jaskóła, W. Osakiewicz, J. Turkiewicz, L. Zemło  
Institute of Nuclear Research, Dept. of Nuclear Reactions, Warsaw  
and

Institute of Experimental Physics, University of Warsaw

The absolute differential cross sections for the  ${}^{149}\text{Sm}(n, \alpha) {}^{146}\text{Nd}$ ,  
 ${}^{171}\text{Yb}(n, \alpha) {}^{168}\text{Er}$ ,  ${}^{173}\text{Yb}(n, \alpha) {}^{170}\text{Er}$  reactions at  $E_n = 14 \text{ MeV}$  and  
 ${}^{171}\text{Yb}(n, \alpha) {}^{168}\text{Er}$ ,  ${}^{173}\text{Yb}(n, \alpha) {}^{170}\text{Er}$  reactions at  $18 \text{ MeV}$  have been  
measured by direct registration of alpha particles. The experimental  
arrangement used in the measurements is described in our earlier work [1].  
The neutrons were obtained from the  ${}^3\text{H}(d, n) {}^4\text{He}$  reaction with deuterons  
accelerated in the 3 MeV Van de Graaff accelerator. The neutron flux

was measured by counting the recoil protons from a thin polyethylene foil. Recoil protons were registered by a CsI(Tl) scintillator followed by photomultiplier and standard electronics. The absolute calibration of the monitor was performed by measuring of the 847 keV  $\gamma$ -transition in  $^{56}\text{Fe}$  produced in the  $^{56}\text{Fe}(n,p)^{56}\text{Mn}$  reaction with successive  $\beta$ -decay of  $^{56}\text{Mn}$ . The cross section for the  $^{56}\text{Fe}(n,p)^{56}\text{Mn}$  reaction was taken as 110 mb and 57 mb for neutron energies equal to 14 and 18 MeV respectively [2]. Uncertainty of the monitor calibration amounts to about 20 %.

The investigated targets were made of oxides and deposited on the thick carbon backings by means of sedimentation from suspensions in isopropyl alcohol.

The energy scale calibration of the alpha spectrometer was performed with employment of alphas from ThC and ThC' and from the reaction  $^{28}\text{Si}(n,\alpha)^{25}\text{Mg}$  produced in the silicon detector by the incident neutrons.

The results of measurements are shown in Tables 1 - 5. In the bottom of each table the energy of neutrons, the angular spread and the energy spread of measurements are also shown. These spreads were calculated by Monte Carlo method [3]. The errors indicated in the tables are only statistical.

1. M.Jaskóła, J.Turkiewicz, L.Zemło, W.Osakiewicz,  
Acta Phys. Pol. B2, 521 /1971/
2. D.C.Santry, J.Butler, Can. J. Phys., 42, 1030 /1964/
3. L.Zemło, INR Report 1464/I/PL/B /1973/

TABLE 1

Differential cross sections for  $^{149}\text{Sm}(n, \alpha)^{146}\text{Nd}$   
 reaction at  $E_n = 14.12 \text{ MeV}$

$E_\alpha$ [MeV]	$\mu\text{b} \cdot \text{sr}^{-1} \text{MeV}^{-1}$	$E_\alpha$ [MeV]	$\mu\text{b} \cdot \text{sr}^{-1} \text{MeV}^{-1}$
15.60	$65 \pm 49$	19.76	$180 \pm 21$
15.79	$116 \pm 46$	19.96	$133 \pm 18$
15.99	$45 \pm 42$	20.16	$130 \pm 17$
16.19	$46 \pm 42$	20.36	$103 \pm 17$
16.39	$140 \pm 39$	20.56	$103 \pm 15$
16.59	$142 \pm 37$	20.75	$124 \pm 15$
16.79	$47 \pm 35$	20.95	$90 \pm 15$
16.98	$130 \pm 35$	21.15	$105 \pm 14$
17.18	$141 \pm 32$	21.35	$128 \pm 14$
17.38	$136 \pm 31$	21.55	$98 \pm 12$
17.58	$131 \pm 30$	21.75	$38 \pm 9$
17.78	$183 \pm 30$	21.94	$19 \pm 8$
17.98	$152 \pm 29$	22.14	$26 \pm 7$
18.17	$200 \pm 27$	22.34	$34 \pm 8$
18.37	$161 \pm 25$	22.54	$34 \pm 7$
18.57	$184 \pm 25$	22.74	$41 \pm 8$
18.77	$160 \pm 24$	22.94	$31 \pm 8$
18.97	$204 \pm 23$	23.13	$34 \pm 7$
19.17	$225 \pm 23$	23.33	$27 \pm 6$
19.37	$235 \pm 23$	23.53	$12 \pm 4$
19.56	$195 \pm 22$	23.73	$3 \pm 2$

Cross section integrated in the 15.60  $\pm$  23.73 MeV range  
 is equal to  $0.913 \pm 0.032 \text{ mb} \cdot \text{sr}^{-1}$ .

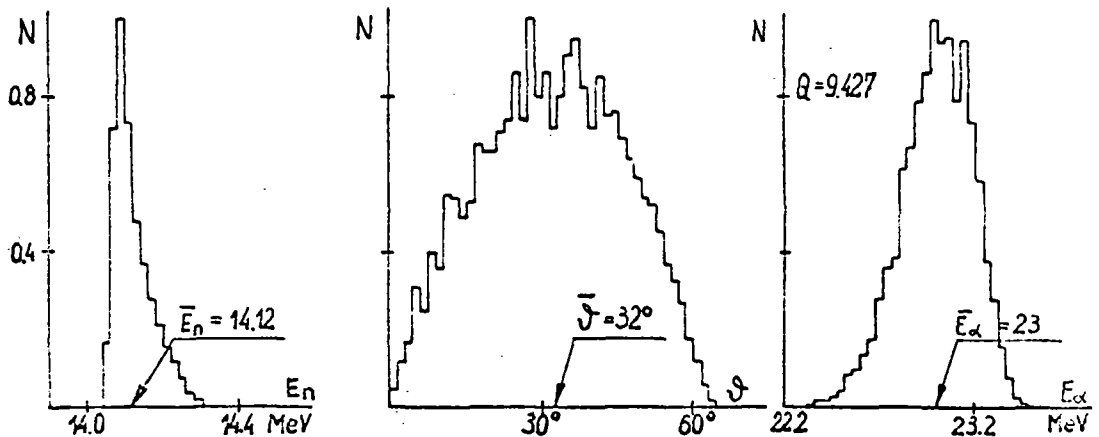


TABLE 2

Differential cross sections for  $^{171}\text{Yb}(n,\alpha)^{168}\text{Er}$   
 reaction at  $E_n = 14.12 \text{ MeV}$

$E_\alpha$ [MeV]	$\mu\text{b} \cdot \text{sr}^{-1} \text{MeV}^{-1}$	$E_\alpha$ [MeV]	$\mu\text{b} \cdot \text{sr}^{-1} \text{MeV}^{-1}$
16.40	$69 \pm 35$	19.97	$129 \pm 15$
16.60	$24 \pm 33$	20.16	$144 \pm 14$
16.80	$14 \pm 31$	20.36	$158 \pm 14$
17.00	$20 \pm 29$	20.56	$121 \pm 12$
17.19	$19 \pm 28$	20.76	$103 \pm 12$
17.39	$34 \pm 27$	20.96	$61 \pm 11$
17.59	$68 \pm 26$	21.15	$48 \pm 10$
17.79	$35 \pm 24$	21.35	$51 \pm 8$
17.99	$35 \pm 23$	21.55	$37 \pm 8$
18.18	$60 \pm 22$	21.75	$38 \pm 7$
18.38	$71 \pm 20$	21.95	$31 \pm 7$
18.58	$39 \pm 19$	22.14	$29 \pm 6$
18.78	$75 \pm 18$	22.34	$22 \pm 6$
18.98	$82 \pm 18$	22.54	$23 \pm 5$
19.17	$91 \pm 17$	22.74	$19 \pm 5$
19.37	$94 \pm 16$	22.94	$20 \pm 4$
19.57	$82 \pm 16$	23.13	$11 \pm 3$
19.77	$90 \pm 15$	23.33	$3 \pm 2$

Cross section integrated in the 16.40  $\pm$  23.33 MeV range is equal to  $0.415 \pm 0.022 \text{ mb} \cdot \text{sr}^{-1}$ .

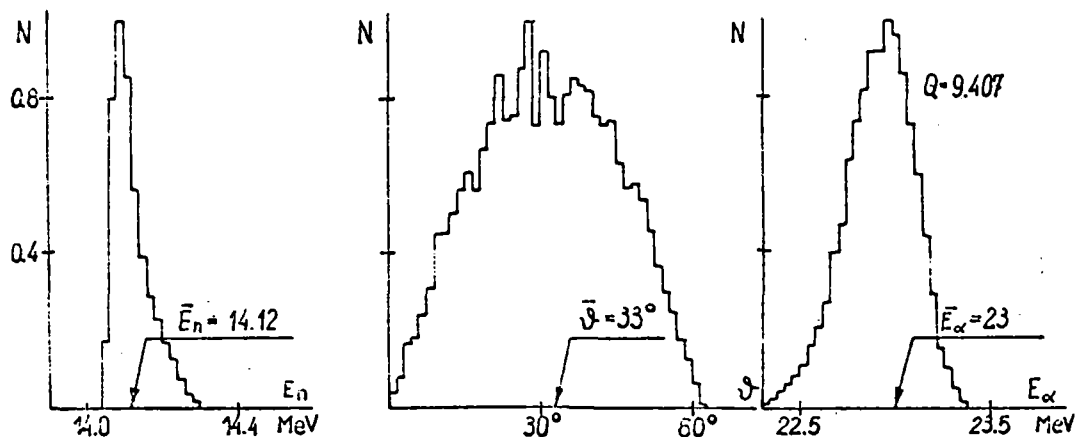


TABLE 3

Differential cross sections for  $^{173}\text{Yb}(n,\alpha)^{170}\text{Er}$   
 reaction at  $E_n = 14.12$  MeV

$E_\alpha$ [MeV]	$\mu\text{b} \cdot \text{sr}^{-1} \text{MeV}^{-1}$	$E_\alpha$ [MeV]	$\mu\text{b} \cdot \text{sr}^{-1} \text{MeV}^{-1}$
16.24	$51 \pm 48$	19.40	$88 \pm 20$
16.43	$17 \pm 45$	19.60	$92 \pm 19$
16.63	$7 \pm 42$	19.80	$103 \pm 18$
16.83	$98 \pm 40$	20.00	$124 \pm 17$
17.03	$62 \pm 38$	20.20	$119 \pm 17$
17.23	$63 \pm 36$	20.39	$135 \pm 16$
17.42	$34 \pm 34$	20.59	$111 \pm 15$
17.62	$62 \pm 32$	20.79	$74 \pm 13$
17.82	$63 \pm 30$	20.99	$54 \pm 12$
18.02	$41 \pm 29$	21.19	$29 \pm 11$
18.22	$109 \pm 28$	21.38	$32 \pm 9$
18.41	$61 \pm 26$	21.58	$0 \pm 8$
18.61	$76 \pm 25$	21.78	$15 \pm 7$
18.81	$92 \pm 23$	21.98	$12 \pm 8$
19.01	$108 \pm 23$	22.18	$22 \pm 6$
19.21	$109 \pm 21$		

Cross section integrated in the 16.24 - 22.18 MeV range is equal to  $0.417 \pm 0.029 \text{ mb} \cdot \text{sr}^{-1}$ .

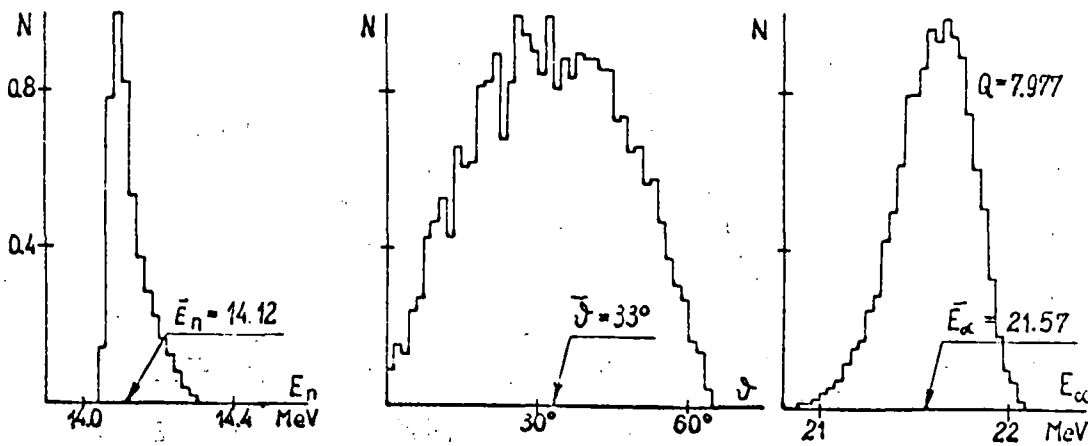


TABLE 4

Differential cross sections for  $^{171}\text{Yb}(n,\alpha)^{168}\text{Er}$   
 reaction  $E_n = 18.18 \text{ MeV}$

$E_\alpha$ [MeV]	$\mu\text{b} \cdot \text{sr}^{-1} \text{MeV}^{-1}$	$E_\alpha$ [MeV]	$\mu\text{b} \cdot \text{sr}^{-1} \text{MeV}^{-1}$
18.82	$170 \pm 79$	23.19	$158 \pm 29$
19.01	$205 \pm 75$	23.39	$126 \pm 27$
19.21	$218 \pm 70$	23.59	$155 \pm 27$
19.41	$169 \pm 66$	23.79	$121 \pm 26$
19.61	$104 \pm 62$	23.99	$148 \pm 25$
19.81	$89 \pm 60$	24.19	$143 \pm 24$
20.01	$138 \pm 56$	24.38	$132 \pm 23$
20.21	$98 \pm 56$	24.58	$183 \pm 23$
20.41	$148 \pm 53$	24.78	$163 \pm 22$
20.61	$95 \pm 51$	24.98	$146 \pm 21$
20.80	$124 \pm 48$	25.18	$91 \pm 18$
21.00	$189 \pm 46$	25.38	$81 \pm 16$
21.20	$195 \pm 44$	25.58	$64 \pm 16$
21.40	$116 \pm 41$	25.78	$66 \pm 14$
21.60	$149 \pm 40$	25.98	$33 \pm 13$
21.80	$127 \pm 39$	26.17	$39 \pm 13$
22.00	$113 \pm 37$	26.37	$34 \pm 12$
22.20	$79 \pm 35$	26.57	$16 \pm 10$
22.40	$156 \pm 33$	26.77	$12 \pm 10$
22.59	$167 \pm 33$	26.97	$11 \pm 10$
22.79	$157 \pm 31$	27.17	$16 \pm 10$
22.99	$111 \pm 30$	27.37	$9 \pm 8$

Cross section integrated in the 18.82 ± 27.37 MeV range is equal to  $1.019 \pm 0.052 \text{ mb} \cdot \text{sr}^{-1}$

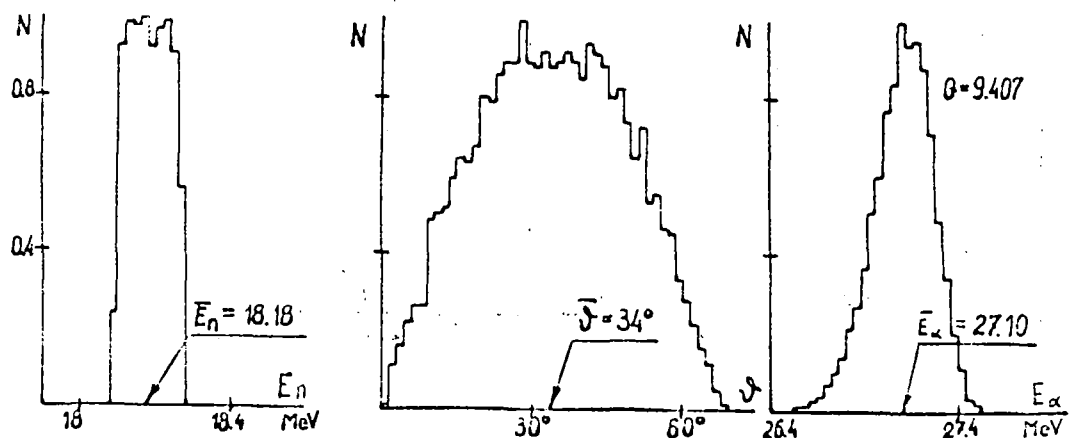
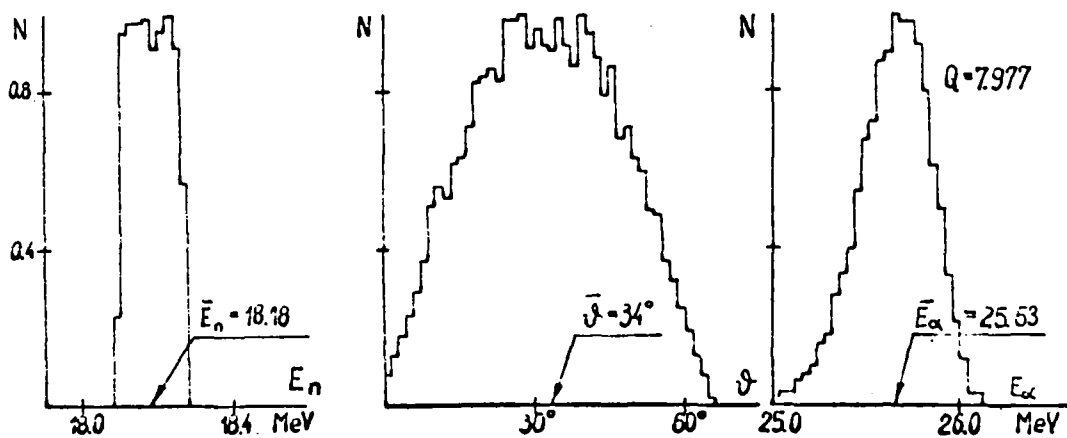


TABLE 5

Differential cross sections for  $^{173}\text{Yb}(n,\alpha)^{170}\text{Er}$   
 reaction at  $E_n = 18.18 \text{ MeV}$

$E_\alpha$ [MeV]	$\mu\text{b} \cdot \text{sr}^{-1} \text{MeV}^{-1}$	$E_\alpha$ [MeV]	$\mu\text{b} \cdot \text{sr}^{-1} \text{MeV}^{-1}$
18.89	178 $\pm$ 73	22.66	142 $\pm$ 31
19.09	117 $\pm$ 69	22.86	134 $\pm$ 29
19.29	182 $\pm$ 65	23.06	127 $\pm$ 29
19.49	212 $\pm$ 62	23.26	142 $\pm$ 27
19.69	206 $\pm$ 59	23.46	172 $\pm$ 26
19.89	191 $\pm$ 56	23.66	134 $\pm$ 24
20.08	101 $\pm$ 52	23.85	110 $\pm$ 23
20.28	95 $\pm$ 52	24.05	83 $\pm$ 22
20.48	165 $\pm$ 49	24.25	98 $\pm$ 21
20.68	119 $\pm$ 48	24.45	95 $\pm$ 20
20.88	136 $\pm$ 45	24.65	98 $\pm$ 19
21.08	126 $\pm$ 42	24.85	59 $\pm$ 18
21.27	180 $\pm$ 40	25.04	38 $\pm$ 16
21.47	176 $\pm$ 40	25.24	46 $\pm$ 15
21.67	140 $\pm$ 37	25.44	47 $\pm$ 14
21.87	119 $\pm$ 36	25.64	10 $\pm$ 12
22.07	154 $\pm$ 35	25.84	37 $\pm$ 11
22.27	134 $\pm$ 34	26.04	15 $\pm$ 12
22.47	143 $\pm$ 31	26.23	16 $\pm$ 11

Cross section integrated in the 18.89  $\pm$  26.23 MeV range is equal to  $0.902 \pm 0.048 \text{ mb} \cdot \text{sr}^{-1}$ .



## CROSS SECTIONS FOR FAST NEUTRON INDUCED REACTIONS ON $^{111}\text{Cd}$ AND $^{112}\text{Cd}$ ISOTOPEs

W. Augustyniak, M. Herman and A. Marcinkowski

Institute of Nuclear Research, Dept. of Nuclear Reactions, Warsaw

Samples of enriched  $^{111}\text{Cd}$  94.52% and  $^{112}\text{Cd}$  95.75% isotopes were irradiated with neutrons from the  $^3\text{H}(d,n)^4\text{He}$  and  $^2\text{H}(d,n)^3\text{He}$  reactions at neutron energies in the range from 3.4 - 18 MeV. The neutron energy was selected by a suitable choice of the emission angle.

The reaction final products were identified by their characteristic  $\gamma$ -ray transitions. The  $\gamma$ -activities were measured with a  $30\text{ cm}^3$   $\text{Ge}(\text{Li})$  spectrometer. Relative detector efficiency for  $\gamma$ -rays in the energy range from 50 keV to 2 MeV was determined using the known intensity relations of  $\gamma$ -transitions in  $^{226}\text{Ra}$ ,  $^{169}\text{Yb}$  and  $^{133}\text{Ba}$  sources [1, 2].

The 48 min, 247 keV,  $\gamma$ -ray activities induced in the cadmium samples were measured and the population of the final nuclei in the  $^{111}\text{Cd}(n,n')^{111\text{m}}\text{Cd}$  and  $^{112}\text{Cd}(n,2n)^{111\text{m}}\text{Cd}$  reactions were extracted. In order to determine the  $^{112}\text{Cd}(n,p)^{112}\text{Ag}$  reaction cross section the 3.2 h, 617 keV,  $\gamma$ -ray activity was followed after irradiation. The measurements were referred to the activities induced in the monitoring reactions  $^{56}\text{Fe}(n,p)^{56}\text{Mn}$  [3] and  $^{64}\text{Zn}(n,p)^{64}\text{Cu}$  [4] at neutron energies ranging from 3-5 MeV.

The attenuation of the  $\gamma$ -rays in the samples was evaluated by the Monte-Carlo method. The decay characteristics of the residual nuclei adopted in the present data analysis were taken from the tables of Lederer et al. [5].

The results of measurements are presented in tables 1 and 2. The errors attached contain statistical errors, errors of detection efficiency determination errors arising from fluctuations of the neutron flux during irradiation, errors of the sample weight and the errors of the cross sections of the monitoring reactions.

List of references

1. Nuclear Data Table Vol. 8 1-2, October 70.
2. P.Alexander and F.Boehm, Nucl. Phys. 46 /1963/ 108
3. D.C.Santry and J.P.Butler, Can.J.Phys. 42 /1964/ 1030
4. BNL-325 Report, Supplement N2, p.30-64-2
5. C.M.Lederer, J.M.Hollander and I.Perlman, Table of Isotopes, Wiley Sons, New York.

TABLE 1

Cross Sections for the  $^{111}\text{Cd}(n, n')^{111\text{m}}\text{Cd}$

$E_n$ MeV	mb
$3.4 \pm 0.2$	$214 \pm 64$
$4.2 \pm 0.7$	$430 \pm 51$
$12.9 \pm 0.2$	$463 \pm 49$
$13.0 \pm 0.3$	$248 \pm 46$
$13.4 \pm 0.3$	$187 \pm 16$
$13.9 \pm 0.3$	$144 \pm 19$
$14.5 \pm 0.3$	$148 \pm 26$
$15.0 \pm 0.3$	$148 \pm 13$
$15.4 \pm 0.3$	$92 \pm 14$
$16.0 \pm 0.3$	$125 \pm 35$
$16.6 \pm 0.1$	$111 \pm 59$

TABLE 2

Cross Sections for the  $^{112}\text{Cd}(n,2n)^{111\text{m}}\text{Cd}$  and  
 $^{112}\text{Cd}(n,p)^{112}\text{Ag}$  Reactions

$E_n$ MeV	$^{112}\text{Cd}(n,2n)^{111\text{m}}\text{Cd}$ mb	$^{112}\text{Cd}(n,p)^{112}\text{Ag}$ mb
$12.9 \pm 0.2$	$638 \pm 45$	
$13.0 \pm 0.3$	$677 \pm 32$	$16.0 \pm 2.9$
$13.4 \pm 0.3$	$616 \pm 28$	$15.7 \pm 1.7$
$13.9 \pm 0.3$	$684 \pm 36$	$15.9 \pm 1.3$
$14.5 \pm 0.3$	$675 \pm 32$	$18.6 \pm 1.6$
$15.0 \pm 0.3$	$647 \pm 30$	$22.4 \pm 1.9$
$15.4 \pm 0.3$	$623 \pm 29$	$19.5 \pm 2.3$
$16.0 \pm 0.3$	$756 \pm 46$	$24.9 \pm 4.4$
$16.6 \pm 0.1$	$664 \pm 42$	$23.8 \pm 5.3$
$17.4 \pm 0.3$	$624 \pm 53$	
$17.9 \pm 0.1$	$479 \pm 42$	

STUDY OF PROTON INELASTIC SCATTERING ON MAGNESIUM  
 ISOTOPEs AT 9.1 MeV

M.Herman, A.Marcinkowski, B.Zwięgliński, W.Augustyniak,  
 J.Bielewicz and W.Zych<sup>\*</sup>

Institute of Nuclear Research, Dept.of Nuclear Reactions, Warsaw

The inelastic scattering of protons on separated magnesium isotopes has been studied at an energy of 9.1 MeV on linear proton accelerator in Świerk. Particle spectra have been measured by two semiconductor

<sup>\*</sup> Present address: Department of Physics, Warsaw Institute of Technology

detectors with an overall energy resolution of 50 keV. One of the detector served as a beam and target monitor and the second one served for the angular distribution measurements. The intensities of inelastic groups have been established with the Berkeley peak-fitting code SAMPO [1]. In tables 1 to 3 the preliminary results of the measurements are collected. The absolute scale has been established by normalizing the cross sections at forward angles to the calculated values obtained with the aid of optical model code SNOOPY [2] and the parameters of Perey [3]. These are not very sensitive to the particular choice of the parameters of the optical model potential.

References:

1. T. Jorma, Routti UCRL-19452
2. P. Schwandt, The Optical-Model Search Routine SNOOPY, University of Wisconsin
3. F.G. Perey, Phys. Rev., 131, 745 1963

TABLE 1

Differential Cross Sections for the  $^{24}\text{Mg}(p,p)^{24}\text{Mg}$   
Reaction at 9.1 MeV<sup>x</sup>

$E_{\text{exc}} - J^{\pi}$	$0 - 0^+$	$1.37 - 2^+$	
$\theta_{\text{c.m.}}$ [deg]	$\sigma$ [mb·sr <sup>-1</sup> ]	$\theta_{\text{c.m.}}$ [deg]	$\sigma$ [mb·sr <sup>-1</sup> ]
36.4	210.0 <sub>±6.0</sub>	36.5	14.2 <sub>±0.7</sub>
		41.7	6.9 <sub>±0.3</sub>
46.7	67.0 <sub>±1.5</sub>	46.8	14.7 <sub>±0.5</sub>

<sup>x</sup> Normalized at 36.4 deg to the optical model value  $\sigma_{\text{el}} = 210 \text{ mb sr}$

TABLE 1 continued

$E_{exc} - J^{\pi}$	$0 - 0^+$	$4.37 - 2^+$	
$\theta_{c.m.}$ [deg]	$\sigma$ [mb·sr <sup>-1</sup> ]	$\theta_{c.m.}$ [deg]	$\sigma$ [mb·sr <sup>-1</sup> ]
51.8	36.7 $\pm$ 1.0	52.0	19.0 $\pm$ 0.6
57.0	18.4 $\pm$ 0.6	57.1	21.6 $\pm$ 0.7
62.0	10.9 $\pm$ 0.3	62.3	20.7 $\pm$ 1.4
67.2	10.1 $\pm$ 0.5	67.4	21.8 $\pm$ 0.6
72.2	12.7 $\pm$ 0.5	72.4	21.7 $\pm$ 0.7
77.3	14.7 $\pm$ 0.7	77.5	22.9 $\pm$ 0.8
82.4	15.2 $\pm$ 0.5	82.6	21.7 $\pm$ 0.6
87.4	19.5 $\pm$ 0.7	87.6	24.7 $\pm$ 0.8
92.4	22.5 $\pm$ 0.8	92.6	24.9 $\pm$ 0.3
97.4	21.7 $\pm$ 0.8	97.6	27.2 $\pm$ 0.8
102.4	19.8 $\pm$ 0.6	102.6	28.8 $\pm$ 0.8
107.3	18.1 $\pm$ 0.8	107.5	30.9 $\pm$ 1.0
112.2	17.1 $\pm$ 0.8	112.4	33.1 $\pm$ 1.0
117.2	14.4 $\pm$ 0.7	117.4	33.8 $\pm$ 0.9
122.0	11.6 $\pm$ 0.3	122.3	33.4 $\pm$ 0.7
127.0	14.9 $\pm$ 0.6	127.1	35.5 $\pm$ 0.9
131.8	14.6 $\pm$ 0.4	132.0	32.6 $\pm$ 0.7
136.7	18.5 $\pm$ 0.6	136.8	33.6 $\pm$ 1.0
141.5	23.2 $\pm$ 0.7	141.7	32.8 $\pm$ 1.0
146.4	21.8 $\pm$ 0.9	146.5	30.8 $\pm$ 0.9
150.2	24.7 $\pm$ 0.8	151.3	28.4 $\pm$ 0.9
156.1	21.6 $\pm$ 0.9	156.1	25.4 $\pm$ 0.9
160.6	23.3 $\pm$ 0.5	160.9	24.5 $\pm$ 0.5
165.6	22.9 $\pm$ 0.9	165.7	21.7 $\pm$ 0.8

TABLE 1 continued

4.12-4 <sup>+</sup>		4.24-2 <sup>+</sup>	
$\theta_{c.m.}$ [deg]	$\bar{\sigma}$ [mb·sr <sup>-1</sup> ]	$\theta_{c.m.}$ [deg]	$\bar{\sigma}$ [mb·sr <sup>-1</sup> ]
36.9	8.9 $\pm$ 0.5	36.9	4.5 $\pm$ 0.4
52.5	5.8 $\pm$ 0.3	52.5	10.9 $\pm$ 0.4
57.7	7.3 $\pm$ 0.4	57.7	10.3 $\pm$ 0.5
62.8	7.5 $\pm$ 0.4	62.9	11.1 $\pm$ 0.3
68.0	9.2 $\pm$ 0.4	68.0	10.1 $\pm$ 0.5
73.1	9.2 $\pm$ 0.4	73.1	9.6 $\pm$ 0.4
78.2	9.9 $\pm$ 0.5	78.2	10.1 $\pm$ 0.5
83.2	10.1 $\pm$ 0.4	83.3	8.0 $\pm$ 0.3
88.3	10.8 $\pm$ 0.5	88.3	7.9 $\pm$ 0.4
93.3	10.5 $\pm$ 0.3	93.3	6.9 $\pm$ 0.2
98.3	10.9 $\pm$ 0.4	98.3	6.1 $\pm$ 0.3
103.2	11.2 $\pm$ 0.4	103.3	5.6 $\pm$ 0.3
108.2	11.7 $\pm$ 0.5	108.2	5.1 $\pm$ 0.3
113.1	11.4 $\pm$ 0.6	113.1	5.1 $\pm$ 0.4
118.0	10.4 $\pm$ 0.5	118.0	4.3 $\pm$ 0.3
122.8	10.2 $\pm$ 0.3	122.9	2.8 $\pm$ 0.1
127.7	9.5 $\pm$ 0.4	127.7	3.7 $\pm$ 0.2
137.3	6.7 $\pm$ 0.3	137.4	4.4 $\pm$ 0.2
142.1	6.2 $\pm$ 0.3	142.1	4.1 $\pm$ 0.2
146.9	4.3 $\pm$ 0.2	146.9	4.9 $\pm$ 0.4
151.6	4.0 $\pm$ 0.2	151.7	5.3 $\pm$ 0.2
156.4	2.1 $\pm$ 0.2	156.4	6.5 $\pm$ 0.2
161.1	2.5 $\pm$ 0.1	161.1	5.4 $\pm$ 0.2
165.9	1.5 $\pm$ 0.1	165.9	6.8 $\pm$ 0.4

TABLE 1 continued

$5.24 - 3^+$	
$\theta_{c.m.}$ [deg]	$\bar{\sigma}$ [mb·sr <sup>-1</sup> ]
36.4	2.0 $\pm$ 0.2
41.5	2.4 $\pm$ 0.2
46.7	1.9 $\pm$ 0.1
57.0	2.2 $\pm$ 0.2
62.1	2.4 $\pm$ 0.1
67.2	2.6 $\pm$ 0.2
72.2	2.8 $\pm$ 0.2
77.3	2.8 $\pm$ 0.2
82.4	2.8 $\pm$ 0.2
87.4	2.5 $\pm$ 0.2
92.4	3.1 $\pm$ 0.1
97.4	3.0 $\pm$ 0.2
102.4	3.2 $\pm$ 0.2
107.3	3.3 $\pm$ 0.2
166.0	4.6 $\pm$ 0.3

TABLE 2

Differential cross sections for the  $^{25}\text{Mg}(p,p')^{25}\text{Mg}$   
reaction at 9.1 MeV<sup>x</sup>

$E_{\text{exc}} - J^{\pi}$	$0. - 5/2^+$	$0.59 - 1/2^+$	
$\theta_{\text{c.m.}}$ [deg]	$\sigma$ [mb·sr <sup>-1</sup> ]	$\theta_{\text{c.m.}}$ [deg]	$\sigma$ [mb·sr <sup>-1</sup> ]
31.1	175.4 <sub>±</sub> 19.9	31.2	0.612 <sub>±</sub> 0.012
36.3	158.3 <sub>±</sub> 2.8	36.4	0.749 <sub>±</sub> 0.049
41.5	122.5 <sub>±</sub> 2.0	41.5	1.020 <sub>±</sub> 0.064
51.8	56.0 <sub>±</sub> 0.9	51.8	1.078 <sub>±</sub> 0.062
62.0	38.9 <sub>±</sub> 0.7	62.1	0.976 <sub>±</sub> 0.065
72.2	36.8 <sub>±</sub> 0.6	72.2	1.085 <sub>±</sub> 0.117
82.3	33.2 <sub>±</sub> 0.5		
92.3	22.4 <sub>±</sub> 0.4	92.4	0.826 <sub>±</sub> 0.060
102.3	14.9 <sub>±</sub> 0.2	102.3	0.915 <sub>±</sub> 0.060
112.2	8.4 <sub>±</sub> 0.2	112.2	0.678 <sub>±</sub> 0.077
122.0	7.3 <sub>±</sub> 0.1		
131.8	9.1 <sub>±</sub> 0.2		
141.5	12.0 <sub>±</sub> 0.2	141.5	0.853 <sub>±</sub> 0.153
151.1	13.4 <sub>±</sub> 0.4	151.2	0.498 <sub>±</sub> 0.099
160.8	15.7 <sub>±</sub> 0.3	160.8	0.527 <sub>±</sub> 0.135

<sup>x</sup> Normalized at 51.8 deg to the optical model value

$$\sigma_{\text{el}} = 56.0 \text{ mb sr}^{-1}$$

TABLE 2 continued

$0.97 - \frac{3}{2}^+$		$1.64 - \frac{7}{2}^+$	
$\theta_{c.m.}$ [deg]	$\bar{\sigma}$ [mb · sr <sup>-1</sup> ]	$\theta_{c.m.}$ [deg]	$\bar{\sigma}$ [mb · sr <sup>-1</sup> ]
31.2	0.776 <sub>±</sub> 0.015	31.3	3.438 <sub>±</sub> 0.164
36.4	1.287 <sub>±</sub> 0.061	36.5	5.165 <sub>±</sub> 0.123
41.6	1.606 <sub>±</sub> 0.082	41.6	6.192 <sub>±</sub> 0.154
51.9	1.705 <sub>±</sub> 0.078	51.9	6.191 <sub>±</sub> 0.129
62.1	1.635 <sub>±</sub> 0.083	62.2	5.874 <sub>±</sub> 0.132
72.3	1.538 <sub>±</sub> 0.075	72.4	5.069 <sub>±</sub> 0.116
82.4	1.772 <sub>±</sub> 0.067	82.5	4.763 <sub>±</sub> 0.143
92.4	1.391 <sub>±</sub> 0.072	92.5	4.237 <sub>±</sub> 0.139
102.4	1.976 <sub>±</sub> 0.083	102.5	4.346 <sub>±</sub> 0.086
112.3	1.565 <sub>±</sub> 0.250	112.4	4.533 <sub>±</sub> 0.063
122.1	2.200 <sub>±</sub> 0.077	122.2	4.927 <sub>±</sub> 0.109
131.9	1.924 <sub>±</sub> 0.063	131.9	5.104 <sub>±</sub> 0.129
141.6	1.854 <sub>±</sub> 0.071	141.6	4.196 <sub>±</sub> 0.117
151.2	1.762 <sub>±</sub> 0.144	151.3	3.923 <sub>±</sub> 0.181
160.8	1.642 <sub>±</sub> 0.087	160.9	3.823 <sub>±</sub> 0.130

TABLE 2 continued

$1.96 - 5/2^+$		$2.56 - 1/2^+$	
$\theta_{c.m.}$ [deg]	$\bar{\sigma}$ [mb · sr <sup>-1</sup> ]	$\theta_{c.m.}$ [deg]	$\bar{\sigma}$ [mb · sr <sup>-1</sup> ]
31.3	1.154 <sub>±0.099</sub>	31.4	0.151 <sub>±0.037</sub>
36.5	1.649 <sub>±0.067</sub>	36.6	0.357 <sub>±0.027</sub>
41.7	1.961 <sub>±0.082</sub>	41.8	0.519 <sub>±0.039</sub>
52.0	1.968 <sub>±0.064</sub>	52.1	0.630 <sub>±0.037</sub>
62.3	1.807 <sub>±0.067</sub>	62.4	0.851 <sub>±0.046</sub>
72.4	1.861 <sub>±0.064</sub>	72.6	0.632 <sub>±0.037</sub>
82.6	1.578 <sub>±0.081</sub>	82.7	0.806 <sub>±0.057</sub>
92.6	1.615 <sub>±0.085</sub>	92.7	0.722 <sub>±0.053</sub>
102.6	1.461 <sub>±0.048</sub>	102.7	0.762 <sub>±0.036</sub>
112.4	1.505 <sub>±0.231</sub>	112.6	0.733 <sub>±0.177</sub>
122.3	1.603 <sub>±0.059</sub>	122.4	0.695 <sub>±0.043</sub>
132.0	1.794 <sub>±0.074</sub>	132.1	0.523 <sub>±0.046</sub>
141.7	1.755 <sub>±0.077</sub>	141.8	0.418 <sub>±0.042</sub>
151.3	1.993 <sub>±0.127</sub>	151.4	0.383 <sub>±0.061</sub>
160.9	2.544 <sub>±0.074</sub>	160.9	0.301 <sub>±0.033</sub>

TABLE 2 continued

$2.74 - \frac{1}{2}^+$ and $2.80 - \frac{3}{2}^+$		$3.40 - \frac{9}{2}^+$ and $3.44 - \frac{3}{2}^-$	
$\Theta_{c.m.}$ [deg]	$\bar{\sigma}$ [mb·sr <sup>-1</sup> ]	$\Theta_{c.m.}$ [deg]	$\bar{\sigma}$ [mb·sr <sup>-1</sup> ]
31.4	1.169 $\pm$ 0.082	31.5	1.633 $\pm$ 0.065
36.6	2.101 $\pm$ 0.058	36.7	1.984 $\pm$ 0.075
41.8	2.075 $\pm$ 0.104	41.9	2.331 $\pm$ 0.104
52.1	2.517 $\pm$ 0.096	52.2	2.690 $\pm$ 0.058
62.4	2.955 $\pm$ 0.135	62.5	2.387 $\pm$ 0.073
72.6	3.056 $\pm$ 0.122	72.8	2.403 $\pm$ 0.076
82.7	2.612 $\pm$ 0.103	82.9	2.473 $\pm$ 0.110
92.8	2.739 $\pm$ 0.292	92.9	2.388 $\pm$ 0.078
102.7	2.841 $\pm$ 0.066	102.9	2.624 $\pm$ 0.066
112.6	2.482 $\pm$ 0.801	112.8	2.594 $\pm$ 0.082
122.4	2.533 $\pm$ 0.114	122.5	2.021 $\pm$ 0.050
132.1	2.901 $\pm$ 0.338	132.2	2.313 $\pm$ 0.056
141.8	2.410 $\pm$ 0.281	141.9	2.061 $\pm$ 0.100
151.4	2.436 $\pm$ 0.136	151.5	1.985 $\pm$ 0.125
160.9	2.970 $\pm$ 0.197	161.0	2.089 $\pm$ 0.077

TABLE 2 continued

$3.90 - (\frac{5}{2}, \frac{5}{2})^+$		$3.97 - \frac{7}{2}^-$	
$\theta_{c.m.}$ [deg]	$\sigma$ [mb · sr <sup>-1</sup> ]	$\theta_{c.m.}$ [deg]	$\sigma$ [mb · sr <sup>-1</sup> ]
31.5	0.735 $\pm$ 0.033	31.6	0.591 $\pm$ 0.032
36.8	1.029 $\pm$ 0.115	36.8	0.807 $\pm$ 0.092
42.0	1.293 $\pm$ 0.156	42.0	0.907 $\pm$ 0.141
52.4	1.932 $\pm$ 0.063	52.4	1.349 $\pm$ 0.093
62.7	1.651 $\pm$ 0.151	62.7	1.281 $\pm$ 0.036
72.9	1.505 $\pm$ 0.135	72.9	1.111 $\pm$ 0.103
83.0	1.716 $\pm$ 0.103	83.1	1.434 $\pm$ 0.126
93.1	1.552 $\pm$ 0.086	93.1	1.602 $\pm$ 0.114
103.0	1.527 $\pm$ 0.175	103.1	1.434 $\pm$ 0.127
122.7	1.583 $\pm$ 0.070	122.7	1.272 $\pm$ 0.124
132.4	1.658 $\pm$ 0.112	132.4	1.461 $\pm$ 0.132
142.0	1.245 $\pm$ 0.137	142.0	1.170 $\pm$ 0.172
161.1	1.162 $\pm$ 0.251	161.1	1.113 $\pm$ 0.150

TABLE 2 continued

$4.06 - \frac{9}{2}^+$		$4.28 - (\frac{1}{2}, \frac{3}{2})^-$	
$\Theta_{c.m.}$ [deg]	$\bar{\sigma}$ [mb · sr <sup>-1</sup> ]	$\Theta_{c.m.}$ [deg]	$\bar{\sigma}$ [mb · sr <sup>-1</sup> ]
31.6	0.672 $\pm$ 0.058	31.6	0.302 $\pm$ 0.046
36.8	1.101 $\pm$ 0.074	36.8	0.503 $\pm$ 0.044
42.0	1.128 $\pm$ 0.118	42.1	0.541 $\pm$ 0.072
52.4	1.058 $\pm$ 0.113	52.5	0.753 $\pm$ 0.037
62.7	1.272 $\pm$ 0.073	62.8	0.718 $\pm$ 0.044
72.9	1.268 $\pm$ 0.180	73.0	0.610 $\pm$ 0.064
83.1	0.795 $\pm$ 0.129		
93.1	0.910 $\pm$ 0.107	93.2	0.499 $\pm$ 0.052
103.1	1.316 $\pm$ 0.132	103.2	0.702 $\pm$ 0.059
122.7	0.940 $\pm$ 0.125	122.8	0.395 $\pm$ 0.039
132.4	1.246 $\pm$ 0.164	132.5	0.612 $\pm$ 0.037
142.0	0.904 $\pm$ 0.206	142.1	0.430 $\pm$ 0.096
161.1	0.707 $\pm$ 0.227	161.1	0.475 $\pm$ 0.099

TABLE 3

Differential cross sections for the  $^{26}\text{Mg}(p,p')^{26}\text{Mg}$  reaction at 9.1 MeV<sup>x</sup>

$E_{\text{exc}} - J^{\pi}$ $0-0^+$		$1.84-2^+$	
$\theta_{\text{c.m.}}$ [deg]	$\sigma$ [mb·sr <sup>-1</sup> ]	$\theta_{\text{c.m.}}$ [deg]	$\sigma$ [mb·sr <sup>-1</sup> ]
31.2	385.8 <sub>+13.5</sub>	31.3	3.6 <sub>+0.2</sub>
36.3	282.2 <sub>+7.0</sub>	36.4	7.1 <sub>+0.3</sub>
41.5	130.8 <sub>+3.5</sub>	41.6	7.2 <sub>+0.3</sub>
46.6	85.8 <sub>+2.2</sub>	46.8	9.0 <sub>+0.3</sub>
51.7	60.6 <sub>+1.2</sub>	51.9	9.8 <sub>+0.4</sub>
56.9	45.5 <sub>+1.3</sub>	57.0	13.3 <sub>+0.5</sub>
62.0	37.4 <sub>+1.4</sub>	62.1	12.6 <sub>+0.5</sub>
67.1	28.7 <sub>+0.6</sub>	67.2	13.1 <sub>+0.3</sub>
72.2	27.6 <sub>+0.8</sub>	72.3	13.7 <sub>+0.5</sub>
77.2	21.5 <sub>+0.6</sub>	77.4	12.8 <sub>+0.4</sub>
82.3	22.4 <sub>+0.9</sub>	82.4	13.4 <sub>+0.6</sub>
87.3	17.6 <sub>+0.5</sub>	87.4	12.5 <sub>+0.4</sub>
92.3	13.5 <sub>+0.5</sub>	92.4	11.8 <sub>+0.4</sub>
97.3	11.1 <sub>+0.4</sub>	97.5	11.4 <sub>+0.4</sub>
102.3	8.0 <sub>+0.3</sub>	102.4	11.2 <sub>+0.4</sub>
107.2	5.9 <sub>+0.2</sub>	107.4	9.6 <sub>+0.4</sub>
112.2	3.8 <sub>+0.2</sub>	112.3	9.9 <sub>+0.4</sub>
117.1	2.9 <sub>+0.2</sub>	117.2	9.0 <sub>+0.3</sub>
122.0	3.5 <sub>+0.2</sub>	122.1	8.8 <sub>+0.3</sub>
126.9	2.8 <sub>+0.2</sub>	127.0	7.7 <sub>+0.3</sub>
131.8	4.0 <sub>+0.1</sub>	131.9	7.4 <sub>+0.3</sub>
136.6	3.6 <sub>+0.2</sub>	136.8	6.6 <sub>+0.2</sub>
141.5	5.5 <sub>+0.2</sub>	141.6	6.6 <sub>+0.2</sub>
146.3	7.3 <sub>+0.3</sub>	146.3	5.7 <sub>+0.3</sub>
151.2	8.8 <sub>+0.3</sub>	151.2	5.2 <sub>+0.2</sub>
156.0	12.0 <sub>+0.4</sub>	156.0	5.0 <sub>+0.2</sub>
160.8	11.8 <sub>+0.4</sub>	160.8	5.0 <sub>+0.3</sub>
165.6	13.6 <sub>+0.6</sub>	165.6	4.6 <sub>+0.3</sub>

<sup>x</sup> Normalized at 31.2 deg to the optical model value  $\tilde{\sigma}_{\text{el}} = 385.8 \text{ mb sr}^{-1}$

TABLE 3 continued

$2.94-2^*$		$3.94-3^*$	
$\Theta_{\text{obs}}$ [deg]	$\sigma$ [mb·sr <sup>-1</sup> ]	$\Theta_{\text{obs}}$ [deg]	$\sigma$ [mb·sr <sup>-1</sup> ]
31.3	2.5±0.2	31.4	1.03±0.14
		36.7	0.99±0.09
41.7	2.5±0.2		
47.0	3.1±0.2		
52.0	3.0±0.2	52.3	0.91±0.09
57.2	3.9±0.2	57.4	1.06±0.09
62.3	3.7±0.3	62.6	1.23±0.15
67.4	3.9±0.2	67.7	0.94±0.06
72.5	3.8±0.2	72.8	1.35±0.11
77.6	3.3±0.2	77.9	1.20±0.08
82.6	2.7±0.2	82.9	1.37±0.15
87.7	2.9±0.2	87.9	1.26±0.11
92.7	2.4±0.2	93.0	1.46±0.12
97.7	2.4±0.2	93.0	1.19±0.11
102.7	2.1±0.1	102.9	1.30±0.08
107.6	2.2±0.1	107.9	1.21±0.11
112.5	2.8±0.1	112.8	1.11±0.08
117.5	3.0±0.2	117.7	1.25±0.09
122.3	3.4±0.2	122.6	1.28±0.09
127.3	3.1±0.2	127.4	1.09±0.08
132.0	3.1±0.2	132.3	1.28±0.06
137.0	3.0±0.1	137.1	1.08±0.06
141.7	3.4±0.1	141.9	0.92±0.08
146.6	3.2±0.2	146.7	0.90±0.09
151.4	3.3±0.2	151.5	0.86±0.06
156.1	2.9±0.2	156.3	0.57±0.06
160.9	3.1±0.2	161.0	0.60±0.04
165.7	2.2±0.2	165.8	0.33±0.06

TABLE 3 continued

4.32-4 <sup>+</sup> and 4.33-(2) and 4.35-3 <sup>+</sup>		4.84-2 <sup>+</sup> and 4.90-4 <sup>+</sup> and 4.97-0 <sup>+</sup>	
$\Theta_{c.m.}$ [deg]	$\sigma$ [mb·sr <sup>-1</sup> ]	$\Theta_{c.m.}$ [deg]	$\sigma$ [mb·sr <sup>-1</sup> ]
31.5	3.01 $\pm$ 0.25	31.7	1.71 $\pm$ 0.19
36.8	3.38 $\pm$ 0.19	36.9	1.86 $\pm$ 0.14
		42.1	1.39 $\pm$ 0.12
		47.3	1.48 $\pm$ 0.14
52.4	3.52 $\pm$ 0.19		
57.5	3.54 $\pm$ 0.19	57.7	2.36 $\pm$ 0.15
62.7	4.00 $\pm$ 0.28	62.9	1.71 $\pm$ 0.07
67.8	4.00 $\pm$ 0.15		
72.9	3.72 $\pm$ 0.20	73.1	2.03 $\pm$ 0.11
78.0	3.95 $\pm$ 0.17	78.2	1.82 $\pm$ 0.05
83.1	4.06 $\pm$ 0.28	83.3	1.73 $\pm$ 0.07
88.1	3.68 $\pm$ 0.19	88.3	1.97 $\pm$ 0.14
93.1	4.00 $\pm$ 0.22	93.3	1.63 $\pm$ 0.12
98.1	3.52 $\pm$ 0.20	98.3	1.77 $\pm$ 0.12
103.1	3.77 $\pm$ 0.17	103.3	1.39 $\pm$ 0.11
108.0	3.94 $\pm$ 0.20	108.2	1.38 $\pm$ 0.11
112.9	3.58 $\pm$ 0.15	113.1	1.51 $\pm$ 0.09
117.8	3.66 $\pm$ 0.17	118.0	1.75 $\pm$ 0.12
122.7	4.20 $\pm$ 0.17	122.9	1.78 $\pm$ 0.11
127.5	3.77 $\pm$ 0.19	122.7	2.12 $\pm$ 0.14
132.4	4.05 $\pm$ 0.14	132.5	2.13 $\pm$ 0.09
137.2	3.52 $\pm$ 0.15	137.3	2.48 $\pm$ 0.12
142.0	3.08 $\pm$ 0.19	142.1	2.12 $\pm$ 0.14
146.8	2.87 $\pm$ 0.15	146.9	2.68 $\pm$ 0.19
151.5	2.86 $\pm$ 0.14	151.7	2.77 $\pm$ 0.12
156.3	2.81 $\pm$ 0.15	156.4	3.28 $\pm$ 0.17
161.1	1.85 $\pm$ 0.14	161.1	3.74 $\pm$ 0.20
165.8	2.15 $\pm$ 0.19	165.9	3.02 $\pm$ 0.20

## THE INVESTIGATION OF $^{158}\text{Eu}$ DECAY

K.J.Blinowska

Institute of Experimental Physics, University of Warsaw

E.F.Wessner

Studiengesellschaft für Atomenergie, Forschungszentrum, Seibersdorf.

$^{158}\text{Eu}$  decays by  $\beta^-$  emission to  $^{158}\text{Gd}$ , which is the double even deformed nucleus. Such nuclei have several possible modes of excitation, rotational and  $\beta$  and  $\gamma$  vibrational levels couple together, which complicates the theoretical description. It was felt, that an investigation of energy levels and transition probabilities in these nuclei would provide valuable information about the correlation of nucleonic motions.

The sources were prepared by means of an  $(n,p)$  reaction in 300 mg  $\text{Gd}_2\text{O}_3$  target, with mass 158 enriched to 92 %. The 14 MeV neutrons were produced by a SAMES generator. The  $^{158}\text{Eu}$  spectra were measured by means of a  $30\text{ cm}^3\text{ Ge/Li}$  spectrometer. PDP-8 computer was used as a multichannel analyser and performed a preliminary data analysis. The results were evaluated by means of a procedure based on Fourier transforms described in Ref. [1] and by a least squares fit.

The energies and the intensities of gamma rays emitted by  $^{158}\text{Eu}$  are presented in Table I. The decay scheme is shown in Fig. 1. The results published in [2] and [3] were helpful in establishing the low lying levels. The log ft values based on gamma - ray intensities given in Table I are presented in Table II.

The spins and parities were proposed on the basis of the log ft values and the transition probabilities. Since the adiabatic assumption of Alaga [4] does not apply for the most branching ratios in  $^{158}\text{Eu}$ , the Michailov's rule [5] was used for estimation of quantum numbers for several levels.

The experimental distribution of the beta strength was compared with that one calculated on the basis of Nilsson model (Fig. 2) using a deformed oscillator potential and taking into account the  $l^2$  term, the pairing interactions and both the quadrupole  $\epsilon_2$  and hexadecapole  $\epsilon_4$  deformations.

References

1. K.J.Blinowska, E.F.Wessner, Nucl. Instr. Meth. 118, 597 /1974/
2. A.F.Kluk et al., Z Physik 253, 1, /1972/
3. H.A.Baader, Risø - M - 1307
4. G.Alaga et al., Mat. Fys. Medd. Dan. Vid. Selsk. 29 No 9 /1955/
5. V.M.Mihailov, Izv. Akad. Nauk SSSR, Ser Fiz. 30, 1334 /1966/.

TABLE I

Energies and relative intensities of gamma rays observed in  $^{158}\text{Eu}$  decay

$\gamma$ -ray energy /keV/	relative intensity	$\gamma$ -ray energy /keV/	relative intensity
79.6 $\pm$ 0.2	46.4 $\pm$ 4.6	1141.7 $\pm$ 0.3	0.83 $\pm$ 0.08
182.1 $\pm$ 0.2	8.2 $\pm$ 1.1	1180.1 $\pm$ 0.3	0.90 $\pm$ 0.20
528.1 $\pm$ 0.2	6.1 $\pm$ 0.5	1183.8 $\pm$ 0.3	9.9 $\pm$ 0.9
606.6 $\pm$ 0.2	13.0 $\pm$ 0.6	1233.4 $\pm$ 0.3	0.69 $\pm$ 0.15
698.7 $\pm$ 0.2	4.0 $\pm$ 0.3	1260.4 $\pm$ 0.3	1.55 $\pm$ 0.20
743.3 $\pm$ 0.2	12.2 $\pm$ 0.9	1263.5 $\pm$ 0.2	7.50 $\pm$ 0.8
750.9 $\pm$ 0.3	0.82 $\pm$ 0.10	1283.7 $\pm$ 0.3	0.23 $\pm$ 0.05
764.0 $\pm$ 0.2	1.15 $\pm$ 0.16	1291.9 $\pm$ 0.3	0.96 $\pm$ 0.15
769.5 $\pm$ 0.2	1.9 $\pm$ 0.2	1300.8 $\pm$ 0.4	0.67 $\pm$ 0.07
779.1 $\pm$ 0.2	2.97 $\pm$ 0.25	1311.7 $\pm$ 0.3	1.06 $\pm$ 0.26
816.5 $\pm$ 0.2	1.08 $\pm$ 0.09	1323.2 $\pm$ 0.4	0.98 $\pm$ 0.9

TABLE I continued

$\gamma$ -ray energy /keV/	relative intensity	$\gamma$ -ray energy /keV/	relative intensity
824.3 $\pm$ 0.2	5.1 $\pm$ 0.4	1347.4 $\pm$ 0.3	5.9 $\pm$ 0.3
828.1 $\pm$ 0.3	0.85 $\pm$ 0.11	1433.1 $\pm$ 0.4	0.31 $\pm$ 0.12
852.6 $\pm$ 0.2	1.49 $\pm$ 0.10	1437.8 $\pm$ 0.4	0.17 $\pm$ 0.07
871.0 $\pm$ 0.2	5.1 $\pm$ 0.5	1529.4 $\pm$ 0.5	0.25 $\pm$ 0.08
897.9 $\pm$ 0.2	42.7 $\pm$ 1.9	1517.4 $\pm$ 0.5	0.12 $\pm$ 0.06
907.1 $\pm$ 0.2	6.0 $\pm$ 0.5	1713.4 $\pm$ 0.3	0.78 $\pm$ 0.10
917.0 $\pm$ 0.3	1.18 $\pm$ 0.14	1768.7 $\pm$ 0.4	0.22 $\pm$ 0.08
922.6 $\pm$ 0.2	5.9 $\pm$ 0.5	1849.3 $\pm$ 0.4	0.60 $\pm$ 0.15
925.7 $\pm$ 0.3	0.60 $\pm$ 0.15	1856.3 $\pm$ 0.5	0.56 $\pm$ 0.12
940.1 $\pm$ 0.3	1.2 $\pm$ 0.3	1883.4 $\pm$ 0.3	4.4 $\pm$ 0.3
944.3 $\pm$ 0.15	100	1929.8 $\pm$ 0.5	0.26 $\pm$ 0.08
953.4 $\pm$ 0.2	5.8 $\pm$ 0.5	1943.7 $\pm$ 0.3	4.8 $\pm$ 0.5
962.2 $\pm$ 0.2	6.0 $\pm$ 0.4	1957.1 $\pm$ 0.4	0.48 $\pm$ 0.10
977.0 $\pm$ 0.15	52.3 $\pm$ 2.1	1964.2 $\pm$ 0.3	0.47 $\pm$ 0.08
986.8 $\pm$ 0.2	4.9 $\pm$ 0.4	2022.8 $\pm$ 0.3	3.4 $\pm$ 0.2
999.1 $\pm$ 0.3	2.0 $\pm$ 0.2	2245.0 $\pm$ 0.4	1.36 $\pm$ 0.15
1003.9 $\pm$ 0.3	1.78 $\pm$ 0.4	2314.4 $\pm$ 1.2	0.19 $\pm$ 0.10
1005.7 $\pm$ 0.3	4.5 $\pm$ 0.6	2366.1 $\pm$ 0.4	2.4 $\pm$ 0.5
1034.8 $\pm$ 0.3	0.46 $\pm$ 0.10	2394.8 $\pm$ 0.6	0.38 $\pm$ 0.10
1061.5 $\pm$ 0.3	1.82 $\pm$ 0.20	2446.9 $\pm$ 0.4	2.6 $\pm$ 0.3
1107.9 $\pm$ 0.2	13.6 $\pm$ 1.0		
1116.0 $\pm$ 0.3	4.6 $\pm$ 0.4		
1137.8 $\pm$ 0.4	0.62 $\pm$ 0.08		

TABLE II

The values of log ft for the levels populated by  $^{158}\text{Eu}$  decay

Energy level /keV/	$\beta$ -feeding /%/	log ft
0	5	8.6
79.55	23.0	7.9
261.6	0.54	9.4
977.2	17.8	7.5
1023.8	21.4	7.3
1041.3	0.005	-
1187.1	1.96	8.3
1195.6	0.92	8.6
1260.4	0.77	8.6
1263.5	2.7	8.1
1265.5	0.15	9.3
1403.2	0.44	8.8
1517.4	0.07	9.4
1793.1	5.5	7.3
1848.1	2.5	7.6
1894.5	0.58	8.2
1930.0	6.1	7.1
1963.8	5.3	7.1
2023.8	2.6	7.4
2269.1	1.35	7.4
2324.8	2.5	7.0
2394.9	0.14	8.2
2446.3	1.2	7.1
2498.6	0.43	7.5

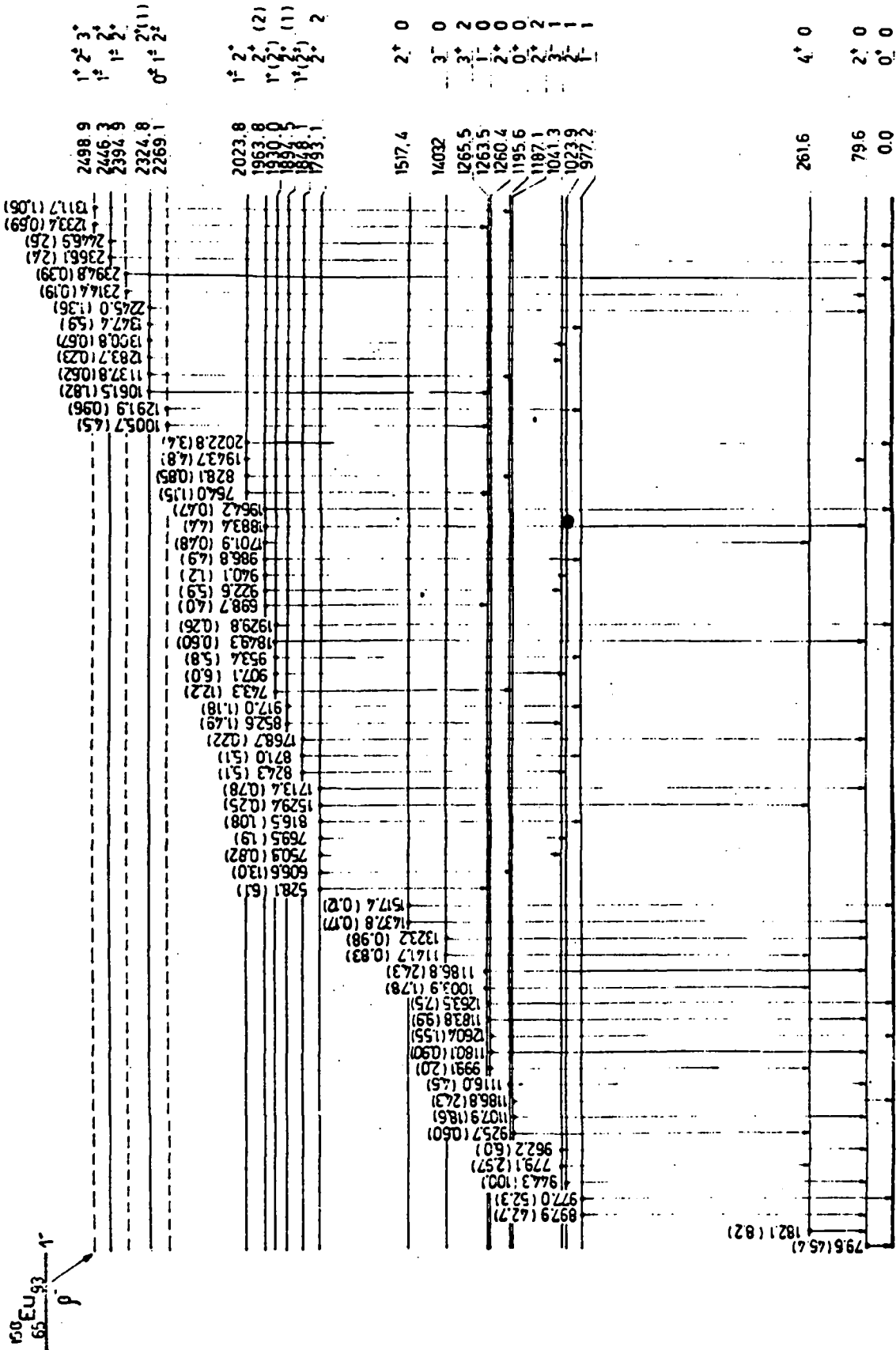


Fig. 1. The decay scheme of  $^{158}\text{Eu}$

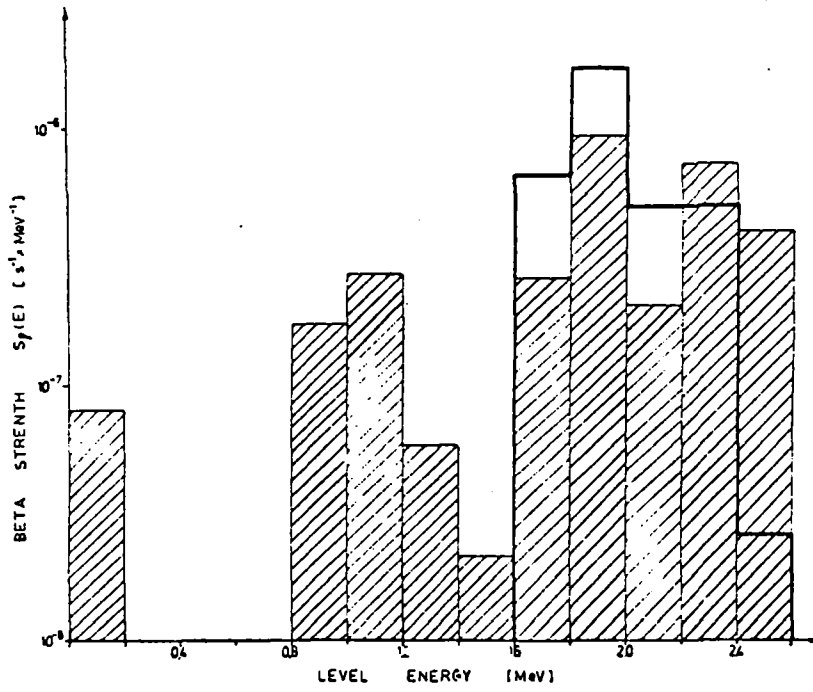


Fig. 2

## LEVELS IN $^{130}\text{Ba}$ FED FROM $^{130}\text{La}$ DECAY

Ch. Droste, T. Morek, M. Nowicki, J. Srebrny, W. Starosta

Institute of Experimental Physics, University of Warsaw

E. Sayed

University College for Women - Ein Shams University, Cairo, Egypt

The experiment was conducted on the 10 MeV proton linear accelerator of the Institute of Nuclear Research at Swierk. The  $^{130}\text{La}$  sources were produced in the  $^{130}\text{Ba} /p, n/ ^{130}\text{La}$  reaction. The energy of the proton beam was 9.5 MeV, the Q - value for the /p, n/ reaction being equal to - 6.5 MeV. 5 mg/cm<sup>2</sup> thick targets of enriched  $^{130}\text{Ba}$  were prepared from  $\text{BaCl}_2$ . After the activation was terminated, the gamma - rays were studied by means of 30 cm<sup>3</sup> Ge /Li/ detector with a resolution /FWHM/ of 2.4 keV and 2.9 keV for  $E_\gamma = 1$  MeV and  $E_\gamma = 2$  MeV respectively.

Measurements were performed of:

- a/ Gamma spectra from the La-Ba decay.
- b/ The decay of the gamma lines; this allowed us to identify the gamma transitions associated with the decay of  $^{130}\text{La}$ .
- c/ Gamma - rays from the La-Ba decay together with gamma - radiation from calibration sources / $^{56}\text{Co}$  or  $^{226}\text{Ra}$ /; This allowed us to improve the quality of gamma energy determination.

The energies and intensities of 28 gamma transitions following radioactive decay of  $^{130}\text{La}$  are listed in Table I. The level scheme of  $^{130}\text{Ba}$  was constructed basing on this data, taking also into account the information about low lying levels available from the previous works [1].

The level spins in  $^{130}\text{Ba}$  were assigned on the basis of log ft values and the rules given by Raman and Gove [2]. Some additional information was obtained when the gamma - transition probabilities were taken into consideration. The proposed decay scheme of  $^{130}\text{La}$  is presented in Fig. 1.

The results were compared with the theoretical collective model of Rohoziński et al. [3]. This model assumes a weak dependence of potential on the gamma deformation. When comparing the energies given by this model with the experimental values for levels with well defined spin and parity, a good fit was obtained /see Table II/. However, we encountered difficulties in explaining some of the experimental data:

1. In the energy region near 1.5 MeV we observed three levels with energies 1361 keV, 1477 keV, 1557 keV and spins 2, 3 or 4. Using this model a multiplet with level spin and parity of  $0^+$ ,  $3^+$ ,  $4^+$ ,  $6^+$  should be expected in the mentioned energy region. We could not observe the  $0^+$  and  $6^+$  levels because of the spin of the ground state of  $^{130}\text{La}$  which equals 3. The  $6^+$  level [ $E_{\text{excit}} = 1593 \text{ keV}$ ] was observed by Rotter et al. [4] and Ward et al. [5] in the  $/\text{HI}; \text{xn}/$  reaction. Among the three mentioned levels, two can have spin and parity  $3^+$  and  $4^+$  /as it is expected from the model/. The presence of the third level is not predicted by this model, however it can be explained by assuming that it is a collective level with  $I = 3^-$  /but there is no experimental evidence for this/.

2. Using this model we could not obtain the reduced transition probability  $B(E2; 2^+ \rightarrow 0^+)$  and the quadrupole moment  $Q_{2+}$  values comparable with the experimental ones.

#### References:

1. A. Abdul - Malek, R.A. Nauman, Nucl. Phys. A 108, 401, /1968/
2. S. Raman, N.B. Gove, Phys. Rev. C7, 1995, /1973/
3. S.G. Rohoziński, J. Srebrny, K. Horbaczewska, Z. Physik 268, 401 /1974/
4. H. Rotter, K.F. Alexander, Ch. Droste, T. Morek, W. Neubert, S. Chojnacki, Nucl. Phys. A133, 643 /1969/
5. D. Ward, F.S. Stephens, R.M. Diamond, Lawrence Radiation Laboratory, University of California, Report UCRL-18667 /1969/.

TABLE I

Gamma-ray energy /keV/	Gamma-ray intensity /arbitrary units/
357.4	100
453.2	4.9
544.5	18.8
550.7	29.8
569.4	2.9
576.0	2.5
649.6	1.7
718.2	3.2
801.2	0.7
822.2	0.9
866.5 / 0.4/	0.5
869.3	2.0
908.0	20.3
936.5	0.8
942.8	1.1
974.9	3.7
1003.6	9.3
1120.2	2.2
1152.3 / 0.3/	0.4
1171.1	4.3
1177.4	2.7
1200.1	3.3
1346.3	1.1
1438.8	2.7
1445.0	1.0
1487.3	0.9
1525.7	7.4
1721.7	2.0



TABLE II

Experimental and calculated energy levels in  $^{130}\text{Ba}$ .  
In the last column spins and parities of all possible levels belonging to the multiplets are given

$I_{\text{exp}}$	$E_{\text{exp}}/\text{keV}/$	$E_{\text{theory}}/\text{keV}/$	$I_{\text{theory}}$
$2^+$	357	363	$2^+$
$2^+, 4^+$	908, 902	895	$2^+, 4^+$
$6^+$	1593	1582	$0^+, 3^+, 4^+, 6^+$
$8^+$	2396	2408	$2^+, 4^+, 5^+, 6^+, 8^+$

HIGH-SPIN EXCITED STATES AND EVIDENCE FOR PARTICLE-CORE  
COUPLING IN THE N=83 NUCLEI  $^{145}_{62}\text{Sm}$  AND  $^{147}_{64}\text{Gd}$

J. Kownacki, Z. Haratym, J. Ludziejewski and Z. Sujkowski  
Institute of Nuclear Research, Dep. Phys. IA, Świerk  
05-400 Otwock, Poland

I. Adam

Charles University, Prague, 12116 Praha 2, Czechoslovakia

H. Ryde

Roskilde University Center, Roskilde, Denmark

High spin states in the  $^{145}\text{Sm}$  and  $^{147}\text{Gd}$  nuclei having one extra neutron outside the N=82 closed shell have been populated through the  $(\alpha, 3n\gamma)$  and  $(\alpha, n\gamma)$  reactions on the  $^{144}\text{Nd}$  and  $^{144}\text{Sm}$  enriched targets. Singles  $\gamma$ -ray,  $\gamma$ - $\gamma$  coincidence spectra, angular and time distribution of  $\gamma$ -rays with respect to the beam bursts have been measured. The level

schema proposed for  $^{145}\text{Sm}$  and  $^{147}\text{Gd}$  on the basis of the obtained results are shown in Fig. 1 and Fig. 2, respectively. From the time distribution of  $\gamma$ -rays it follows that the  $13/2^+$  excited states populated in these nuclei show the half life time  $T_{1/2} = 15.5 \pm 2.0$  ns in  $^{145}\text{Sm}$  and  $T_{1/2} = 23.5 \pm 5.0$  ns in  $^{147}\text{Gd}$ .

The hindrance factor:

$$G(\lambda=3) = \frac{B(E3)_{\text{exp}}}{B(E3, 1i_{13/2} \rightarrow 2f_{7/2})}$$

calculated for these half-life values are equal to 8.2 and 11.5 for  $^{145}\text{Sm}$  and  $^{147}\text{Gd}$  respectively. This enhancements of the E3 transitions indicates that the  $13/2^+$  states contain important contribution of the  $13/2^+$  member of the  $(2f_{7/2} \otimes 3^-)$  multiplet:

$$|13/2^+\rangle = |1i_{13/2}\rangle + \epsilon |(2f_{7/2} \otimes 3^-)_{13/2^+}\rangle$$

with  $\epsilon^2 = 40\%$  for  $^{145}\text{Sm}$  and  $\epsilon^2 = 59\%$  for  $^{147}\text{Gd}$ .

Also the lowest  $9/2^-$  states should be a mixing of the  $9/2^-$  member of the  $(2f_{7/2} \otimes 2^+)$  multiplet and the  $1h_{9/2}$  single particle state, while the lowest  $11/2^-$  states may be interpreted as being due to the coupling of a particle in the  $2f_{7/2}$  orbital to the  $2^+$  one - phonon state in the  $^{144}\text{Sm}$  and  $^{146}\text{Gd}$  core, respectively. The simplest and most probable interpretation of the ground state  $7/2^-$  and the  $3/2^-$  state is to describe them as due to the single-particle orbitals  $2f_{7/2}$  and  $2p_{3/2}$ , respectively.

The higher-lying states may be interpreted as due to the coupling of a neutron in the  $2f_{7/2}$ ,  $1h_{9/2}$  or  $1i_{13/2}$  orbital to the  $4^+$  and  $6^+$  two proton states in the  $^{144}\text{Sm}$  and  $^{146}\text{Gd}$  core, resulting in three particle states. The largest possible spin values achieved in the  $\nu(1i_{13/2})\pi(2d_{5/2}^2)$  and  $\nu(1i_{13/2})\pi(2d_{5/2}1g_{7/2})$  coupling are indeed  $21/2^+$  and  $25/2^+$  respectively.

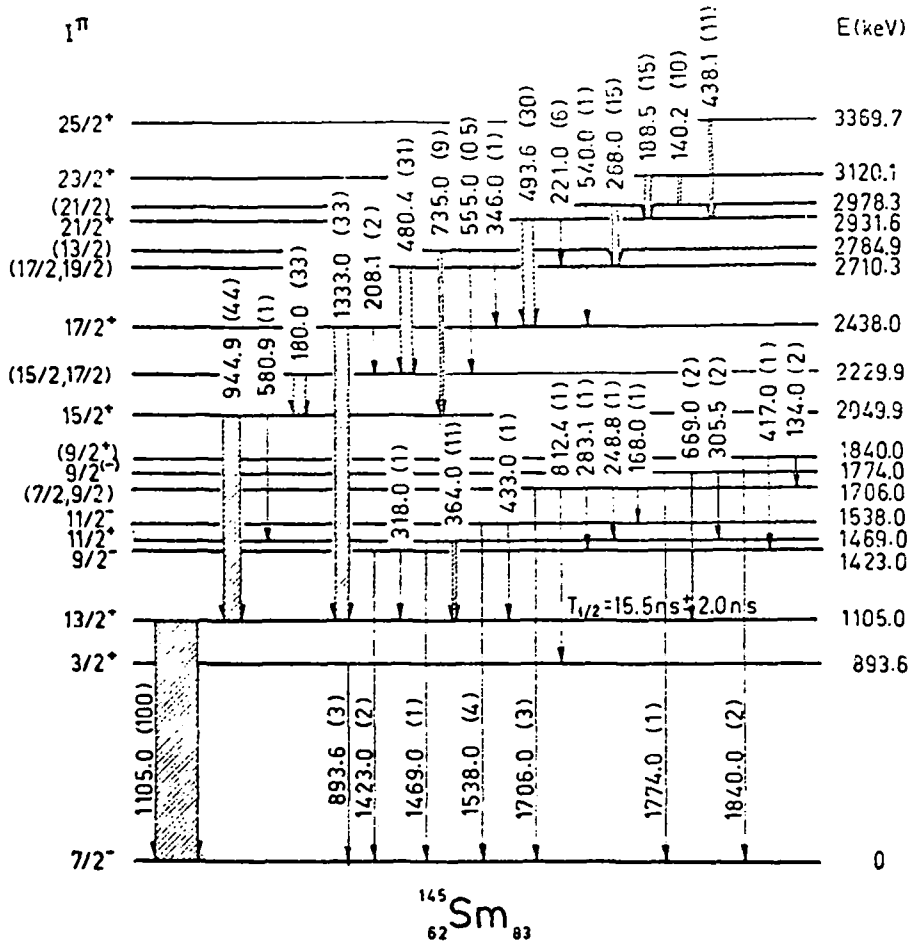


Fig. 1. Level scheme proposed for  $^{145}\text{Sm}_{83}$

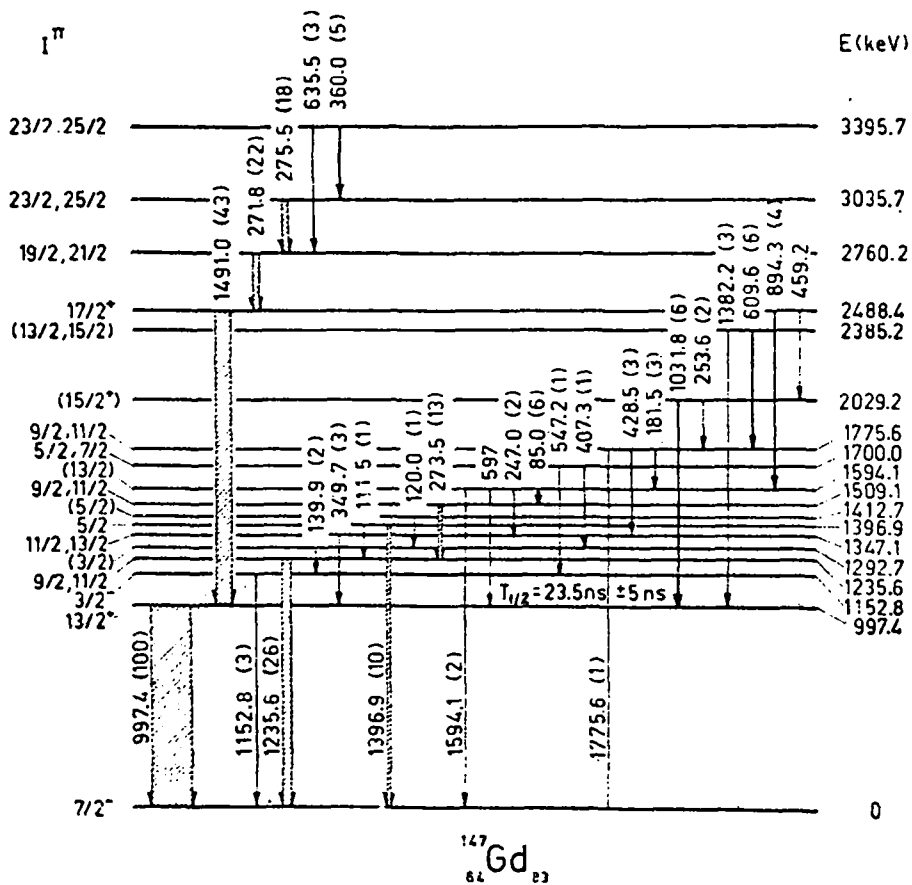


Fig. 2. Level scheme proposed for  $^{147}\text{Gd}_{83}$

HIGH-SPIN STATES IN  $^{144}_{60}\text{Nd}_{84}$  OBSERVED  
IN THE  $(\alpha, 2n)$  REACTION

L.E. De Geer and A. Kerek

Research Institute for Physics, 10405 Stockholm 50, Sweden

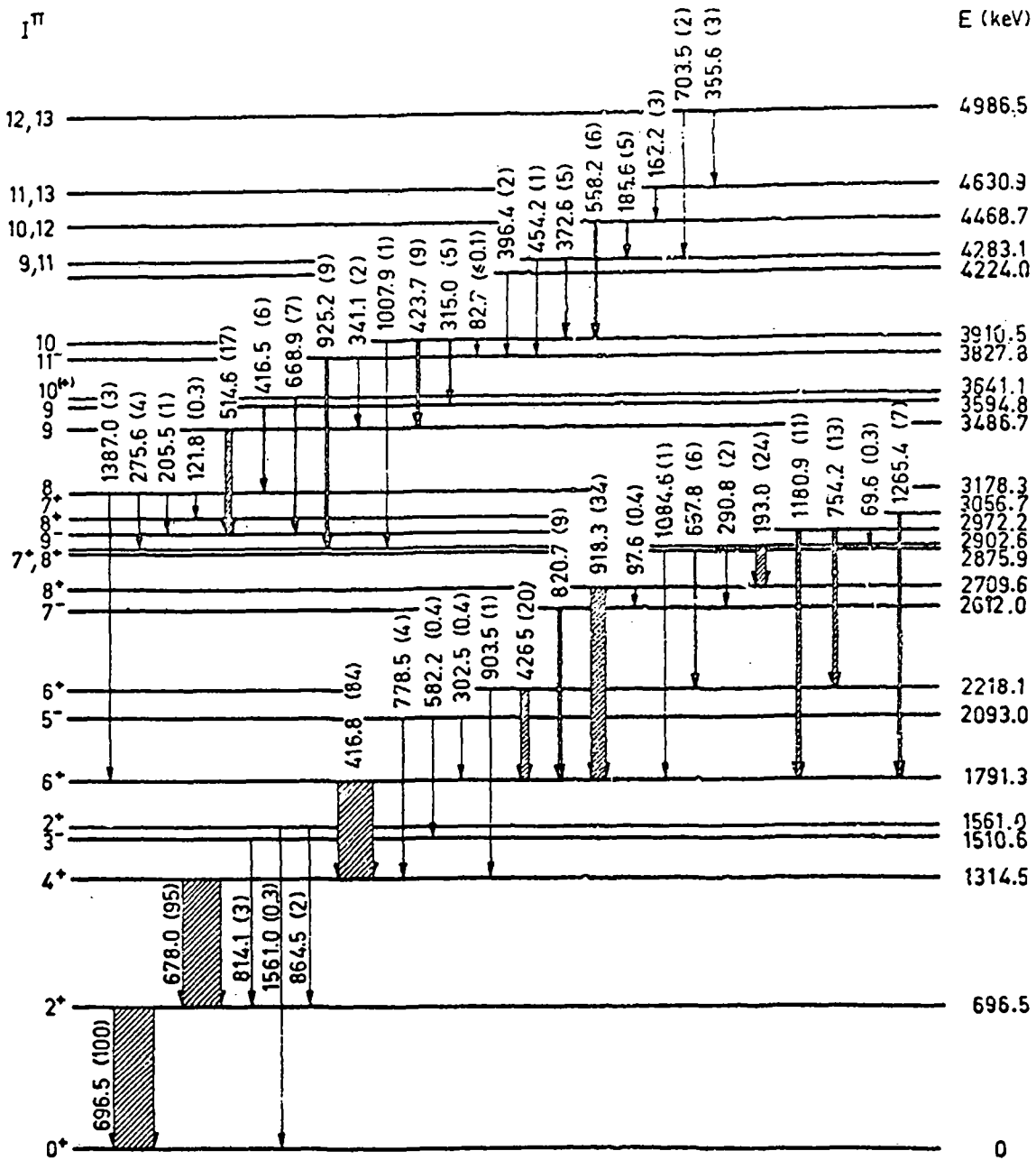
Z. Haratym, J. Kownacki and J. Ludziejewski

Institute of Nuclear Research, Dep. Phys. IA, Świerk

05-400 Otwock, Poland

The excited states of  $^{144}\text{Nd}$  have been studied using the  $^{142}\text{Ce}$   $^{142}\text{Ce}(\alpha, 2n\gamma)^{144}\text{Nd}$  reaction. Singles  $\gamma$ -ray,  $\gamma$ - $\gamma$  coincidence spectra, angular and time distributions of  $\gamma$ -rays with respect to the beam bursts have been measured by means of Ge(Li) detectors. The results obtained allowed to construct the level schema of  $^{144}\text{Nd}$  shown in Fig. 1. Energies and intensities /in parantheses/ are given. No isomeric states with half life longer than 1 ns have been found.

The majority of the observed states with spin values up to 12 can be explained as two-quasiparticle states. Several of the highest-spin states can be explained qualitatively as fourquasiparticle states.



$^{144}_{60}\text{Nd}_{84}$

Fig. 1. Level scheme proposed for  $^{144}_{60}\text{Nd}_{84}$



STATE COMMITTEE FOR NUCLEAR ENERGY

PROGRESS REPORT  
ON NUCLEAR DATA IN ROMANIA  
during the year 1974

compiled by  
S. RAPEANU,  
G. VASILIU

BUCHAREST, 1975

## INTRODUCTION

The report on the nuclear data activities in Romania presents the work carried out during 1974 as follows:

A. A brief review of activities connected with the computerising of compilation and evaluation processes of neutron nuclear data and the calculation of multigroup constants for reactors, activities which had an increased importance during this period.

B. A brief review of the activities concerning experimental measurements of neutron and non-neutron data.

C. A brief review of some activities regarding data compilation on reactions of producing strange particles.

D. Reports and abstracts regarding results obtained in the enumerated fields, published or to be published.

They do not claim to be complete or formal. In consequence their quoting or reproduction will be done only with permission of the authors.

Both theoretical and experimental works on nuclear data were carried on according to the National Nuclear Program, in accordance with "own requirements" and at the same time with the WRENDA requirements for data.

The above-mentioned activities were mainly carried out within the Institute for Atomic Physics - P.O.B. 5206, Bucharest, Romania, and the Institute for Nuclear Technology, P.O.B. 5204, Bucharest, Romania.

The new list of Romanian Nuclear Data Committee's members is given.

So as in previous years, part of the research was developed in collaboration with similar institutes abroad or during specialization stages.

We wish to thank the institutes and specialists that have cooperated with us or that have accepted Romanian specialists in their laboratories offering them optimum working conditions.

At the same time, we have benefited of the permanent support of I.A.E.A. and especially of the Nuclear Data Section, for which we express our grateful thanks.

We hope that in the future also, the multiple and efficient collaboration in this field will develop.

A. A BRIEF REVIEW OF THE ACTIVITIES OF COMPILATION, EVALUATION AND CALCULATION OF MULTIGROUP CONSTANTS FOR NEUTRON NUCLEAR DATA.

During 1974 this activity has developed significantly within the I.A.P. Nuclear Data Laboratory, as follows:

The DANEX experimental neutron nuclear data library was created, adopting a format similar to the CSISRS library and to that adopted by I.A.E.A. The storage is done on 9 track magnetic tape. Programs INDEX, SINTEX-1, SINTEX-2 and REDEX are used to introduce data on the magnetic tape and for their selective retrieval.

In the storage manner adopted, besides integral, differential and partial cross-sections, a number of quantities are introduced, characterizing thermal neutrons (frequency distribution functions  $f(\omega)$ ,  $g(\nu)$ ,  $\rho(\beta)$ , the scattering law

$s(\alpha, \beta)$  scattering cross-section of bound atom, etc.).

At present in the DANEX library are introduced neutron data for Be, O,  $D_1^2$ ,  $D_2O$ , Th-232, U-235, U-238, compiled in part within the laboratory and in part received through the kindness of the I.A.E.A. Nuclear Data Section.

With the view to later processing of data for evaluation by means of the PREG-1 and PREG-2 programs data processing is carried out using a DANEX tape as input. As output is obtained another tape containing renormalized numerical data, selected for a given element and ordered according to energies in a format compatible with the subsequent processing programs.

Further, by means of the LISTPLOT program, the cross-sections, the errors in cross-section and in energy are plotted on the printer to determine the discrepancies and gaps allowing the elimination of some data.

The fitting of experimental data is done by means of the SPN-SIGMA-FIT program by cubic splines, optimized by an  $\chi^2$  criterion. The last three programs are mutually compatible as input-output and start from a data tape of the DANEX library. To cover gap regions and to clarify some discrepancies in the experimental data, and in general for theoretical calculations, several programs were adopted or created, namely:

- In the field of thermal neutrons by means of the program SEINT, the neutron scattering law is calculated, as well as the total scattering cross-section, the inelastic cross-section, the elastic cross-section, the transport cross-section.

- In the field of fast neutrons program JUPITOR was adapted for computing the total, elastic, reaction cross-sections and the angular distributions through the coupled

channel theory.

- By means of one of the above mentioned programs preliminary evaluations for Be were performed.

An ABBN multigroup constant library for fast reactors was created. The EXDATA code prepares the tape of evaluated data using as input the DANEM evaluated data library. This tape is used by the ETDAN code for computing self-shielding factors in the resonance zone, as well as the infinite dilution sections and the inelastic transfer matrix for energy structures up to 50 groups.

The ETLIB code allows all necessary operations with multigroup data stored on the tape. The library contains at present ABBM multigroup constants for Be, U-235, U-238, Pu-239, Np-237, Th-232, D, O-16 in various energy structures.

In the field of thermal reactor data the efforts were concentrated on adapting some computing codes on generating, preparing and handling the data as follows:

- generating, from the scattering law of thermal multigroup sections (30 groups) through the BLITHE code;

- putting into operation the library of epithermal and fast multigroup data (code BINHDT, NUTAPE-II).

The BRT-1v UNIVAC 1108 code was also adapted for the IBM-370/135 (DOS) system, testing on a number of 9 cases.

The code HRG-3 was put into operation for the calculation of the epithermal and fast spectrum (and of multigroup cell constants) allowing thus, in conjunction with BRT-2R a complete description of a spectrum in a thermal reactor cell.

At the same time, within the Institute for Nuclear Technology (I.N.T.) nuclear data activity is closely connected

with core physics calculations for thermal and fast reactors, fuel burn-up, shielding, neutron dosimetry and the calculations regarding nuclear fuel development.

Interest is directly connected with evaluated nuclear data which can be transformed in multigroup model as well as general microscopic multigroup sets.

In collaboration with the I.A.P. nuclear data laboratory, a calculation program for generating multigroup data in ABBN scheme was elaborated.

I.N.T. is also concerned in the improvement of multigroup nuclear data using integral experiments.

In this respect a neutron standard spectrum generating facility was built.

#### B. BRIEF REVIEW ON ACTIVITIES REGARDING EXPERIMENTAL NUCLEAR DATA MEASUREMENTS.

Within the nuclear physics sections of the I.A.P., the activity of obtaining experimental nuclear data was continued and developed in 1974.

As regards the material basis which lied at the bed-rock of these measurements, it did not indicate an obvious development during this period.

It is however to be mentioned that the semiconductor detectors and most of the new modules and electronic devices were of own production.

The main facilities used were:

- the U-120 cyclotron, tandem F-M, betatrons, and the VVR-S reactor.

At the cyclotron were approached the subjects for which the weak energy resolution of the bombarding beam had no influence on the accuracy and value of experimental results.

The following measurements were carried out:

- neutron interaction with energies of the MeV order with the isotopes of boron;
- obtaining and study of new fissionable isomers of the Am, Pu, U, region;
- measuring the angular distributions of neutrons resulted from reactions (p, n) and ( $\alpha$ , n) on medium nuclei;
- simulation of irradiation defects produced by fast neutrons by irradiation with alpha particles.

Another category of measurements performed at the cyclotron was that connected with obtaining of non-neutron data of large use in the economical and social life as for instance:

- measurement of excitation functions of some reactions to determine the optimum output of producing new radioisotopes which had to producing isotopes of Fe, F, Co, Ga and I within the I.A.P.;
- measuring production sections of fluorescence X rays by charged particle and neutron activation.

This activity is supported in part by I.A.E.A.

The first results of these measurements were used to determine the concentration of elements in soil and subsoil and in a number of applications in metallurgy, mining and medicine.

Another group of measurements aimed at accumulating new informations on the atom nucleus and the mechanisms of producing

nuclear reactions:

- measurements on the lifetime of excited nuclear states in the range  $10^{-10}$  -  $10^{-15}$  sec by the method of attenuating the Doppler (DSMA) and Planger shift;

- obtaining of new isomers and determination of g factors for medium nuclei.

This category of measurements was much developed especially at the I.A.P. tandem, namely:

- $\gamma$  spectroscopy in heavy ion reactions,

- study of analog isobar resonances and of some anomalies in the excitation functions (d, p), and (p, p) on opening other channels,

- measurement of angular distributions for the particles resulted from reactions with transfer of one or more nucleons,

- measurement of internal conversion X rays and of gamma rays

We appreciate that the results obtained are of real value by the novelty of their scientific content.

Using the betatron accelerators, a number of measurements were performed on the cross-section of the reaction  $Ta^{181}(\gamma, xn)$  as well as the delayed released gamma rays by photofission of natural and enriched uranium.

At the I.A.P. reactor the research carried out was meant to supply new neutron data:

- study of the behaviour of some material for thermal, epithermal neutron transmission and simultaneously of neutrons and gamma rays,

- analysis by the method of delayed neutrons of U and Th from geological samples,

- calculation of correlation coefficients between neutron reduced widths and the binding energy of the neutron in nuclei of isotonic group,

- high accuracy absolute determination of neutron fission cross-section of  $^{235}\text{U}$  (also object of I.A.E.A. contract).

By thermal neutron techniques determination were made on static and dynamic structure for some metals and molecular systems in liquid and solid state.

#### C. SHORT REVIEW ON THE ACTIVITY OF COMPILATION OF DATA FOR STRANGE PARTICLE PRODUCTION

In the High Energy Laboratory of the Institute for Atomic Physics, the activity of compilation of data on reactions with strange particle production has been continued. During the year 1974 in collaboration with the Joint Institute for Nuclear Research - Dubna, the University of Bucharest and the University of Helsinki (the BUDHE Collaboration), the data on cross-sections for strange particle production in proton-proton collisions have been compiled. Also, the compilation of cross-sections for strange particle production in  $\pi^-p$  collisions has been up dated.

The group activity has been extended to data compilation on mean strange particle multiplicities. Moreover, the dependence of the mean multiplicities of strange particle production on energy has been investigated, the available data being parametrized in a fashion interpretable within the framework of some theoretical models. A comparative study of the dependence on energy of the mean multiplicities of strange and non-strange particles has been done.

ROMANIAN NUCLEAR DATA COMMITTEE

1. N. Andreescu : Institute for Nuclear Technologies  
(co-opted) Colibași - Pitești
2. G. Baciuc : Institute for Atomic Physics  
Bucharest
3. V. Cuculeanu : Institute for Nuclear Technologies  
Colibași - Pitești
4. M. Ivașcu : Institute for Atomic Physics  
Bucharest
5. N. Mateescu : Institute for Atomic Physics  
Bucharest
6. M. Petrașcu : Institute for Atomic Physics  
Bucharest
7. S. Râpeanu : Institute for Atomic Physics  
(chairman) State Committee for Nuclear Energy  
Bucharest
8. G. Vasiliu : Institute for Atomic Physics  
(co-opted) Bucharest

D.1. INDEX, SINTEX AND REDEX - PROGRAMS FOR THE STORAGE AND RETRIEVAL OF THE EXPERIMENTAL NEUTRON NUCLEAR DATA -  
S. Mateescu, G. Vasiliu

According to I.A.E.A. recommendations concerning computerised neutron nuclear data libraries, the program INDEX assures the storage of the typical neutronic nuclear data on magnetic tapes.

The program SINTEX retrieves compressed information regarding the institute, laboratory, first author, isotope and reaction type, energy range, number of experimental points, for a fast and qualitative analysis of the data.

The program REDEX retrieves and prints all information regarding a given isotope for one or more reaction types.

2. PREG-1 AND PREG-2 - PROGRAMS FOR THE PROCESSING OF THE NEUTRON NUCLEAR DATA - G. Vasiliu, S. Mateescu

The program PREG-1 selects from a DANEX tape a minimum quantity of information for identification of data and numerical data, generating an output tape BL 1 for a given isotope and reaction type.

Any later processing of these data can start with this tape which is shorter than the original DANEX tape.

The program PREG-2, using the BL 1 tape generated by PREG-1 as input, made uniform the data units, made the renormalization of the data and excludes some data.

As output the program PREG-2 generates the tapes BL 2 or BL 3, respectively.

3. LISTPLOT - A PROGRAM FOR THE PLOTTING OF THE EXPERIMENTAL AND/OR COMPUTED NEUTRON DATA - G. Vasiliu, S. Mateescu

Using as input the tape BL 2 generated by PREG-2, the program LISTPLOT made on the printer, a plot of nuclear cross-sections, energy errors and cross-sections errors from different references with different signs. The plot is made on 11 energy subranges between  $10^{-3}$  eV and 20 MeV with a particular scale for

each range or with a scale for all ranges.

According to the extreme values ratio of the quantity to be plotted, the scales can be lin-lin, log-lin, and sqrt-lin.

Because of the large number of points the program made averaged values for the all points arising from one reference to be plotted at one energy.

This type of plot is used for the analysis and selection of the data according their quality for evaluation.

Using the tape BL 3 with the complet processed data, the program permites the plotting with the same sign of the weighted averaged data to choose the knots for their fitting with the programe SPN-SIGMA-FIT.

4. SPN-SIGMA-FIT - PROGRAM FOR FITTING OF NUCLEAR DATA -  
- S. Râpeanu, G. Vasiliu, S. Mateescu

The program SPN-SIGMA-FIT represents a chain of two programs, SPN for fitting of the data using cubic splines and the program SIGMA for the optimization of the spline's parameters by  $\chi^2$  criterion. Both SPN and SIGMA programs, contain subroutines for the calculation of interpolated cross-sections, for plotting the experimental, computed and optimised data.

They print also tables containing energies, experimental cross-sections by initial and optimised splines and suitable errors, allowing a fast analysis of the results.

5. SEINT - A PROGRAM FOR THE CALCULATION OF SCATTERING LAW  
AND OF SOME NEUTRON CROSS-SECTIONS IN THERMAL ENERGY RANGE  
- C. Munteanu, N. Mateescu

The program computes the scattering law of neutron, the total scattering cross-section, the inelastic cross-section, the elastic cross-section and the transport cross-section for thermal neutrons.

The incoherent approximation is taken into account and the multiphonic extension is used.

For  $2W > 6$  the program uses "the short time" extension.

6. A MODIFIED VERSION OF THE PROGRAM JUPITOR FOR THE CALCULATION OF THE CROSS SECTIONS BY THE COUPLED CHANNEL THEORY -

S. Mateescu, E. Bădescu, N. Drăgan

The program computes the total, elastic and reaction cross-sections, and the angular distributions of the secondary neutrons. Using the coupled channel theory for nuclear reactions (T. Tamura), the program takes into account the case of collective nuclei: vibrationales (permanently deformed) and rotationales (temporary deformed). The original version has been phased and requests now only 165 k bytes memory. It is compatible with IBM-IAP computer.

7. COMPUTATION PROGRAM FOR GENERATION OF GROUP CONSTANTS FOR FAST REACTORS - D. Gheorghe, V. Cuculeanu

The program conceived in the year 1973 was accomplished and the first execution tests were done.

Using the A.B.B.N. schema, the code computes the multigroup cross-sections (total, fission, capture, elastic and inelastic scattering) for infinite dilution, the selfshielding factors for six dilutions, the average number of neutrons per fission, the mean logarithmic energy decrease per scattering and the average cosine of the scattering angle.

The code accepts maximum 50 groups.

The code is optimized, using a 189 kbytes memory, and a file on disk of 20 cylinders.

Up to now we have made calculations for U-235, U-238, Pu-239 with 26 groups and for Be, Nb, O, D with 40 groups.

In order to develop this program we intend to introduce special subroutines to compute the elastic scattering matrix and the multigroup constants for the  $P_N$  approximations.

8. BRT-2R- AN IBM 370/135 VERSION OF THE BRT-1 CODE - I. Preda

BRT-2R is a transport code which computes the thermal neutron spectrum depending on the position into one reactor cell.

Initiated by Honeck, the code has been developed and improved by C.L. Bennet et al. (BNWL 1434), on UNIVAC 1108 computer. The subroutines SETDAR, OPDMWT, CLDAWT, have been removed depending on the UNIVAC 1108 system.

Consequently we lost some facilities of the program as the random access possibility to the library.

The main modifications have been: passing to the sequential access to the data library for thermal neutrons by modifications of the RBLITHE code, which generates the thermal multigroup constants from the scattering kernels and by rewriting the TAPISO subroutine.

The other insignificant modifications are: the changing of specific formats of the UNIVAC-1108 version and the reducing of some code dimensions (consequently the program allows up to 20 spaced points and 5 mixtures).

The program has been multiphased too, and has been checked for 9 control cases.

9. PRESENT STATUS OF THE MULTIGROUP NUCLEAR DATA SET FOR FAST BREEDER REACTORS AT THE INSTITUTE FOR NUCLEAR TECHNOLOGY -

V. Cuculeanu, D. Mocioiu

During the year 1974 we have made a great effort in order to implement at I.N.T. a nuclear data file containing the A.B.B.N. set, 1964 and 1972 versions, and those published by Cosini and Salvatores [RT/FI (72)44] .

He and Cl were taken from Huschke's paper [KFK - 770] .

We have now data for Mn and Co.

We have also given attention to the development of the computer codes for processing basic multigroup data in such a way to be compatible with criticality calculating codes.

In this respect, we can mention the PRESEC code, which calculates the macroscopic cross-sections for the homogeneous zones and the BIZON code used for the fast reactor two-region cylindrical cells in square lattice.

10. INES - INT - STANDARD NEUTRON SPECTRUM IN THE INTERMEDIATE ENERGY RANGE - I.Gîrlea, A.Thurzo, B.Cîrstoiu, P.Ilie,

L. Moisin

In order to establish neutron properties of the INES-INT facility during 1974 neutron measurements and calculations begun.

The flux characteristics in the empty cavity have been measured as follows: absolute thermal flux, spatial distribution of thermal neutrons and Cd ratio. These measurements have been necessary for the knowing of the neutron properties of INES - INT facility and for the establishing of

experimental conditions for comparison between the following system: INES-INT - Bucharest Romania, - Mol, CEN/SCK Belgium and NISSUS - Imperial College of Science and Technology - London - England.

Calculations have shown the spectra in the two systems Mol and INES - INT are the same (or identical within calculations approximation scheme) but differ to some extent from NISSUS spectrum, due different geometry of the English driver.

The measurements of neutronic spectrum by spectrometric method with semiconductors with  $\text{Li}^6$  deposits have been carried out by joint efforts of CEN/SCK Mol and INT.

On this occasion, the experimental conditions necessary for measurements (as reactor power, detector locations) have been established.

#### 11. STATISTICAL PARAMETERS FOR TWO La ISOTOPES FROM

#### $^{134}\text{Ba}(p,n)^{134}\text{La}$ AND $^{136}\text{Ba}(p,n)^{136}\text{La}$ REACTIONS -

Elena Nicuți, R. Dumitrescu

The level density parameter "a" is of essential importance for the nuclear level density calculation generally used in cross-section evaluation in the frame of the statistical model of the nuclear reactions.

Although, in the last time, the pre-equilibrium decay model was successful in explanation of the apparent variation, with bombarding energy of the level density parameter of a certain nucleus, however, the absolute value predicting of the cross-sections remains an open problem yet.

As a result of the experimental evidence accumulated, it has remained an established fact that, the more precise determination of the level density parameter can be obtained from angular distributions of the emitted particles in reactions with compound - nucleus formation, on condition that the real statistical character of the respective reaction be verified.

This condition is realised by choosing low energies for projectile particle and for emitted particle especially at a backward angle against the bombardment particle direction, where the mechanism of reaction is practically statistical.

In this sense, the present work had as purpose the determination of the statistical parameters of some elements situated in the heavy mass region to complete the picture of the statistical parameter values for isotopes unstudied yet.

Thus, was studied the lantan element through two of its isotopes namely  $^{134}\text{La}$  and  $^{136}\text{La}$  as residual nuclei in  $^{134}\text{Ba}(p,n)^{134}\text{La}$  and  $^{136}\text{Ba}(p,n)^{136}\text{La}$  reactions. The information concerning level densities was obtained from statistical emission study of the neutrons resulted from the reactions afore mentioned and the analysis of the experimental results was made in the frame of the Fermi-gas model of the nucleus.

The values of the level density parameter "a" and of the nuclear temperature T for the isotope  $^{134}\text{La}$  were extracted from an energy spectrum at  $130^\circ$  angle, at excitation energy of 3 MeV and for a bombarding energy  $E_p = 9.158$  MeV. The values of the some parameters for the isotope  $^{136}\text{La}$  were extracted from an energy spectrum at  $150^\circ$ , at excitation energy of 4 MeV and the same bombarding energy.

The results obtained are indicated in table I and they are in very good accord with the values published by other authors for some elements situated in this mass region.

Table I

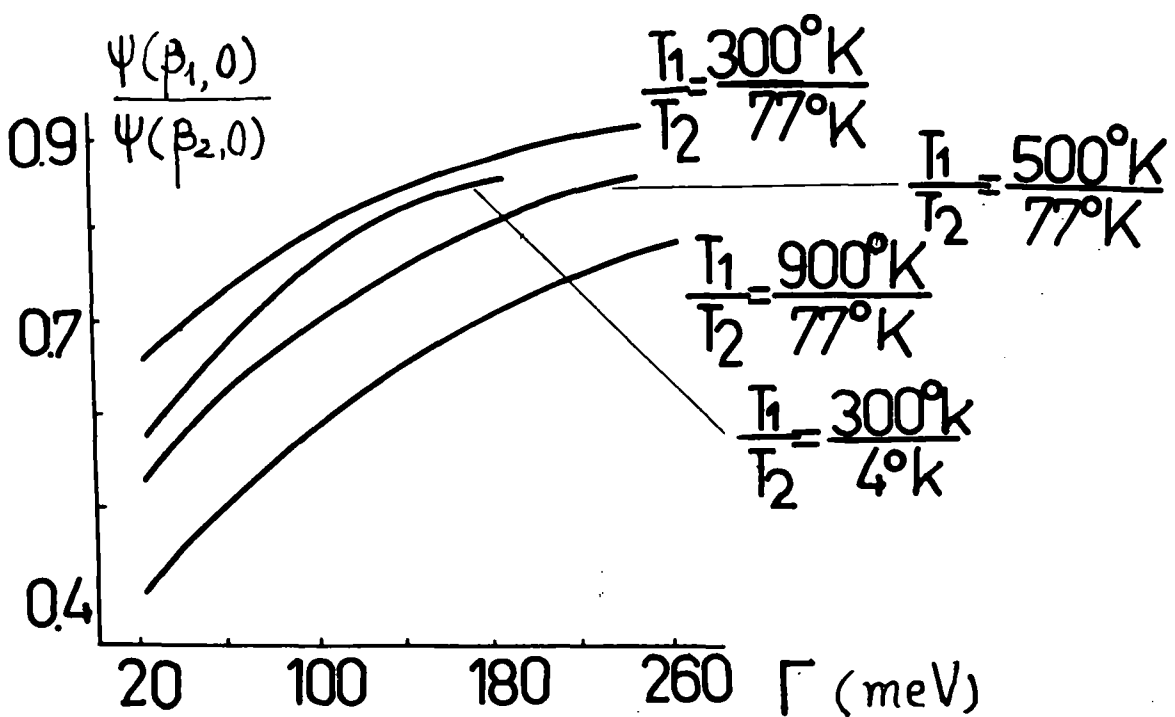
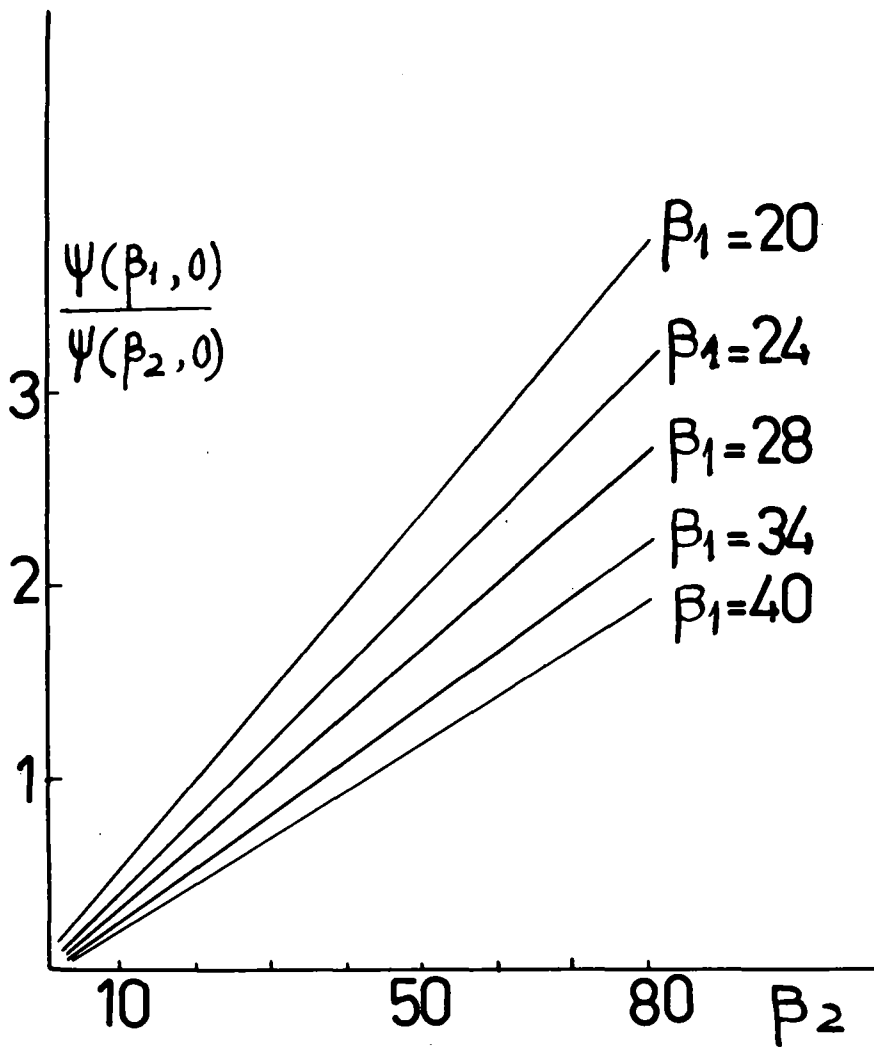
Element	Parameter	
	a(MeV <sup>-1</sup> )	T(MeV)
$^{134}\text{La}$	17.2 ± 4.1	0.579 ± 0.069
$^{136}\text{La}$	17.3 ± 4.1	0.633 ± 0.075

The curves of angular distribution were also analysed at the mentioned bombarding energy for some intervals of excitation energy in  $^{134}\text{La}$  and  $^{136}\text{La}$ .

The value practically constant of the double-differential section at angles larger than  $90^\circ$ , on all considered excitation energy region is a proof that in our case, the emission at backward angles is purely statistical and that the values of the parameters obtained in the present work are reliable.

## 12. THEORETICAL AND EXPERIMENTAL RESEARCHES OF DOPPLER EFFECT ON THE NEUTRON RESONANCES - V.Mateiciuc, M.Constantinescu, T.Stadnicov.

The shape of the neutron absorption line for an atom which is bound in a crystal lattice, was calculated by Lamb. In this case, the neutron cross-section for a weak lattice binding, in the neighbourhood of the ab-



sorption resonance is given by the following relation:

$$\sigma(\beta, x) = \sigma_p + \left(\frac{E_0}{E_n}\right)^{1/2} \sigma_0 \Psi(\beta, x)$$

where,  $\sigma_p$  is the potential cross section,  $E_0$  and  $E_n$  are the neutron energies in laboratory coordinates,  $\sigma_0$  defines the total cross section for  $x = 0$  and  $\Psi(\beta, x)$  is the so called Doppler function.

For two temperatures, the ratio of the neutron cross-sections is:

$$\sigma_1/\sigma_2 = \Psi(\beta_1, x)/\Psi(\beta_2, x)$$

When  $x = 0$ , the Doppler function depends only of  $\beta$ , which is given by the relation:

$$\beta = \frac{2\Delta}{\Gamma}$$

Where,  $\Delta$  is a function of the temperature and  $\Gamma$  the total neutron width.

The Doppler functions can be calculated for different temperatures and  $\Gamma$  widths.

Two problems can be resolved:

- when the ratio  $\sigma_1/\sigma_2$  at two temperatures  $T_1$  and  $T_2$  is known, the total neutron width can be calculated, and,

- when the total neutron width,  $\Gamma$ , and the neutron cross section,  $\sigma_1$ , at room temperature are known, the neutron cross section,  $\sigma_2$ , for the other temperature can be calculated.

Fig. 1 represents the ratio of Doppler functions for different  $\beta_1$ , and  $\beta_2$ , and Fig.2, the variation of  $\Psi(\beta_1, 0)/\Psi(\beta_2, 0)$  versus  $\Gamma$  for different temperatures.

The curves of fig. 1, can be used in the determination of the neutron cross section for other temperatures and the curves of fig. 2 for the total  $\Gamma$  width determination.

Experimentally, these graphics have been verified for the nuclear parameters determination at 6.24 eV resonance of  $^{121}\text{Sb}$ .

13. THE EFFECTIVE CROSS SECTION OF THE  $^{181}\text{Ta}(\gamma, xn)$  REACTION -

D. Catană, G. Baciuc. V.I.R. Niculescu

The systematics of the giant dipole resonance, which characterizes the absorption of electromagnetic radiation by nuclei in the energy range from about 10 to 30 MeV, is of a great interest today. Such experimental results are necessary in order to check different competing nuclear models for computation of photoabsorption cross-section; these cross-sections are needed in the evaluation of the  $(n, \gamma)$  cross-sections.

In a continuing series of experiments, the photonuclear group at the Betatron Laboratory has undertaken to conduct such a survey. The measurements reported here on the  $^{181}\text{Ta}$  nucleus is part of the investigation regarding heavy nuclei.

The yield curve of the  $^{181}\text{Ta}(\gamma, xn)$  reaction has been measured from the threshold of the reaction up to 23 MeV with 0.1 MeV spacing, and a statistical error less than 1%. The computation of the total photoneutron cross-section from the measured yield curve of  $^{181}\text{Ta}(\gamma, xn)$  reaction is based on the least structure solution with  $S_2$  smoothing matrix, using the corresponding forward-direction thick-target bremsstrahlung (FDTTB) spectrum for a Ta target of  $0.382 \text{ g.cm}^{-2}$  thickness.

The multiplicity correction for  $(\gamma, 2n)$  reaction contribution cannot be directly evaluated when a low efficiency system is used, which is the case in our experiment (about 10%). Consequently, this contribution to the measured total photoneutron cross-section of  $^{181}\text{Ta}(\gamma, xn)$  reaction has been estimated by considering  $(\gamma, 2n)$  data from measurements by Bergère et al.

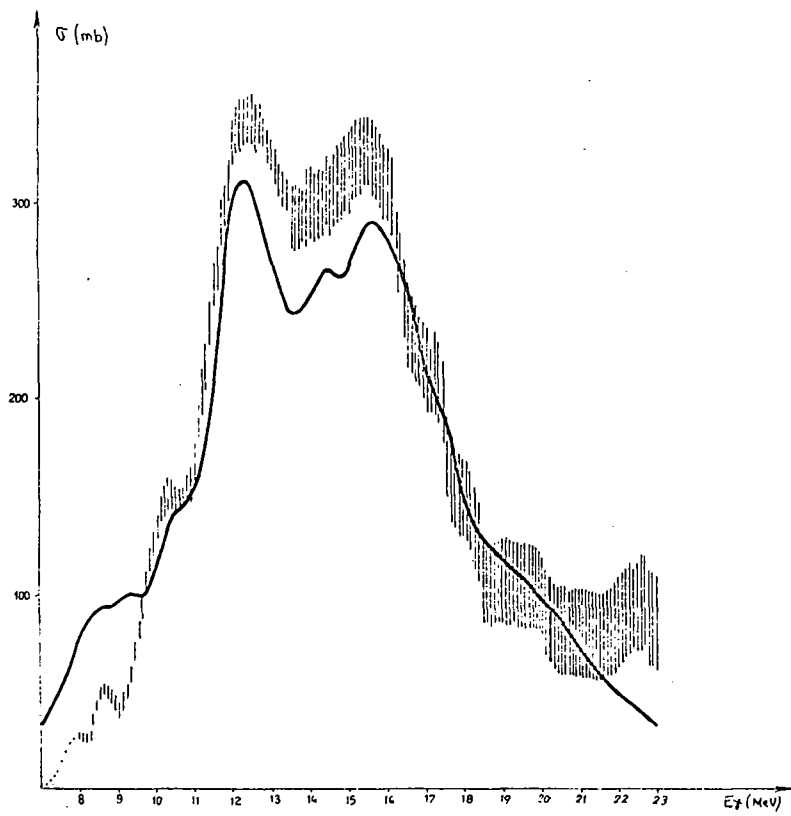
In fig. 1, the total photoabsorption cross-section is represented by bars indicating the uncertainties due to experimental error in the measured yield curve.

Also in fig. 1, the computed total  $E_1$  photoabsorption cross-section for  $^{181}\text{Ta}$  under the approximation of single-parcicle transitions' is given.

14. DELAYED GAMMA RAYS EMITTED IN NATURAL AND ENRICHED URANIUM PHOTOFISSION WITH BETATRON BREMSSTRAHLUNG -

V. Galațanu, M. Grecescu, G. Baciuc

The purpose of this investigation is the determination of absolute yields for the production of delayed gamma-rays emitted after uranium



photofission with a bremsstrahlung beam. The necessity for these nuclear data was emphasized by T.A. Byer in the Draft Working Paper for IWGNSRD on Non-Neutron Data Needs for Safeguards Development Purposes at a I.A.E.A. meeting in 1972.

The dependence of the absolute yield versus end-point energy of the bremsstrahlung was measured for natural uranium in the energy range 8-16 MeV. Some illustrative results for the most prominent gamma rays are given in Table 1. At 16 MeV, the absolute yield were measured versus the concentration of  $^{235}\text{U}$  in different enriched samples. Some preliminary results are given in Table 2. For most observed gamma-rays, the yield is increasing linearly with the  $^{235}\text{U}$  concentration with the exception of those belonging to  $^{104}\text{Tc}$  and  $^{132}\text{Te}$  which are decreasing linearly. The data processing is still in progress.

15. MEASUREMENTS OF STATICAL AND DYNAMICAL STRUCTURE  
FACTORS FOR SOME METALS AND MOLECULAR SYSTEMS IN LIQUID  
AND SOLID STATE - V. Trepăduş, I. Pădureanu, O. Dumitru

The statical and dynamical structure factors for Cu and Al-alloys were measured by thermal neutron scattering.

We have tried to put in evidence the clustering near the melting point.

Information about pair-interaction-potential were obtained starting from the liquid state theories existing at present. For this, the structure factors were measured over a large range of the momentum transfer, covering a large domain of temperature. The measurements were corrected for multiple scattering, resolution, absorption, etc.

16. CROSS SECTIONS FOR STRANGE PARTICLE PRODUCTION IN  $\Pi^+$   
INDUCED REACTIONS - T. Beşliu, M.Gavrilaş, I.Berceanu,  
S. Berceanu, C.V.Kautiş, A.L.M.Mihul, T.Nygren,  
K.V.Laurikainen. EL-7380, JINR Commun. (Dubna)

A computerized compilation of cross sections for strange particle production in the collisions of the  $\Pi^+$  mesons with protons, neutrons and deuterium is presented. 256 reactions with strange particle production have been compiled. For reactions with more than 5 data points, plots of the dependence of the cross-sections on primary energy are presented.

T a b l e 1

Absolute yields (quanta/gram.Röntgen)

$T_i = 2.5 \text{ h}$        $T_m = 2.5 \text{ h}$

$E_\gamma$ (keV)	$T_p$ (h)	$E_{ir}^\gamma$ (MeV)								
		8	9	10	11	12	13	14	15	16
228.6	10	18.2±0.6	19.2±0.6	19.9±0.6	21.5±0.6	24.1±0.7	28.4±0.8	32.4± 0.9	41.4± 1.2	45.4± 1.5
249.63	26	17.1±0.5	17.8±0.6	21.2±0.6	44.1±1.4	66.0±1.9	76.9±2.2	84.6± 2.5	105.8± 3.4	124.2± 4.0
293.26	10	31.7±0.9	32.8±0.9	34.6±1.0	35.1±1.0	38.0±1.1	39.8±1.2	42.7± 1.3	49.5± 1.6	54.2± 2.0
306.8	0.5	48.3±1.6	52.4±1.8	55.8±2.0	104.7±3.3	210.5±6.1	250.4±7.5	304.3± 9.0	375.1±10.9	428.5±14.5
357.96	0.5	19.8±0.6	21.1±0.6	29.2±0.9	41.6±1.2	50.9±1.6	57.8±2.0	69.5± 2.2	86.3± 2.5	94.4± 3.0
529.90	26		12.9±0.3	16.8±0.4	29.7±0.9	41.7±1.2	52.3±1.6	57.8± 2.0	73.3± 2.3	84.6± 2.5
555.57	26		2.9±0.1	3.9±0.2	8.5±0.3	10.7±0.4	12.4±0.4	15.5± 0.5	18.0± 0.6	22.0± 0.7
641.22	0.5		52.4±1.8	90.2±2.8	167.1±5.0	241.3±7.0	279.7±8.4	343.1±10.0	381.3±11.9	435.5±13.0
657.92	10		19.2±0.6	40.2±1.2	64.9±1.8	87.0±2.6	103.4±3.0	130.2± 3.8	158.1± 4.5	180.5± 5.5
667.69	26			9.4±0.3	10.7±0.4	13.4±0.4	15.6±0.5	20.5± 0.6	28.1± 0.8	34.8± 1.0
724.4	0.5		21.6±0.6	32.5±0.9	41.8±1.2	52.8±1.6	62.1±1.8	79.2± 2.4	96.0± 2.9	114.5± 3.5
743.28	10			153.7±4.5	158.4±4.6	164.8±4.7	174.4±5.0	185.5± 5.3	203.8± 6.0	235.2± 7.0
749.84	10			5.3±0.2	8.3±0.3	10.5±0.4	13.5±0.5	16.8± 0.6	20.1± 0.6	26.5± 0.8
772.55	26			7.1±0.3	8.1±0.3	10.2±0.4	11.9±0.4	15.6± 0.5	21.6± 0.7	26.8± 0.8
1260.45	10			14.6±0.5	22.2±0.7	26.4±0.8	31.3±1.0	34.5± 1.2	41.0± 1.3	50.7± 1.5
1383.97	10			2.0±0.1	5.4±0.2	7.9±0.3	8.9±0.3	10.5± 0.4	12.9± 0.4	15.7± 0.5
1435.74	0.5	77.8±2.2	94.3±2.5	98.5±2.6	150.3±4.2	221.1±6.5	253.8±7.5	286.8± 7.7	373.7±10.6	414.3±13.0

T a b l e 2

Absolute yields (quanta/gram.Röntgen)

$T_i = 2.5 \text{ h}; T_m = 2.5 \text{ h } E_{ir}^Y = 16 \text{ MeV}$

$E_Y$ (keV)	Isotope	$T_{1/2}$	$T_p$ (h)	$U^{235}$ concentration			
				0.72%	5.2%	16.6%	93.1%
228.16	$^{132}_{52}\text{Te}$	78.2 h	10	45.4 ± 1.5	45.0 ± 1.4	44.4 ± 1.3	38.7 ± 1.0
249.63	$^{135}_{54}\text{Xe}$	9.16h	26	124.2 ± 4.0	150.0 ± 4.5	212.0 ± 6.0	613.4 ± 18.0
293.26	$^{143}_{58}\text{Ce}$	33.0 h	10	54.2 ± 2.0	70.4 ± 2.3	117.0 ± 3.3	409.2 ± 11.9
306.8	$^{101}_{43}\text{Tc}$	14.0 m	0.5	428.5 ± 14.5	465.3 ± 16.0	560.5 ± 19.0	1187.7 ± 31.0
357.96	$^{104}_{43}\text{Tc}$	18 m	0.5	94.4 ± 3.0	91.2 ± 2.7	83.7 ± 2.5	32.2 ± 0.9
529.90	$^{133}_{53}\text{I}$	20.9 h	26	84.6 ± 2.5	93.4 ± 2.8	119.2 ± 3.4	262.7 ± 8.0
555.57	$^{91m}_{39}\text{Y}$	49.71m	26	22.0 ± 0.7	26.8 ± 0.8	38.5 ± 1.2	101.1 ± 3.0
641.22	$^{142}_{57}\text{La}$	92.4 m	0.5	435.5 ± 13.0	479.8 ± 15.1	598.5 ± 18.1	1180.3 ± 30.0
657.92	$^{97}_{41}\text{Nb}$	71 m	10	180.5 ± 5.5	207.5 ± 6.1	269.6 ± 8.2	598.1 ± 17.5
667.69	$^{132}_{53}\text{I}$	2.28h	26	34.8 ± 1.0	39.6 ± 1.2	51.0 ± 1.6	111.3 ± 3.5
724.4	$^{105}_{44}\text{Ru}$	4.44h	0.5	114.5 ± 3.5	130.0 ± 4.0	160.1 ± 5.0	395.8 ± 12.1
743.28	$^{97m}_{41}\text{Nb}$	59 s	10	235.2 ± 7.0	266.1 ± 8.1	349.5 ± 10.8	773.7 ± 20.5
749.84	$^{91}_{38}\text{Sr}$	9.48h	10	26.5 ± 0.8	32.3 ± 1.0	47.4 ± 1.6	122.5 ± 3.9
772.5	$^{132}_{53}\text{I}$	2.8 h	26	26.8 ± 0.8	30.5 ± 1.0	39.1 ± 1.2	85.0 ± 2.5
1260.45	$^{135}_{53}\text{I}$	6.72h	10	50.7 ± 1.5	57.8 ± 1.8	77.1 ± 2.3	171.6 ± 5.2
1383.97	$^{92}_{38}\text{Sr}$	2.71h	10	15.7 ± 0.5	23.7 ± 0.7	47.4 ± 1.4	194.0 ± 6.0
1435.74	$^{138}_{55}\text{Cs}$	32.3 m	0.5	414.3 ± 13.0	468.4 ± 14.5	626.5 ± 18.5	1426.8 ± 40.0

17. ON MULTIPLICITY SYSTEMATICS OF  $\pi^0$ ,  $K_S^0$  AND  $\Lambda$  PRODUCTION IN HIGH ENERGY COLLISIONS - S. Berceanu, T. Ponta . E1-7501, JINR Commun. Dubna.

It is shown that the experimental data on  $\pi^0$ ,  $K_S^0$  and  $\Lambda$  multiplicities in  $\pi^-p$  and  $pp$  collisions can be parametrized by a unique function within the framework of the Koba, Nielsen and Olesen semiinclusive scaling prediction on larger energy ranges than those quoted earlier. However, the ratios of moments  $\langle n_c^q \rangle \langle n \rangle^{-q} \langle n_c \rangle^{-1}$  seem to increase with energy.

18. ON REGULARITIES OF STRANGE PARTICLE PRODUCTION IN HIGH ENERGY COLLISIONS - S. Berceanu. E1-8559, JINR Commun. Dubna.

Available data on total strange particle cross-sections ( $\overset{\vee}{K}K$  and  $Y^0K$ ) from  $\pi^+p$  and  $pp$  collisions are surveyed. Fits and comments on the change with energy of average multiplicities of  $\pi^\pm$ ,  $K^\pm$ ,  $\overset{\vee}{p}$ ,  $\Lambda/\Sigma^0$ ,  $K^0/\overset{\vee}{K}^0$  from  $pp$  collisions and  $\Lambda/\Sigma^0$  and  $K^0/\overset{\vee}{K}^0$  from  $\pi^-p$  collisions are presented.

REPUBLIC OF SOUTH AFRICA

PROGRESS REPORT TO THE INDC

1974

Compiled by D. Reitmann

1. PHYSICS DIVISION, ATOMIC ENERGY BOARD, PELINDABA, TRANSVAAL

The major facilities used for neutron physics research remained unchanged. They are the 20 MW research reactor, Safari I, and the pulsed 3 MV Van de Graaff accelerator with terminal bunching and an on-line computer.

1.1 Neutron capture reactions

C. Hofmeyr

The results obtained from thermal neutron capture in  $^{58}\text{Ni}$  were reported at the "Second International Symposium on Neutron Capture Gamma-Ray Spectroscopy and Related Topics", Petten, Sept. 1974. Coincidence measurements with two Ge(Li)-detectors on the gamma-ray cascade following neutron capture were found to be feasible, utilizing the data-link to the on-line computer. Under the given experimental conditions a five-day run is normally sufficient to see a good fraction of the lines observed in singles spectra by sorting 4K-channel spectra into up to 32 preselected windows.

1.2 Scattering of fast neutrons

E. Barnard, D.T.L. Jones, J.G. Malan and D. Reitmann

The results of a comprehensive study of fast neutron scattering from cesium have been published<sup>1)</sup>. An investigation of fast neutron interactions with titanium, which was carried out in co-operation with a group from the Argonne National Laboratory, has also led to publication<sup>2)</sup>. Good progress was made with the measurement of fast neutron scattering

cross sections for  $^{103}\text{Rh}$ . The effective cross section for excitation of the 40 keV isomeric state obtained from detailed microscopic inelastic scattering cross sections, agrees remarkably well with the activation results of Santry and Butler<sup>3)</sup>. The level and decay scheme of  $^{103}\text{Rh}$  exhibits some very interesting properties and Hauser-Feshbach calculations of inelastic scattering cross sections seem to require unusual treatment of the optical model potential. Preliminary results were presented at the conference on Nuclear Cross Sections and Technology, Washington, March 1975.

- 1) Z. Physik 271(1974)1
- 2) Nucl. Phys. A229(1974)189
- 3) Can. J. Phys. 52(1974)1421

### 1.3 (p,n) reactions

E. Barnard, J.A.M. de Villiers, J.G. Malan and P. van der Merwe

Some additional measurements were made on the  $^{71}\text{Ga}(p,n)^{71}\text{Ge}$  reaction, the analysis of the level and decay scheme for  $^{71}\text{Ge}$  up to 1.3 MeV was completed and the results were published<sup>1)</sup>. A similar investigation of the  $^{73}\text{Ge}(p,n)^{73}\text{As}$  reaction was also completed and published<sup>2)</sup>.

- 1) Nucl. Phys. A227(1974)399
- 2) Nucl. Phys. A240(1975)273

## 2. SOUTHERN UNIVERSITIES NUCLEAR INSTITUTE, FAURE, CAPE PROVINCE

The major research facility is a 5.5 MV pulsed Van de Graaff accelerator. The research program covered a wide variety of topics in basic and applied science, of which the most relevant are listed below:

### 2.1 Neutron induced reactions

#### 2.1.1 The level structure of $^{115}\text{In}$ from $(n,n'\gamma)$ measurements

I.J. van Heerden and W.R. McMurray

A large amount of data relating to the level structure

of  $^{115}\text{In}$  has been explained quantitatively by coupling a  $1 g_{9/2}$  hole state to a  $2^+$  excitation of the even  $^{116}\text{Sn}$  core. These data were observed by Coulomb excitation<sup>1)</sup> with  $^{16}\text{O}$  and  $^{12}\text{C}$  ions and by inelastic scattering of 12 MeV deuterons<sup>2)</sup> and of 7.04 MeV protons<sup>3)</sup>. Several  $^{115}\text{In}$  levels have however been observed which cannot be fitted into this hole-vibration picture. In recent  $\beta$ -decay studies of  $^{115}\text{Cd}$  and  $^{115\text{m}}\text{Cd}$ , Graeffe et al.<sup>4)</sup> have shown states in  $^{115}\text{In}$  at 934.4, 1133.0, 1292.2, 1419.4 and 1450.1 keV, whereas Bachlin et al.<sup>5)</sup> observed states at 828 and 864 keV, to which they have assigned spins and parities of  $3/2^+$  and  $1/2^+$  or  $3/2^+$  respectively. The strongly enhanced E2 transition between these two levels, formed the basis for Bachlin et al. suggesting that the 828 and 864 keV levels may form the beginning of a  $K = 1/2$  rotational band based on the Nilsson state  $\frac{1}{2}^+$  [431].

The present work was initiated to possibly reveal further members of the proposed rotational band. All reactions studied such as Coulomb excitation, transfer reactions and inelastic scattering are comparatively selective regarding the nature of populated states. The  $(n, n'\gamma)$  reaction is not so selective regarding excitation mode and might make it possible to also observe deformed states in a nucleus with a spherical ground state.

In previous  $(n, n'\gamma)$  measurements carried out with neutrons produced in the  $^7\text{Li}(p, n)^7\text{Be}$  reaction, it was found that scattering of the 430 and 477 keV  $\gamma$ -rays produced in the  $(p, n)$  and  $(p, p')$  reactions on  $^7\text{Li}$ , caused a large low-energy  $\gamma$ -ray background. This made it impossible to observe low energy  $\gamma$ -rays resulting from the  $(n, n'\gamma)$  reaction on  $^{115}\text{In}$ . We therefore repeated our previous measurements using the  $\text{T}(p, n)$  reaction as our source of neutrons.

Gamma rays from levels in  $^{115}\text{In}$  were observed following inelastic neutron scattering at several neutron energies up to 2.5 MeV. A consistent level scheme was deduced taking into account the  $\gamma$ -ray threshold energies, and the shapes

of the excitation curves. The observed  $\gamma$ -ray yields have been determined using the SAMPO programme and corrected for incident neutron flux, gamma attenuation in the scatterer, detection efficiency and for the effect of the time-gate used to depress neutron induced  $\gamma$ -rays in the Ge(Li) detector. Inelastic neutron scattering cross sections as a function of neutron energy are at present being compared with Hauser-Feshbach calculations, corrected for level width fluctuations, using the NEARREX programme.

As a start, optical model parameters obtained from neutron elastic scattering<sup>4)</sup> were used, and it was found that these did not give best fits to the excitation curves of levels with known  $J^\pi$  as at 933.6 keV ( $7/2^+$ ), 941.2 keV ( $5/2^+$ ), 1448.4 keV ( $9/2^+$ ) and 1462.4 keV ( $7/2^+$ ). These parameters were therefore adjusted and the values which, up to now, have given the best fits are:

$V_o = 48.9$  MeV (Saxon-Woods form),  $W_o = 5.8$  MeV (surface derivative form),  $V_{so} = 8.00$  MeV,  $a = 0.66$  fm,  $b = 0.48$  fm and  $R = 1.25 A^{1/3}$  fm.

- 1) F.S. Dietrich, B. Herskind, R.A. Naumann, R.G. Stokstad and G.E. Walker Nucl. Phys. A155 (1970) 209
- 2) S.A. Hjorth and L.H. Allen, Ark. Phys. 33(1967)121
- 3) R.D. Sharp and W. Buechner, Phys. Rev. 112(1958)897
- 4) G. Graeffe, C.W. Tang, C.D. Coryell and G.E. Gordon, Phys. Rev. 149(1966)884
- 5) A. Bächlin, B. Fogelberg and S.G. Malmskog, Nucl. Phys. A96(1967)539

#### 2.1.2 Study of the level structure of $^{232}\text{Th}$

W.R. McMurray and I.J. van Heerden (SUNI),  
E. Barnard and D.T.L. Jones (AEB)

We have continued the investigation of the level structure of  $^{232}\text{Th}$  using the  $(n,n')$  and  $(n,n'\gamma)$  reactions. During 1974 additional measurements of the inelastic neutron

spectra were obtained over the neutron energy range 500 to 1600 keV using the Van de Graaff accelerator at the AEB, Pretoria. Better resolution was achieved with a flight path of 2 m. A low background resulted from efficient shielding of the detector placed at  $125^\circ$  to the incident neutron beam. Elastic scattering cross sections will also be obtained to complete this part of the study. Measurements of the  $(n,n'\gamma)$  angular distributions are still required to complete the gamma measurements for this project.

2.1.3  $^{114,116}\text{Cd}$  level structure from the  $(n,n'\gamma)$  reaction  
D.R. Gill<sup>a)</sup>, N. Ahmed<sup>a)</sup>, W.J. McDonald<sup>a)</sup>, G.C. Neilson<sup>a)</sup>  
S.A. ElBakr<sup>b)</sup>, I.J. van Heerden and W.K. Dawson<sup>a)</sup>

The even-A Cadmium isotopes exhibit level schemes which in previous investigations have been attributable to collective vibrations. No  $(n,n'\gamma)$  studies of the  $^{114,116}\text{Cd}$  nuclei have as yet been reported, probably due to the large quantities of separated isotopes required by conventional techniques. The present study was carried out using the close neutron source-to-scatter geometry and data analysis techniques described previously<sup>1,2)</sup> which allowed the use of small scattering samples of about 4 g each. In most of this work the  $^3\text{H}(p,n)$  reaction was used as a neutron source, the tritium target consisting of tritium embedded in metallic erbium deposited on a Ta backing.

In the  $^{114}\text{Cd}$  nucleus, analysis of the excitation function confirms the spins of the 558, 1134, 1210, 1284, 1365 and 1733 keV levels as 2,0, 2, 4,2 and 4 respectively. The  $\gamma$ -ray excitation cross section for the 1306 keV level is too weak to confirm the  $J^\pi = 0^+$  assignment, as most of its strength decays by internal conversion<sup>3)</sup>. In addition to these, the spin of the level at 1843 has been determined as 1. The doublet at 1861 and 1865 keV agrees with  $J = (0)$  and 1 assignment respectively.

In  $^{116}\text{Cd}$  results, we have confirmed the spins of the levels 513, 1213, 1220 and 1381 keV as 2, 2, 4 and 0 respectively. Also, the spin of the 1283, 1644 and 1917 levels have been assigned to be 0, (2,3) and 0 respectively. Only tentative spin assignments could be made to the levels above 1900 keV.

These results have been presented in a recent publication<sup>4)</sup>.

- a) Nuclear Research Centre, University of Alberta, Edmonton, Canada
  - b) Dept. of Physics, University of Manitoba, Winnipeg, Canada
- 1) S.A. Elbakt, I.J. van Heerden, W.K. Dawson, W.J. McDonald and G.C. Neilson, Nucl. Instr. 97(1971)283
  - 2) S.A. Elbakt, I.J. van Heerden, W.K. Dawson, W.J. McDonald and G.C. Neilson, Nucl. Phys. A211(1973)493
  - 3) A. Bachlin, N.E. Holmberg and G. Backstrom, Nucl. Phys. 80(1966)154
  - 4) D.R. Gill, N. Ahmed, W.J. McDonald, G.C. Neilson, S.A. Elbakt, I.J. van Heerden and W.K. Dawson, Nucl. Phys. A229(1974)397

#### 2.1.4 Polarization in neutron-deuteron scattering

M. Steinbock, F.D. Brooks (UCT)

I.J. van Heerden (SUNI)

Further studies have been made of the polarization  $P_{nd}$  in neutron-deuteron elastic scattering at energies in the range 7.9 - 21.6 MeV, using the deuterated anthracene scintillation polarimeter described in previous reports<sup>1)</sup>. Analysis of the data obtained at 7.9, 16.4 and 21.6 MeV is now nearing completion. The present preliminary values at 16.4 MeV are consistent with the distribution predicted by the phase analysis and with previous measurements for incident neutrons and protons. A detailed comparison will be made between the proton and neutron data at this energy and at the other energies under study to determine whether anything of significance can be deduced relative to the charge symmetry of nuclear forces.

- 1) Annual Research Reports SUNI-23(1972), item 2.1.7;  
and SUNI-27 (1973), item 2.1.6.1

2.1.5 Angular correlation of neutrons from  $^{252}\text{Cf}$  spontaneous fission

J.S. Pringle and F.D. Brooks

In an attempt to gain further insight into fission neutron emission processes, an investigation is being undertaken of the angular correlation of prompt neutrons emitted in  $^{252}\text{Cf}$  spontaneous fission. A neutron-neutron angular correlation measurement was reported in 1948 by de Benedetti et al.<sup>1)</sup> for thermal neutron induced fission of  $^{235}\text{U}$ . However, to the best of our knowledge no further reports of any experiments of this kind have appeared in the literature.

In the present experiment, two neutron detectors are used to measure the fission neutron coincidence rate for pairs of neutrons emitted at relative angles ranging from  $0^\circ$  to  $180^\circ$ . The measured singles rates in the two detectors and the coincidence rate are used to calculate a ratio  $R(\theta)$  which is proportional to the angular correlation function. The ratio  $R(\theta)$  is defined so as to be independent of the experimental geometry and insensitive to small variations in the detector efficiencies. In the measurements made at small angles  $\theta \lesssim 40^\circ$ , shadow shields are used and corrections are made to eliminate false coincidences arising from a single neutron scattering between the two detectors.

The experimental results were compared with a computer-generated distribution of  $R(\theta)$ . This distribution was generated by a Monte Carlo calculation in which an evaporation model was used to describe the neutron emission in fission. The fission process was simulated step-by-step for a large number of fissions ( $4 \times 10^4$ ), the behaviour of the "fissioning nucleus" and the subsequent "fission fragments" being selected in a random manner from existing possibilities. The choices made in the selection process were weighted according to the probability of their occurrence as defined by the model. "Prompt neutrons" emitted from the fissions were tracked, their energy spectrum was accumulated and the probabilities of their detection by "detectors" having the same properties

as those used in the actual experiment were determined. Several cross checks were included at intermediate stages in the simulation to confirm the validity of the calculation. One such check was a comparison of the computer-generated angular distribution of neutrons relative to the direction of motion of the light fragment with the experimental measurement of Bowman et al<sup>2)</sup>.

It is clear from these comparisons that a simple evaporation model in which it is assumed that all prompt neutrons are emitted isotropically in the frames of the fully accelerated fragments is unable to account accurately for the experimental measurements. At present the model is being extended to include a scission neutron component<sup>2)</sup> and also to allow for the anisotropic emission of neutrons in the fragment frames as proposed by Ericson and Strutinski<sup>3)</sup>. Further experiments, on both  $^{252}\text{Cf}$  and  $^{235}\text{U}$ , coupled with more elaborate fission models promise to yield much evidence on the nature of neutron emission in fission.

- 1) S. de Benedetti, J.E. Francis, W.M. Preston and T.W. Bonner, Phys. Rev. 74(1948)1645
- 2) H.R. Bowman, S.G. Thompson, J.C.D. Milton and W.J. Swiatecki, Phys. Rev. 126(1962)2120
- 3) T. Ericson and B. Strutinski, Nucl. Phys. 8(1958)284

#### 2.1.6 Direct excitation of analogue dipole states in $^{28}\text{Al}$ K. Bharuth-Ram, S.M. Perez, F.D. Brooks, W.R. McMurray and S. Wynchank

Studies of analogue dipole states in  $^{28}\text{Al}$  via the  $^{28}\text{Si}(n,p)^{28}\text{Al}$  reaction are continuing. The experiments outlined in a previous report<sup>1)</sup> were carried out using a counter telescope consisting of three Si surface barrier detectors one of which was also the target for the (n,p) reaction. This detector and the center detector of the telescope formed the two sides of a time-of-flight system

which was used to select protons against a background of deuterons and heavier particles arising from competing reactions in silicon.

The analyses carried out during the past year have revealed appreciable and unexpected time-walk effects in the constant fraction discriminators. The data have had to be reanalysed in consequence, and new methods of analysis have had to be devised to deal with the low energy region ( $E_p < 6$  MeV) where the effects of time walk were most serious. No final results are available as yet from the analysis and it might prove necessary to repeat some of the measurements.

1) SUNI-28(1973)Item 2.1.7

## 2.2 (p,n $\gamma$ ) Reactions

I.J. van Heerden, R.J. van Reenen, J.V. Pilcher and W.R. McMurray

Studies of (p,n) and (p,n $\gamma$ ) reactions have proved to be successful in determining the level structure of many nuclei in the mass region  $A = 45$  to  $65$ . In many cases the reaction Q-values are well suited to the available 5,5 MeV proton energy, allowing the excitation of the interesting lower energy levels. The mentioned mass region is of interest insofar as a number of nuclear models are applicable so that acquired experimental data become immediately useful in evaluating the success of the various models.

In an effort to determine parameters of levels in  $^{65}\text{Zn}$  via the  $^{65}\text{Cu}(p,n\gamma)$  reaction, angular distribution measurements were obtained at various proton energies<sup>1)</sup>. It was found that these distributions were inconsistent probably as a result of instabilities in the monitoring system. It will therefore be necessary to repeat these measurements for the completion of the project.

The study of the properties of excited levels in  $^{49}\text{V}$  and  $^{50}\text{Cr}$  using the (p,n $\gamma$ ) reaction of  $^{49}\text{Ti}$  and  $^{50}\text{V}$  has been

continued<sup>2)</sup>. Gamma-rays from reactions on  $^{50}\text{V}$  were positively identified by comparing  $\gamma$ -ray spectra obtained from natural and enriched  $\text{V}_2\text{O}_5$  targets. Additional particle-gamma coincidence measurements are being planned to separate  $\gamma$ -rays produced in the  $(p,n\gamma)$  and  $(pp'\gamma)$  reactions on  $^{50}\text{V}$ .

1) Report SUNI-28(1973), Item 2.2.1

2) Report SUNI-28(1973), Item 2.2.2

---

PROGRESS REPORT FROM YUGOSLAVIA

I. NEUTRON DATA

NEUTRON CAPTURE DIFFERENTIAL CROSS SECTION FROM THE SEMIDIRECT CAPTURE MODEL

A.Likar, M.Potokar and F.Cvelbar

Institute "Jožef Stefan", Ljubljana, Yugoslavia  
 The differential cross section formula from neutron radiative capture is derived on the grounds of the direct-semidirect model. Numerical results for neutron capture to three single particle levels in  $^{88}\text{Sr}$  are considered. It is found that the anisotropy in general is not small and is also dependent on the incident particle-target nucleus coupling interaction used in the calculation.

It is found that the anisotropy in general is not small and is also dependent on the incident particle-target nucleus coupling interaction used in the calculation.

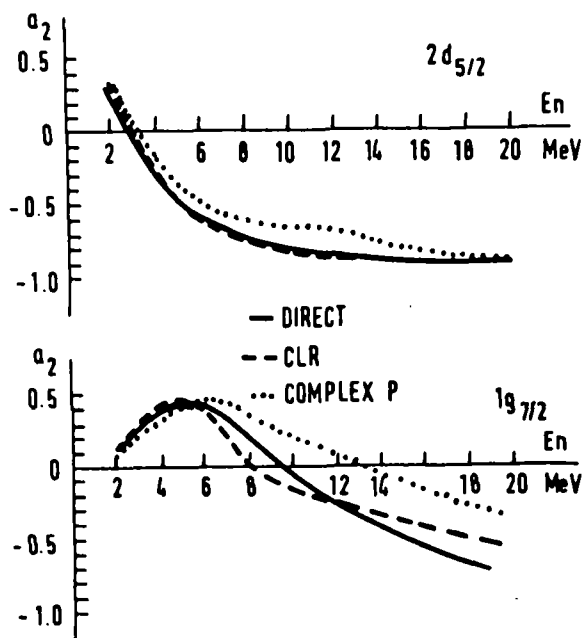


Fig.1 Neutron energy dependence of the  $a_2$  coefficient from the  $2d_{5/2}$  and  $1g_{7/2}$  capture in  $^{88}\text{Sr}$ , calculated according to direct capture model and two approaches of the direct-semidirect capture model.

Reported to the IIInd Int. Symposium on Neutron Capture Gamma Ray Spectroscopy and Related Topics, Petten, 1974

THE MECHANISM OF THE RADIATIVE NEUTRON CAPTURE IN HEAVIER NUCLEI WITH CLOSED NEUTRON SHELLS AT THE EXCITATION ENERGIES OF DIPOLE GIANT RESONANCES

M.Potokar, A.Likar and F.Cvelbar

Institute "Jožef Stefan", Ljubljana, Yugoslavia  
 The present experimental data on fast neutron radiative capture in  $^{208}\text{Pb}$ ,  $^{138}\text{Ba}$ ,  $^{88}\text{Sr}$  and  $^{40}\text{Ca}$  is sufficient to show that direct-semidirect model does not account for the capture

dynamics satisfactorily. However, the recently proposed re-  
 fined direct-semidirect model, which involves the complex  
 coupling interaction between the incident nucleon and the  
 target nucleus reproduces the experimental results well.  
 This may be an indication that some more complex configu-  
 rations cannot be ignored when describing the reaction me-  
 chanism.

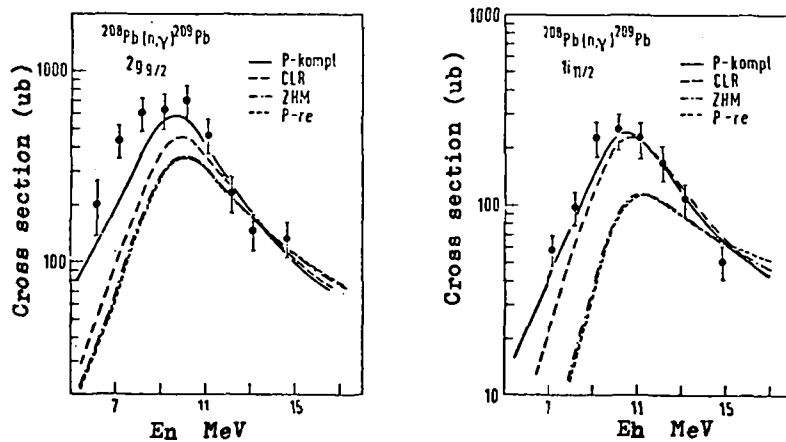


Fig.1. The experimental excitation functions for the radiative capture of fast neutrons to the ground and first excited single particle state of  $^{209}\text{Pb}$  ( $6^-$ ) compared with the excitation functions calculated according to different approaches to the DSD model. The corresponding values of free parameters  $V_1$  and  $W_1$  are given in the Table.

Reported to the Second International Symposium on Neutron  
 Capture Gamma Ray Spectroscopy and Related Topics, Petten, 1974

#### RECENT TRENDS IN FAST NUCLEON CAPTURE STUDIES

M. Potokar

Institute "Jožef Stefan", Ljubljana, Yugoslavia

With the appearance of a new generation of nucleon radiative capture data, namely the excitation functions for fast neutron capture to particular final states of the residual nucleus, it was possible to make a further step in the theoretical description of the observed data. The original direct-semi-direct (DSD) model (<sup>1,2</sup>) assumed that two processes are important in the fast nucleon capture reaction; direct dipole capture in the average nuclear field and semi-direct capture connected with the dipole excitation of the target nucleus by inelastic scattering of the incoming nucleon to a single par-

ticle bound state, in the first step, and with the radiative deexcitation of the target nucleus, in the second step. This model has now been refined by allowing the coupling between the incident nucleon and the vibrating target nucleus to be complex (<sup>3</sup>). The imaginary coupling was introduced in a semi-phenomenological way. The parameters attributed to it were taken from the imaginary part of the symmetry optical potential in the same way as the parameters of the real coupling were in accordance with the real part of the symmetry optical potential.

The meaning of the imaginary term has been traced into the formal derivation of the model on the basis of the Feshbach's unified reaction theory.

References:

1. G.E.Brown, Nucl. Phys. A95 (1964) 339
2. C.F.Clement, A.M.Lane and J.R.Rook, Nucl.Phys. 66 (1965) 273, 293
3. M.Potokar, Phys.Lett. 46B (1973) 346
4. M.Potokar, thesis, unpublished

Reported to the Annual Meeting of Yugoslav Nuclear Physicists, Čortanovci 1974

PERSPECTIVES OF LOW ENERGY ACCELERATORS IN FAST NEUTRON CAPTURE STUDIES

F.Cvelbar

Institute "Jožef Stefan", Ljubljana, Yugoslavia  
The present status of research in the field of fast neutron radiative capture is briefly described and perspectives for future study are indicated. Special attention is paid to the measurements of prompt  $\gamma$ -ray spectra and excitation functions leading to the excitation of particular final states in nuclei studied. Comparison of these data with the results of the calculation on the basis of the semidirect capture theory is discussed. The first results of the measurements of the angular distribution of capture  $\gamma$ -rays is considered from the theoretical and experimental point of view.

IAEA Meeting on the Use of Low Energy Accelerators, Zagreb, 1974

ANGULAR DISTRIBUTION OF NEUTRON CAPTURE  $\gamma$ -RAYS IN THE SEMI-DIRECT CAPTURE MODEL

A. Likar, M. Potokar and F. Cvelbar  
 Institute "Jožef Stefan", Ljubljana, Yugoslavia  
 The angular distribution of prompt  $\gamma$ -rays from the radiative capture of a neutron in the region of giant dipole resonance is calculated according to the semi-direct radiative capture model. Results are compared with a few available experimental values. For further analysis more experimental data are needed.

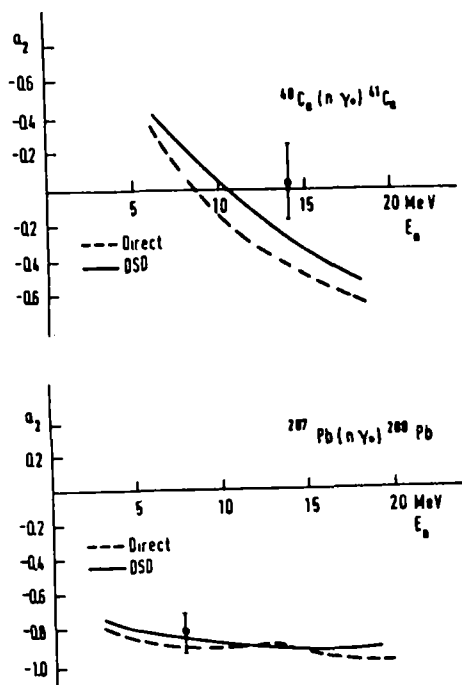


Fig.1 Comparison of experimental and calculated  $a_2$  coefficient for the reaction  $^{40}\text{Ca}(n, \gamma)^{41}\text{Ca}$  a) and for the reaction  $^{207}\text{Pb}(n, \gamma)^{208}\text{Pb}$  b).

To be submitted for publication in Phys.Lett.

1. B. Antolković, Z. Dolenc: The neutron-induced  $^{12}\text{C}(n,n')3\alpha$  reaction at 14.4. MeV in a kinematically complete experiment, Nucl. Phys. A237(1975)235

A three-particle coincidence measurement of the  $n+^{12}\text{C} \rightarrow n+3\alpha$  reaction at  $E_n=14.4$  MeV has been performed. The reaction proceeds via several sequential decay processes. The inelastic scattering of the incoming neutron on  $^{12}\text{C}$  and the subsequent  $3\alpha$  decay of 9.36, 10.84, 11.83 and 12.71 MeV excited states of  $^{12}\text{C}$  amounts 90% of the total yield. 10% of the total cross section is attributed to the  $^{12}\text{C}(n,\alpha)^9\text{Be}(n,2\alpha)$  reaction proceeding through an intermediate  $^9\text{Be}$  state at 2.43 MeV. The density distribution of  $3\alpha$  correlation spectra are consistent with  $I^\pi$  assignment  $3^-, 1^-$  and  $1^+$  anticipated for the 9.63, 10.84 and 12.71 MeV states of  $^{12}\text{C}$  respectively. However, for the 11.83 MeV state of  $^{12}\text{C}$  the spin and parity value  $1^-$  is suggested.

2. B. Antolković, J. Hudomalj,:  $3\alpha$  decay of the 10.84 and 11.83 MeV states of  $^{12}\text{C}$ , Nucl. Phys. A237 (1975) 253

The theoretical density distributions for the  $^{12}\text{C} - 3\alpha$  break-up have been compared with those obtained experimentally for the 10.84 and 11.83 MeV states of  $^{12}\text{C}$ . The good fit obtained for the  $I^\pi = 1^{-1}$  state at 10.84 MeV has confirmed the validity of the theoretical approach used in the present calculation. The theoretical density distribution for the  $^{12}\text{C}_{11.83} - 3\alpha$  break-up has been computed for both tentative spin assignments  $1^-$  and  $2^-$ . To explain experimental data on  $\alpha - \alpha$  correlation spectrum it is necessary to accept the  $1^-$  value for the spin and parity of the 11.83 MeV state of  $^{12}\text{C}$ .

3. M. Turk, B. Antolković, D. Winterhalter: Three-body breakup of  $^{14}\text{N}$  induced by fast neutrons, Fizika 7 (1975) 23

The correlation spectra of the three-body breakup of the  $n+^{14}\text{N}$  system have been studied at incident neutron energies 14.4 and 18.2 MeV. The Dalitz plot analysis shows that the sequential decay proceeds either through the ground state of  $^8\text{Be}$  at the 8.9-, 9.2-, 11.3-, 12.6- and 14.0-MeV states of  $^{11}\text{B}$ , the last three being excited with 18.2 MeV neutrons. A level in  $^{11}\text{B}$  at an excitation of 12.56 MeV has been assumed to be the lowest  $T=3/2$  state in  $^{11}\text{B}$ . However, the presence of this resonance in the  $^7\text{Li}(\alpha, \alpha)^7\text{Li}$  reaction as well as in the present experiment suggests that it also contains some  $T=1/2$  admixtures. The relative contributions of the various decay modes have been calculated and given in a tabular form.

4. B. Antolković, M. Turk: Role of quasifree processes in 14.4 MeV neutron induced multiparticle breakup on light nuclei, Proceed of the Intern. Conference "Clustering Phenomena in Nuclei", Maryland 21-25 April 1975

An experimental study of  $n+^6\text{Li} \rightarrow n+\alpha+d$  and  $n+^{10}\text{B} \rightarrow \alpha+d+n$  reactions at 14.4 MeV gave indication on the presence of quasifree processes. The data of the  $^6\text{Li}(h, n\alpha)d$  reaction were analysed in the frame of the PWIA. The extracted Fourier transform agrees with the calculated one using Hankel wave function and a cut off radius of 2.7 fm. No contribution of the QF process has been found in the analysis of the three body breakup reaction  $n+^{10}\text{B} \rightarrow \alpha + \alpha + t$ . However, by applying a simple PWIA to the experimental data of the four body breakup  $n+^{10}\text{B} \rightarrow \alpha + \alpha + d + n$ , a well resolved low momentum lump is obtained which is in favour of a quasifree process and

can be explained by the  ${}^8\text{Be}_{2.9}(n,n)$  and  ${}^8\text{Be}_{2.9}(n,\alpha)$  quasi elastic and quasi reaction processes, with deuteron being a spectator particle.

5. B. Antolković: Neutron induced multiparticle break-up of light nuclei in nuclear emulsions, IAEA Meeting on "Utilization of Low Energy Accelerators", Zagreb, 1974

The review of the investigations of the neutron induced three- and four-particle breakup reactions on light nuclei which can be performed with low-voltage accelerators is given.

The following topics are discussed

- Interest of such a study from the fundamental as well as applied points of view.
- Description of the nuclear emulsion technique and data processing of a "storage experiment".
- Experimental features of the kinematically complete experiment and representation of data by generalized Dalitz plots, illustrated by several representative correlation spectra of the neutron-induced multiparticle breakup reactions on light nuclei.
- Comparison of the nuclear emulsion technique with respect to the other measuring techniques both to the character of data and to the costs they impose.

STUDY OF SOME SYSTEMATIC TRENDS AND NONEQUILIBRIUM  
EFFECTS IN (n,2n) REACTIONS AROUND 14MeV

E. Holub and N. Cindro

Institute "Rudjer Bošković", Zagreb, Yugoslavia

The mechanism of (n,2n) reactions has arisen considerable interest in view of contradictory conclusions drawn in recent systematic studies (1-7) and also in view of the growing awareness of the role of nonequilibrium processes in the (n,2n) reactions (8,9).

Total (n,2n) cross sections at  $14.6 \pm 0.3$  MeV for the  $^{84}\text{Sr}$ ,  $^{86}\text{Sr}$ ,  $^{88}\text{Sr}$ ,  $^{93}\text{Nb}$ ,  $^{113}\text{In}$ ,  $^{134}\text{Ba}$  and  $^{136}\text{Ba}$  targets were measured using the activation technique and a Ge(Li) detection system. Isomeric cross section ratios were calculated on the basis of the statistical theory using the shifted Fermi-gas and supraconductivity models. Theoretical results are compared with experimental data. In several cases ( $^{88}\text{Sr}$ ,  $^{93}\text{Nb}$ ,  $^{109}\text{Ag}$ ,  $^{134}\text{Ba}$ ,  $^{136}\text{Ba}$  and  $^{138}\text{Ba}$ ), it was not possible to measure total cross sections, and therefore the theoretical prediction of the isomeric cross section ratio was used to determine the total (n,2n) cross section. The results obtained in this work are shown in Table 1. These results and other recent literature data are analysed in terms of the neutron excess of residual nuclei  $(N-Z)_R$  at a constant value of the residual excitation energy. The systematics of recent data fit a smooth gross trend well and show that there are no significant minima in the total (n,2n) cross section mass dependency in the neighbourhood of closed neutron and proton shells ( see Figs. 1 and 2.) Evidence for the existence of

the preequilibrium mechanisms in (n,2n) reactions around 14 MeV at higher residual excitation energies ( $\sim 6$  MeV) was found in the systematic deviation of experimental (n,2n) data data from statistical predictions ( Pearlstein semiempirical formula) (Fig. 3.).

References:

- 1) P. Hille, Nucl. Phys. A107 (1968) 49
- 2) A. Chatterjee and S. Chatterjee, Nucl. Phys A125 (1969) 593
- 3) S.M. Qaim, Nucl. Phys. A185 (1972) 614
- 4) S.M. Qaim, Nucl. Phys. A224 (1974) 319
- 5) E. Holub, Master's Theses, Univ. of Zagreb, 1974
- 6) E. Kondaiah, J. Phys. A7 (1974) 1457
- 7) E. Holub and N. Cindro, To be published in J. Phys. G: Nucl. Phys.
- 8) Proceedings of the International Symposium on Fast neutron induced reactions, Smolenice, ČSSR, September 1974, To be published in Acta Physica Slovaca.
- 9) E. Holub and N. Cindro, Phys. Lett. 56B (1975) 143
- 10) S. Pearlstein, Nuclear Data A3 (1967) 327.

Table 1. Results for (n,2n) cross sections obtained in this work, compared with the statistical theory.

$E_n = 14.6 \pm 0.3$  MeV

Target	Res. Nucl.	(N-Z) <sub>R</sub>	t <sub>1/2</sub>	I <sub>R</sub>	$\sigma_{\text{exp}}$ (mb) present work	$\sigma_{\text{cal}}$ (mb) <sup>a)</sup> present work	$\sigma_{\text{stat.th.}}$ (mb)
<sup>84</sup> <sub>38</sub> Sr	<sup>83t</sup> Sr	7	32.4 h	1/2 <sup>-</sup>	594±57		665 <sup>a)</sup>
<sup>86</sup> <sub>38</sub> Sr	<sup>85m</sup> Sr	9	70 m	1/2 <sup>-</sup>	270±50		
	<sup>85g</sup> Sr	9	64 d	9/2 <sup>+</sup>	676±40		
	<sup>85t</sup> Sr	9			946±90		790 <sup>a)</sup>
<sup>88</sup> <sub>38</sub> Sr	<sup>87m</sup> Sr	11	2.83 h	1/2 <sup>-</sup>	283±23		
	<sup>87g</sup> Sr	11	stab.	9/2 <sup>+</sup>		765±74	
	<sup>87t</sup> Sr	11				1003±94	963 <sup>a)</sup>
<sup>93</sup> <sub>41</sub> Nb	<sup>92m</sup> Nb	10	10.16 d	2 <sup>+</sup>	484±50		
	<sup>92g</sup> Nb	10	350 y	7 <sup>+</sup>		1078±111	
	<sup>92t</sup> Nb	10				1562±161	1526 <sup>b)</sup>
<sup>113</sup> <sub>49</sub> In	<sup>112m</sup> In	14	20.7 m	4 <sup>+</sup>	1188±69		
	<sup>112g</sup> In	14	14 m	1 <sup>+</sup>	303±17		
	<sup>112t</sup> In	14			1491±86		1529 <sup>a)</sup>
<sup>134</sup> <sub>56</sub> Ba	<sup>133m</sup> Ba	21	38.9 h	11/2 <sup>-</sup>	728±40		
	<sup>133g</sup> Ba	21	7.2 y	1/2 <sup>-</sup>		423±23	
	<sup>133t</sup> Ba	21				1151±63	1722 <sup>a)</sup>
<sup>136</sup> <sub>56</sub> Ba	<sup>135m</sup> Ba	23	28.7 h	11/2 <sup>-</sup>	1053±36		
	<sup>135g</sup> Ba	23	stab.	3/2 <sup>+</sup>		329±11	
	<sup>135t</sup> Ba	23				1382±47	1726 <sup>a)</sup>

a)  $\sigma_{\text{calc}}$  is composed of a measured  $\sigma_m$  (or  $\sigma_g$ ) and a calculated  $\sigma_g$  (or  $\sigma_m$ ) cross section.

a) S. Pearlstein, Nucl. Data A3 (1967) 327

b) M. Häring, H. Vonach and E.J. Feicht, Z. Physik 244 (1971) 352

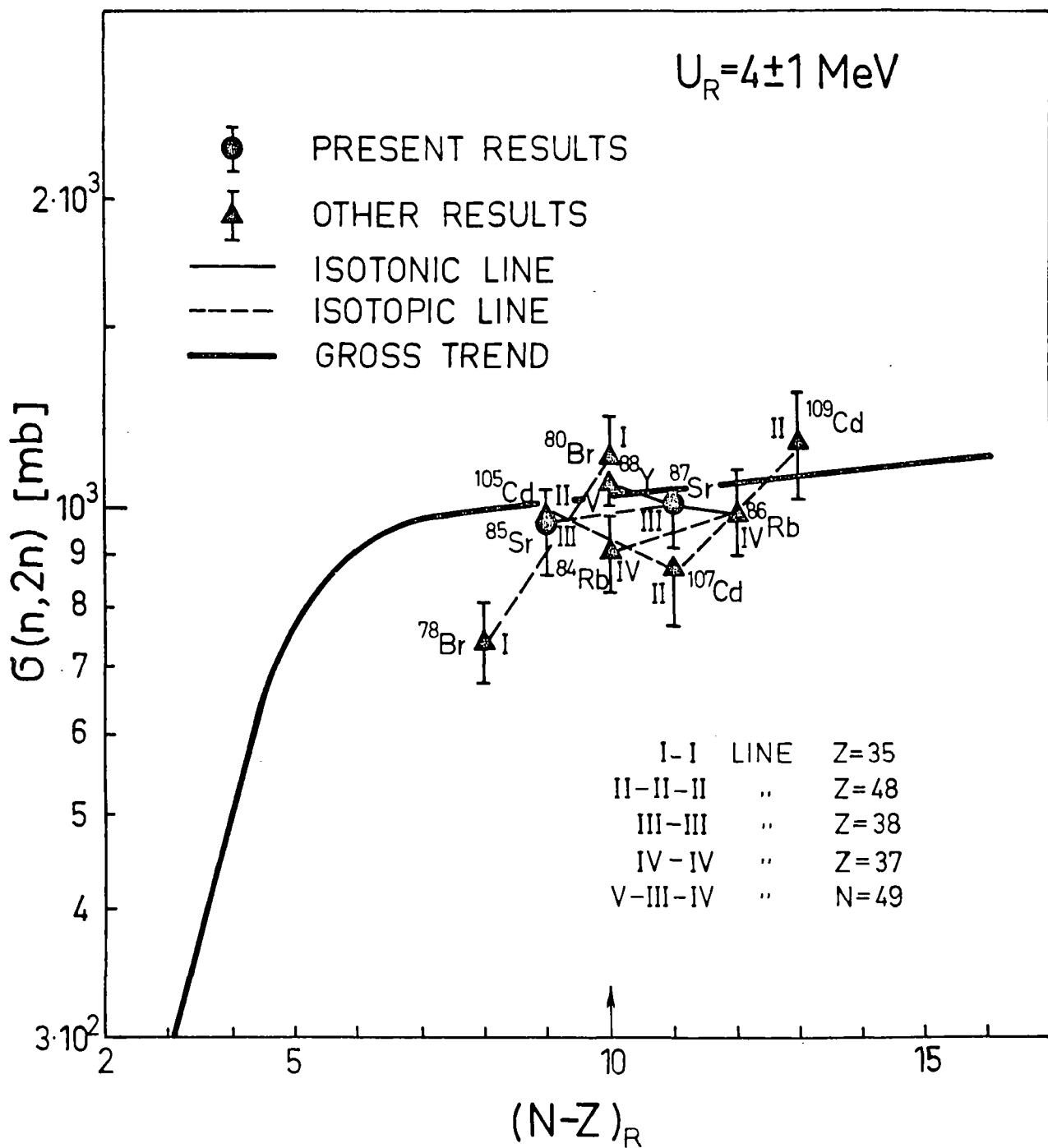


Fig. 1. The experimental cross sections  $G(n, 2n)$  vs.  $(N-Z)_R$  at  $U_R = 4 \pm 1$  MeV. The experimental results follow the gross trend (heavy solid) line and are given in detail only around  $(N-Z)_R = 10$ .

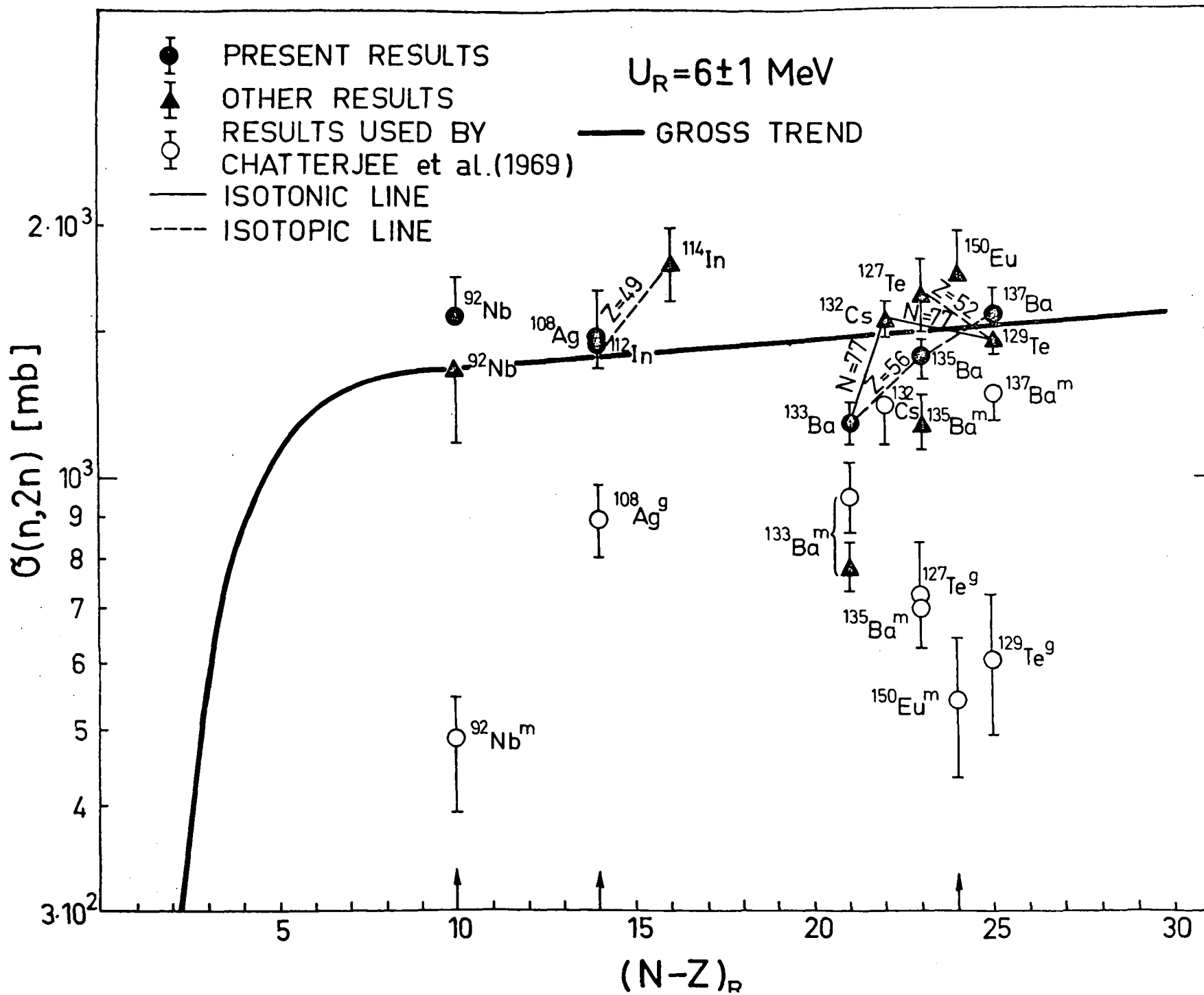


Fig. 2. The same as Fig. 1, but for  $U_R = 6 \pm 1$  MeV region. The experimental results are given in detail only around  $(N-Z)_R = 10, 14$  and  $24$ .

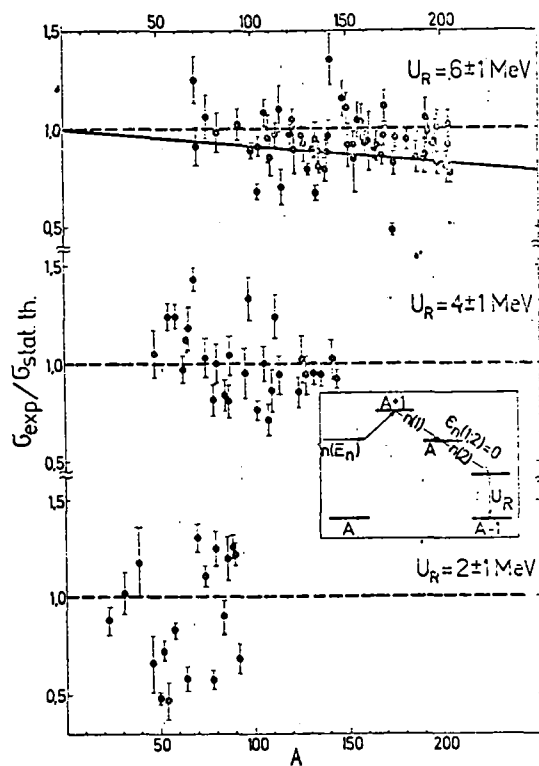


Fig. 3. Ratios of experimental (n,2n) cross sections to the statistical calculations of Paerlstein (10) versus the atomic masses of target nuclei. The full line in the upper part of the figure represents the best  $\chi^2$ -fit to the data using a linear function  $y = \sigma_{\text{exp}}/\sigma_{\text{stat. th.}} = aA + b$ .

II. NON-NEUTRON DATA

THE STRUCTURE OF THE PHOTONUCLEAR GIANT RESONANCE IN  $^{90}\text{Zr}$

D. Brajnik, D. Jamnik, G. Kernel, M. Korun, U. Miklavžič, B. Pucelj  
and A. Stanovnik

Institute "Jožef Stefan", Ljubljana, Yugoslavia

From spectra of photoprotons measured at different end point energies of bremsstrahlung cross sections for  $\gamma, p_0$  reaction and for  $\gamma, p$  reactions leading to three groups of excited states in  $^{89}\text{Y}$  have been determined. In contrast to the  $\gamma, p_0$  reaction the cross sections for the photoproton reactions leading to the excited states in  $^{89}\text{Y}$  show considerable contribution in the region of the expected  $T + 1$  resonance.

The isospin splitting of the dipole resonance is also supported by the measured ratio of the cross sections for the  $\gamma, np$  and  $\gamma, 2n$  reaction which is greater than expected from the statistical calculation of the assumed two-step process for both reactions.

The  $\gamma, np$  and  $\gamma, 2n$  cross sections have been determined by the method of Penfold and Leiss from the measurements of the residual activity.

Reported to the International Conference on Nuclear Structure and Spectroscopy, Amsterdam 1974.

$^{90}\text{Zr} \gamma, p_1 / ^{89}\text{Y}$  and  $^{90}\text{Zr} \gamma, n_1 / ^{89}\text{Zr}$  REACTIONS CROSS SECTIONS IN THE REGION OF GIANT DIPOLE RESONANCE

D. Brajnik, D. Jamnik, G. Kernel, M. Korun, U. Miklavžič, B. Pucelj, A. Stanovnik

Institute "Jožef Stefan", Ljubljana, Yugoslavia  
Cross sections for the reactions  $^{90}\text{Zr} \gamma, p_1 / ^{89}\text{Y}$ , and  $^{90}\text{Zr} \gamma, n_1 / ^{89}\text{Zr}$ , leading to the 909 keV isomeric state of  $^{89}\text{Y}$ ,  $t_{1/2} = 16$  sec. and 588 keV isomeric state of  $^{89}\text{Zr}$ ,  $t_{1/2} = 4.18$  min. were determined by measuring the induced activity at different bremsstrahlung and point energies. In both cases gamma rays were measured with a Ge /Li/ detector. Irradiation and counting times were chosen to be four times  $t_{1/2}$ . A specially designed electronic controller provided the required timing and acquisition of data.

Reported to the Annual Meeting of Yugoslav Nuclear Physicists, Čortanová 1974.

ANGULAR DISTRIBUTIONS OF GAMMA RAYS FROM BOUND STATES ALIGNED  
BY PHOTONUCLEON REACTIONS

G. Kernel

Institute "Jožef Stefan", Ljubljana, Yugoslavia

An expression for the angular distribution of deexcitation gamma rays from excited nuclear states populated in photonuclear reactions was obtained. The main advantage of such experiments for the study of reaction channel configurations is the incoherent contribution of different particle partial waves. The expression simplifies considerably in the region of the giant dipole resonance. Particularly when the photonuclear reaction is performed on a  $J = 0^+$  nucleus, only three photonuclear parameters define the  $A_0$  and  $A_2$  Legendre polynomial coefficients. In addition, a restriction is imposed by the dominance of the non-spin-flip transition in the photonuclear process, thus limiting the alignments of the residual nuclear states. Therefore, some spectroscopic informations about the nuclear levels involved are also gained from such experiments.

Reported to the International Conference on Nuclear Structure and Spectroscopy, Amsterdam 1974.

Study of anomalies in the  $K_{\beta}/K_{\alpha}$  ratios  
observed following K electron capture

G. Paić and V. Pečar

Institute "Ruđer Bošković", Zagreb, Yugoslavia

Measurements of  $K_{\beta}/K_{\alpha}$  ratios in the region has been performed using nuclei decaying via K-electron capture. Measurements of the  $K_{\beta}/K_{\alpha}$  ratio has been performed for Ti, V, Cr, Fe, Cu and Zn. The results show that a marked difference between the  $K_{\beta}/K_{\alpha}$  ratios measured by that method and by x-ray excitation exists for nuclei with  $Z < 28$ . The ratio for these nuclei is lower when the excitation is via electron capture.

$K_{\alpha}/K_{\beta}$  Ratio for Cu Measured by Different Modes  
of Excitation

G. Paić, M. Antić, M. Krčmar, and S. Blagus  
Institute "Ruđer Bošković", Zagreb, Yugoslavia

In order to treat the  $K_{\alpha}/K_{\beta}$  ratios with confidence, it is necessary to ascertain that the most frequently used techniques of excitation do not affect the value of the  $K_{\alpha}/K_{\beta}$  ratio. Several authors have recently measured the  $K_{\alpha}/K_{\beta}$  ratio for different elements. The results have been subject to a rather large scatter depending on the mode of excitation. It is very difficult to reconcile the existing discrepancies, and we therefore performed a measurements of the  $K_{\alpha}/K_{\beta}$  ratio for

copper by three different techniques of excitation but using the same detector system and the same evaluation procedure. The excitations used were:

- (i) electron-capture mode,
- (ii) bremsstrahlung spectrum + Mo K-x rays at  $E_{e1} = 30$  kV, and
- (iii) protons of 162 keV.

The data as determined from the present experiment are in agreement with the latest theoretical estimate of Scofield, which includes the effect of nonzero overlap of the wave functions from different subshells. That treatment yields a  $K_{\alpha}/K_{\beta}$  ratio of 7.24. The present experiment yields equal values for  $K_{\alpha}/K_{\beta}$  ratios obtained from x-ray excitation and electron capture with  $\sim 1$  percent errors. Such precision in the knowledge of  $K_{\alpha}/K_{\beta}$  makes the use of these ratios for applied purposes such as detector efficiency determinations and thickness measurements possible. The relatively important error in proton excitation data prevents us from drawing the conclusion whether the lower  $K_{\alpha}/K_{\beta}$  ratio is due to the higher probability for the formation of multiple vacancies, as observed for heavy ions at higher energies.

### Radioisotope production

G. Paić, M. Vlatković, S. Kaučić, B. Vekić, I. Šlaus, J. Nosil  
Institute "Rudjer Bošković", Zagreb, Yugoslavia

The Ga<sup>67</sup> production with 14 MeV deuterons has been increased to the level of 1500 mCi/year and further increase is planned for the next year.

The 28 MeV alpha beam has been used for production of Rb<sup>81</sup> from Br in order to develop a Kr generator for lung ventilation studies.

### Neutron dosimetry

N. Stipčić, I. Šlaus, G. Paić, K. Kovačević  
Institute "Rudjer Bošković", Zagreb, Yugoslavia

A small volume thin Si detector has been tested for neutron dosimetry. The response of the detector to monoenergetic 14 MeV and 2.7 MeV neutrons and to neutrons obtained with 14 MeV deuterons on an internal Aluminum target in the cyclotron has been measured. The efficiency of the detector satisfies the general requirements for neutron dosimetry in biological research.

II. NON-NEUTRON DATA

STRUCTURE OF THE PHOTONUCLEAR GIANT RESONANCE IN  $^{90}\text{Zr}$

D. Brajnik, D. Jamnik, G. Kernel, M. Korun, U. Miklavžič, B. Pucelj  
and A. Stanovnik

From spectra of photoprotons measured at different end point energies of bremsstrahlung cross sections for  $\gamma, p_0$  reaction and for  $\gamma, p$  reactions leading to three groups of excited states in  $^{89}\text{Y}$  have been determined. In contrast to the  $\gamma, p_0$  reaction the cross sections for the photoproton reactions leading to the excited states in  $^{89}\text{Y}$  show considerable contribution in the region of the expected  $T + 1$  resonance.

The isospin splitting of the dipole resonance is also supported by the measured ratio of the cross sections for the  $\gamma, np$  and  $\gamma, 2n$  reaction which is greater than expected from the statistical calculation of the assumed two-step process for both reactions.

The  $\gamma, np$  and  $\gamma, 2n$  cross sections have been determined by the method of Penfold and Leiss from the measurements of the residual activity.

Reported to the International Conference on Nuclear Structure and Spectroscopy, Amsterdam 1974.

$^{90}\text{Zr} \gamma, p_1 / ^{89}\text{Y}$  and  $^{90}\text{Zr} \gamma, n_1 / ^{89}\text{Zr}$  REACTIONS CROSS SECTIONS IN THE REGION OF GIANT DIPOLE RESONANCE

D. Brajnik, D. Jamnik, G. Kernel, M. Korun, U. Miklavžič, B. Pucelj,  
A. Stanovnik

Cross sections for the reactions  $^{90}\text{Zr} \gamma, p_1 / ^{89}\text{Y}$ , and  $^{90}\text{Zr} \gamma, n_1 / ^{89}\text{Zr}$ , leading to the 909 keV isomeric state of  $^{89}\text{Y}$ ,  $t_{1/2} = 16$  sec. and 588 keV isomeric state of  $^{89}\text{Zr}$ ,  $t_{1/2} = 4.18$  min. were determined by measuring the induced activity at different bremsstrahlung end point energies. In both cases gamma rays were measured with a Ge /Li/ detector. Irradiation and counting times were chosen to be four times  $t_{1/2}$ . A specially designed electronic controller provided the required timing and acquisition of data.

Reported to the Annual Meeting of Yugoslav Nuclear Physicists, Čortanovci 1974.

ANGULAR DISTRIBUTIONS OF GAMMA RAYS FROM BOUND STATES ALIGNED  
BY PHOTONUCLEON REACTIONS

G. Kernel

An expression for the angular distribution of deexcitation gamma rays from excited nuclear states populated in photonuclear reactions was obtained. The main advantage of such experiments for the study of reaction channel configurations is the incoherent contribution of different particle partial waves. The expression simplifies considerably in the region of the giant dipole resonance. Particularly when the photonuclear reaction is performed on a  $J = 0^+$  nucleus, only three photonuclear parameters define the  $A_0$  and  $A_2$  Legendre polynomial coefficients. In addition, a restriction is imposed by the dominance of the non-spin-flip transition in the photonuclear process, thus limiting the alignments of the residual nuclear states. Therefore, some spectroscopic informations about the nuclear levels involved are also gained from such experiments.

Reported to the International Conference on Nuclear Structure and Spectroscopy, Amsterdam 1974.